WSRC-TR-99-00262, Rev. 0

# Composition and Property Measurements for PHA Phase 1 Glasses



by

T. B. Edwards

Westinghouse Savannah River Company
Savannah River Site
Aiken, South Carolina 29808

J. R. Harbour

R. J. Workman

DOE Contract No. **DE-AC09-96SR18500**

WSRC-TR-99-00262
Revision 0

Keywords: Coupled Operations
DWPF, PCT, PCCS,
Liquidus Temperature,
Salt Disposition, Viscosity

Retention Time: Permanent

# COMPOSITION AND PROPERTY MEASUREMENTS FOR PHA PHASE 1 GLASSES (U)

T. B. Edwards
J. R. Harbour
R. J. Workman

Westinghouse Savannah River Company
Savannah River Technology Center
Aiken, SC 29808

SAFETY • RESPONSIBILITY • SECURITY
SRS
SAVANNAH RIVER SITE

PREPARED FOR THE U.S. DEPARTMENT OF ENERGY UNDER CONTRACT NO. DE-AC09-96SR18500

## DISCLAIMER

# COMPOSITION AND PROPERTY MEASUREMENTS FOR PHA PHASE 1 GLASSES (U)

August 4, 1999

Document Approvals

| | |
|---|---|
| Thomas B. Edwards | 8/29/99 |
| **T. B. Edwards**, Author<br>Statistical Consulting Section | Date |
| John R Harbour | 8/31/99 |
| **J. R. Harbour**, Author<br>Immobilization Technology Section | Date |
| Rhonda J. Workman | 8/31/99 |
| **R. J. Workman**, Author<br>Immobilization Technology Section | Date |
| | 8/30/99 |
| **K. G. Brown**, Technical Review<br>Immobilization Technology Section | Date |
| Carol M Jantzen | 8/30/99 |
| **C. M. Jantzen**, Technical Review<br>Immobilization Technology Section | Date |
| | 9/7/99 |
| **R. C. Tuckfield**, Manager<br>Statistical Consulting Section | Date |
| Ed Holtzscheiter | 9-2-99 |
| **E. W. Holtzscheiter**, Manager Immobilization Technology Section<br>Authorized Derivative Classifier | Date |

This page intentionally left blank.

# TABLE OF CONTENTS

This page intentionally left blank.

# SUMMARY AND CONCLUSION

The results presented in this report are for six Phase 1 Precipitate Hydrolysis Aqueous (PHA) glasses, each of which was targeted to contain 26 wt% simulated PUREX sludge on an oxide basis. The target PHA and MST (monosodium titanate) concentrations were varied from 7 to 10 to 13 wt % oxides for PHA and at 1.25 and 2.5 wt % oxides of washed MST.

The models currently in the Product Composition Control System (PCCS) used by the Defense Waste Processing Facility (DWPF) were used to predict durability, homogeneity, liquidus, and viscosity for these six glasses. All six glasses were predicted to be phase separated (i.e., outside the property acceptance region for the homogeneity constraint), and consequently prediction of glass durability is precluded with the current DWPF models. If one ignores the homogeneity constraint, the measured durabilities were within the 95% prediction limits of the model. Further efforts are required to resolve this issue on phase separation (inhomogeneity).

The liquidus model predicted acceptable liquidus temperatures for all six glasses. The approximate (bounding) liquidus temperatures that were measured (<900°C) were well below the model predictions. The measured viscosities were below the predictions of the model and therefore, conservative to the upper limit of viscosity. The predictions are not conservative to the lower limit however, with the lowest measured viscosity value of ~30 poise at 1150°C. The 30-poise viscosity value corresponds to the glass with the highest levels of PHA and MST.

All six of these glasses were durable when compared to the EA (Environmental Assessment) glass (as determined by the 7-day Product Consistency Test, PCT) and processible (based upon approximate measurements of viscosity and liquidus temperature). Therefore, the results imply that the DWPF would be able to run these six glass formulations at 26 wt % PUREX waste loading. However, the effect of kinetics on phase separation (both crystalline and amorphous) for these glasses was not determined since it was beyond the scope of this task.

Acceptable product quality and processability for these Phase 1 glasses promoted the continuation of the phased approach for this PHA variability study as planned. At least 19 additional glasses have been fabricated and are currently being tested under this task. At the end of this task all results will be combined and a final analysis performed.

# INTRODUCTION

One of the Alternative Salt Disposition Flowsheets being considered would require that the Defense Waste Processing Facility (DWPF) vitrify a coupled feed containing high level waste (HLW) and Precipitate Hydrolysis Aqueous (PHA). A Technical Task Request (TTR) [1] was received by the Savannah River Technology Center (SRTC) requesting that a glass variability study be conducted to explore the processability and product quality of the glass composition region for this alternative to the In-Tank Precipitation (ITP) Process. A Task Technical and Quality Assurance (TT&QA) plan [2] was issued by SRTC in response to the TTR. The objective of this task is to obtain information on the feasibility of incorporating anticipated levels of PHA into DWPF glass with and without doubling the nominal levels of monosodium titanate (MST).

A set of target compositions from which the glasses supporting this task are to be selected was provided in the memorandum appearing as Attachment I of this report. Process and product property predictions for these glasses are also provided in that attachment. The candidate glasses identified involved three sludge types: Purex, HM, and Blend; covered sludge loadings (in the glass) of 22, 26, and 30 oxide weight percent (wt%); utilized PHA loadings (in the glass) of 7, 10, and 13 oxide wt%; and included MST concentrations (in the glass) at 1.25 and 2.5 wt%. For each composition, the remainder of the glass consisted of Frit 202. The glasses, batched, and fabricated using the Purex sludge at a target loading of 26 wt% of the glass were selected to comprise Phase 1 of this study. The general, target compositions of these glasses are provided in Table 1.

**Table 1: General Composition of the PHA Phase 1 Glasses**

| Glass ID | Purex Sludge | PHA | MST | Frit 202 |
|---|---|---|---|---|
| pha07 | 26% | 7% | 1.25% | 65.75% |
| pha08 | 26% | 10% | 1.25% | 62.75% |
| pha09 | 26% | 13% | 1.25% | 59.75% |
| pha10 | 26% | 7% | 2.5% | 64.50% |
| pha11 | 26% | 10% | 2.5% | 61.50% |
| pha12 | 26% | 13% | 2.5% | 58.50% |

The properties of interest for these glasses included durability (as measured by the 7-day Product Consistency Test (PCT) [3]), viscosity at 1150 °C, and liquidus temperature. The purpose of this report is to provide and investigate comparisons between

- the measured and target compositions of this set of Phase 1 PHA glasses and
- the property measurements and their predictions.

# RESULTS AND DISCUSSION

The six glasses comprising Phase 1 of the PHA study were designated as pha07 through pha12. Composition and property measurements of these glasses were conducted in parallel with the six glasses comprising Phase 1 of the other ITP replacement alternative, designated as the CST (Crystalline Silicotitanate) study. This approach helps ensure that the PHA and CST glasses are fabricated, characterized, and analyzed under very similar conditions. The CST Phase 1 results were reported in [4], and included in the attachments of that report are the analytical plans that were used to generate the measurements required to support both (PHA and CST) studies. These plans, which are identified in the discussion that follows, were prepared to support the overall Task Technical and QA plan [2] and the analytical study plan [5]. The results of these measurements (both composition and properties) are presented in this section.

## Chemical Compositions

Table 2 provides the target oxide compositions for each of the PHA glasses fabricated with Purex sludge. See Attachment I of this report for details on the development of these target compositions. The Phase 1 glasses, as previously stated, appear as pha07 through pha12 in Table 2.

**Table 2: Target Oxide Composition (in weight percents, wt%'s) of the PHA Glasses Fabricated with Purex Sludge**

| Sludge | MST | PHA | Frit 202 | Glass ID | $Al_2O_3$ | $B_2O_3$ | BaO | CaO | $Cr_2O_3$ | CuO | $Fe_2O_3$ | $K_2O$ | $Li_2O$ | MgO | MnO | $Na_2O$ |
|---|---|---|---|---|---|---|---|---|---|---|---|---|---|---|---|---|
| 22 | 1.250 | 7 | 69.750 | pha01 | 2.540 | 7.974 | 0.084 | 0.945 | 0.106 | 0.568 | 9.899 | 3.350 | 4.785 | 1.448 | 1.727 | 7.869 |
| 22 | 1.250 | 10 | 66.750 | pha02 | 2.522 | 8.803 | 0.084 | 0.941 | 0.106 | 0.791 | 9.897 | 4.730 | 4.579 | 1.389 | 1.727 | 8.017 |
| 22 | 1.250 | 13 | 63.750 | pha03 | 2.504 | 9.632 | 0.084 | 0.936 | 0.106 | 1.014 | 9.894 | 6.110 | 4.373 | 1.329 | 1.727 | 8.165 |
| 22 | 2.500 | 7 | 68.500 | pha04 | 2.532 | 7.876 | 0.084 | 0.943 | 0.106 | 0.568 | 9.898 | 3.350 | 4.699 | 1.423 | 1.727 | 7.944 |
| 22 | 2.500 | 10 | 65.500 | pha05 | 2.514 | 8.705 | 0.084 | 0.939 | 0.106 | 0.791 | 9.896 | 4.730 | 4.493 | 1.364 | 1.727 | 8.092 |
| 22 | 2.500 | 13 | 62.500 | pha06 | 2.496 | 9.534 | 0.084 | 0.934 | 0.106 | 1.014 | 9.893 | 6.110 | 4.288 | 1.304 | 1.727 | 8.240 |
| 26 | 1.250 | 7 | 65.750 | pha07 | 2.901 | 7.660 | 0.099 | 1.092 | 0.125 | 0.576 | 11.685 | 3.365 | 4.510 | 1.381 | 2.041 | 8.116 |
| 26 | 1.250 | 10 | 62.750 | pha08 | 2.883 | 8.488 | 0.099 | 1.088 | 0.125 | 0.800 | 11.683 | 4.745 | 4.305 | 1.322 | 2.041 | 8.264 |
| 26 | 1.250 | 13 | 59.750 | pha09 | 2.865 | 9.317 | 0.099 | 1.083 | 0.125 | 1.023 | 11.681 | 6.125 | 4.099 | 1.262 | 2.041 | 8.412 |
| 26 | 2.500 | 7 | 64.500 | pha10 | 2.894 | 7.561 | 0.099 | 1.090 | 0.125 | 0.576 | 11.684 | 3.365 | 4.425 | 1.356 | 2.041 | 8.191 |
| 26 | 2.500 | 10 | 61.500 | pha11 | 2.876 | 8.390 | 0.099 | 1.086 | 0.125 | 0.800 | 11.682 | 4.745 | 4.219 | 1.297 | 2.041 | 8.339 |
| 26 | 2.500 | 13 | 58.500 | pha12 | 2.858 | 9.219 | 0.099 | 1.081 | 0.125 | 1.023 | 11.680 | 6.125 | 4.013 | 1.237 | 2.041 | 8.487 |
| 30 | 1.250 | 7 | 61.750 | pha13 | 3.263 | 7.345 | 0.114 | 1.239 | 0.144 | 0.585 | 13.472 | 3.380 | 4.236 | 1.314 | 2.355 | 8.363 |
| 30 | 1.250 | 10 | 58.750 | pha14 | 3.245 | 8.174 | 0.114 | 1.234 | 0.144 | 0.808 | 13.470 | 4.760 | 4.030 | 1.255 | 2.355 | 8.511 |
| 30 | 1.250 | 13 | 55.750 | pha15 | 3.227 | 9.003 | 0.114 | 1.230 | 0.144 | 1.031 | 13.467 | 6.140 | 3.824 | 1.195 | 2.355 | 8.659 |
| 30 | 2.500 | 7 | 60.500 | pha16 | 3.256 | 7.246 | 0.114 | 1.237 | 0.144 | 0.585 | 13.471 | 3.379 | 4.150 | 1.289 | 2.355 | 8.438 |
| 30 | 2.500 | 10 | 57.500 | pha17 | 3.238 | 8.075 | 0.114 | 1.233 | 0.144 | 0.808 | 13.469 | 4.759 | 3.945 | 1.230 | 2.355 | 8.586 |
| 30 | 2.500 | 13 | 54.500 | pha18 | 3.220 | 8.904 | 0.114 | 1.228 | 0.144 | 1.031 | 13.466 | 6.139 | 3.739 | 1.170 | 2.355 | 8.734 |

**Table 2: Target Oxide Composition (in weight percents, wt%'s) of the PHA Glasses Fabricated with Purex Sludge (continued)**

| Sludge | MST | PHA | Frit 202 | Glass ID | NiO | $P_2O_5$ | PbO | $SiO_2$ | $TiO_2$ | $U_3O_8$ | ZnO | $ZrO_2$ | $F^-$ | $Cl^-$ | $(SO_4)^=$ |
|---|---|---|---|---|---|---|---|---|---|---|---|---|---|---|---|
| 22 | 1.250 | 7 | 69.750 | pha01 | 0.930 | 0.030 | 0.096 | 53.684 | 1.128 | 2.003 | 0.086 | 0.109 | 0.032 | 0.240 | 0.173 |
| 22 | 1.250 | 10 | 66.750 | pha02 | 0.930 | 0.030 | 0.096 | 51.404 | 1.127 | 2.003 | 0.086 | 0.109 | 0.032 | 0.240 | 0.173 |
| 22 | 1.250 | 13 | 63.750 | pha03 | 0.930 | 0.030 | 0.096 | 49.124 | 1.125 | 2.003 | 0.086 | 0.109 | 0.032 | 0.240 | 0.173 |
| 22 | 2.500 | 7 | 68.500 | pha04 | 0.930 | 0.030 | 0.096 | 52.734 | 2.226 | 2.003 | 0.086 | 0.109 | 0.032 | 0.240 | 0.173 |
| 22 | 2.500 | 10 | 65.500 | pha05 | 0.930 | 0.030 | 0.096 | 50.454 | 2.225 | 2.003 | 0.086 | 0.109 | 0.032 | 0.240 | 0.173 |
| 22 | 2.500 | 13 | 62.500 | pha06 | 0.930 | 0.030 | 0.096 | 48.174 | 2.224 | 2.003 | 0.086 | 0.109 | 0.032 | 0.240 | 0.173 |
| 26 | 1.250 | 7 | 65.750 | pha07 | 1.099 | 0.036 | 0.114 | 50.766 | 1.126 | 2.367 | 0.102 | 0.129 | 0.038 | 0.283 | 0.205 |
| 26 | 1.250 | 10 | 62.750 | pha08 | 1.099 | 0.036 | 0.114 | 48.486 | 1.125 | 2.367 | 0.102 | 0.129 | 0.038 | 0.283 | 0.205 |
| 26 | 1.250 | 13 | 59.750 | pha09 | 1.099 | 0.036 | 0.114 | 46.206 | 1.124 | 2.367 | 0.102 | 0.129 | 0.038 | 0.283 | 0.205 |
| 26 | 2.500 | 7 | 64.500 | pha10 | 1.099 | 0.036 | 0.114 | 49.816 | 2.224 | 2.367 | 0.102 | 0.129 | 0.038 | 0.283 | 0.205 |
| 26 | 2.500 | 10 | 61.500 | pha11 | 1.099 | 0.036 | 0.114 | 47.536 | 2.223 | 2.367 | 0.102 | 0.129 | 0.038 | 0.283 | 0.205 |
| 26 | 2.500 | 13 | 58.500 | pha12 | 1.099 | 0.036 | 0.114 | 45.256 | 2.222 | 2.367 | 0.102 | 0.129 | 0.038 | 0.283 | 0.205 |
| 30 | 1.250 | 7 | 61.750 | pha13 | 1.268 | 0.041 | 0.132 | 47.849 | 1.125 | 2.731 | 0.118 | 0.149 | 0.043 | 0.327 | 0.236 |
| 30 | 1.250 | 10 | 58.750 | pha14 | 1.268 | 0.041 | 0.132 | 45.569 | 1.123 | 2.731 | 0.118 | 0.149 | 0.043 | 0.327 | 0.236 |
| 30 | 1.250 | 13 | 55.750 | pha15 | 1.268 | 0.041 | 0.132 | 43.289 | 1.122 | 2.731 | 0.118 | 0.149 | 0.043 | 0.327 | 0.236 |
| 30 | 2.500 | 7 | 60.500 | pha16 | 1.268 | 0.041 | 0.132 | 46.899 | 2.223 | 2.731 | 0.118 | 0.149 | 0.043 | 0.327 | 0.236 |
| 30 | 2.500 | 10 | 57.500 | pha17 | 1.268 | 0.041 | 0.132 | 44.619 | 2.221 | 2.731 | 0.118 | 0.149 | 0.043 | 0.327 | 0.236 |
| 30 | 2.500 | 13 | 54.500 | pha18 | 1.268 | 0.041 | 0.132 | 42.339 | 2.220 | 2.731 | 0.118 | 0.149 | 0.043 | 0.327 | 0.236 |

Predictions for the properties of interest generated for these target compositions by the models utilized by the Defense Waste Processing Facility (DWPF) are also included in the discussion provided in Attachment I. These properties, for a given composition, relate to its processability and its product quality. For a given composition, acceptable property characteristics and reliable property predictions (using the current DWPF models) are of interest. Comparisons between property predictions and property measurements are provided for these Phase 1 PHA glasses in the discussion that follows.

Initially, glasses were batched and fabricated to the target compositions corresponding to rows pha07 though pha12 of Table 2. In addition to the Phase 1 glasses (both PHA and CST), a standard glass (Batch 1) and a standard uranium-bearing glass were included in the planning of these analyses (for possible bias correction). An analytical plan (in the form of a memorandum) was provided to assist the SRTC-Mobile Laboratory (SRTC-ML) in conducting these analyses (see Attachment II of [4]).

Glasses were batched using the appropriate combinations of Purex sludge, glass formers, PHA, and MST. The simulated Purex sludge was batched from dry chemicals (e.g., reagent grade nitrates, carbonates, and oxides) and has an oxide composition provided in Table 3 of Attachment I of this report. PHA was batched from chemicals and has an oxide composition provided in Table 2 of Attachment I. A basic MST solution was obtained from D. Hobbs. This material was washed and then dried. The composition of MST was determined by the SRTC-ML and is presented in Table 1 of Attachment I. Frit 202, Lot 14 was obtained from the DWPF. The Frit 202 composition is given in Table 7 of Attachment I.

For each glass, the combined powders (~60 grams) were added to a 100 mL Pt-Au crucible and placed in a calibrated furnace, heated to 1150°C at a rate of 10°C/minute, and then held for four hours at 1150°C. The crucible was then removed and the glass immediately poured onto a clean stainless steel plate.

Table A.1 in Appendix A provides the composition measurements obtained by the SRTC-ML for the plan covering these analyses. As indicated in this table, two dissolution methods were used to perform these analyses: peroxide fusion and microwave. The SRTC-ML was unable to successfully complete the first block of B, Ca, and Si measurements (for samples prepared using peroxide fusion). Thus, the first block was split, and a sample of the Batch 1 standard glass was inserted to begin a new block designated as block 1b. Exhibit A.1 in Appendix A provides a plot of the measurements by glass sample id by oxide. There is somewhat more scatter in the $Fe_2O_3$ values than in some of the other oxides measured from samples prepared using the microwave method. The large scatter among the boron measurements for several glasses and among the silicon measurements for a few glasses prompted a request for the SRTC-ML to rerun the block that was split. Table A.2 in Appendix A provides the results from this set of analyses for B, Ca, and Si. Exhibit A.2 in Appendix A provides plots of these new measurements by glass sample id for the oxides of these three elements. Even though the $SiO_2$ values for some of the glasses still appear to be somewhat excessively scattered, these values were used to replace the original B, Ca, and Si measurements for the analyses that follow.

A review of the results from the standards was used to provide insight into the possibility that the ICP calibration contributes (in a systematic way) to the variation seen in the oxide measurements for the Phase 1 glasses. Exhibit A.3 in Appendix A provides plots of the oxide measurements per analytical block by oxide. Table 3 provides the average measured composition for the two standards included in this analytical plan. The reference values for the standards are also provided in this table.

**Table 3: Measurements from Glass Standards**

| | std (Batch 1) | | | u-std (Uranium-bearing Standard) | | |
|---|---|---|---|---|---|---|
| | Analytical Block | | | Analytical Block | | |
| | 1 | 2 | Reference | 1 | 2 | Reference |
| **Oxide** | **3 obs** | **3 obs** | **Value** | **2 obs** | **2 obs** | **Value** |
| **$Al_2O_3$** | 4.661 | 4.711 | 4.877 | 3.826 | 3.855 | 4.100 |
| **$B_2O_3$** | 8.275 | 7.878 | 7.777 | 9.402 | 9.338 | 9.209 |
| **CaO** | 1.269 | 1.330 | 1.220 | 1.361 | 1.396 | 1.301 |
| **$Cr_2O_3$** | 0.103 | 0.097 | 0.107 | 0.240 | 0.224 | 0.000 |
| **CuO** | 0.386 | 0.378 | 0.399 | 0.006 | 0.014 | 0.000 |
| **$Fe_2O_3$** | 11.690 | 12.701 | 12.839 | 11.938 | 12.639 | 13.196 |
| **$K_2O$** | 3.425 | 3.256 | 3.327 | 3.030 | 2.903 | 2.999 |
| **$Li_2O$** | 4.335 | 4.062 | 4.429 | 2.928 | 2.734 | 3.057 |
| **MgO** | 1.366 | 1.403 | 1.419 | 1.126 | 1.117 | 1.210 |
| **MnO** | 1.670 | 1.648 | 1.726 | 2.653 | 2.582 | 2.892 |
| **$Na_2O$** | 9.571 | 8.807 | 9.003 | 12.617 | 11.701 | 11.795 |
| **NiO** | 0.713 | 0.728 | 0.751 | 1.014 | 1.025 | 1.120 |
| **$SiO_2$** | 52.627 | 46.280 | 50.220 | 49.953 | 42.786 | 45.353 |
| **$TiO_2$** | 0.670 | 0.688 | 0.677 | 0.981 | 0.986 | 1.049 |
| **$U_3O_8$** | 0.590 | 0.590 | 0.000 | 2.187 | 2.329 | 2.406 |
| **$ZrO_2$** | 0.088 | 0.096 | 0.098 | 0.007 | 0.014 | 0.000 |
| **Sum of Oxides** | 101.479 | 94.705 | 98.869 | 103.325 | 95.711 | 99.687 |

The analytical results from the Batch 1 samples were used to bias-correct for a possible ICP calibration effect (a block effect) in the other measurements.[1] This was accomplished for each oxide in turn by taking the original oxide measurement, noting its block, and then multiplying the measurement by the ratio of the corresponding reference value for Batch 1 divided by the average oxide measurement for Batch 1 in that block. This approach was used to bias-correct the composition measurements of the Phase 1 and standard glasses.

Exhibit A.4 in Appendix A provides plots of these measurements for each oxide over all of the glasses (including the standards), and Table 4 provides summary information for these measurements. The sums of oxides for the target, measured, and measured bias-corrected compositions are also provided. A review of these sums shows that they all are within the interval of 95 to 105 weight percent with the smallest value being 95.6 wt% for the measured composition of pha07 and the largest being 100.8 wt% for the bias-corrected composition of pha11. One observation from this exhibit and table is that the TiO2 measurements are consistently low for the PHA glasses even though the Batch 1 and uranium-standard measurements are more near their respective targets. This problem was discussed in [4] and

1 Bias corrections of this type have been advantageous (see for example "A Statistical Review of Data from the SRTC Mobile Laboratory," WSRC-RP-98-00430, Revision 0, June 15, 1998) but not always. In some instances, bias correction does not improve the accuracy of the results. Measurements are bias-corrected in this report, and bias-corrected values are considered in the comparisons that follow. Conclusions, developed from these comparisons, that are insensitive to the way the glass compositions are represented (target, measured, or bias-corrected) demonstrate robustness to which representation might be nearer the true composition for each glass.

is also described in Appendix B of this report. Some other trends are seen in the plots of Exhibit A.4 and in Table 4, but no other problems were identified.

**Table 4: Target, Measured and Bias-Corrected Compositions (in wt%) for the Phase 1 Glasses**

| | *Batch 1* | | | *Uranium Standard (u-std)* | | | *pha07* | | |
|---|---|---|---|---|---|---|---|---|---|
| | Target | Measured | Measured Bias-cor. | Target | Meas. Meas. | Bias-cor. | Target | Measured | Measured Bias-cor. |
| $Al_2O_3$ | 4.877 | 4.544 | 4.877 | 4.100 | 3.755 | 4.030 | 2.901 | 2.650 | 2.758 |
| $B_2O_3$ | 7.777 | 7.814 | 7.777 | 9.209 | 9.257 | 9.220 | 7.660 | 7.688 | 7.403 |
| CaO | 1.220 | 1.173 | 1.220 | 1.301 | 1.263 | 1.313 | 1.092 | 1.119 | 1.051 |
| $Cr_2O_3$ | 0.107 | 0.105 | 0.107 | 0 | 0.248 | 0.271 | 0.125 | 0.121 | 0.129 |
| CuO | 0.399 | 0.381 | 0.399 | 0 | 0.011 | 0.012 | 0.576 | 0.492 | 0.514 |
| $Fe_2O_3$ | 12.839 | 13.311 | 12.839 | 13.196 | 13.561 | 13.076 | 11.685 | 10.308 | 10.855 |
| $K_2O$ | 3.327 | 3.244 | 3.327 | 2.999 | 2.909 | 2.984 | 3.365 | 3.084 | 3.071 |
| $Li_2O$ | 4.429 | 4.632 | 4.429 | 3.057 | 2.971 | 2.838 | 4.510 | 4.236 | 4.468 |
| MgO | 1.419 | 1.413 | 1.419 | 1.210 | 1.186 | 1.191 | 1.381 | 1.382 | 1.417 |
| MnO | 1.726 | 1.730 | 1.726 | 2.892 | 2.783 | 2.776 | 2.041 | 1.863 | 1.938 |
| $Na_2O$ | 9.003 | 9.045 | 9.003 | 11.795 | 11.798 | 11.744 | 8.116 | 8.071 | 7.910 |
| NiO | 0.751 | 0.766 | 0.751 | 1.120 | 1.087 | 1.065 | 1.099 | 0.866 | 0.902 |
| $SiO_2$ | 50.220 | 48.705 | 50.22 | 45.353 | 45.300 | 46.711 | 50.766 | 50.274 | 51.040 |
| $TiO_2$ | 0.677 | 0.666 | 0.677 | 1.049 | 0.962 | 0.979 | 1.126 | 0.691 | 0.689 |
| $U_3O_8$ | 0 | 0.295 | 0.295 | 2.406 | 2.311 | 2.311 | 2.367 | 2.633 | 2.633 |
| $ZrO_2$ | 0.098 | 0.090 | 0.098 | 0 | 0.009 | 0.010 | 0.129 | 0.128 | 0.137 |
| Sum of Oxides | 98.869 | 97.972 | 99.221 | 99.687 | 99.485 | 100.604 | 98.939 | 95.647 | 96.958 |

| | *pha08* | | | *pha09* | | | *pha10* | | |
|---|---|---|---|---|---|---|---|---|---|
| | Target | Meas. Meas. | Bias-cor. | Target | Measured | Measured Bias-cor. | Target | Meas. Meas. | Bias-cor. |
| $Al_2O_3$ | 2.883 | 2.711 | 2.822 | 2.865 | 2.707 | 2.817 | 2.894 | 2.636 | 2.743 |
| $B_2O_3$ | 8.488 | 8.766 | 8.435 | 9.317 | 9.410 | 9.068 | 7.561 | 7.985 | 7.693 |
| CaO | 1.088 | 1.129 | 1.060 | 1.083 | 1.099 | 1.032 | 1.090 | 1.109 | 1.043 |
| $Cr_2O_3$ | 0.125 | 0.113 | 0.120 | 0.125 | 0.113 | 0.121 | 0.125 | 0.113 | 0.121 |
| CuO | 0.800 | 0.693 | 0.725 | 1.023 | 0.761 | 0.795 | 0.576 | 0.501 | 0.523 |
| $Fe_2O_3$ | 11.683 | 10.626 | 11.201 | 11.681 | 9.951 | 10.475 | 11.684 | 9.701 | 10.205 |
| $K_2O$ | 4.745 | 4.352 | 4.335 | 6.125 | 5.294 | 5.273 | 3.365 | 3.123 | 3.111 |
| $Li_2O$ | 4.305 | 4.080 | 4.304 | 4.099 | 4.037 | 4.259 | 4.425 | 4.295 | 4.533 |
| MgO | 1.322 | 1.331 | 1.365 | 1.262 | 1.272 | 1.304 | 1.356 | 1.337 | 1.370 |
| MnO | 2.041 | 1.875 | 1.950 | 2.041 | 1.905 | 1.981 | 2.041 | 1.853 | 1.928 |
| $Na_2O$ | 8.264 | 8.391 | 8.222 | 8.412 | 8.374 | 8.206 | 8.191 | 8.341 | 8.178 |
| NiO | 1.099 | 0.861 | 0.897 | 1.099 | 0.857 | 0.893 | 1.099 | 0.838 | 0.873 |
| $SiO_2$ | 48.486 | 50.006 | 50.778 | 46.206 | 48.081 | 48.940 | 49.816 | 51.343 | 52.180 |
| $TiO_2$ | 1.125 | 0.698 | 0.697 | 1.124 | 0.707 | 0.705 | 2.224 | 1.369 | 1.365 |
| $U_3O_8$ | 2.367 | 2.161 | 2.161 | 2.367 | 2.565 | 2.565 | 2.367 | 2.409 | 2.409 |
| $ZrO_2$ | 0.129 | 0.126 | 0.134 | 0.129 | 0.132 | 0.140 | 0.129 | 0.126 | 0.134 |
| Sum of Oxides | 98.950 | 97.963 | 99.250 | 98.958 | 97.306 | 98.618 | 98.943 | 97.171 | 98.504 |

| | *pha11* | | | *pha12* | | |
|---|---|---|---|---|---|---|
| | Target | Measured | Measured Bias-cor. | Target | Meas. Meas. | Bias-cor. |
| $Al_2O_3$ | 2.876 | 2.664 | 2.773 | 2.858 | 2.626 | 2.733 |
| $B_2O_3$ | 8.390 | 8.967 | 8.646 | 9.219 | 9.724 | 9.375 |
| CaO | 1.086 | 1.102 | 1.036 | 1.081 | 1.114 | 1.047 |
| $Cr_2O_3$ | 0.125 | 0.117 | 0.124 | 0.125 | 0.111 | 0.119 |
| CuO | 0.800 | 0.676 | 0.707 | 1.023 | 0.818 | 0.855 |
| $Fe_2O_3$ | 11.682 | 9.879 | 10.403 | 11.680 | 10.344 | 10.880 |
| $K_2O$ | 4.745 | 4.255 | 4.239 | 6.125 | 5.514 | 5.491 |
| $Li_2O$ | 4.219 | 4.091 | 4.315 | 4.013 | 3.929 | 4.145 |
| MgO | 1.297 | 1.285 | 1.317 | 1.237 | 1.230 | 1.261 |
| MnO | 2.041 | 1.840 | 1.914 | 2.041 | 1.837 | 1.910 |
| $Na_2O$ | 8.339 | 8.432 | 8.266 | 8.487 | 8.543 | 8.373 |
| NiO | 1.099 | 0.861 | 0.898 | 1.099 | 0.849 | 0.885 |
| $SiO_2$ | 47.536 | 51.236 | 52.113 | 45.256 | 48.669 | 49.502 |
| $TiO_2$ | 2.223 | 1.337 | 1.334 | 2.222 | 1.350 | 1.346 |
| $U_3O_8$ | 2.367 | 2.462 | 2.462 | 2.367 | 2.456 | 2.456 |
| $ZrO_2$ | 0.129 | 0.122 | 0.130 | 0.129 | 0.122 | 0.129 |
| Sum of Oxides | 98.954 | 99.415 | 100.764 | 98.962 | 99.327 | 100.600 |

## PCT Results

The six PHA glasses making up Phase 1, after being batched and fabricated, were subjected to the 7-day Product Consistency Test (PCT) as an assessment of their durabilities [3]. More specifically, Method A of the PCT (ASTM C1285) was used for these measurements. Since durability is a critical product quality metric for vitrified nuclear waste, a review of the PCTs for these initial glasses was seen as a prerequisite for additional testing of these glasses. The PCTs were to be conducted in triplicate for the Phase 1 glasses. In addition, PCTs were also conducted in triplicate for samples of the Environmental Assessment (EA) glass, the ARM glass, and a blank (ASTM Type I water). An analytical plan supporting these tests was provided in the form of a memorandum (see Attachment III of [4]). This plan assisted the SRTC-ML in measuring the compositions of the solutions resulting from these PCTs. Of primary interest were the concentrations (in parts per million, ppm) of boron (B), lithium (Li), sodium (Na), and silicon (Si). Samples of a multi-element solution standard were also included in this analytical plan (as a check on the accuracy of the Inductively Coupled Plasma (ICP) – Emission Spectrometer used for these measurements).

The results from these tests are given in Table A.3 of Appendix A. Any measurement determined to be below detection was replaced by ½ of the detection limit in subsequent analyses. PCT leachate concentrations are typically normalized using the cation composition (expressed as a weight percent) in the glass to obtain a grams-per-liter (g/L) leachate concentration. The normalization of the PCTs is usually conducted using the measured compositions of the glasses. This is the preferred normalization process for the PCTs. For completeness, the target cation compositions will also be used to conduct this normalization.

As is the usual convention, the common logarithm of the normalized PCT (normalized leachate, NL) for each element of interest will be determined and used for comparison. To accomplish this computation, one must

1. Determine the common logarithm of the elemental parts per million (ppm) leachate concentration for each of the triplicates and each of the elements of interest (these values are provided in Table A.3 of Appendix A),

2. Average the common logarithms over the triplicates for each element of interest, and then

Normalizing Using Measured Composition (preferred method)

3. Subtract a quantity equal to 1 plus the common logarithm of the average cation measured concentration (expressed as a weight percent of the glass) from the average computed in step 2.

Or

Normalizing Using Target Composition

3. Subtract a quantity equal to 1 plus the common logarithm of the target cation concentration (expressed as a weight percent of the glass) from the average computed in step 2.

As a preliminary step to completing these normalizations of the PCTs, a review of the elemental ppm data was conducted. Exhibit A.5 in Appendix A provides plots of the leachate concentrations by sample id and by element with and without the EA and the blank samples. No problems are seen in these data, in that the results are reasonably consistent across all Phase 1 and standard glasses. Table 5 provides a look at the results from the three analyses of the multi-element standard solution that were included in the analytical plan. These results also indicate consistent and reasonably accurate results from these analyses.

**Table 5: Measurements of Standard Solution**

| Sequence | B (ppm) | Si (ppm) | Na (ppm) | Li (ppm) |
|---|---|---|---|---|
| 1 | 20.5 | 53.0 | 86.6 | 10.1 |
| 2 | 21.0 | 51.1 | 86.0 | 10.3 |
| 3 | 20.6 | 50.0 | 83.8 | 10.1 |
| Average | 20.7 | 51.4 | 85.5 | 10.2 |
| Reference | 20.0 | 50.0 | 81.0 | 10.0 |
| % difference | 3.5% | 2.7% | 5.5% | 1.7% |

Table 6 provides the results from the normalization process using the information in Table 4 and Table A.3. Exhibit A.6 in Appendix A provides scatter plots for these results offering an opportunity to investigate the consistency in the leaching across the elements for the glasses of this study. This consistency is typically demonstrated by a high degree of linear correlation among the values. PCT normalized using target, measured, and bias-corrected compositions are investigated. A high degree of correlation between each pair of elements is seen for these data. The smallest correlation (95%) is between Na and Si for the PCTs normalized using the bias-corrected compositions.

**Table 6: Normalized PCTs**

| Glass ID | Composition | log NL [B(g/L)] | log NL [Si(g/L)] | log NL [Na(g/L)] | log NL [Li(g/L)] | NL B(g/L) | NL Si(g/L) | NL Na(g/L) | NL Li(g/L) |
|---|---|---|---|---|---|---|---|---|---|
| ARM | reference comp. [6] | -0.2220 | -0.5076 | -0.2258 | -0.1677 | 0.60 | 0.31 | 0.59 | 0.68 |
| EA | reference comp. [6] | 1.2485 | 0.6195 | 1.1569 | 0.9997 | 17.72 | 4.16 | 14.35 | 9.99 |
| | measured | -0.0238 | -0.2692 | -0.0623 | 0.0093 | 0.95 | 0.54 | 0.87 | 1.02 |
| pha07 | measured, bias-cor. | -0.0074 | -0.2758 | -0.0535 | -0.0139 | 0.98 | 0.53 | 0.88 | 0.97 |
| | target | -0.0223 | -0.2734 | -0.0647 | -0.0179 | 0.95 | 0.53 | 0.86 | 0.96 |
| | measured | 0.0096 | -0.2554 | 0.0058 | 0.0503 | 1.02 | 0.56 | 1.01 | 1.12 |
| pha08 | measured, bias-cor. | 0.0263 | -0.2621 | 0.0147 | 0.0271 | 1.06 | 0.55 | 1.03 | 1.06 |
| | target | 0.0236 | -0.2420 | 0.0125 | 0.0270 | 1.06 | 0.57 | 1.03 | 1.06 |
| | measured | 0.0864 | -0.2332 | 0.0779 | 0.1132 | 1.22 | 0.58 | 1.20 | 1.30 |
| pha09 | measured, bias-cor. | 0.1025 | -0.2409 | 0.0867 | 0.0899 | 1.27 | 0.57 | 1.22 | 1.23 |
| | target | 0.0907 | -0.2159 | 0.0759 | 0.1065 | 1.23 | 0.61 | 1.19 | 1.28 |
| | measured | -0.0456 | -0.2723 | -0.0573 | 0.0095 | 0.90 | 0.53 | 0.88 | 1.02 |
| pha10 | measured, bias-cor. | -0.0294 | -0.2793 | -0.0488 | -0.0140 | 0.93 | 0.53 | 0.89 | 0.97 |
| | target | -0.0219 | -0.2592 | -0.0495 | -0.0035 | 0.95 | 0.55 | 0.89 | 0.99 |
| | measured | 0.0371 | -0.2609 | 0.0323 | 0.0830 | 1.09 | 0.55 | 1.08 | 1.21 |
| pha11 | measured, bias-cor. | 0.0529 | -0.2683 | 0.0409 | 0.0597 | 1.13 | 0.54 | 1.10 | 1.15 |
| | target | 0.0660 | -0.2284 | 0.0371 | 0.0695 | 1.16 | 0.59 | 1.09 | 1.17 |
| | measured | 0.1748 | -0.2054 | 0.1433 | 0.1777 | 1.50 | 0.62 | 1.39 | 1.51 |
| pha12 | measured, bias-cor. | 0.1907 | -0.2128 | 0.1520 | 0.1545 | 1.55 | 0.61 | 1.42 | 1.43 |
| | target | 0.1980 | -0.1739 | 0.1462 | 0.1685 | 1.58 | 0.67 | 1.40 | 1.47 |

As seen in Table 6, the durabilities for the PHA Phase 1 glasses are much better than that of EA. (This is indicated for each glass by its normalized leachate being much smaller than that of EA.). Figure 1 provides an opportunity for a closer look at these results using measured and bias-corrected compositions. Figure 1 is a plot of the DWPF model that relates the logarithm of the normalized PCT (in this case for B) to a linear function of a free energy of hydration term ($\Delta G_p$, kcal/100g glass) derived from the glass (measured and bias-corrected) compositions [6]. Prediction limits (at 95% confidence) for individual PCT results are also plotted around this linear fit. The PCT results for EA (shown as a diamond), ARM (shown as a "z"), and the PHA glasses (each shown as an "x") are presented on this plot. Note that the PHA results reveal acceptable PCTs and that the PCTs are well predicted by the current DWPF durability model for boron. Figure 2 provides a plot of the boron results based upon target compositions. Exhibit A.7 in Appendix A provides similar plots of the PHA durability measurements versus the DWPF durability models for B, Si, Na, and Li. The behavior seen in the plots for Si, Na, and Li is similar to that demonstrated by the B results: acceptable and predictable durabilities.

**Figure 1.**
**Log NL(B) (g/L) By del Gp**
**(Using PHA Measured & Bias-corrected compositions and reference compositions for EA and ARM)**

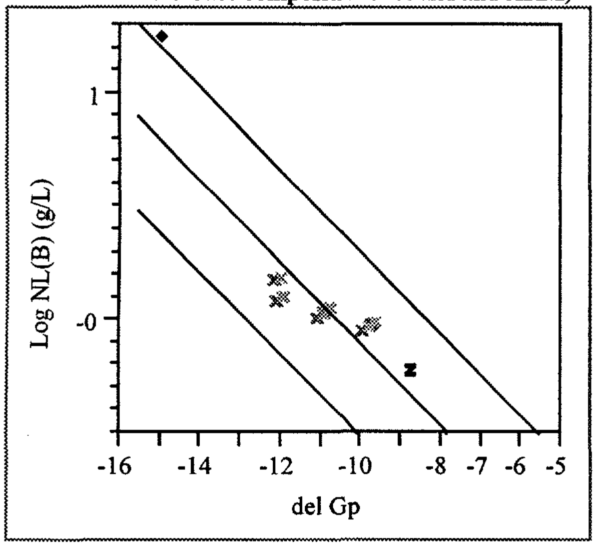


**Figure 2.**
**Log NL(B) (g/L) By del Gp**
**(Using target PHA compositions and reference compositions for EA and ARM)**

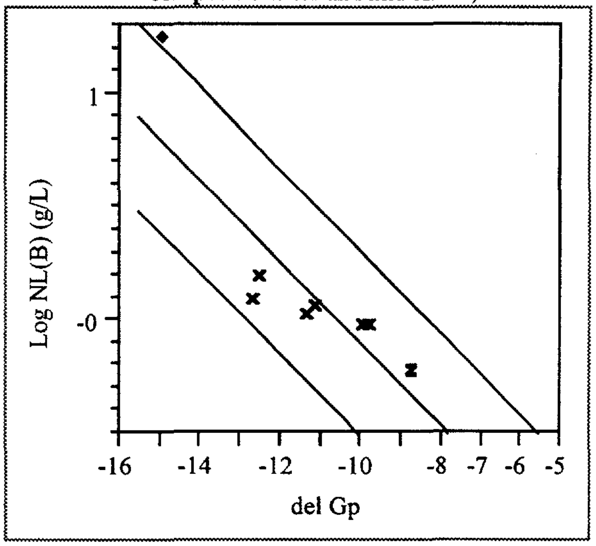


## Viscosity at 1150 °C

Viscosity measurements were made on the six Phase 1 PHA glasses at SRTC using a Harrop, high-temperature viscometer [7]. The viscosity (in Poise) of each of these glasses at 1150 °C is to be estimated from a Fulcher equation fitted to a set of viscosity measurements taken over an appropriate range of temperatures. The functional form of the (three-parameter) Fulcher equation (expressed in Poise) used to fit these data is given by equation (1):

$$\ln \hat{\eta} = A + \frac{B}{(T - C)} \qquad (1)$$

where A, B, and C represent the parameters of the natural logarithm (ln) model that are to be determined from the available measurements (represented by $\eta$, expressed in Poise) at various temperatures (represented by T). The fitted model is then used to predict the viscosity of a given glass at 1150 °C.

Although no definitive error analysis has been completed on the use of the Harrop viscometer, SRTC has conducted several sets of viscosity measurements using this viscometer with good results [8]. Two crucible/spindle sets were used in conducting these measurements, which were sequenced according to the plan provided in Attachment IV of [4]. This plan covered the CST and PHA Phase 1 glasses and called for these measurements to be followed by measurements of the Batch 1 standard glass with both crucible/spindle sets. Measurements of the Batch 1 glass conducted before the planned measurements were reported in [8]. Exhibit A.8 of Appendix A provides the measured viscosities, the results of the Fulcher fit, and the prediction at 1150 °C for each of the PHA Phase 1 glasses along with the ending Batch 1 results. The information presented in this exhibit (along with predictions from the DWPF viscosity model and the Batch 1 results from [8]) is summarized in Table 7.

**Table 7: Viscosity Results (in Poise) at 1150 °C By Glass ID**

| Glass ID | Viscosity (Poise) @ 1150 °C | Predicted (measured composition) | Predicted (bias-corrected composition) | Predicted (target composition) |
|---|---|---|---|---|
| Batch 1 | 48.6, 49.7, 46.4 | 44.2 (Sharp-Schurtz) | | 56.2 |
| pha07 | 52.6 | 65.7 | 66.1 | 58.0 |
| pha08 | 39.5 | 53.3 | 54.1 | 42.7 |
| pha09 | 31.8 | 42.7 | 44.0 | 30.5 |
| pha10 | 50.9 | 67.5 | 68.2 | 55.3 |
| pha11 | 37.7 | 59.4 | 60.7 | 40.4 |
| pha12 | 29.2 | 42.1 | 43.4 | 28.5 |
| Batch 1 | 48.9, 47.3 | 44.2 (Sharp-Schurtz) | | 56.2 |

The melt viscosities at 1150°C for the six PHA glasses are all well within the DWPF operating range, although lower than the viscosities of the sludge-only glasses that have been run in the DWPF for the last several years. Therefore, processing these glasses in the DWPF would evidently not be a problem from a viscosity perspective.

There are several interesting trends observed in the data. Whether one uses the measured or bias-corrected measured compositions to calculate viscosities using the current model, the model viscosities are always higher than the measured viscosities. On the other hand, the measured viscosities are closer to the predicted viscosities using the target compositions.

Another trend observed in these data is a decrease in viscosity as the PHA concentration is increased in the glass from 7 to 13 wt %. At a fixed PHA concentration, the viscosity decreases slightly as the MST concentration increases.

## Liquidus Temperature ($T_L$)

As plans were being made to measure the $T_L$'s for these glasses, it was thought that there may not sufficient quantities of these glasses to support all of these measurements. This led to a second set of six glasses (with the same target compositions as the first set) being batched and fabricated. It was intended that these re-batched glasses be used to conduct isothermal liquidus temperature measurements. However, a problem in the compositions of these glasses was discovered (see Appendix B for a full discussion of these re-batched glasses), so the original six glasses were used for the liquidus temperature measurements.

The standard ASTM procedure for measuring liquidus temperature uses a gradient furnace. The equipment for determining liquidus temperature by this method is being installed and tested within SRTC in a clean laboratory. Due to the presence of depleted uranium in the glass samples (as well as the early stage of equipment setup), we were not able to use this method for liquidus determination. A decision was therefore made to perform isothermal holds using reasonable quantities of the glass to bound the liquidus temperature as determined by XRD.

XRD was selected as the method of detection for crystal formation in these glasses. It is estimated that the sensitivity of XRD (non-quantitative) is ~ 0.7 to 1 wt% for a crystalline phase (in this case, Trevorite) [9]. Therefore, for this type of measurement, absence of detection of a crystalline phase was evidence that the liquidus temperature is less than the temperature of that isothermal hold. On the other hand, detection of Trevorite (or any other primary crystalline phase) indicates that the liquidus temperature is higher than the temperature of the isothermal hold.

Each glass underwent an isothermal hold at 900°C. Approximately 5 grams of glass were placed in a small platinum crucible and transferred to a furnace already heated to 1150°C. After a four-hour hold period, the temperature was reduced to 900°C and held at that temperature for 24 hours. The crucible was then removed from the furnace and the glass allowed to cool within the crucible at room temperature. For these experiments, twelve glasses were treated together. The twelve glasses consisted of the six CST and six PHA glasses containing 26 wt% Purex simulated sludge. Therefore, the CST and PHA glasses experienced essentially identical heat treatments. The six PHA glasses at 900°C were submitted for XRD analysis. Care was taken to obtain glass that was not part of the top glass surface. The glass pieces, although mainly from the bulk, usually included part of the bottom surface (i.e., that surface in contact with the crucible).

The XRD analysis revealed no crystals in any of the glasses to the detection limit of the technique (~0.7 to 1.0 wt%). Therefore, the approximate liquidus temperatures for the six PHA glasses are bounded by the values of Table 8:

**Table 8: Liquidus Temperatures**

| GLASS ID | LIQUIDUS TEMPERATURE |
|---|---|
| pha07 | <900°C |
| pha08 | <900°C |
| pha09 | <900°C |
| pha10 | <900°C |
| pha11 | <900°C |
| pha12 | <900°C |

To the detection capabilities of XRD, the liquidus temperatures for these glasses are likely well below the nominal PAR value of 1025 °C [10] and readily meet DWPF processing requirements for liquidus. The model predictions for these six glasses ranged from 988°C to 1012°C using targeted chemical compositions, from 954°C to 973°C using measured compositions, and 959°C to 980°C using bias-corrected compositions. These data suggest that the predictions may be conservative for these glasses. A new liquidus temperature model is being developed with a goal of preventing unnecessarily conservative constraints on this property.

## Surface Crystallization

For liquidus temperature measurements, crystal formation is considered only in the interior or bulk glass region. Therefore, samples submitted for XRD analysis were bulk samples. However, crystals can form at the interface of the glass and the crucible and/or the glass and air. For completeness, the detection of these surface crystals on the top of the glass is provided in Table 9 as a function of temperature. Only 900°C data are provided since XRD revealed no crystals in the six glasses isothermally held at 900°C for 24 hours. Consequently, no higher temperature isothermal holds were conducted.

**Table 9. Surface Crystals for the Six PHA Glasses as Function of Temperature after the 24 hour heat treatment.**

| | pha07 | pha08 | pha09 | pha10 | pha11 | pha12 |
|---|---|---|---|---|---|---|
| 1150°C | No test | No test | No test | No test | No test | No test |
| 1000°C | No test | No test | No test | No test | No test | No test |
| 950°C | No test | No test | No test | No test | No test | No test |
| 900°C | None | None | None | None | None | None |

As shown in Table 9, no surface crystallization was detected for any of the glasses at these temperatures.

## Phase Separation

The formation of separate amorphous phases in glass is referred to as amorphous phase separation or inhomogeneity. Crystal formation, as determined by liquidus temperature measurements on the other hand, may indicate a "separation of phases," but reflects crystalline particles within the glass matrix. Amorphous phase separation is to be avoided since the models currently used to predict durability do not apply for glasses predicted to be phase separated. The limit for the homogeneity constraint in the

PCCS is nominally (for the Property Acceptance Region, PAR) a value of 211 [10]. For the measurement acceptance region (MAR), the value will be even higher. In order for a glass to pass this constraint, the calculated value from chemical composition of the glass must be greater than the MAR value. The homogeneity values calculated using the targeted and measured chemical compositions are all below the PAR value. Thus, all of these PHA Phase 1 glasses are predicted to be phase separated. Their predicted values are given in Table 10:

**Table 10: Homogeneity Property Predictions**

| | Homogeneity Property Prediciton Based on (Acceptability Requires a Value > 211) | | |
|---|---|---|---|
| Glass ID | Target Composition | Measured Composition | Bias-Corrected Composition |
| pha07 | 207.9 | 197.1 | 201.3 |
| pha08 | 207.5 | 202.9 | 207.2 |
| pha09 | 207.2 | 198.3 | 202.4 |
| pha10 | 206.1 | 196.3 | 200.4 |
| pha11 | 205.8 | 200.5 | 204.7 |
| pha12 | 205.4 | 202.0 | 206.1 |

The homogeneity constraint was developed for a glass compositional region that included PHA. Therefore, the predictability of phase separation by this model should be correct. A significant search for phase separation in these glasses is beyond the scope of work for this task, except when routine SEM analysis is performed. For these six glasses one SEM analysis was performed for glass pha12. No apparent phase separation was observed using this procedure.

However, detection of phase separation is not straight forward. Absence of detection of phase separation by SEM does not imply absence of phase separation. The scale and contrast may be such that other techniques such as SAXS or TEM are required to definitively identify phase separation. In addition, no acid etching or other techniques were used in sample preparation for the SEM analysis since this is also outside the scope of this task. In addition, macroscopic phase separation was not investigated. Finally, the effect of kinetics on phase separation (both crystalline and amorphous) for these glasses was not determined since it was beyond the scope of this task.

# CONCLUSIONS

The results presented in this report are for six Phase 1 PHA glasses, each of which was targeted to contain 26 wt% simulated PUREX sludge on an oxide basis. The target PHA and MST concentrations were varied from 7 to 10 to 13 wt % oxides for PHA and at 1.25 and 2.5 wt % oxides of washed MST.

The models currently in DWPF's PCCS were used to predict durability, homogeneity, liquidus, and viscosity for these six glasses. All six glasses were predicted to be phase separated (i.e., outside the property acceptance region for the homogeneity constraint), and consequently prediction of glass durability is precluded with the current DWPF models. If one ignores the homogeneity constraint, the measured durabilities were within the 95% prediction limits of the model. Further efforts are required to resolve this issue on phase separation (inhomogeneity).

The liquidus model predicted acceptable liquidus temperatures for all six glasses. The approximate (bounding) liquidus temperatures that were measured (<900°C) were well below the model predictions. The measured viscosities were below the predictions of the model and therefore, conservative to the upper limit of viscosity. The predictions are not conservative to the lower limit however, with the lowest measured viscosity value of ~30 poise at 1150°C. The 30-poise viscosity value corresponds to the glass with the highest levels of PHA and MST.

All six of these glasses were durable when compared to the EA glass (as determined by the 7-day PCT) and processible (based upon approximate measurements of viscosity and liquidus temperature). Therefore, the results imply that the DWPF would be able to run these six glass formulations at 26 wt % PUREX waste loading. However, the effect of kinetics on phase separation (both crystalline and amorphous) for these glasses was not determined since it was beyond the scope of this task.

Acceptable product quality and processability for these Phase 1 glasses promoted the continuation of the phased approach for this PHA variability study as planned. At least 19 additional glasses have been fabricated and are currently being tested under this task. At the end of this task all results will be combined and a final analysis performed.

# REFERENCES

[1] Elder, H. H., "Technical Task Request: DWPF Waste Qualification – DWPF Coupled Operation Chemistry," HLW-SDT-TTR-99-07.0, February 2, 1999.

[2] Harbour, J. R. and T. B. Edwards, "Technical Task and QA Plan: DWPF Coupled Operation Chemistry – PHA Glass Testing," WSRC-RP-99-00218, Revision 1, April 23, 1999.

[3] ASTM C1285-94, "Standard Test Methods for Determining Chemical Durability of Nuclear Waste Glasses: The Product Consistency Test (PCT)," 1994.

[4] Edwards, T. B., J. R. Harbour, and R. J. Workman, "Composition and Property Measurements for CST Phase 1 Glasses (U)," WSRC-TR-99-00245, Revision 0, July 27, 1999.

[5] Harbour, J. R. and T. B. Edwards, "Analytical Study Plan-PHA: DWPF Coupled Operation Chemistry – PHA Glass Testing," WSRC-RP-99-00315, Revision 0, April 14, 1999.

[6] Jantzen, C. M., J. B. Pickett, K. G. Brown, T. B. Edwards, and D. C. Beam, "Process/Product Models for the Defense Waste Processing Facility (DWPF): Part I. Predicting Glass Durability from Composition Using a Thermodynamic Hydration Energy Reaction Model (THERMO) (U)," WSRC-TR-93-672, Rev. 1, September 28, 1995.

[7] Schumacher, R. F. and D. K. Peeler, "Establishment of Harrop, High-Temperature Viscometer," WSRC-RP-98-00737, Revision 0, September 1998.

[8] Schumacher, R. F., R. J. Workman, J. R. Harbour, and T. B. Edwards, "Measurements of DWPF Glass Viscosity – Interim Report," WSRC-RP-99-00350, Revision 0, May 5, 1999.

[9] Cicero, C. A., S. L. Marra, and M. K. Andrews, "Phase Stability Determinations of DWPF Waste Glasses (U)," WSRC-TR-93-227, Revision 0, 1993.

[10] Brown, K. G. and R. L. Postles, "SME Accepability Determination for DWPF Processs Control (U)," WSRC-TR-95-0364, Revision 3, February 21, 1996.

# APPENDIX A.

## Supplemental Tables and Exhibits

**This page intentionally left blank.**

## Table A.1: Composition Measurements (expressed as cation wt%'s)

| Planning | Sample | Peroxide Fusion Dissolution | | | | | | Microwave Dissolution | | | | | | Microwave Dissolution | | | | | | | | | | | | |
|---|---|---|---|---|---|---|---|---|---|---|---|---|---|---|---|---|---|---|---|---|---|---|---|---|---|---|
| Glass ID | Glass ID | Block | Seq | Lab ID | B | Si | Ca | Block | Seq | Lab ID | Na | Li | K | Block | Seq | Lab ID | Ni | Fe | Mn | Cr | Mg | Cu | Ti | Zr | Al | U |
| pha11 | pha09 | 1 | 3 | n10pf11 | 2.72 | 22.1 | 0.878 | 1 | 25 | n10mw11 | 6.51 | 1.91 | 4.520 | 1 | 7 | n10mw1 | 0.674 | 6.85 | 1.53 | 0.084 | 0.761 | 0.595 | 0.436 | 0.095 | 1.46 | 2.17 |
| pha11 | pha09 | 2 | 20 | n10pf12 | 2.95 | 22 | 0.826 | 2 | 3 | n10mw12 | 6.11 | 1.84 | 4.380 | 2 | 17 | n10mw12 | 0.680 | 7.30 | 1.46 | 0.073 | 0.771 | 0.619 | 0.423 | 0.099 | 1.40 | 2.14 |
| pha11 | pha09 | 1 | 14 | n10pf21 | 2.22 | 19.1 | 0.861 | 1 | 3 | n10mw21 | 6.40 | 1.96 | 4.430 | 1 | 28 | n10mw21 | 0.639 | 6.47 | 1.45 | 0.078 | 0.763 | 0.592 | 0.409 | 0.093 | 1.46 | 2.15 |
| pha11 | pha09 | 2 | 5 | n10pf22 | 2.93 | 21.7 | 0.778 | 2 | 23 | n10mw22 | 5.83 | 1.79 | 4.250 | 2 | 10 | n10mw22 | 0.701 | 7.22 | 1.46 | 0.074 | 0.774 | 0.625 | 0.427 | 0.103 | 1.41 | 2.24 |
| pha09 | pha08 | 1 | 11 | n11pf11 | 2.23 | 20.1 | 0.858 | 1 | 28 | n11mw11 | 6.34 | 1.93 | 3.620 | 1 | 9 | n11mw11 | 0.701 | 7.43 | 1.51 | 0.082 | 0.798 | 0.566 | 0.426 | 0.091 | 1.49 | 1.81 |
| pha09 | pha08 | 2 | 3 | n11pf12 | 2.56 | 22.2 | 0.785 | 2 | 12 | n11mw12 | 6.00 | 1.87 | 3.630 | 2 | 26 | n11mw12 | 0.658 | 7.45 | 1.38 | 0.071 | 0.803 | 0.549 | 0.396 | 0.092 | 1.38 | 1.79 |
| pha09 | pha08 | 1 | 13 | n11pf21 | 2.21 | 19.7 | 0.857 | 1 | 23 | n11mw21 | 6.60 | 1.98 | 3.700 | 1 | 4 | n11mw21 | 0.694 | 7.27 | 1.53 | 0.082 | 0.848 | 0.565 | 0.443 | 0.094 | 1.44 | 1.86 |
| pha09 | pha08 | 2 | 25 | n11pf22 | 2.58 | 21.5 | 0.875 | 2 | 26 | n11mw22 | 5.96 | 1.80 | 3.500 | 2 | 20 | n11mw22 | 0.653 | 7.58 | 1.39 | 0.073 | 0.761 | 0.536 | 0.410 | 0.095 | 1.43 | 1.87 |
| pha10 | pha11 | 1b | 14 | n3pf11 | 2.48 | 21.9 | 0.899 | 1 | 7 | n3mw11 | 6.53 | 1.95 | 3.630 | 1 | 22 | n3mw11 | 0.660 | 6.52 | 1.42 | 0.084 | 0.740 | 0.531 | 0.784 | 0.085 | 1.38 | 2.02 |
| pha10 | pha11 | 2 | 21 | n3pf12 | 2.91 | 22.7 | 0.766 | 2 | 19 | n3mw12 | 5.98 | 1.81 | 3.410 | 2 | 15 | n3mw12 | 0.682 | 6.94 | 1.42 | 0.074 | 0.784 | 0.544 | 0.763 | 0.091 | 1.41 | 2.11 |
| pha10 | pha11 | 1b | 5 | n3pf21 | 2.76 | 22.5 | 0.854 | 1 | 14 | n3mw21 | 6.34 | 1.98 | 3.520 | 1 | 17 | n3mw21 | 0.680 | 6.80 | 1.46 | 0.083 | 0.774 | 0.546 | 0.836 | 0.090 | 1.44 | 2.06 |
| pha10 | pha11 | 2 | 17 | n3pf22 | 2.82 | 23.3 | 0.796 | 2 | 5 | n3mw22 | 6.17 | 1.86 | 3.570 | 2 | 9 | n3mw22 | 0.686 | 7.38 | 1.40 | 0.078 | 0.801 | 0.540 | 0.823 | 0.094 | 1.41 | 2.16 |
| pha12 | pha12 | 1 | 6 | n5pf11 | 2.90 | 21.3 | 0.848 | 1 | 2 | n5mw11 | 6.60 | 1.87 | 4.730 | 1 | 25 | n5mw11 | 0.654 | 6.60 | 1.43 | 0.079 | 0.735 | 0.643 | 0.798 | 0.088 | 1.44 | 2.08 |
| pha12 | pha12 | 2 | 13 | n5pf12 | 2.93 | 20.8 | 0.808 | 2 | 10 | n5mw12 | 6.12 | 1.76 | 4.500 | 2 | 25 | n5mw12 | 0.701 | 7.54 | 1.35 | 0.071 | 0.745 | 0.656 | 0.799 | 0.092 | 1.40 | 2.05 |
| pha12 | pha12 | 1b | 9 | n5pf21 | 2.90 | 21.3 | 0.821 | 1 | 10 | n5mw21 | 6.49 | 1.91 | 4.660 | 1 | 18 | n5mw21 | 0.675 | 6.96 | 1.48 | 0.082 | 0.740 | 0.657 | 0.830 | 0.086 | 1.33 | 2.04 |
| pha12 | pha12 | 2 | 10 | n5pf22 | 3.27 | 22.9 | 0.795 | 2 | 18 | n5mw22 | 6.14 | 1.76 | 4.420 | 2 | 18 | n5mw22 | 0.640 | 7.84 | 1.43 | 0.073 | 0.748 | 0.658 | 0.810 | 0.094 | 1.39 | 2.16 |
| pha08 | pha10 | 1b | 13 | n6pf11 | 2.41 | 23.5 | 0.849 | 1 | 26 | n6mw11 | 6.28 | 1.96 | 2.630 | 1 | 26 | n6mw11 | 0.631 | 6.43 | 1.43 | 0.076 | 0.787 | 0.392 | 0.825 | 0.085 | 1.41 | 2.02 |
| pha08 | pha10 | 2 | 6 | n6pf12 | 2.35 | 21.3 | 0.755 | 2 | 6 | n6mw12 | 6.12 | 2.02 | 2.670 | 2 | 2 | n6mw12 | 0.712 | 7.17 | 1.50 | 0.079 | 0.816 | 0.407 | 0.793 | 0.102 | 1.42 | 2.10 |
| pha08 | pha10 | 1 | 4 | n6pf21 | 2.25 | 23.2 | 0.885 | 1 | 6 | n6mw21 | 6.39 | 2.10 | 2.600 | 1 | 20 | n6mw21 | 0.643 | 6.35 | 1.44 | 0.081 | 0.807 | 0.397 | 0.809 | 0.092 | 1.38 | 1.97 |
| pha08 | pha10 | 2 | 19 | n6pf22 | 2.60 | 24.2 | 0.799 | 2 | 20 | n6mw22 | 5.96 | 1.90 | 2.470 | 2 | 23 | n6mw22 | 0.648 | 7.19 | 1.37 | 0.073 | 0.815 | 0.404 | 0.856 | 0.094 | 1.37 | 2.08 |
| pha07 | pha07 | 1 | 2 | n9pf11 | 2.14 | 23.1 | 0.905 | 1 | 13 | n9mw11 | 6.10 | 2.04 | 2.650 | 1 | 11 | n9mw11 | 0.668 | 6.99 | 1.44 | 0.084 | 0.807 | 0.387 | 0.406 | 0.090 | 1.41 | 2.21 |
| pha07 | pha07 | 2 | 27 | n9pf12 | 2.28 | 22.4 | 0.789 | 2 | 25 | n9mw12 | 5.83 | 1.90 | 2.490 | 2 | 4 | n9mw12 | 0.690 | 7.56 | 1.42 | 0.082 | 0.828 | 0.392 | 0.417 | 0.098 | 1.38 | 2.16 |
| pha07 | pha07 | 1b | 6 | n9pf21 | 2.43 | 22.3 | 0.944 | 1 | 4 | n9mw21 | 6.30 | 2.03 | 2.610 | 1 | 6 | n9mw21 | 0.682 | 6.92 | 1.46 | 0.087 | 0.878 | 0.388 | 0.414 | 0.095 | 1.43 | 2.24 |
| pha07 | pha07 | 2 | 23 | n9pf22 | 2.39 | 21.4 | 0.827 | 2 | 27 | n9mw22 | 5.72 | 1.90 | 2.490 | 2 | 3 | n9mw22 | 0.682 | 7.37 | 1.45 | 0.078 | 0.820 | 0.404 | 0.421 | 0.097 | 1.39 | 2.32 |
| std | std | 1 | 1 | stdpf11 | 2.36 | 21.7 | 1.030 | 1 | 1 | stdmw11 | 7.09 | 2.06 | 2.870 | 1 | 1 | stdmw11 | 0.582 | 8.30 | 1.33 | 0.073 | 0.856 | 0.321 | 0.399 | 0.066 | 2.48 | <1.00 |
| std | std | 1 | 15 | stdpf12 | 2.57 | 24.9 | 0.979 | 1 | 15 | stdmw12 | 7.08 | 2.02 | 2.880 | 1 | 14 | stdmw12 | 0.555 | 8.61 | 1.31 | 0.071 | 0.839 | 0.309 | 0.410 | 0.066 | 2.46 | <1.00 |
| std | std | 1b | 1 | stdpf12B | 2.44 | 23.2 | | 1 | 29 | stdmw13 | 7.13 | 1.96 | 2.780 | 1 | 29 | stdmw13 | 0.544 | 7.62 | 1.24 | 0.068 | 0.776 | 0.295 | 0.396 | 0.063 | 2.46 | <1.00 |
| std | std | 1b | 15 | stdpf13 | 2.25 | 22.5 | 1.020 | 2 | 1 | stdmw21 | 6.64 | 1.98 | 2.750 | 2 | 1 | stdmw21 | 0.600 | 8.69 | 1.31 | 0.070 | 0.864 | 0.305 | 0.423 | 0.073 | 2.59 | <1.00 |
| std | std | 2 | 1 | stdpf21 | 2.50 | 21.6 | 0.956 | 2 | 15 | stdmw22 | 6.59 | 1.87 | 2.640 | 2 | 14 | stdmw22 | 0.564 | 8.91 | 1.27 | 0.065 | 0.833 | 0.310 | 0.401 | 0.072 | 2.51 | <1.00 |
| std | std | 2 | 15 | stdpf22 | 2.50 | 22.3 | 0.923 | 2 | 29 | stdmw23 | 6.37 | 1.81 | 2.720 | 2 | 29 | stdmw23 | 0.553 | 9.05 | 1.25 | 0.064 | 0.841 | 0.290 | 0.413 | 0.069 | 2.38 | <1.00 |
| std | std | 2 | 29 | stdpf23 | 2.34 | 21 | 0.972 | . | . | | | | | . | . | | | | | | | | | | | |
| u-std | u-std | 1 | 8 | ustdpf11 | 2.72 | 19.9 | 1.000 | 1 | 8 | ustdmw11 | 9.32 | 1.35 | 2.540 | 1 | 8 | ustdmw11 | 0.808 | 8.46 | 2.09 | 0.168 | 0.700 | <0.010 | 0.590 | <0.010 | 2.06 | 1.89 |
| u-std | u-std | 1b | 8 | ustdpf12 | 2.92 | 21.7 | 1.040 | 1 | 22 | ustdmw12 | 9.40 | 1.37 | 2.490 | 1 | 21 | ustdmw12 | 0.786 | 8.24 | 2.02 | 0.161 | 0.658 | <0.010 | 0.586 | <0.010 | 1.99 | 1.82 |
| u-std | u-std | 2 | 8 | ustdpf21 | 2.87 | 20.3 | 1.010 | 2 | 8 | ustdmw21 | 8.83 | 1.29 | 2.410 | 2 | 8 | ustdmw21 | 0.852 | 8.83 | 2.02 | 0.160 | 0.673 | 0.011 | 0.603 | 0.010 | 2.04 | 1.98 |
| u-std | u-std | 2 | 22 | ustdpf22 | 2.93 | 19.7 | 0.986 | 2 | 22 | ustdmw22 | 8.53 | 1.25 | 2.410 | 2 | 21 | ustdmw22 | 0.759 | 8.85 | 1.98 | 0.147 | 0.674 | 0.011 | 0.579 | 0.011 | 2.04 | 1.97 |

**Table A.2: Re-Analysis of the First Block of B, Ca, and Si Measurements**

| Planning | Sample | Peroxide Fusion Dissolution | | | | | |
|---|---|---|---|---|---|---|---|
| Glass ID | Glass ID | Block | Seq | Lab ID | B | Si | Ca |
| std | std | 1 | 1 | stdpf11 | 2.59 | 24.1 | 0.910 |
| pha07 | pha07 | 1 | 2 | n9pf11 | 2.50 | 25.6 | 0.811 |
| pha11 | pha09 | 1 | 3 | n10pf11 | 2.82 | 23.2 | 0.745 |
| pha08 | pha10 | 1 | 4 | n6pf21 | 2.41 | 24.8 | 0.798 |
| pha12 | pha12 | 1 | 6 | n5pf11 | 2.90 | 23.4 | 0.813 |
| u-std | u-std | 1 | 8 | ustdpf11 | 2.86 | 23.3 | 0.980 |
| pha09 | pha08 | 1 | 11 | n11pf11 | 3.09 | 25.2 | 0.790 |
| pha09 | pha08 | 1 | 13 | n11pf21 | 2.66 | 24.6 | 0.778 |
| pha11 | pha09 | 1 | 14 | n10pf21 | 2.99 | 23 | 0.793 |
| std | std | 1 | 15 | stdpf12 | 2.59 | 25.1 | 0.898 |
| pha10 | pha11 | 1 | 19 | n3pf21 | 2.65 | 24.6 | 0.752 |
| pha07 | pha07 | 1 | 20 | n9pf21 | 2.38 | 24.6 | 0.772 |
| u-std | u-std | 1 | 22 | ustdpf12 | 2.98 | 23.4 | 0.965 |
| pha12 | pha12 | 1 | 23 | n5pf21 | 2.98 | 23.9 | 0.769 |
| pha08 | pha10 | 1 | 27 | n6pf11 | 2.56 | 25.7 | 0.819 |
| pha10 | pha11 | 1 | 28 | n3pf11 | 2.76 | 25.2 | 0.836 |
| std | std | 1 | 29 | stdpf13 | 2.53 | 24.6 | 0.912 |

## Table A.3: Composition of PCT Leachate Solutions

| Original Sample ID | Planning Sample ID | Lab ID | Seq | Concentrations in ppm (as reported) B | Si | Na | Li | Concentrations in ppm (after correcting for dilution) B | Si | Na | Li | Common Logarithm of ppm Concentrations log[B] | log[Si] | log[Na] | log[Li] |
|---|---|---|---|---|---|---|---|---|---|---|---|---|---|---|---|
| std | *std* | std | 1 | 20.5 | 53 | 86.6 | 10.1 | 20.50 | 53.00 | 86.60 | 10.10 | 1.3118 | 1.7243 | 1.9375 | 1.0043 |
| pha09 | *pha11* | v13 | 3 | 21.8 | 80.1 | 44.8 | 14.6 | 36.33 | 133.50 | 74.67 | 24.33 | 1.5603 | 2.1255 | 1.8731 | 1.3862 |
| pha08 | *pha09* | v14 | 4 | 16.5 | 79.5 | 39.2 | 12.7 | 27.50 | 132.50 | 65.33 | 21.17 | 1.4393 | 2.1222 | 1.8151 | 1.3257 |
| pha09 | *pha11* | v47 | 5 | 21.8 | 79.2 | 45.2 | 14.8 | 36.33 | 132.00 | 75.33 | 24.67 | 1.5603 | 2.1206 | 1.8770 | 1.3921 |
| pha12 | *pha12* | v05 | 6 | 26.6 | 82.1 | 52.4 | 16.1 | 44.33 | 136.84 | 87.34 | 26.83 | 1.6467 | 2.1362 | 1.9412 | 1.4287 |
| ARM | *ARM* | v34 | 7 | 12.3 | 40.1 | 24.7 | 9.6 | 20.50 | 66.83 | 41.17 | 16.00 | 1.3118 | 1.8250 | 1.6146 | 1.2041 |
| blank | *blank* | v25 | 9 | 0.25 | <0.180 | <0.530 | 0.028 | 0.42 | 0.15 | 0.44 | 0.05 | -0.3802 | -0.8239 | -0.3549 | -1.3310 |
| pha10 | *pha08* | v07 | 10 | 13.1 | 78.1 | 32.2 | 12.2 | 21.83 | 130.17 | 53.67 | 20.33 | 1.3391 | 2.1145 | 1.7297 | 1.3082 |
| pha09 | *pha11* | v15 | 13 | 20.6 | 77.2 | 43.8 | 14.4 | 34.33 | 128.67 | 73.00 | 24.00 | 1.5357 | 2.1095 | 1.8633 | 1.3802 |
| ARM | *ARM* | v55 | 15 | 12.6 | 39.6 | 26.4 | 9.56 | 21.00 | 66.00 | 44.00 | 15.93 | 1.3222 | 1.8196 | 1.6435 | 1.2023 |
| EA | *EA* | v48 | 16 | 387 | 593 | 1090 | 121 | 645.01 | 988.35 | 1816.70 | 201.67 | 2.8096 | 2.9949 | 3.2593 | 2.3046 |
| pha07 | *pha07* | v62 | 17 | 13.9 | 75.3 | 32.1 | 12.6 | 23.17 | 125.50 | 53.50 | 21.00 | 1.3649 | 2.0987 | 1.7284 | 1.3222 |
| ARM | *ARM* | v45 | 19 | 13 | 41.9 | 25.7 | 9.71 | 21.67 | 69.83 | 42.83 | 16.18 | 1.3358 | 1.8441 | 1.6318 | 1.2091 |
| pha07 | *pha07* | v27 | 21 | 13 | 75.1 | 30.9 | 11.7 | 21.67 | 125.17 | 51.50 | 19.50 | 1.3358 | 2.0975 | 1.7118 | 1.2900 |
| pha11 | *pha10* | v59 | 23 | 18.4 | 78.4 | 41.4 | 14 | 30.67 | 130.67 | 69.00 | 23.33 | 1.4867 | 2.1162 | 1.8389 | 1.3680 |
| std | *std* | std | 24 | 21 | 51.1 | 86 | 10.3 | 21.00 | 51.10 | 86.00 | 10.30 | 1.3222 | 1.7084 | 1.9345 | 1.0128 |
| pha11 | *pha10* | v22 | 25 | 17.8 | 79.7 | 39.6 | 13.7 | 29.67 | 132.84 | 66.00 | 22.83 | 1.4723 | 2.1233 | 1.8196 | 1.3586 |
| EA | *EA* | v26 | 27 | 359 | 556 | 1080 | 120 | 598.35 | 926.69 | 1800.04 | 200.00 | 2.7770 | 2.9669 | 3.2553 | 2.3010 |
| pha12 | *pha12* | v24 | 29 | 25.8 | 84.3 | 50.6 | 15.9 | 43.00 | 140.50 | 84.34 | 26.50 | 1.6335 | 2.1477 | 1.9260 | 1.4233 |
| pha11 | *pha10* | v43 | 30 | 18.4 | 78.3 | 40.3 | 13.7 | 30.67 | 130.50 | 67.17 | 22.83 | 1.4867 | 2.1156 | 1.8272 | 1.3586 |
| pha08 | *pha09* | v39 | 31 | 17 | 76.6 | 37.4 | 12.9 | 28.33 | 127.67 | 62.33 | 21.50 | 1.4523 | 2.1061 | 1.7947 | 1.3324 |
| pha10 | *pha08* | v29 | 33 | 13.8 | 77.2 | 32.8 | 12.3 | 23.00 | 128.67 | 54.67 | 20.50 | 1.3617 | 2.1095 | 1.7377 | 1.3118 |
| pha12 | *pha12* | v35 | 35 | 29 | 88.9 | 55.8 | 17.5 | 48.33 | 148.17 | 93.00 | 29.17 | 1.6843 | 2.1708 | 1.9685 | 1.4649 |
| blank | *blank* | v60 | 37 | 0.414 | <0.180 | <0.530 | 0.04 | 0.69 | 0.15 | 0.44 | 0.07 | -0.1611 | -0.8239 | -0.3549 | -1.1761 |
| pha10 | *pha08* | v20 | 39 | 13.3 | 75.5 | 32.6 | 12.2 | 22.17 | 125.84 | 54.33 | 20.33 | 1.3457 | 2.0998 | 1.7351 | 1.3082 |
| pha08 | *pha09* | v65 | 40 | 16.6 | 77.6 | 37 | 12.7 | 27.67 | 129.34 | 61.67 | 21.17 | 1.4420 | 2.1117 | 1.7901 | 1.3257 |
| EA | *EA* | v46 | 42 | 374 | 559 | 1050 | 115 | 623.35 | 931.69 | 1750.04 | 191.67 | 2.7947 | 2.9693 | 3.2430 | 2.2826 |
| pha07 | *pha07* | v17 | 46 | 13.8 | 77.2 | 30.4 | 11.9 | 23.00 | 128.67 | 50.67 | 19.83 | 1.3617 | 2.1095 | 1.7047 | 1.2974 |
| std | *std* | std | 47 | 20.6 | 50 | 83.8 | 10.1 | 20.60 | 50.00 | 83.80 | 10.10 | 1.3139 | 1.6990 | 1.9232 | 1.0043 |

**Notes:**

(1). Values that are below detection (indicated by a "<") were converted to ½ the detection limit.

(2) Although somewhat confusing, two sample id columns are provided in this table. The planning sample id was used to label the samples for use by the SRTC-ML. These sample id's were different (unintentionally) from the original sample id's. References to and analyses of these data will be identified using the original sample id's.

**Exhibit A.1: Measurements by Glass Sample ID by Oxide**

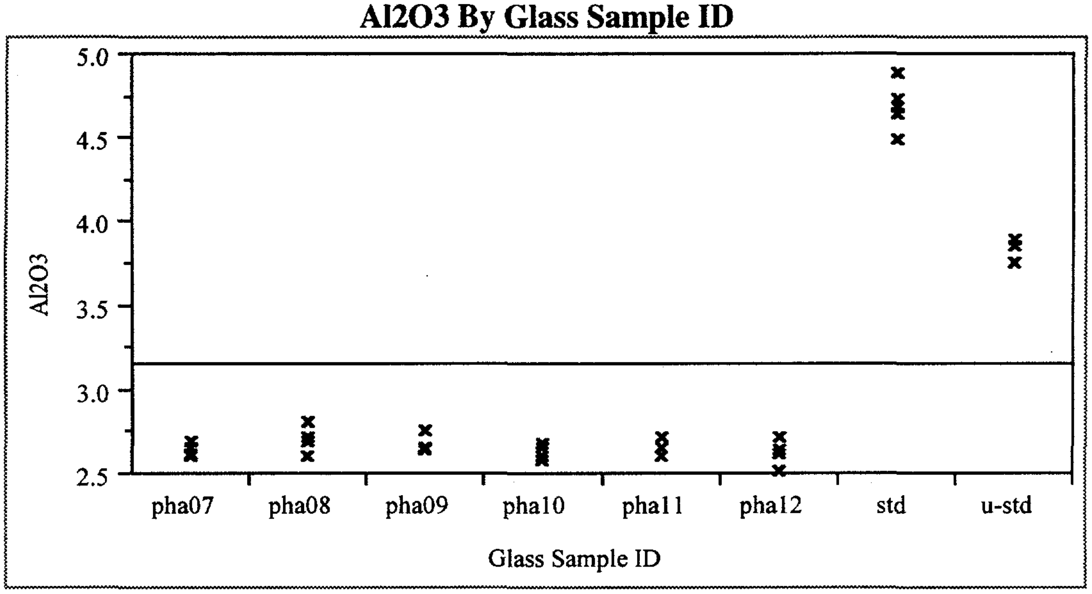


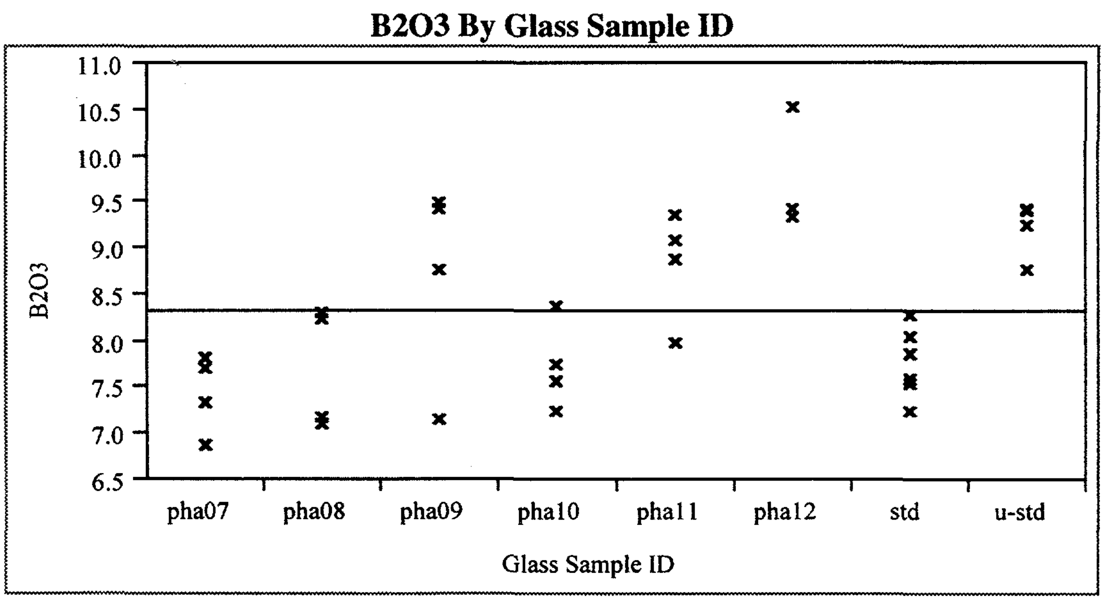

**Exhibit A.1: Measurements by Glass Sample ID by Oxide**
**(continued)**

**CaO By Glass Sample ID**

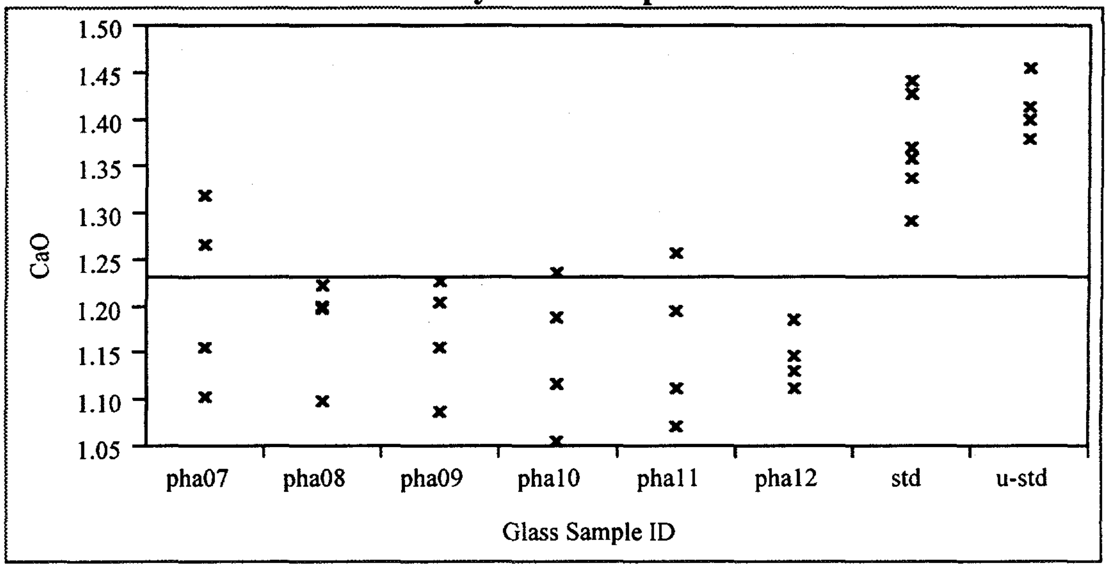


**Cr2O3 By Glass Sample ID**

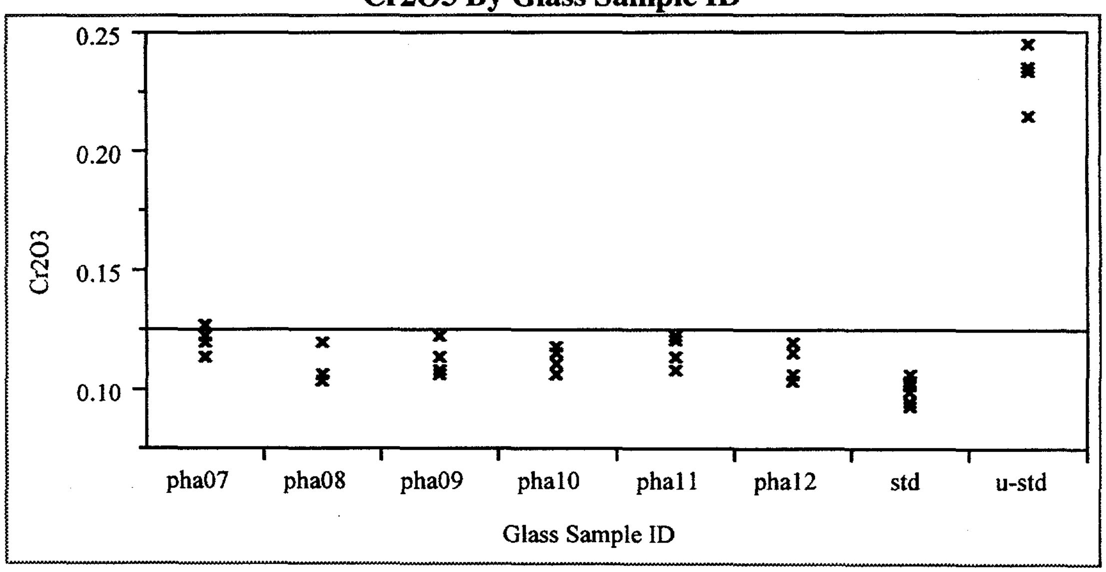

**Exhibit A.1: Measurements by Glass Sample ID by Oxide**
**(continued)**

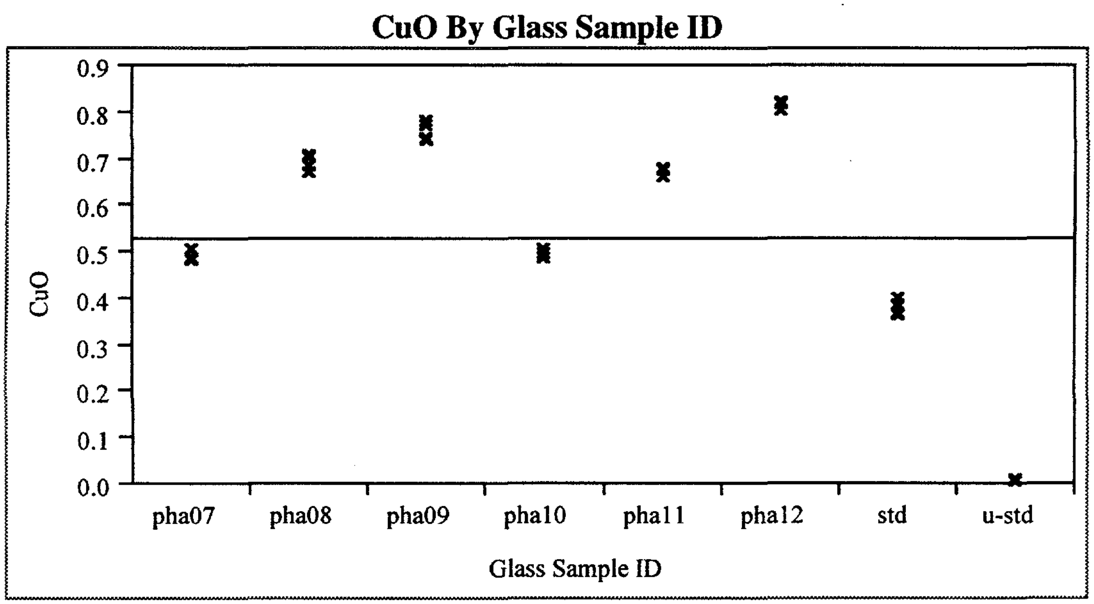


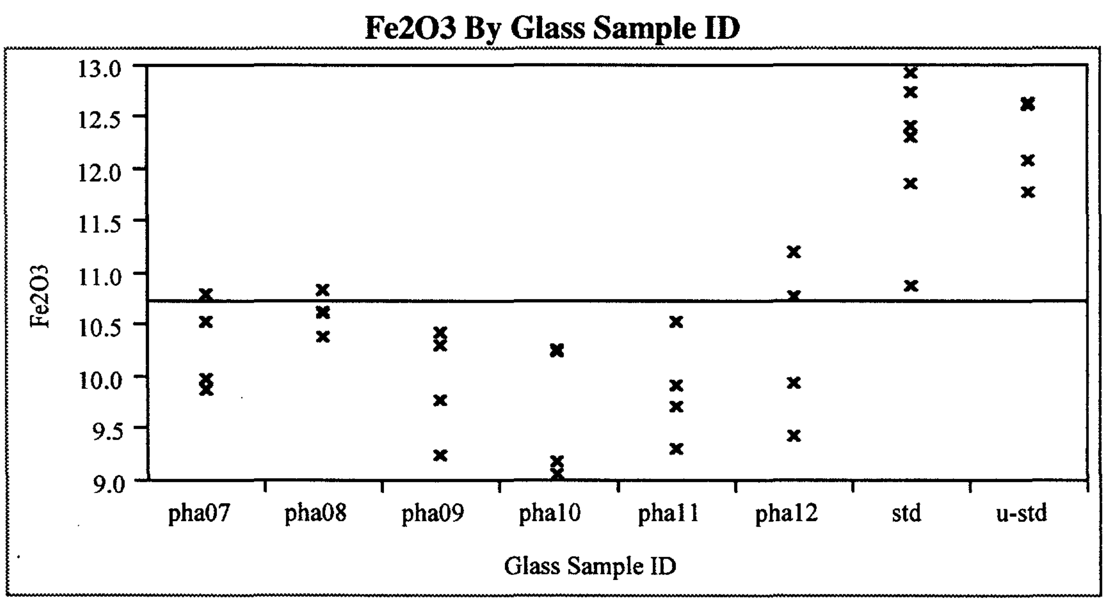

**Exhibit A.1: Measurements by Glass Sample ID by Oxide**
**(continued)**

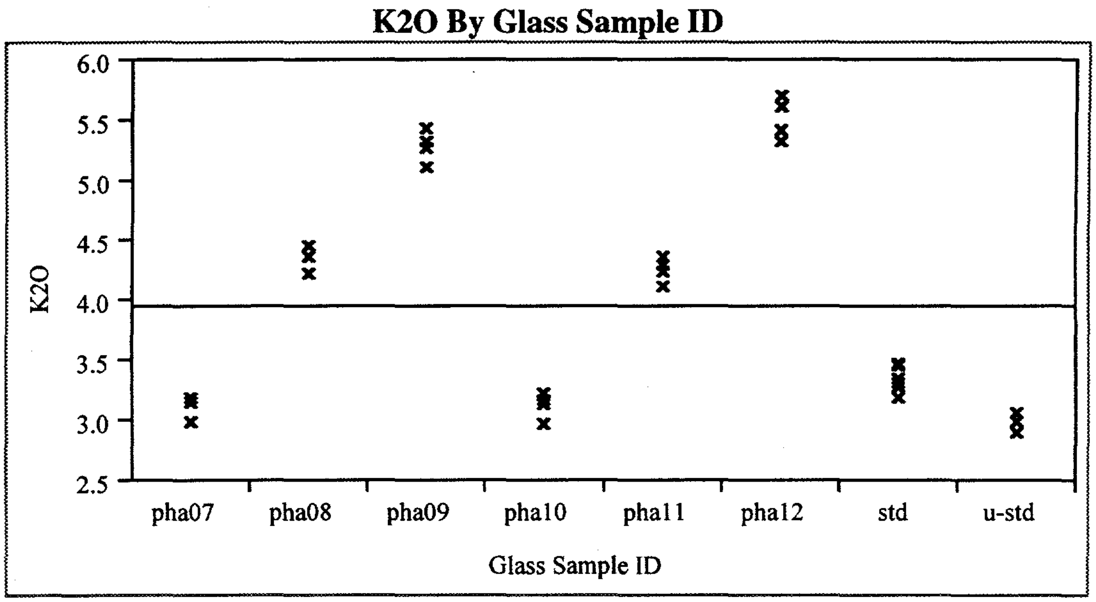


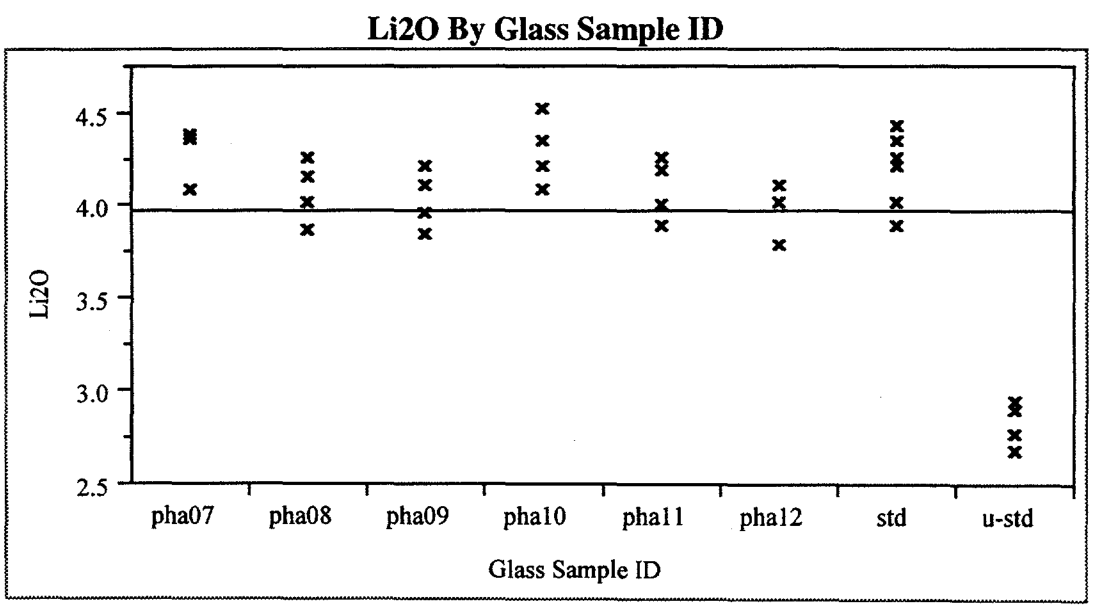

**Exhibit A.1: Measurements by Glass Sample ID by Oxide**
**(continued)**

## MgO By Glass Sample ID

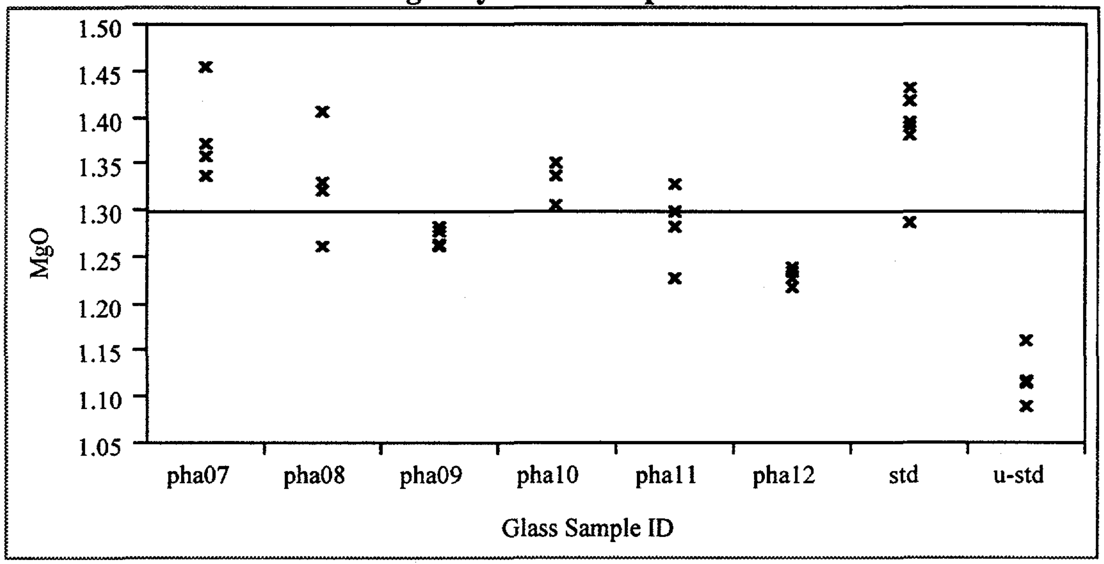


## MnO By Glass Sample ID

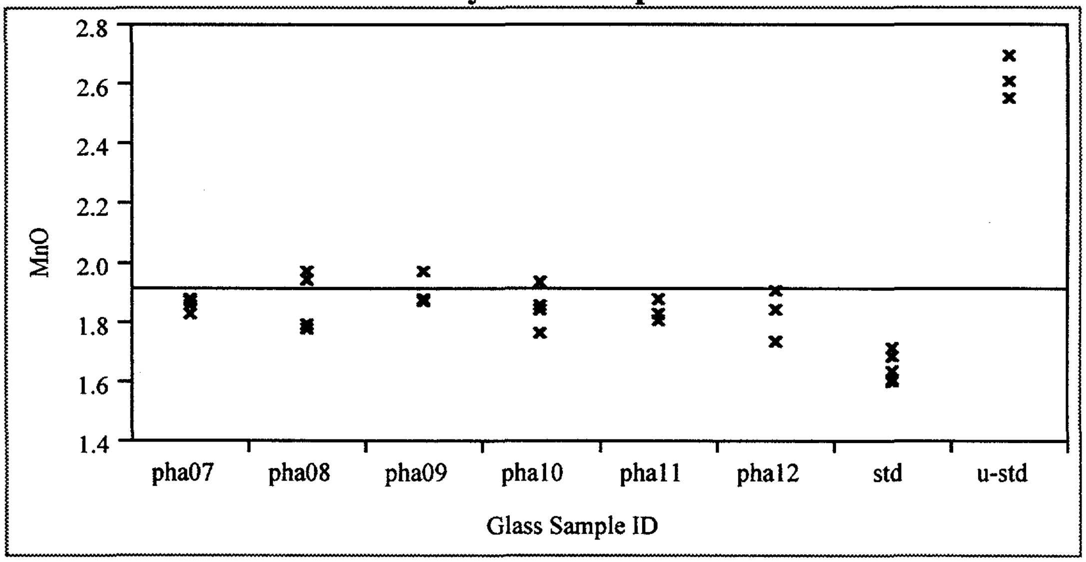

**Exhibit A.1: Measurements by Glass Sample ID by Oxide**
**(continued)**

## Na2O By Glass Sample ID

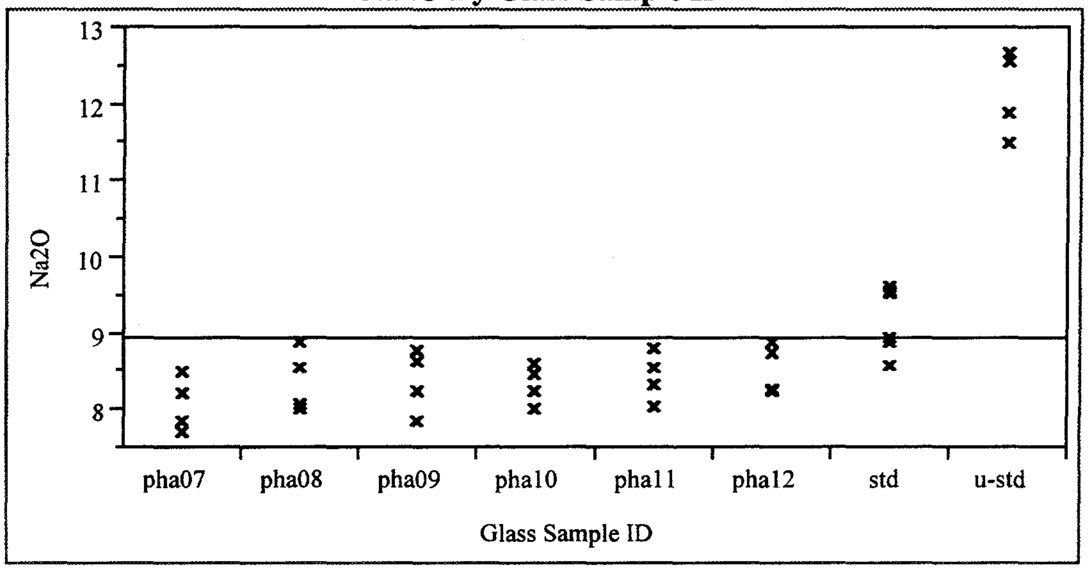


## Nb2O5 By Glass Sample ID

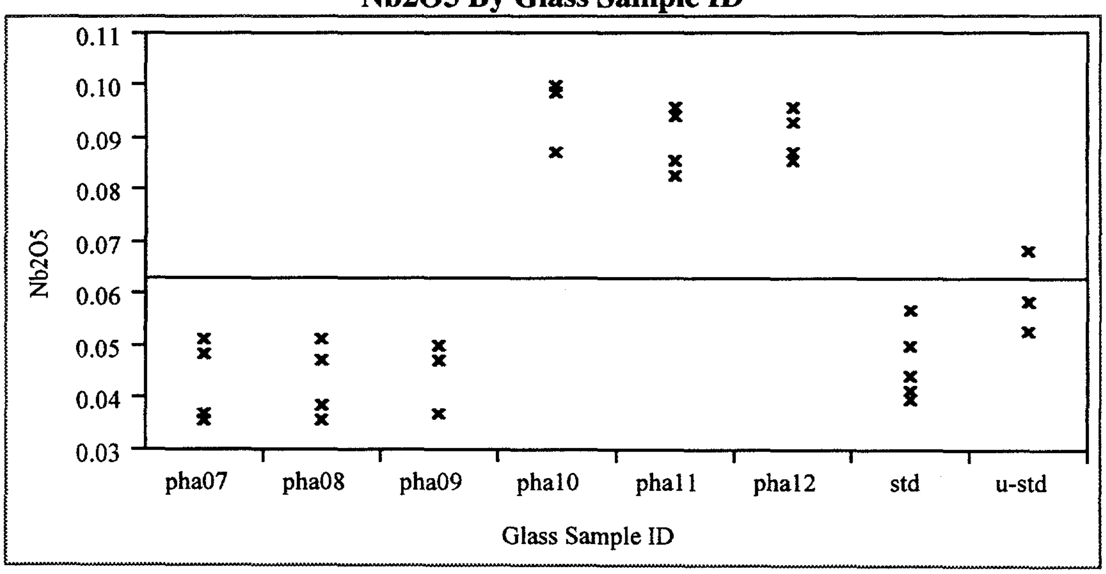

**Exhibit A.1: Measurements by Glass Sample ID by Oxide**
**(continued)**

## NiO By Glass Sample ID

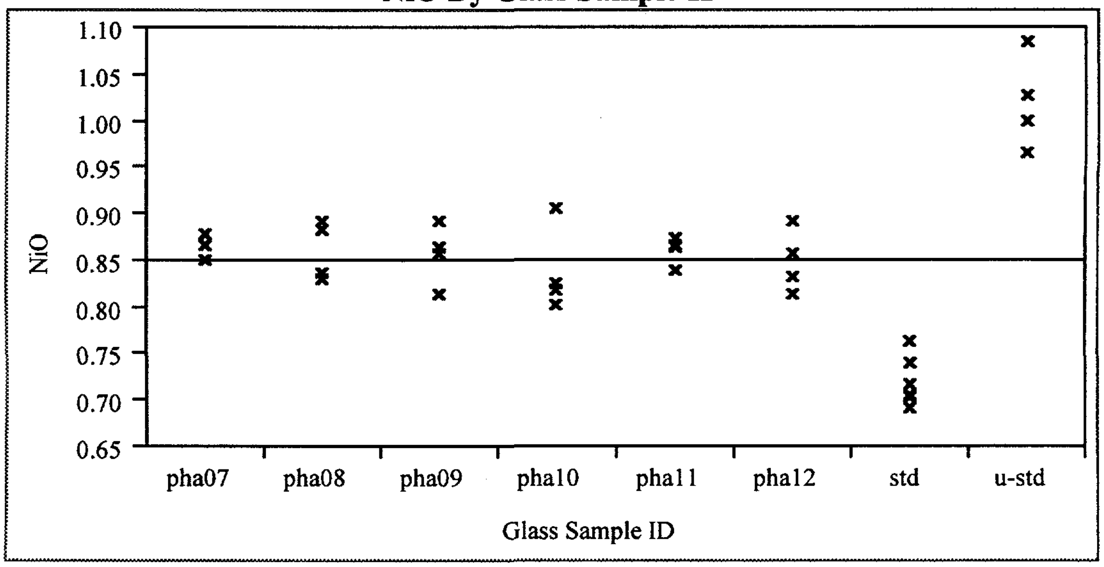


## SiO2 By Glass Sample ID

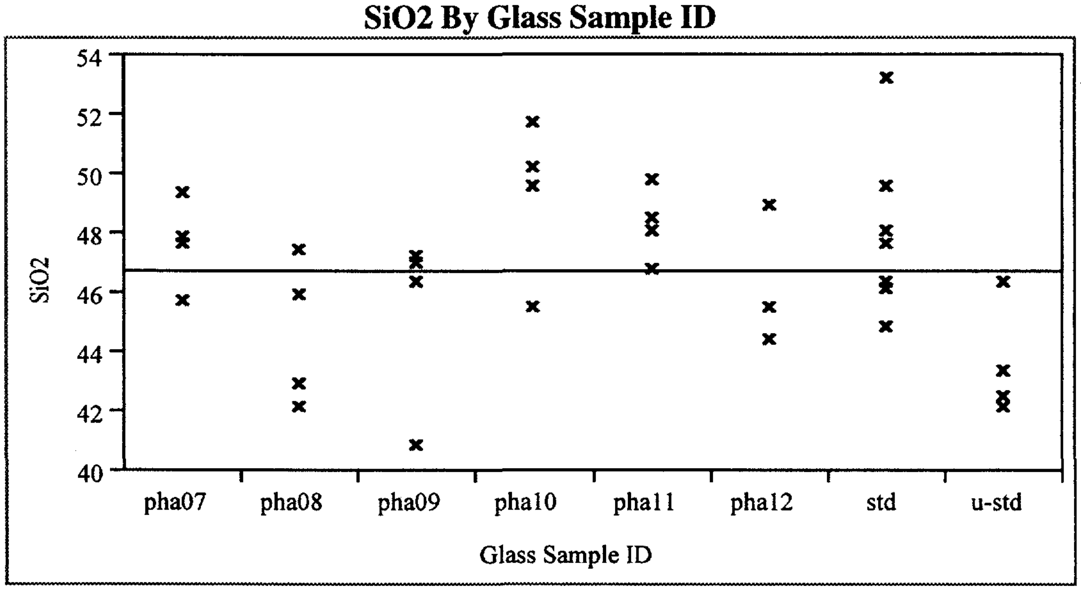

**Exhibit A.1: Measurements by Glass Sample ID by Oxide**
**(continued)**

## TiO2 By Glass Sample ID

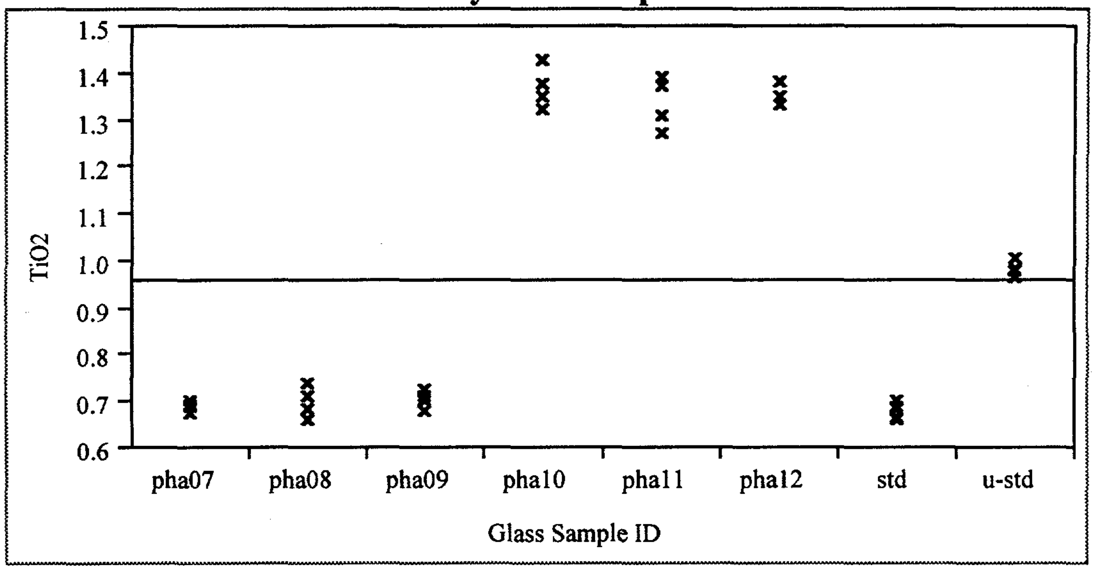


## U3O8 By Glass Sample ID

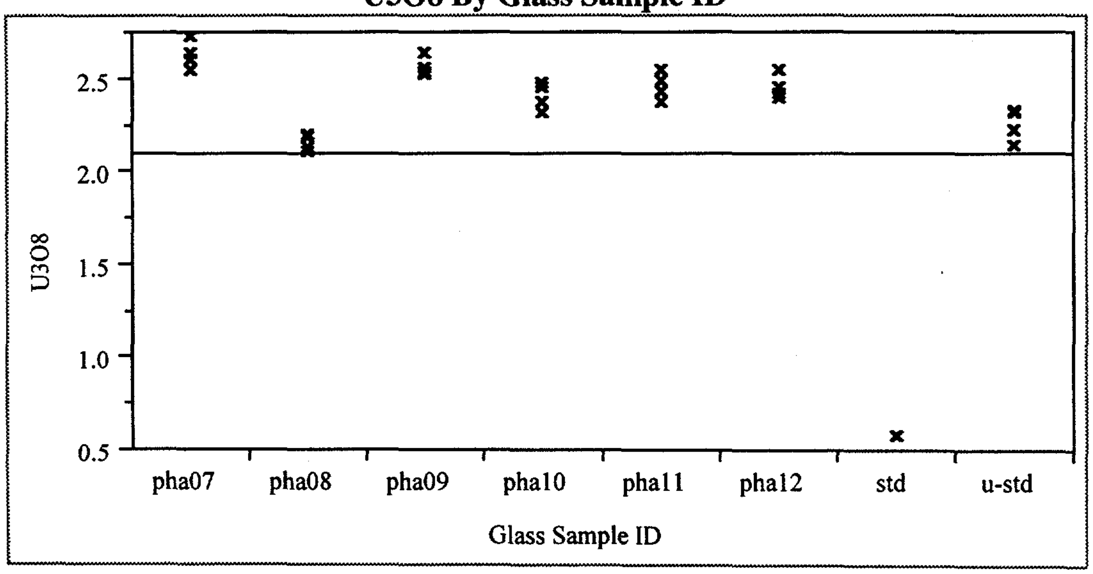

**Exhibit A.1: Measurements by Glass Sample ID by Oxide**
**(continued)**

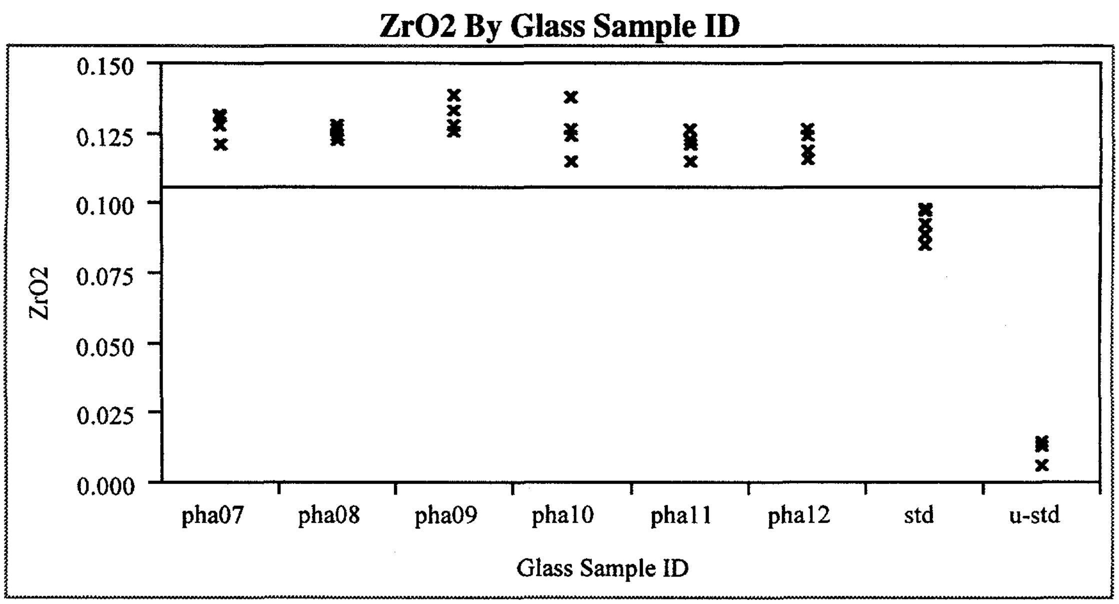


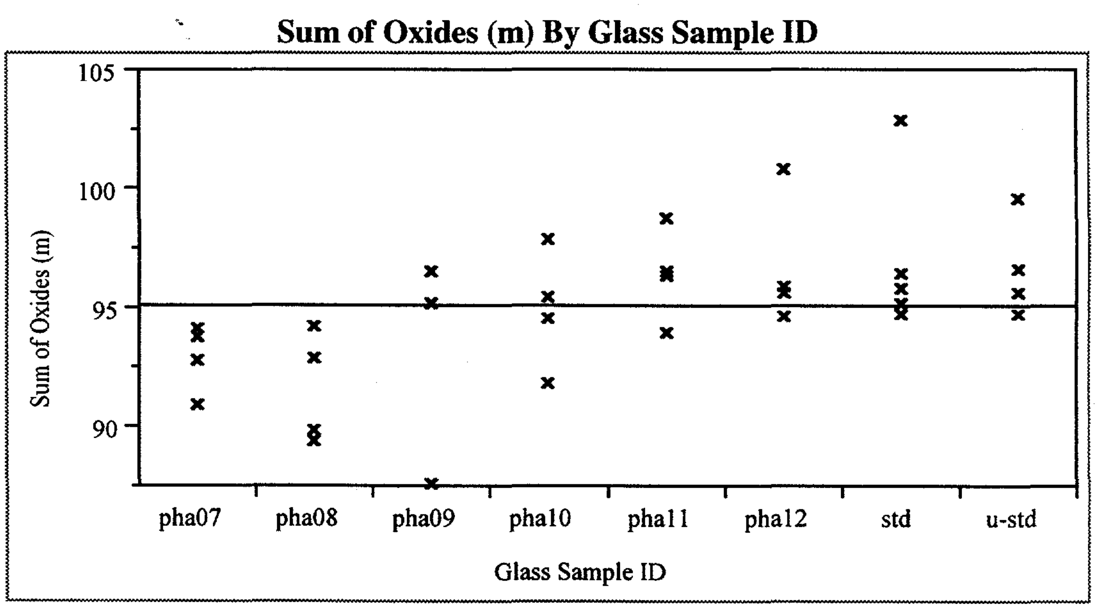

**Exhibit A.2: Second Set of Block 1 B, Ca, and Si Measurements by Glass Sample ID**

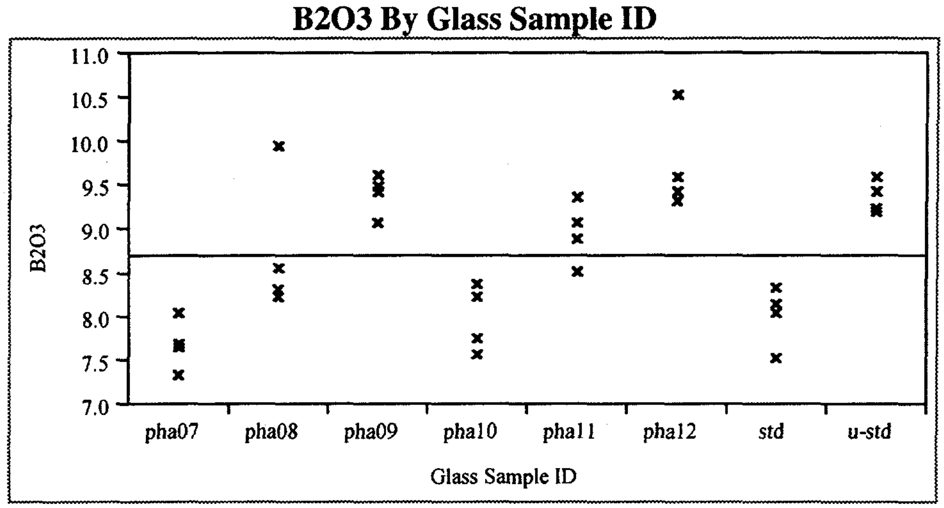


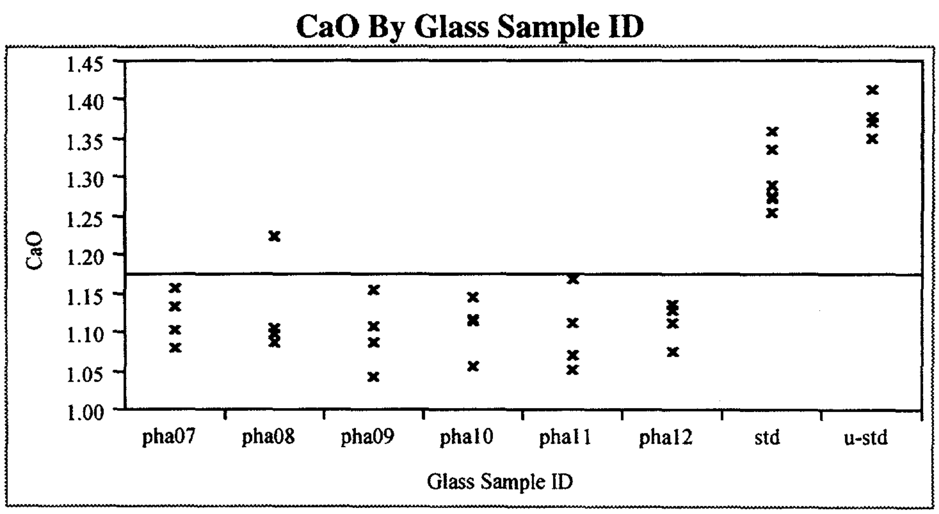


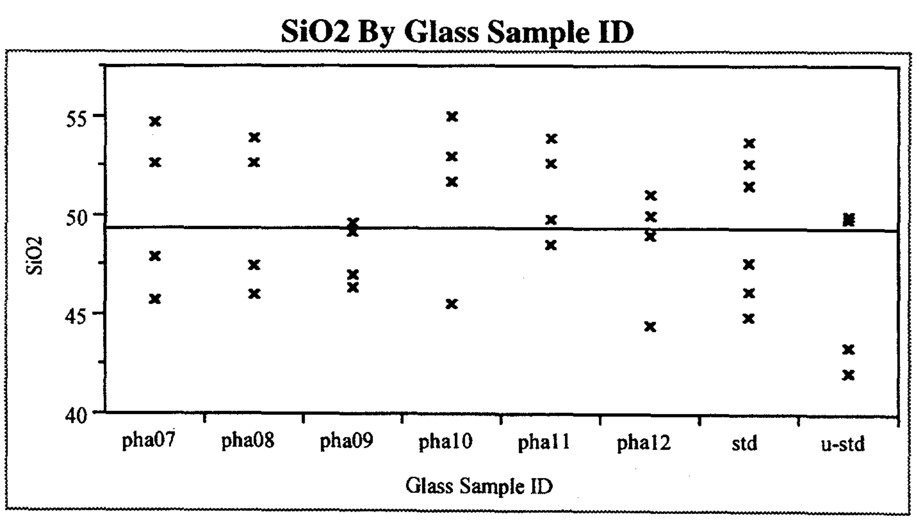

**Exhibit A.3: Measurements of Glass Standards by Oxide**
(+ u-std; small square Batch 1 standard)

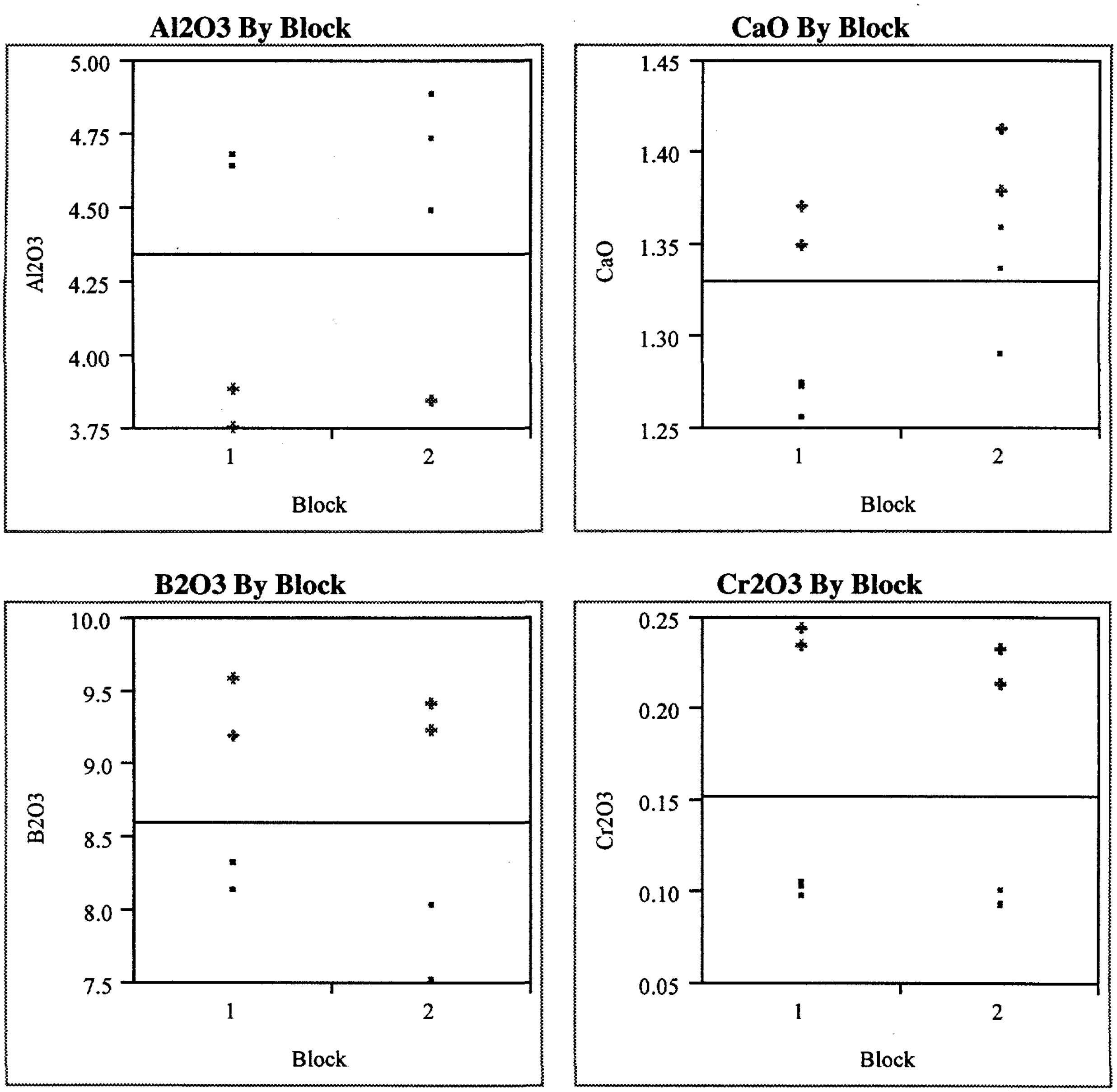

**Exhibit A.3: Measurements of Glass Standards by Oxide**

(+ u-std; small square Batch 1 standard)

(continued)

**CuO By Block**

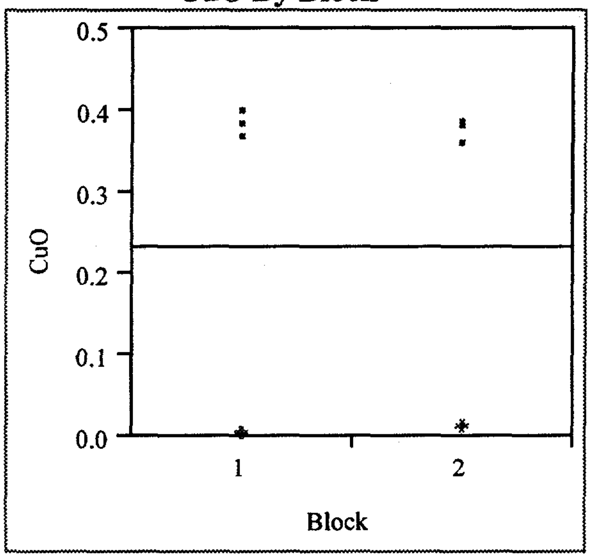


**K2O By Block**

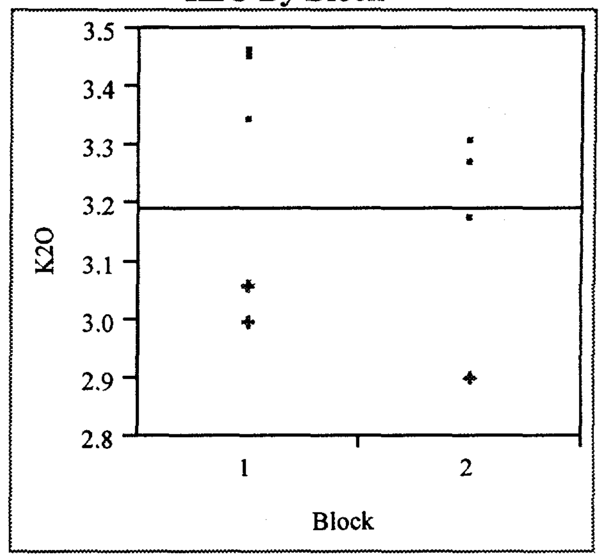


**Fe2O3 By Block**

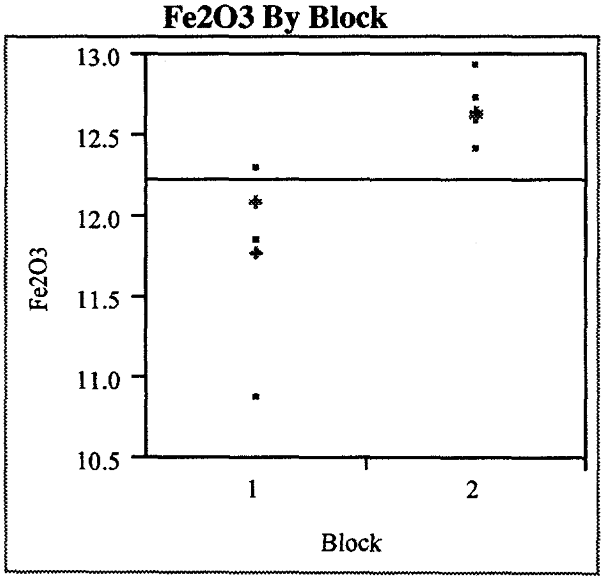


**Li2O By Block**

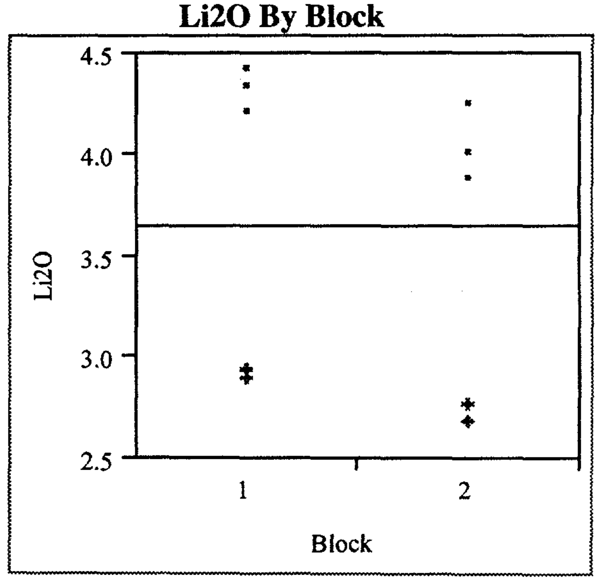

**Exhibit A.3: Measurements of Glass Standards by Oxide**
(+ u-std; small square Batch 1 standard)
(continued)

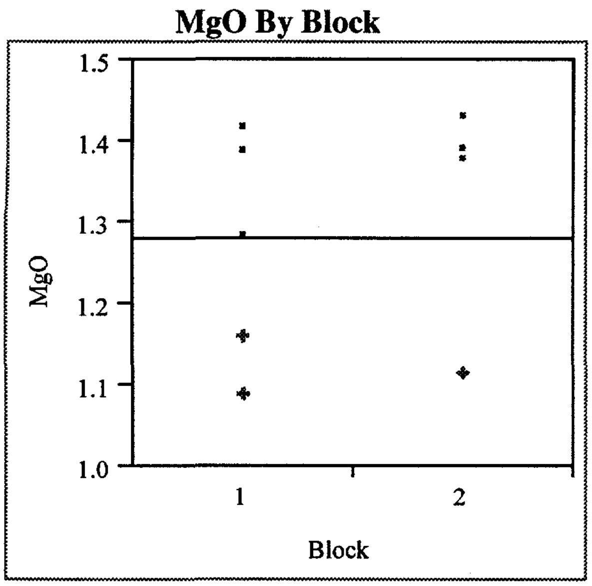


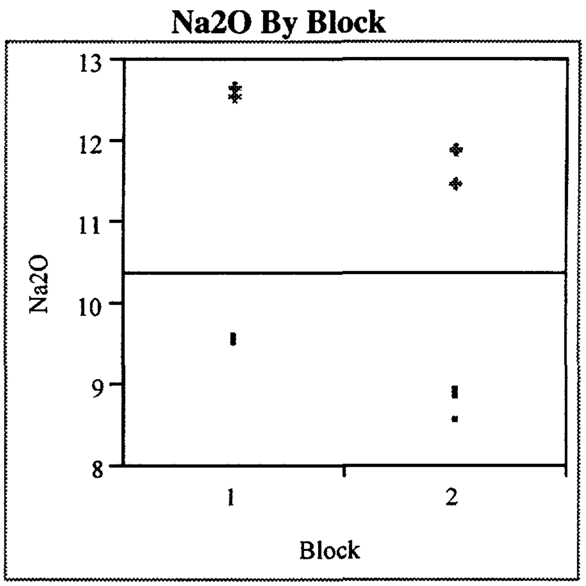


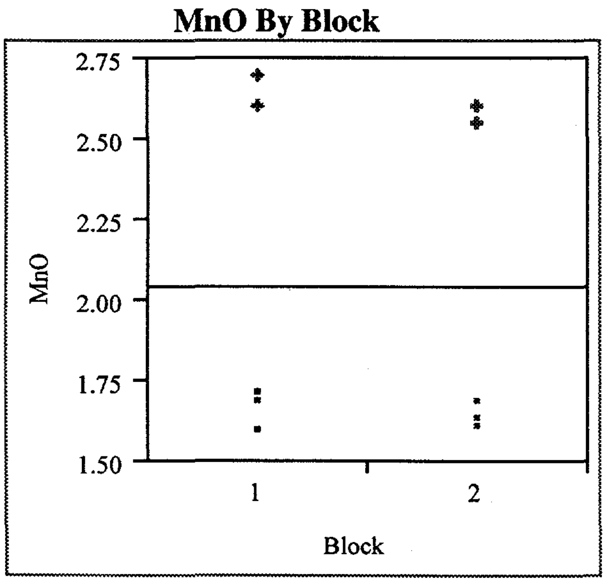


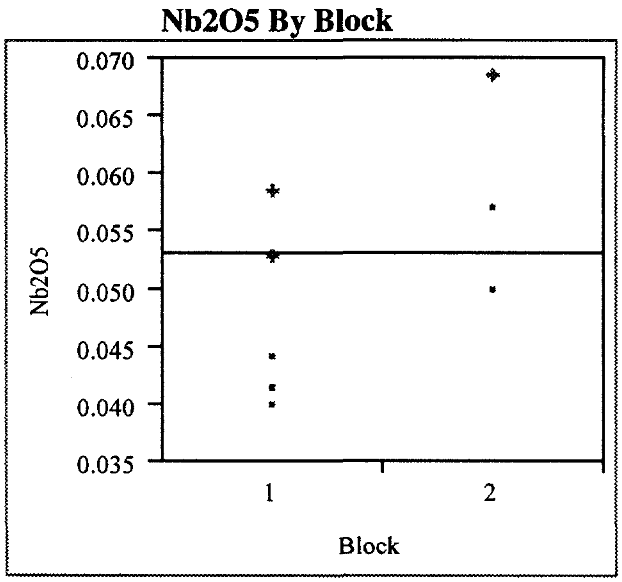

**Exhibit A.3: Measurements of Glass Standards by Oxide**

(+ u-std; small square Batch 1 standard)

(continued)

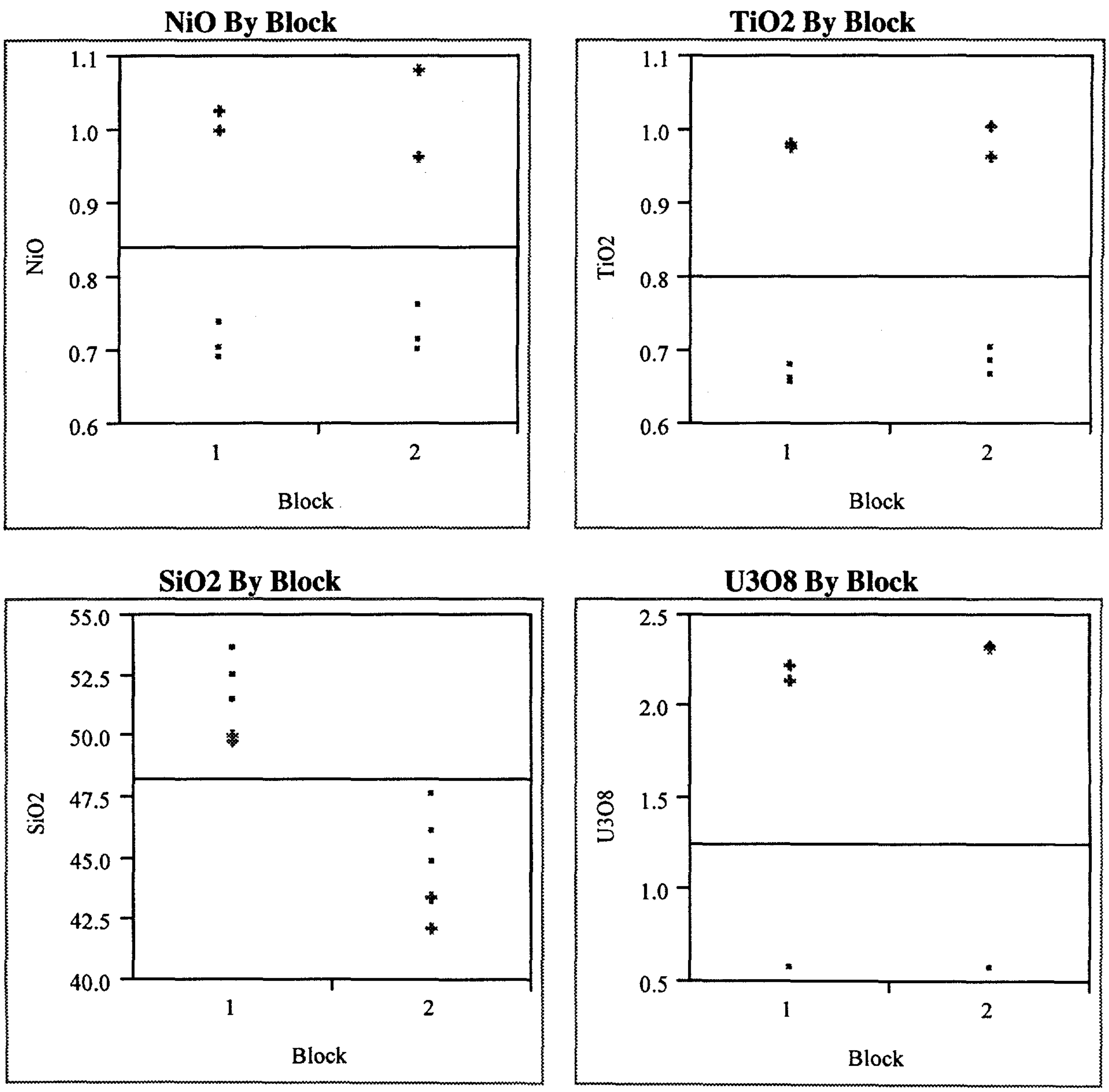

**Exhibit A.3: Measurements of Glass Standards by Oxide**

(+ u-std; small square Batch 1 standard)

(continued)

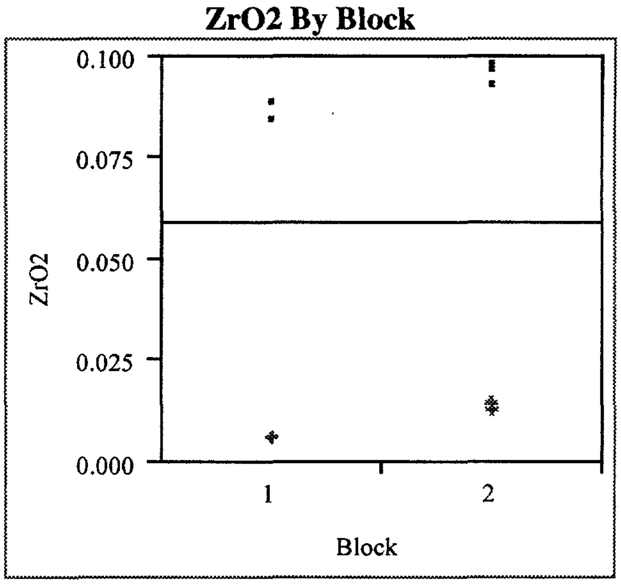

**Exhibit A.4: Comparisons of Measurements versus Target Compositions**
(concentrations in weight percents)

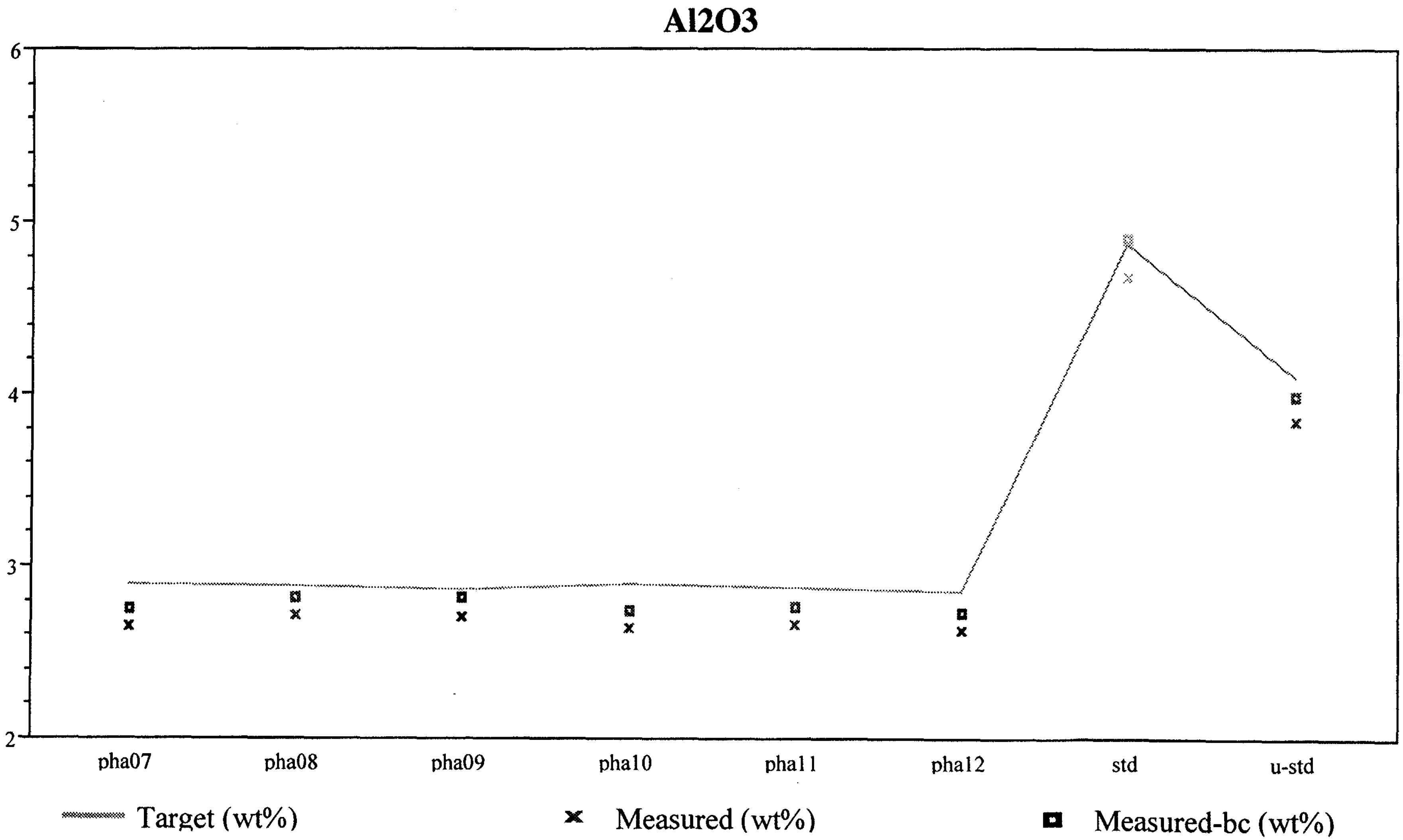

**Exhibit A.4: Comparisons of Measurements versus Target Compositions**
(concentrations in weight percents)

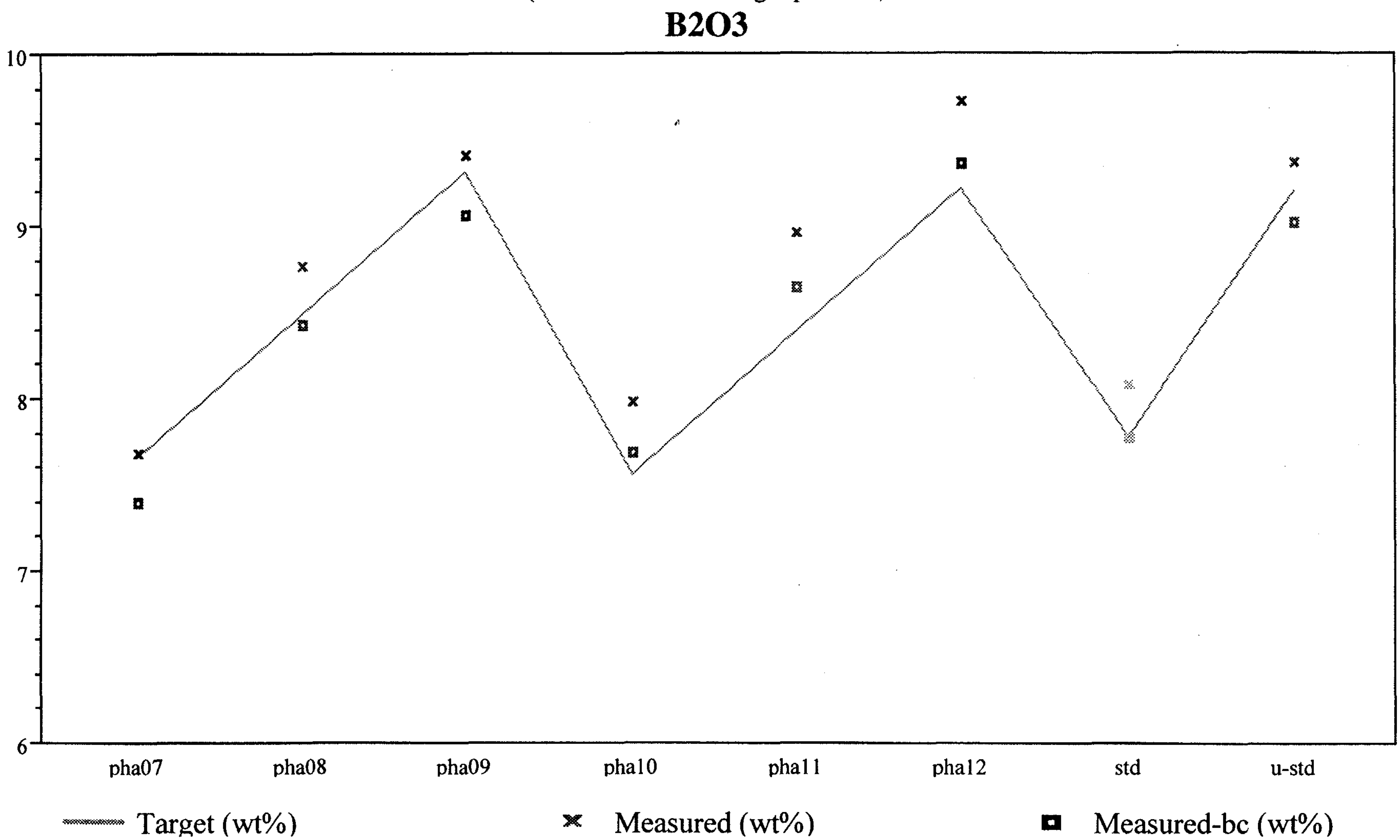

**Exhibit A.4: Comparisons of Measurements versus Target Compositions**
(concentrations in weight percents)

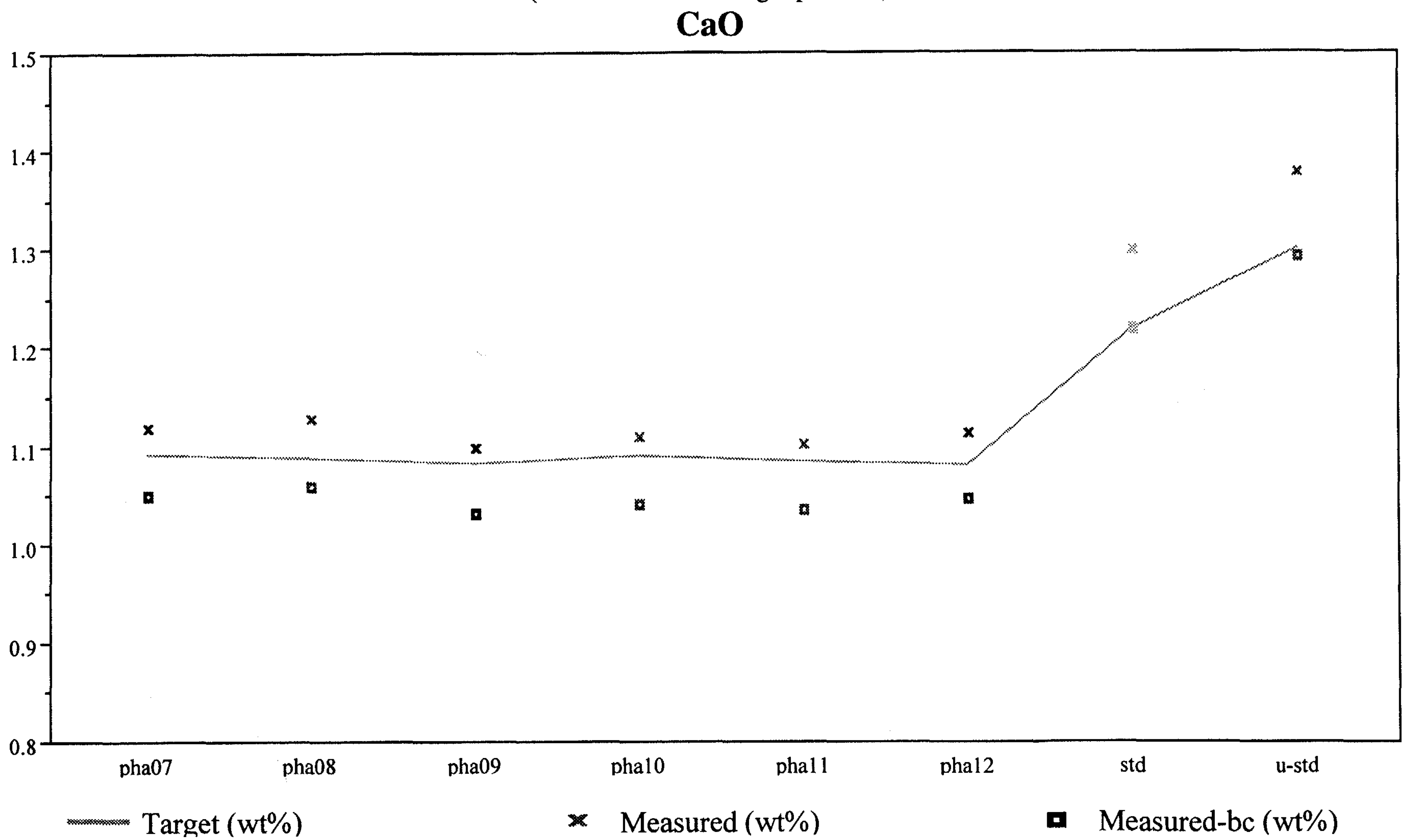

**Exhibit A.4: Comparisons of Measurements versus Target Compositions**
(concentrations in weight percents)

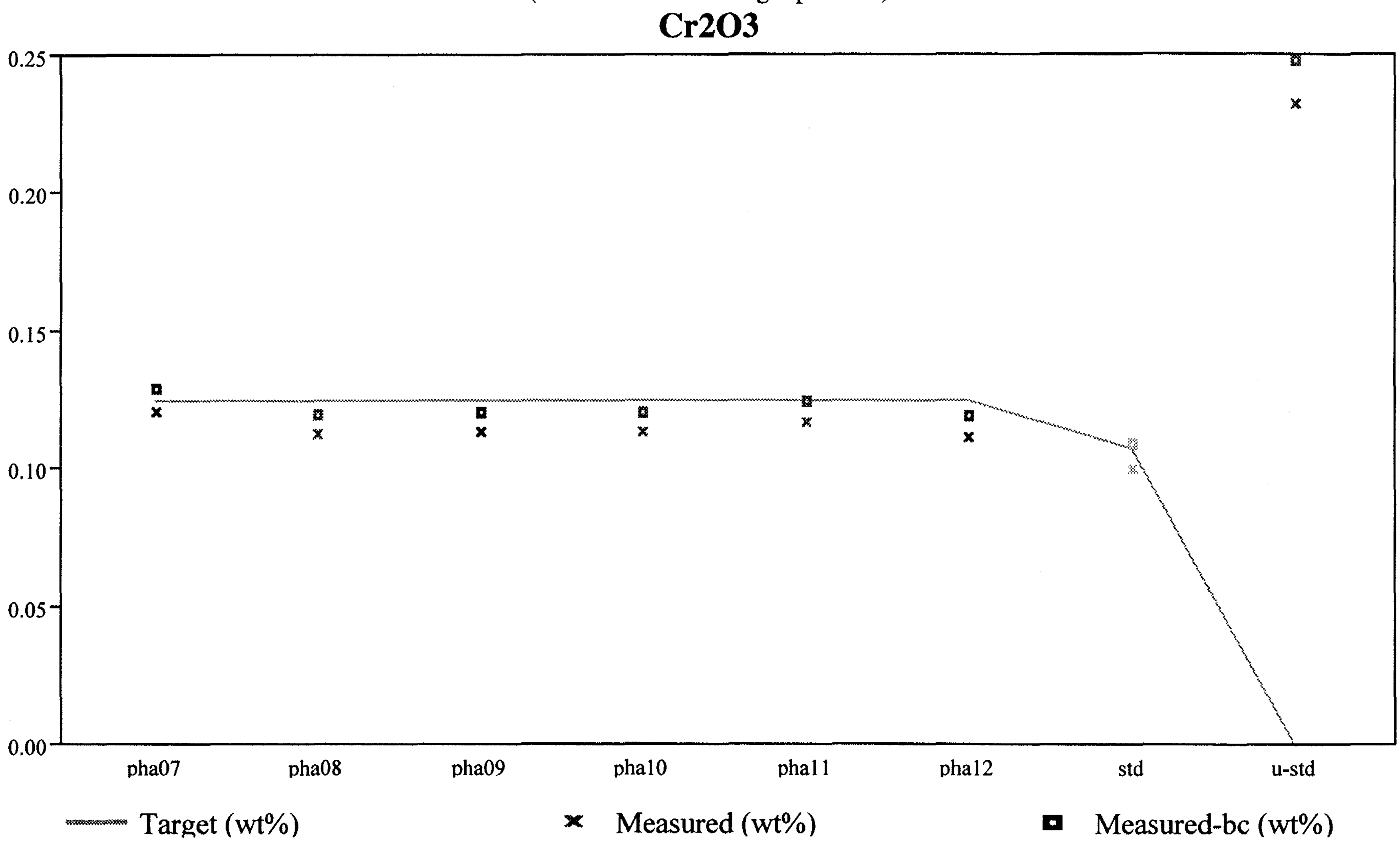

**Exhibit A.4: Comparisons of Measurements versus Target Compositions**
(concentrations in weight percents)

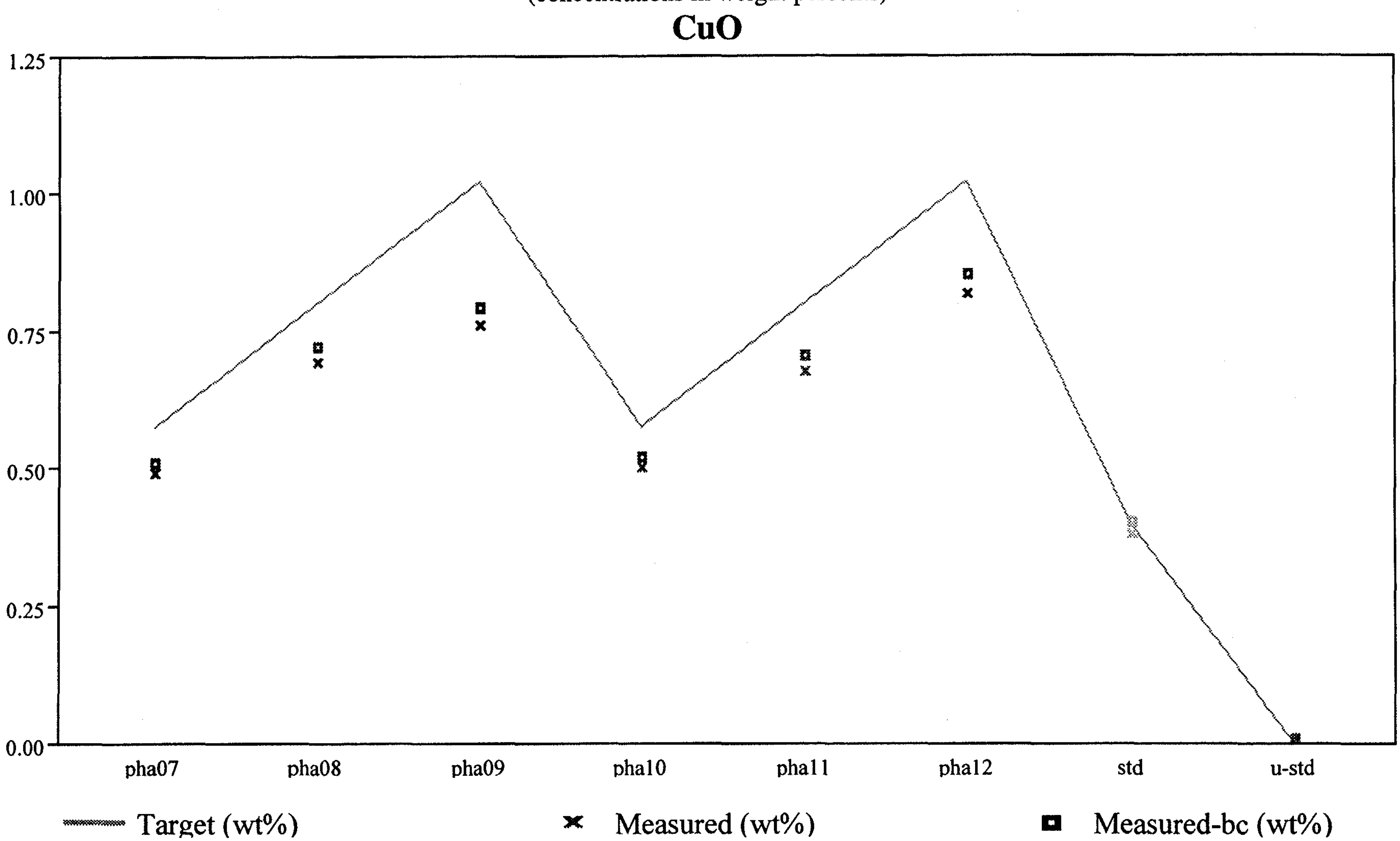

**Exhibit A.4: Comparisons of Measurements versus Target Compositions**
(concentrations in weight percents)

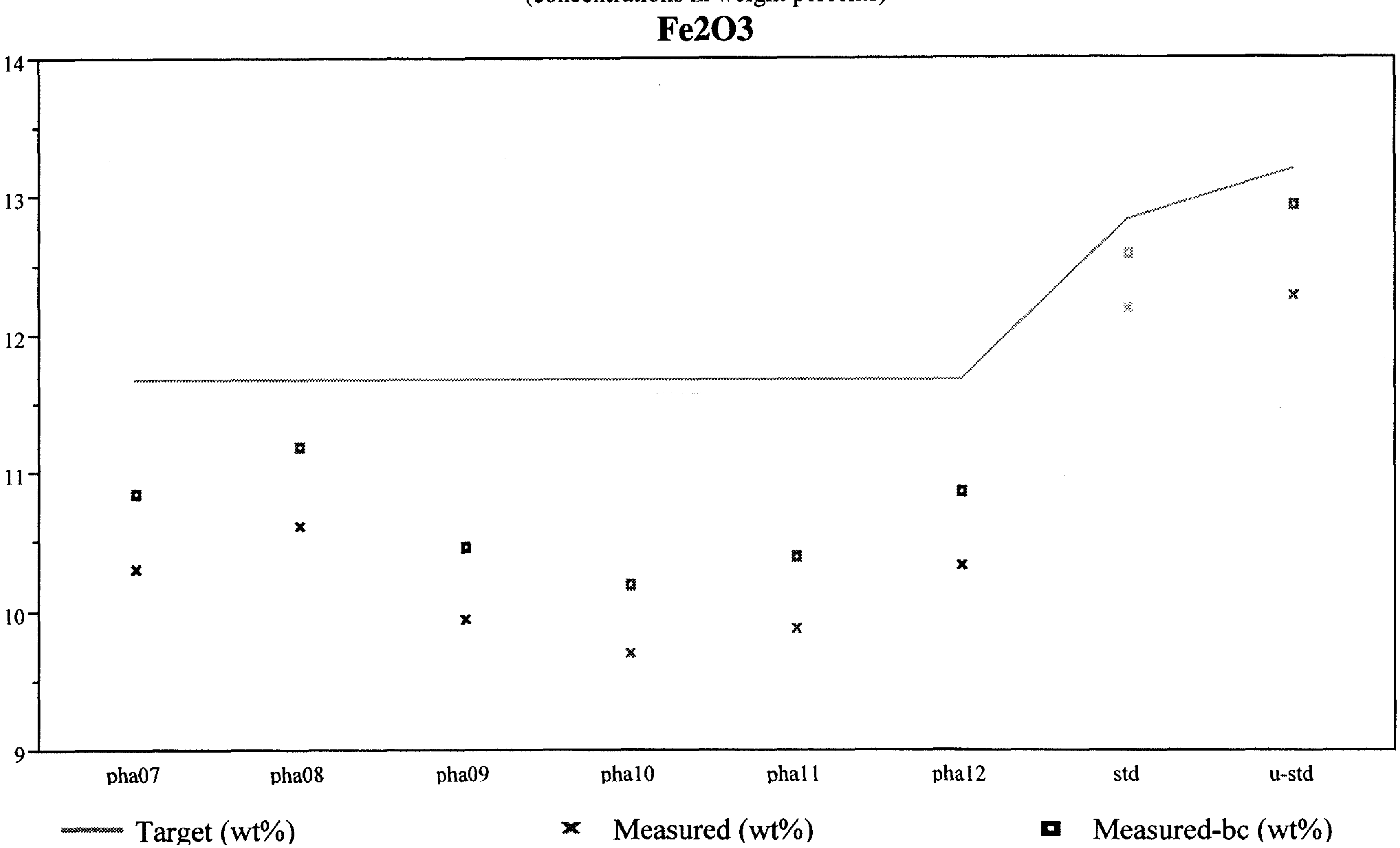

**Exhibit A.4: Comparisons of Measurements versus Target Compositions**
(concentrations in weight percents)

# K2O

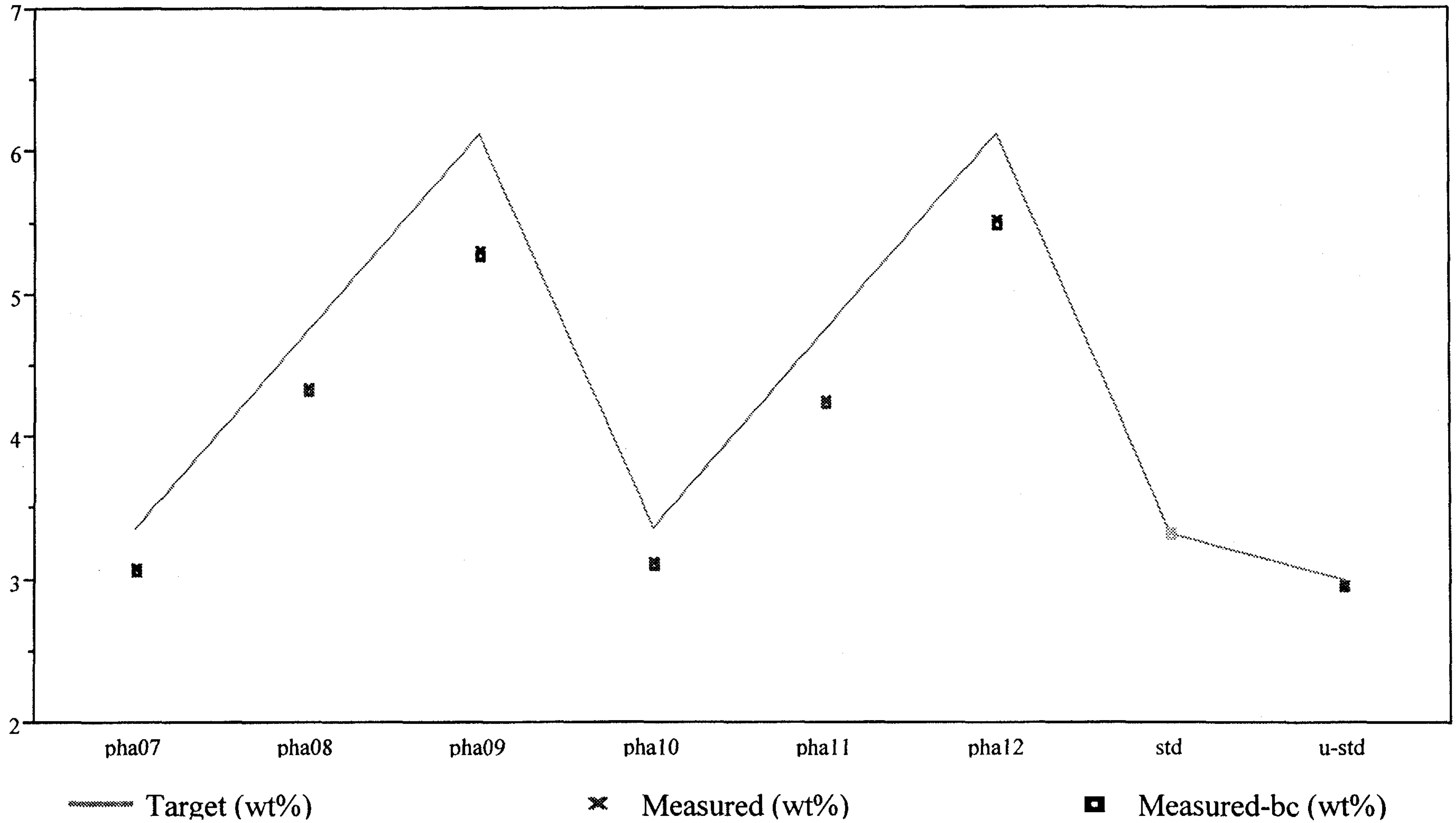

**Exhibit A.4: Comparisons of Measurements versus Target Compositions**
(concentrations in weight percents)

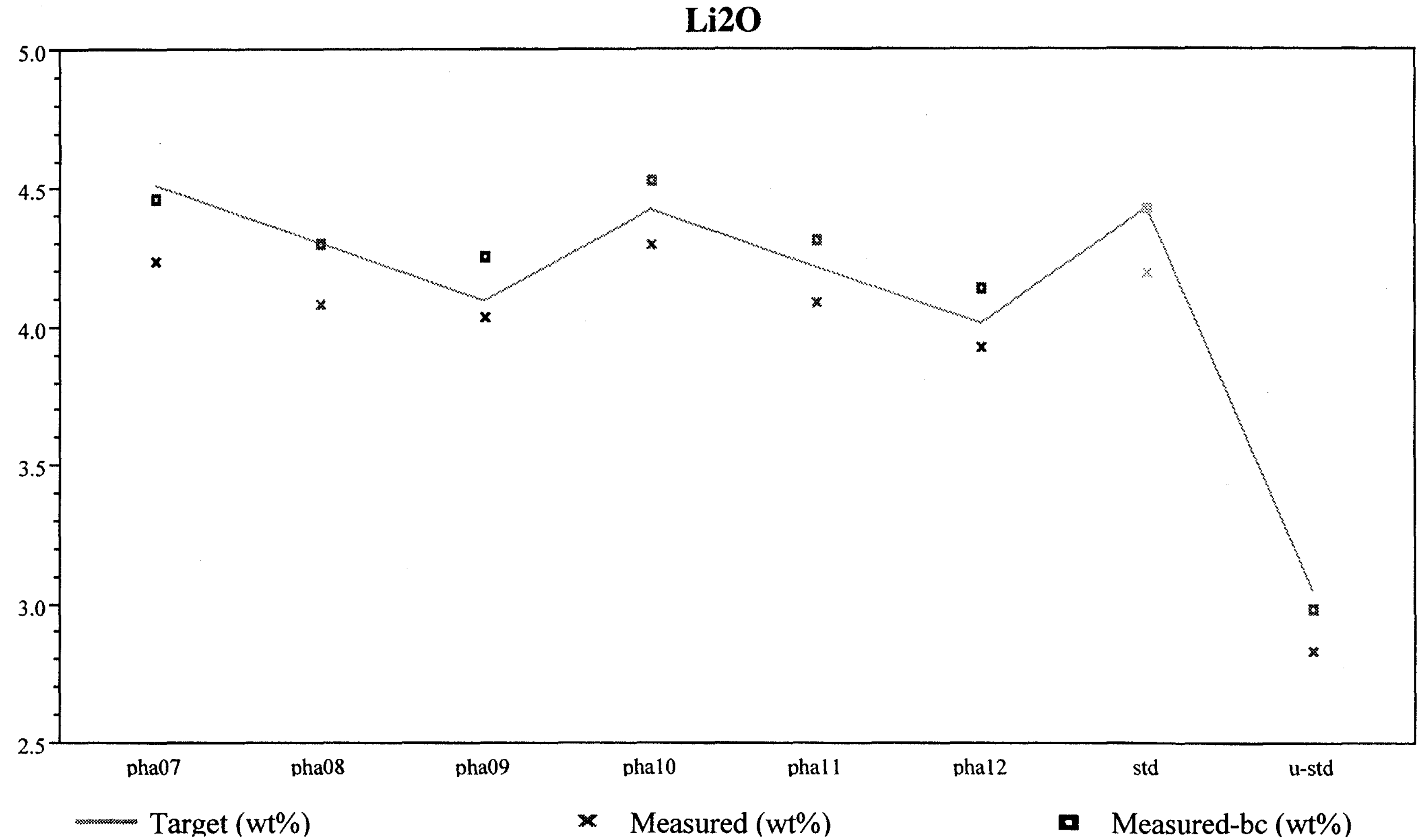

**Exhibit A.4: Comparisons of Measurements versus Target Compositions**
(concentrations in weight percents)

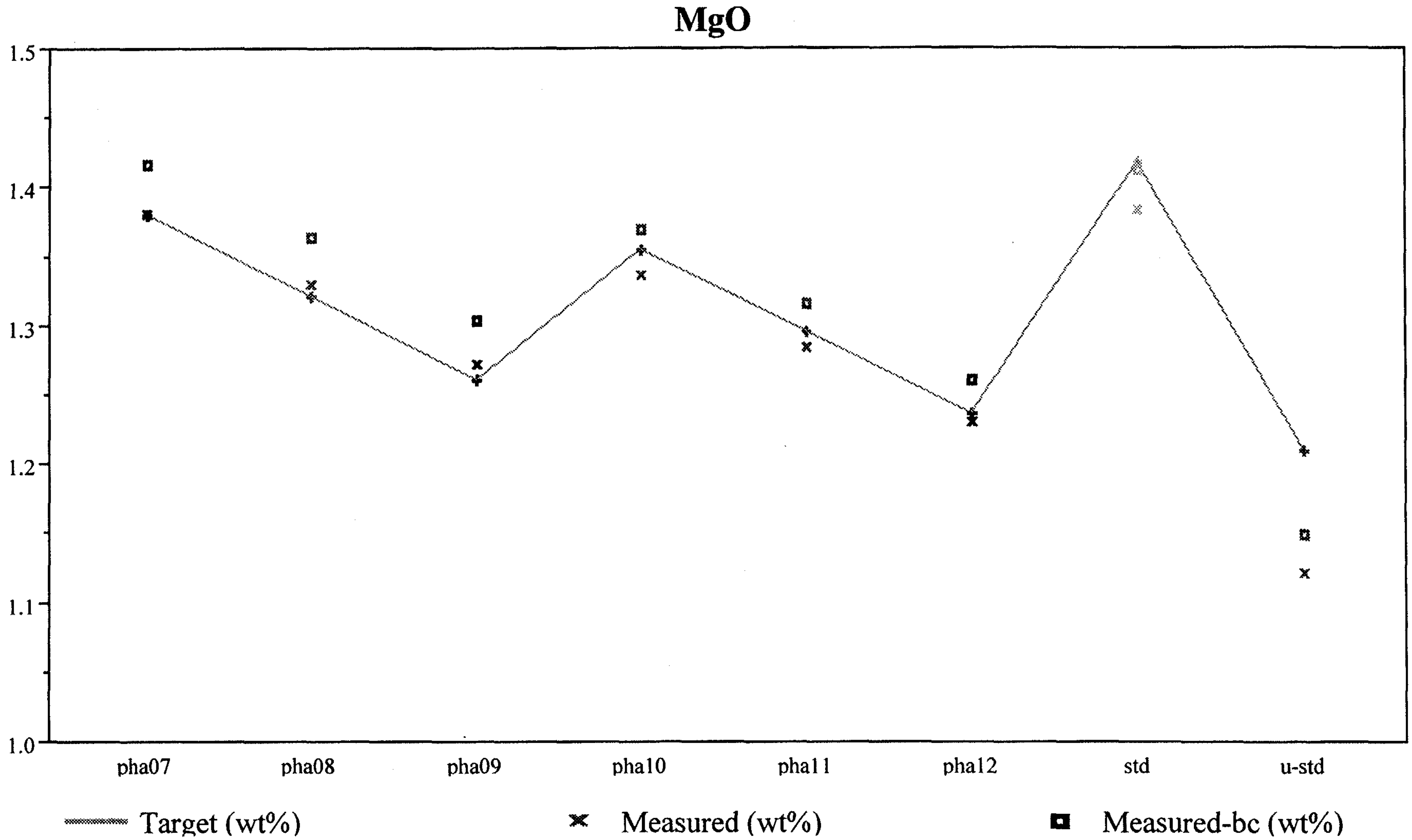

**Exhibit A.4: Comparisons of Measurements versus Target Compositions**
(concentrations in weight percents)

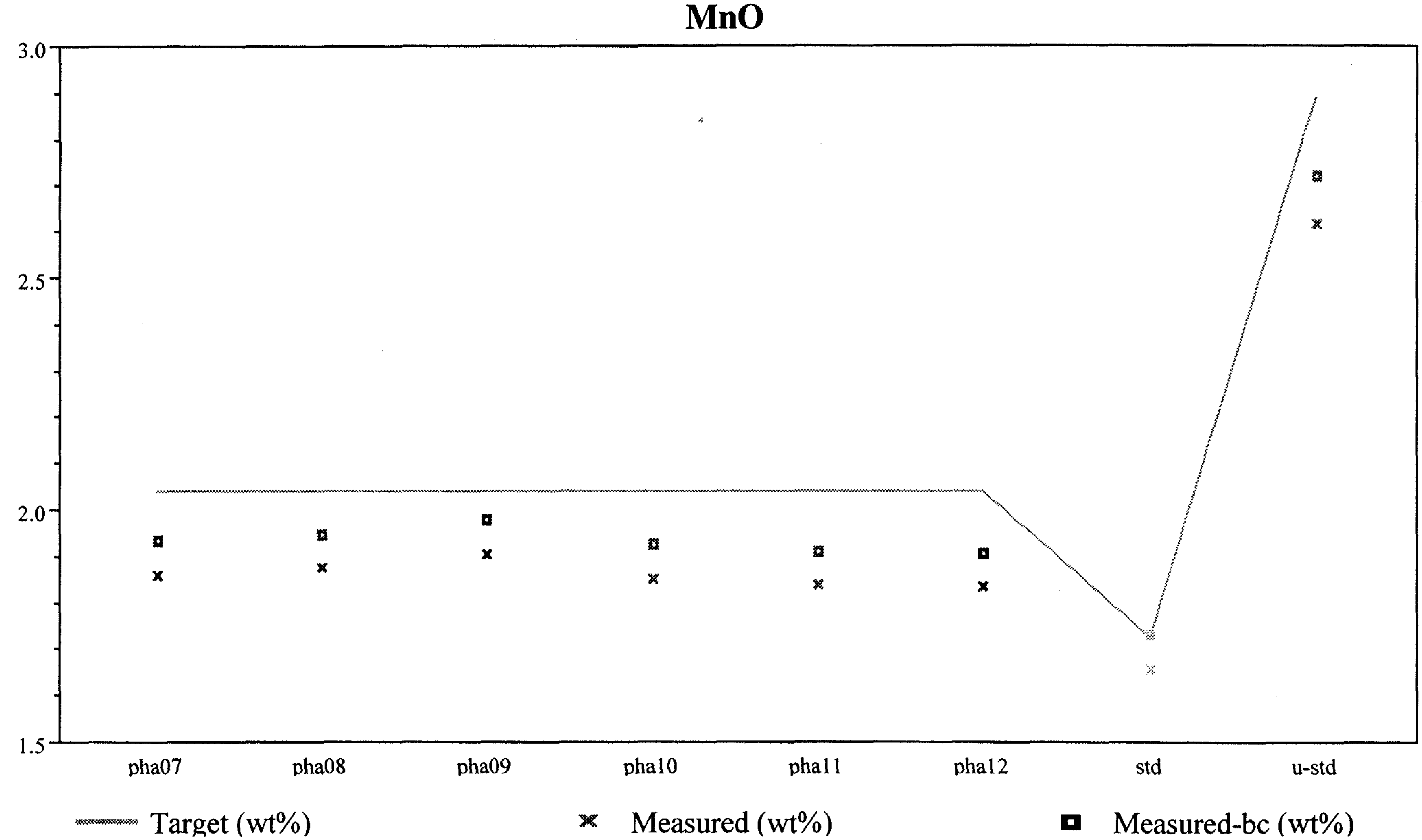

**Exhibit A.4: Comparisons of Measurements versus Target Compositions**
(concentrations in weight percents)

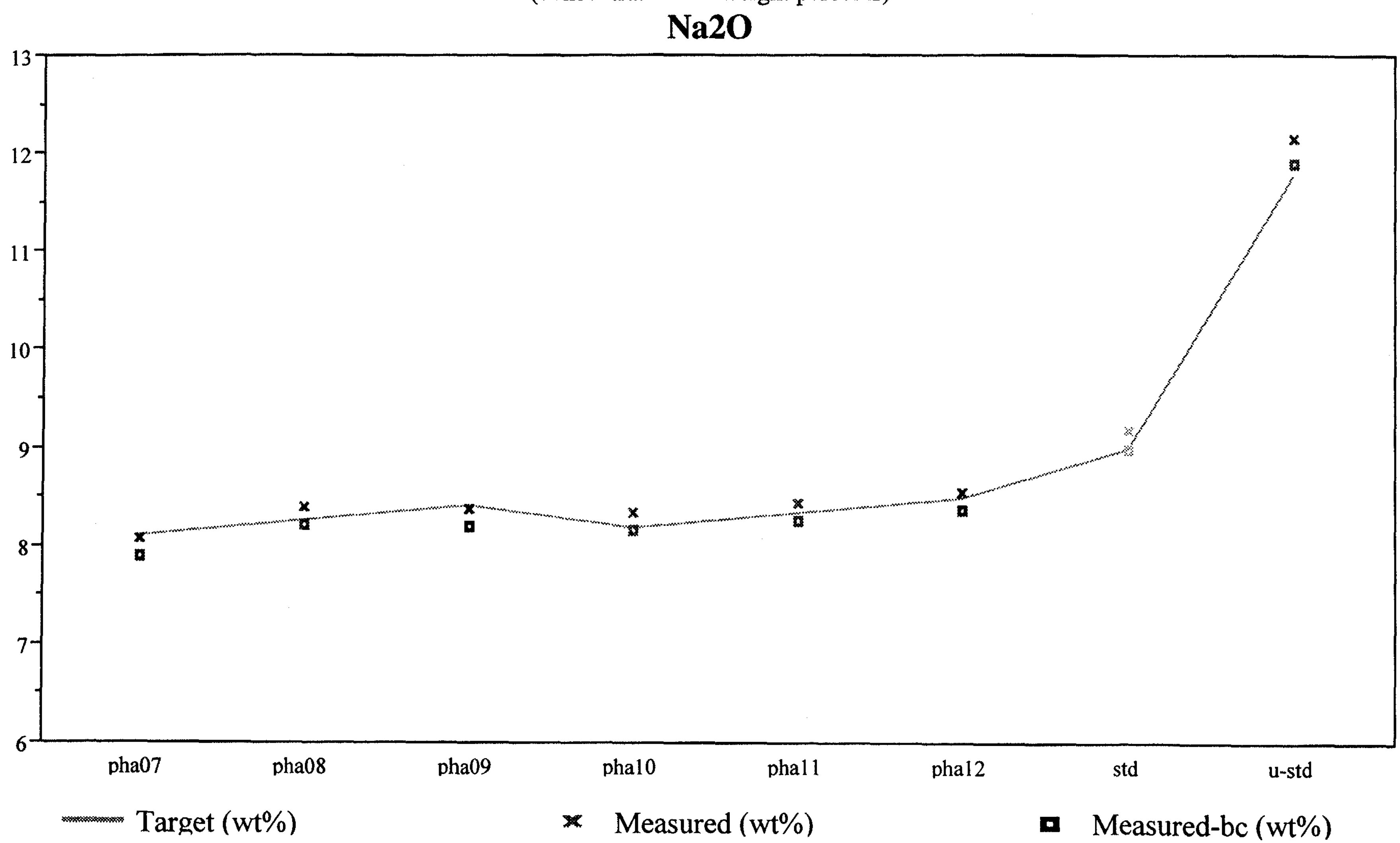

**Exhibit A.4: Comparisons of Measurements versus Target Compositions**
(concentrations in weight percents)

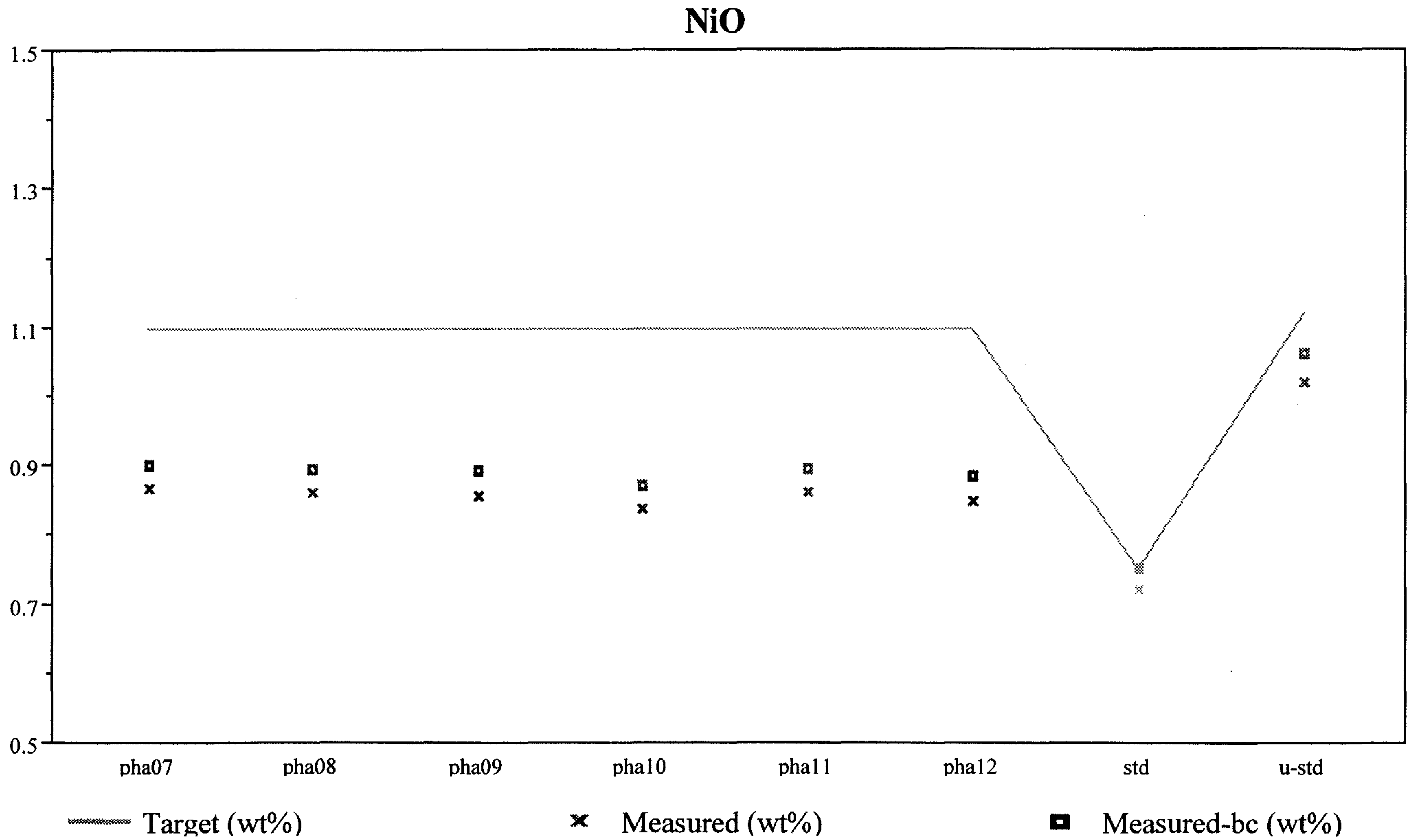

**Exhibit A.4: Comparisons of Measurements versus Target Compositions**
(concentrations in weight percents)

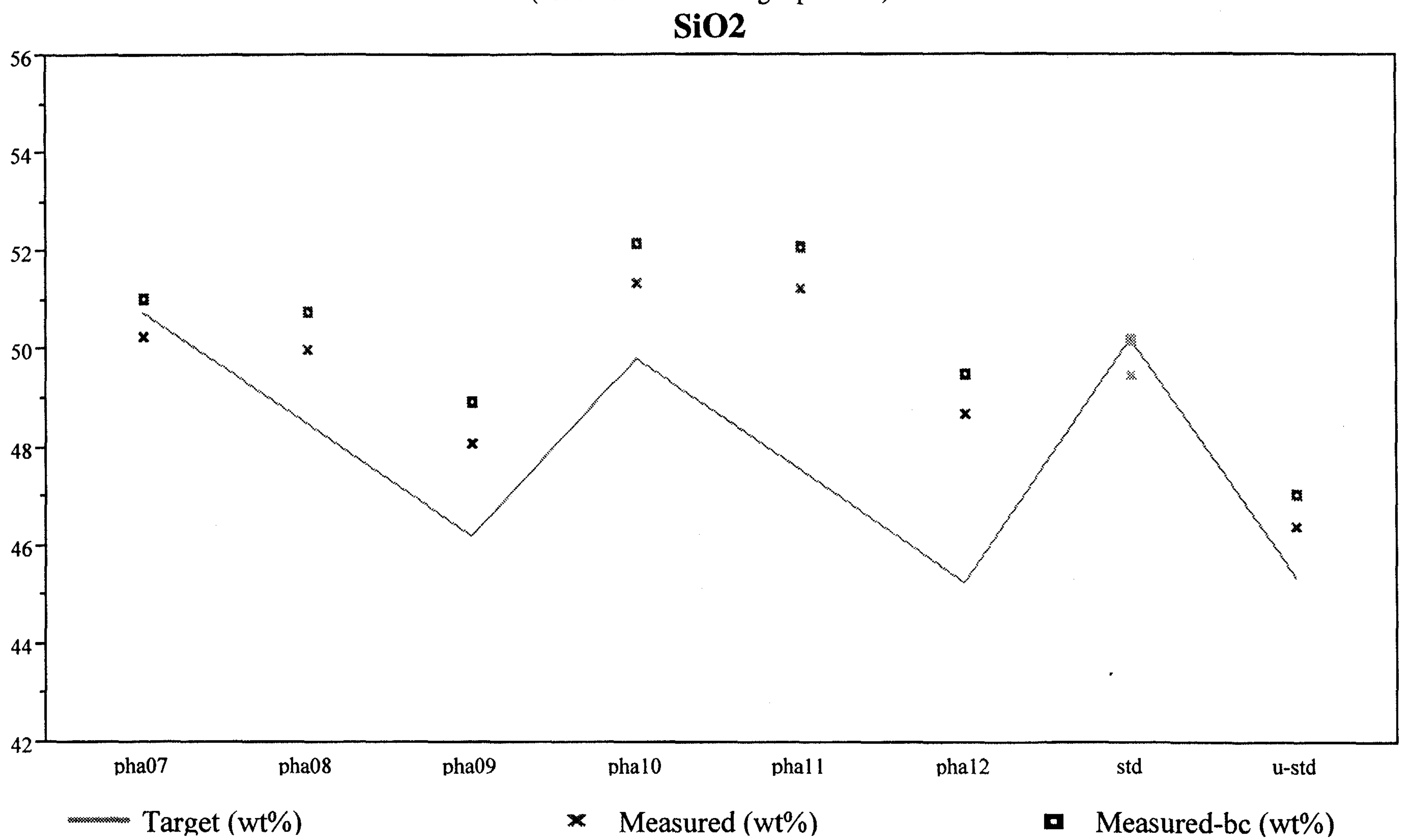

**Exhibit A.4: Comparisons of Measurements versus Target Compositions**
(concentrations in weight percents)

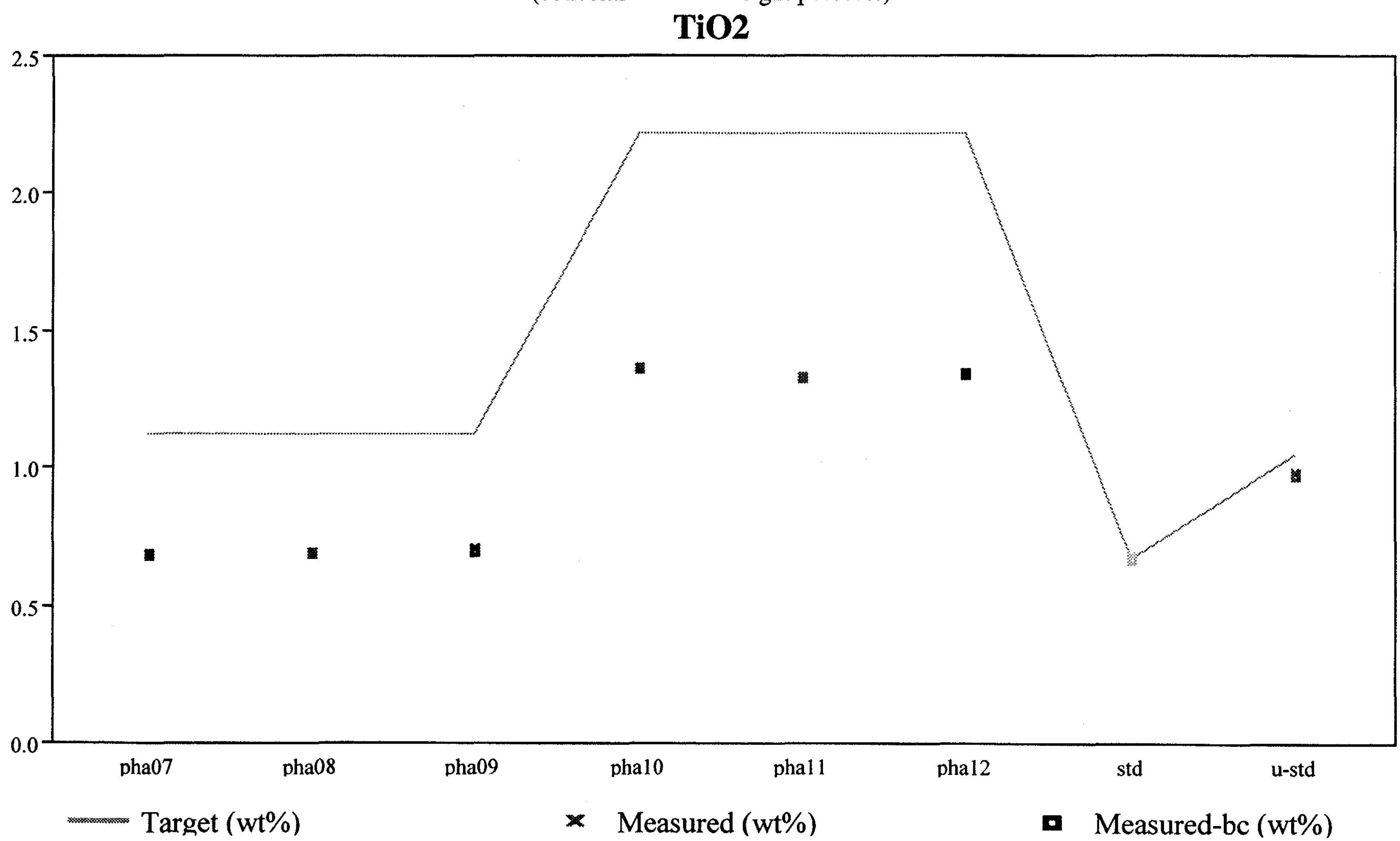

**Exhibit A.4: Comparisons of Measurements versus Target Compositions**
(concentrations in weight percents)

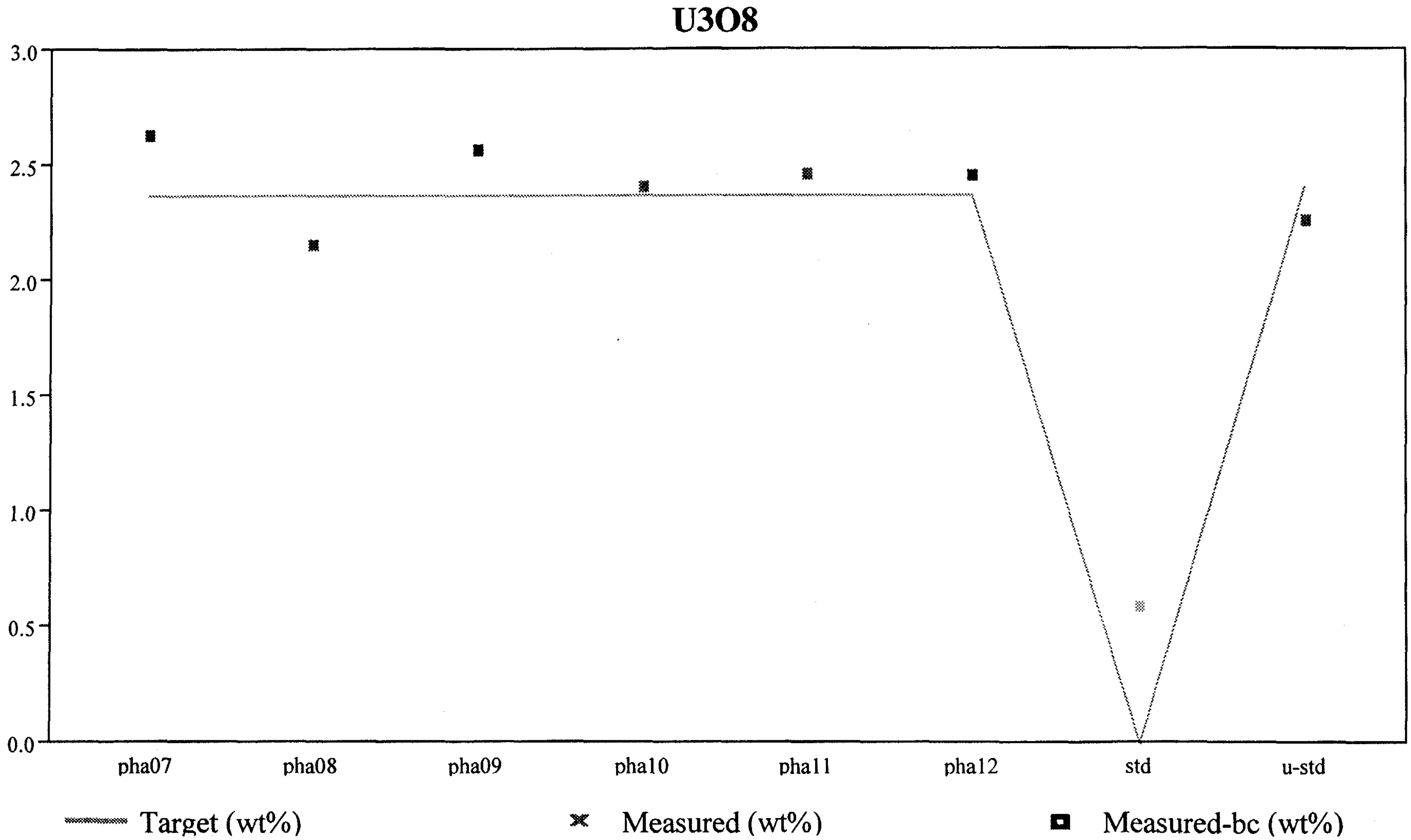

**Exhibit A.4: Comparisons of Measurements versus Target Compositions**
(concentrations in weight percents)

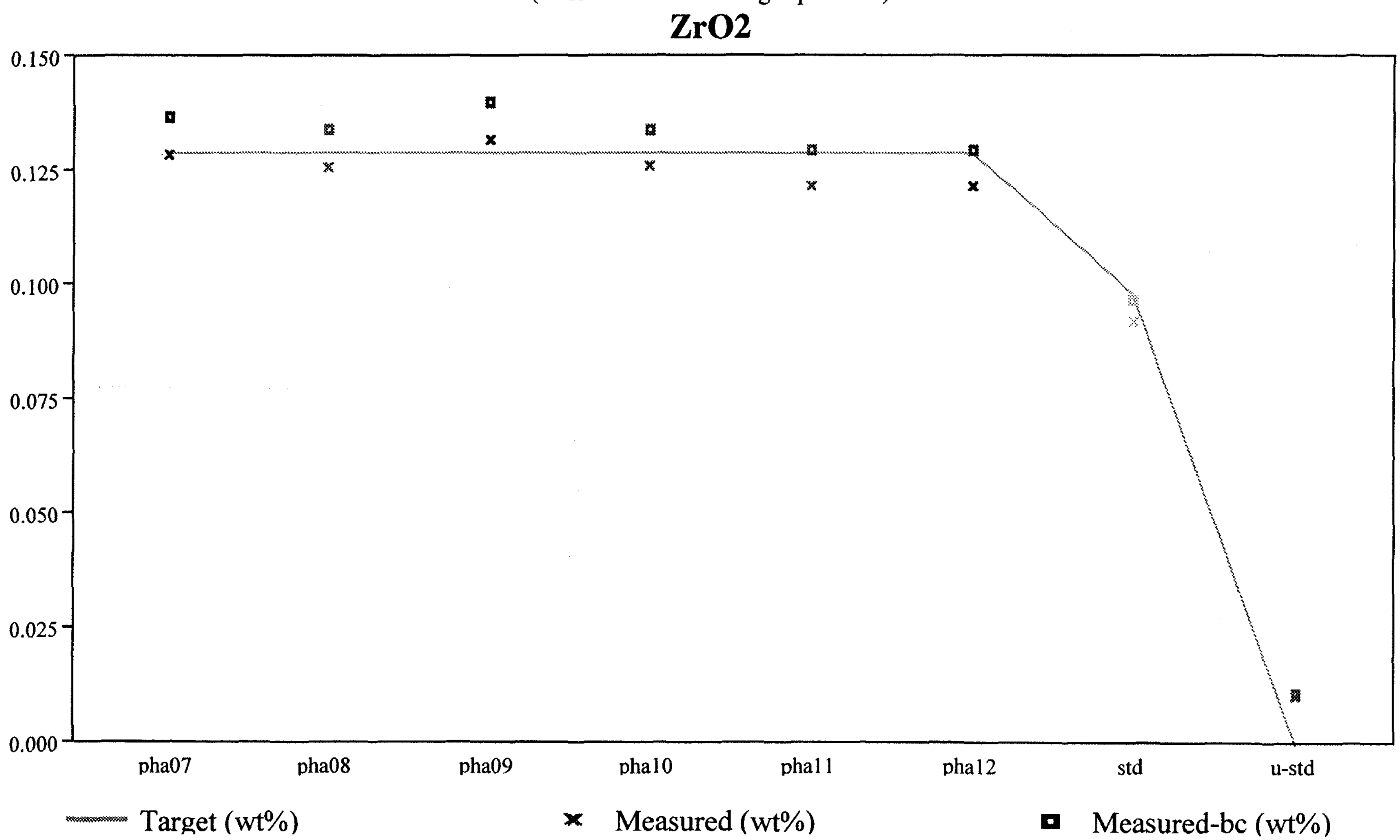

**Exhibit A.4: Comparisons of Measurements versus Target Compositions**
(concentrations in weight percents)

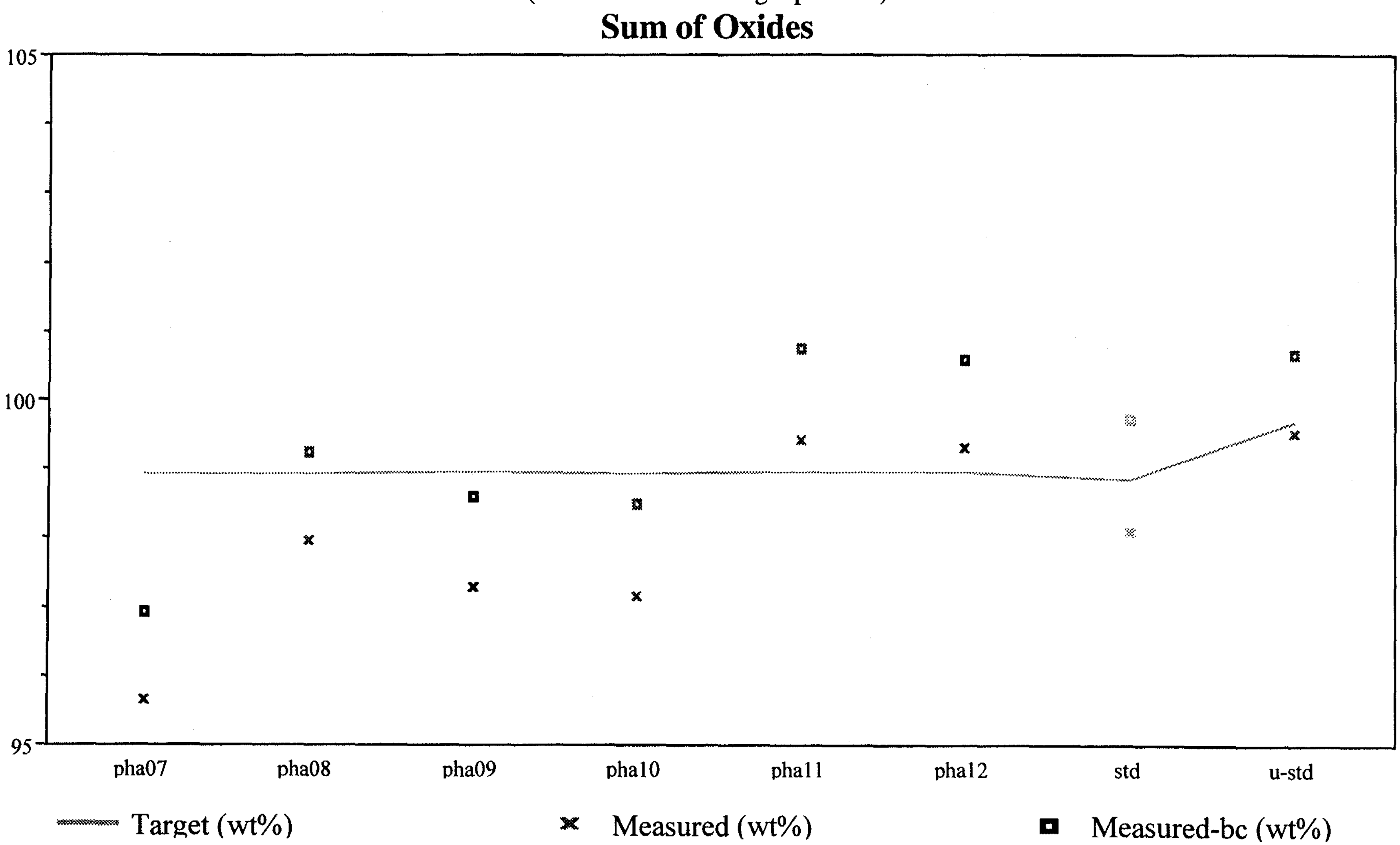

**Exhibit A.5: Plots of the Leachate Concentrations by Sample ID by Element**

## B (ppm) By Sample ID

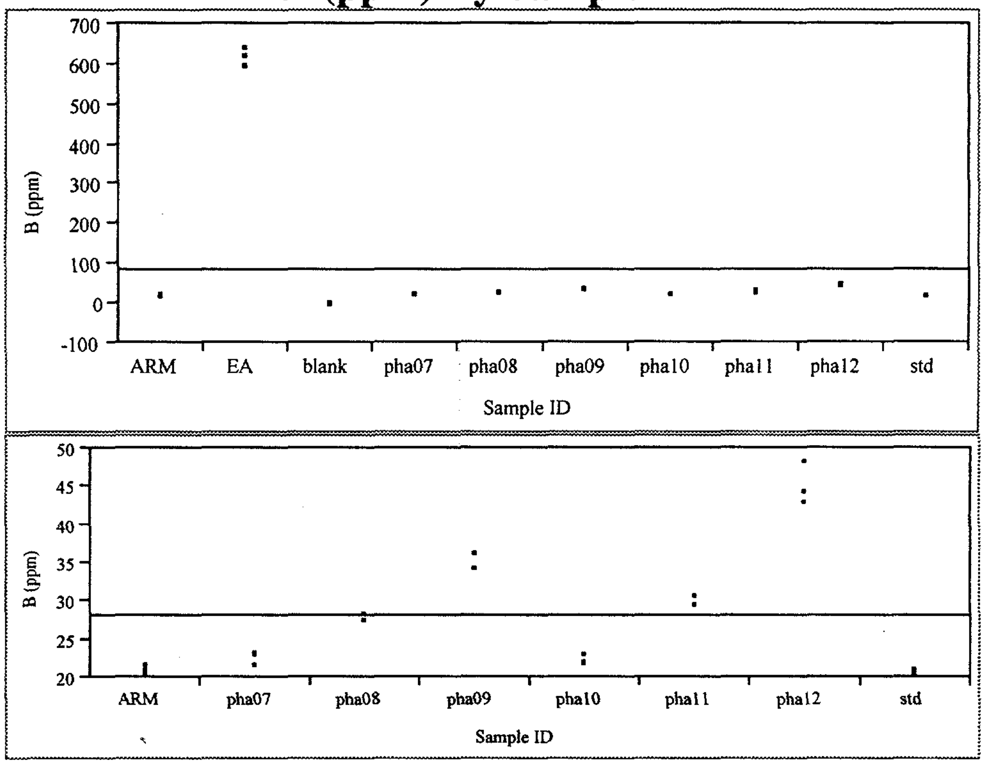


## Si (ppm) By Sample ID

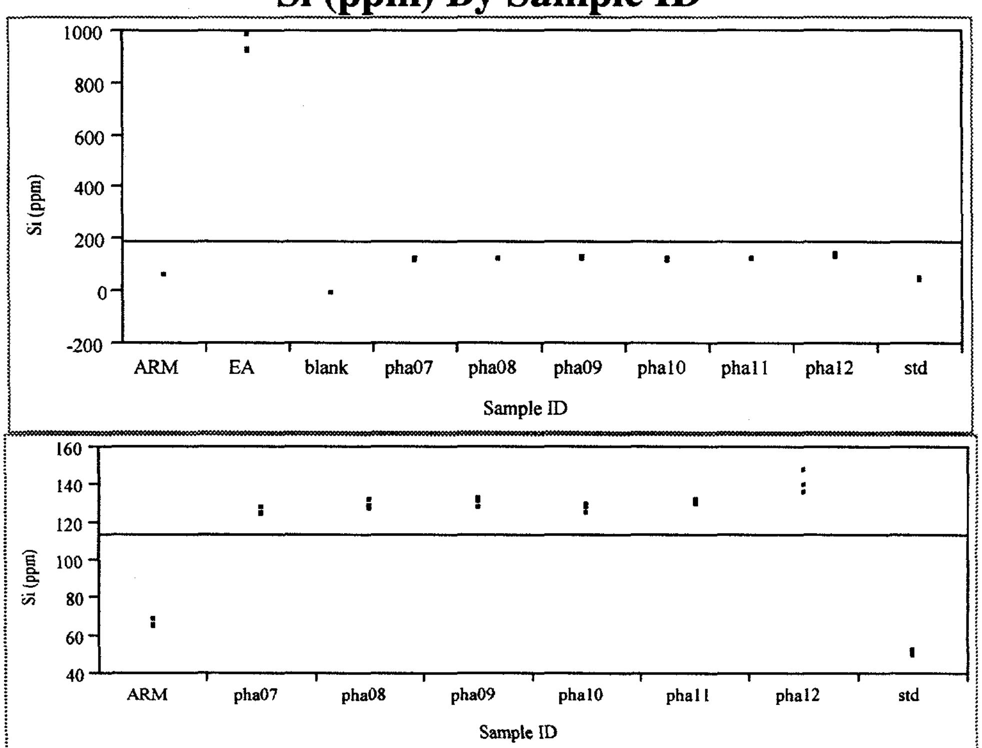

**Exhibit A.5: Plots of the Leachate Concentrations by Sample ID by Element**
**(continued)**

# Na (ppm) By Sample ID

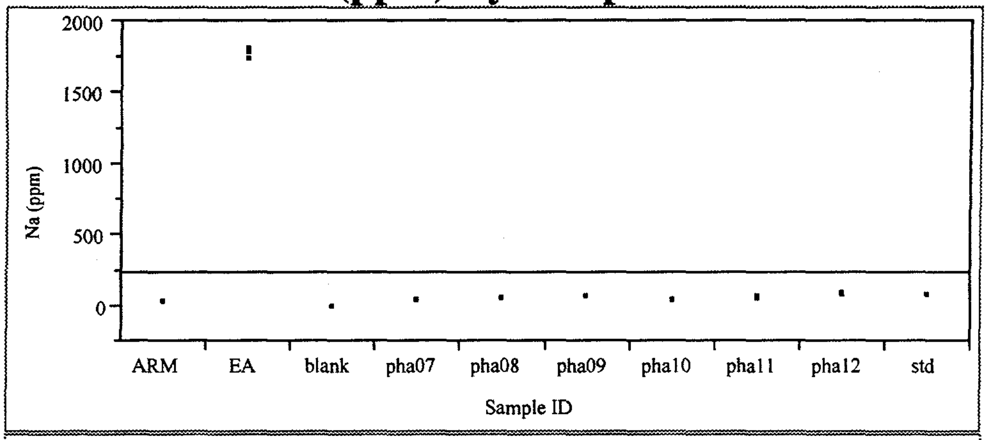


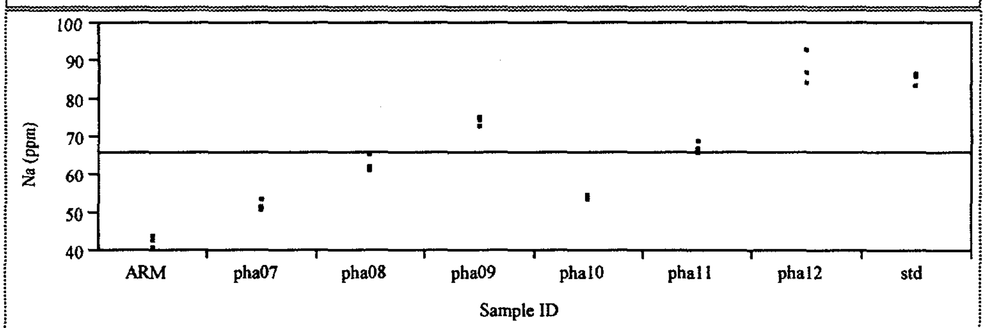


# Li (ppm) By Sample ID

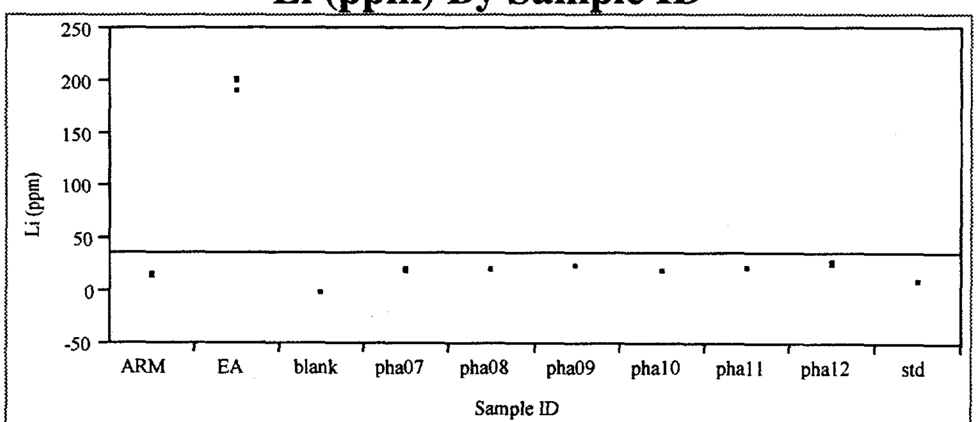


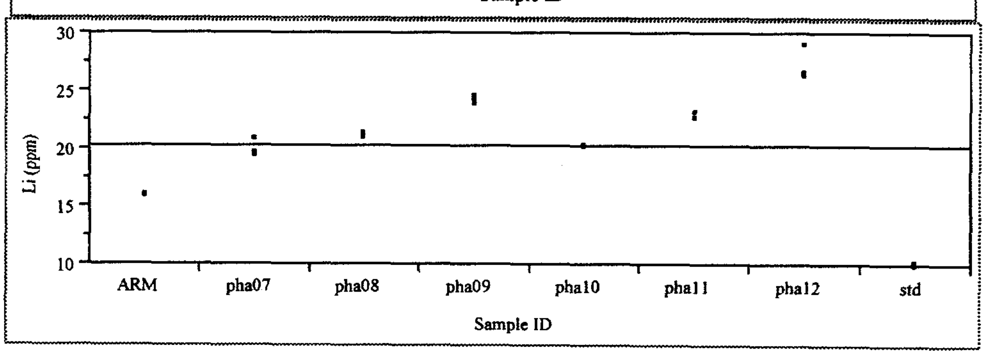

## Exhibit A.6: Scatter Plots of the Normalized PCT's

### Correlations Using Target Compositions

| Variable | log NL[B g/L] | log NL[Si g/L] | log NL[Na g/L] | log NL[Li g/L] |
|---|---|---|---|---|
| log NL[B g/L] | 1.0000 | 0.9901 | 0.9828 | 0.9881 |
| log NL[Si g/L] | 0.9901 | 1.0000 | 0.9904 | 0.9893 |
| log NL[Na g/L] | 0.9828 | 0.9904 | 1.0000 | 0.9911 |
| log NL[Li g/L] | 0.9881 | 0.9893 | 0.9911 | 1.0000 |

### Correlations Using Measured Compositions

| Variable | log NL[B g/L] | log NL[Si g/L] | log NL[Na g/L] | log NL[Li g/L] |
|---|---|---|---|---|
| log NL[B g/L] | 1.0000 | 0.9775 | 0.9831 | 0.9917 |
| log NL[Si g/L] | 0.9775 | 1.0000 | 0.9530 | 0.9564 |
| log NL[Na g/L] | 0.9831 | 0.9530 | 1.0000 | 0.9957 |
| log NL[Li g/L] | 0.9917 | 0.9564 | 0.9957 | 1.0000 |

### Correlations Using Bias-Corrected Measured Compositions

| Variable | log NL[B g/L] | log NL[Si g/L] | log NL[Na g/L] | log NL[Li g/L] |
|---|---|---|---|---|
| log NL[B g/L] | 1.0000 | 0.9765 | 0.9831 | 0.9916 |
| log NL[Si g/L] | 0.9765 | 1.0000 | 0.9502 | 0.9535 |
| log NL[Na g/L] | 0.9831 | 0.9502 | 1.0000 | 0.9957 |
| log NL[Li g/L] | 0.9916 | 0.9535 | 0.9957 | 1.0000 |

## Scatterplot Matrix

### PCT Normalized Using

**Target Compositions** | **Measured Compositions** | **Bias-Corrected Compositions**

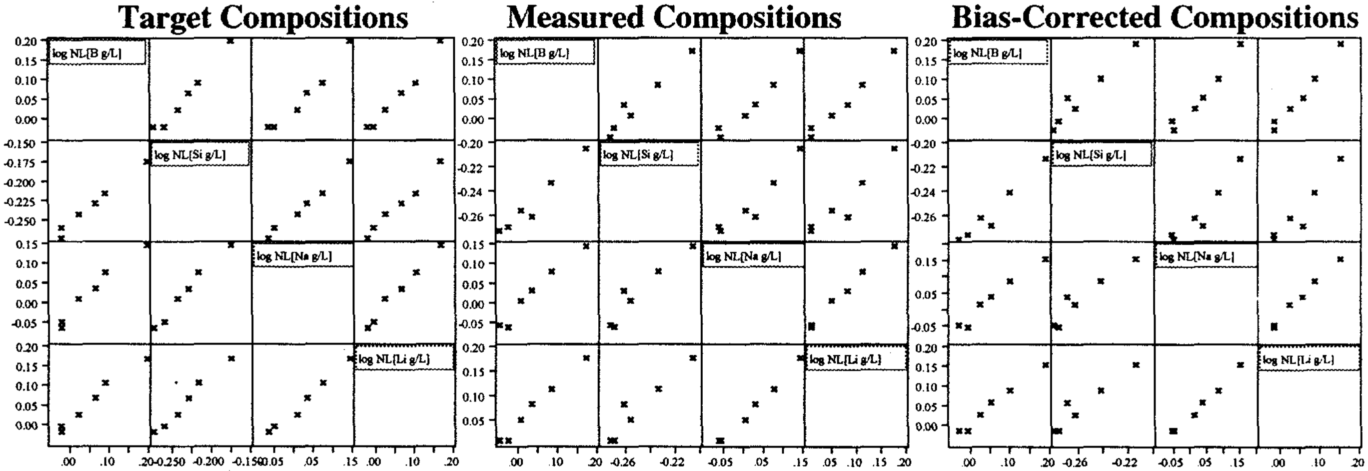

**Exhibit A.7: Durability Predictions versus Measured**

**Log NL(B) (g/L) By del Gp(m)**
**(based on measured and bias-corrected compositions)**

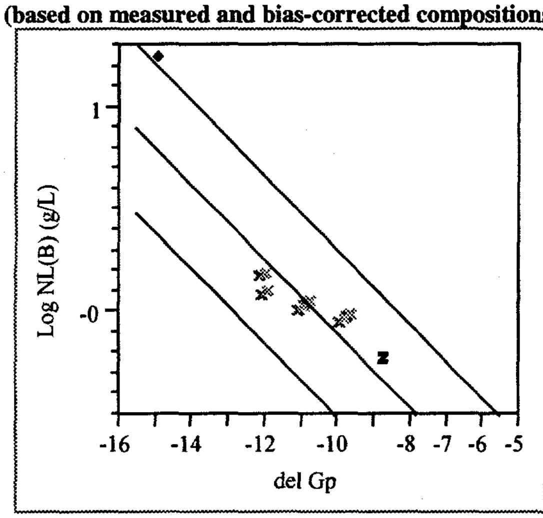


**Log NL(B) (g/L) By del Gp(m)**
**(based on target composition)**

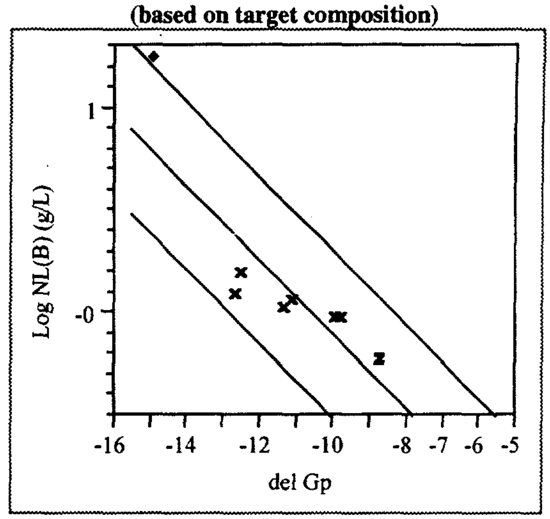


**Log NL(Si) (g/L) By del Gp(m)**
**(based on measured and bias-corrected compositions)**

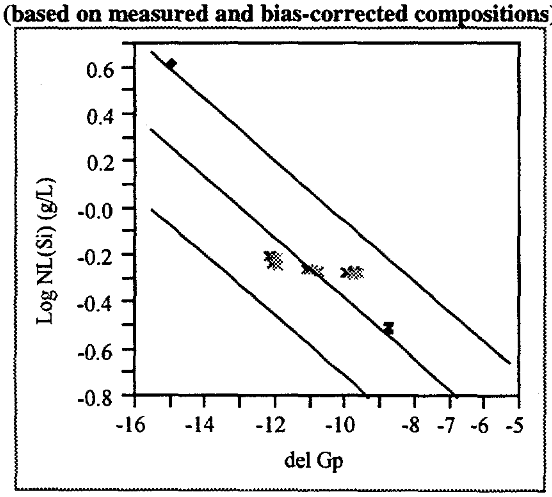


**Log NL(Si) (g/L) By del Gp(m)**
**(based on measured and bias-corrected compositions)**

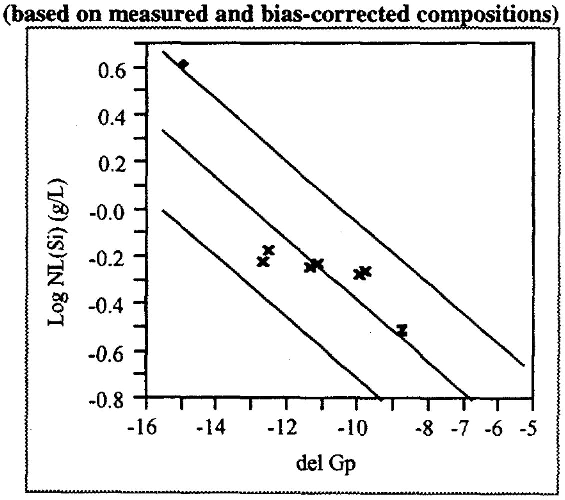

**Exhibit A.7: Durability Predictions versus Measured**
**(Continued)**

**Log NL (Na) (g/L) By del Gp(m)**
**(based on measured and bias-corrected compositions)**

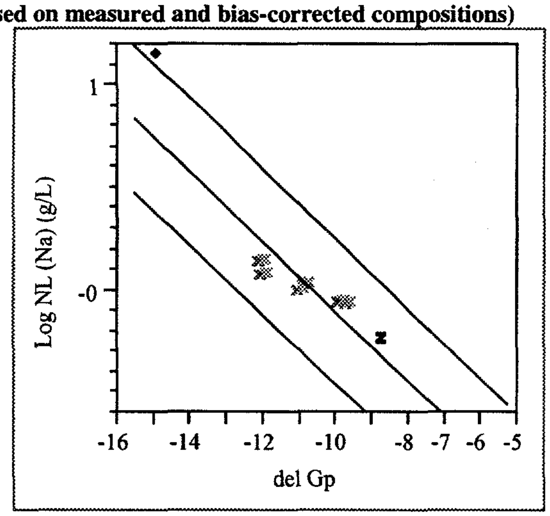


**Log NL (Na) (g/L) By del Gp(m)**
**(based on measured and bias-corrected compositions)**

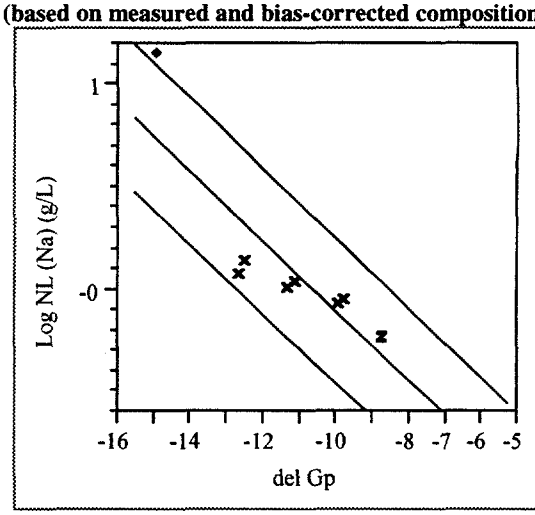


**log[NL(Li) g/L] By del Gp(m)**
**(based on measured and bias-corrected compositions)**

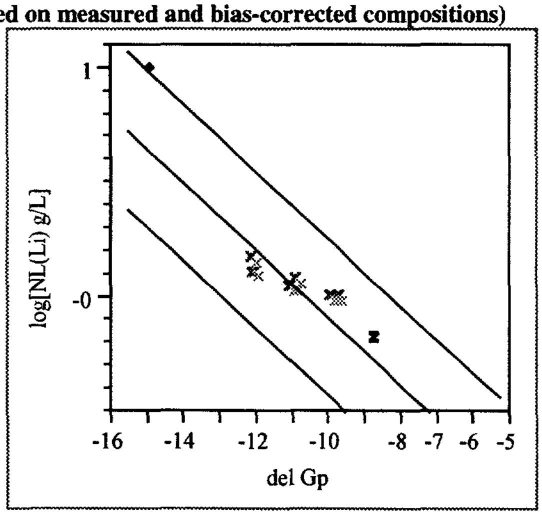


**log[NL(Li) g/L] By del Gp(m)**
**(based on measured and bias-corrected compositions)**

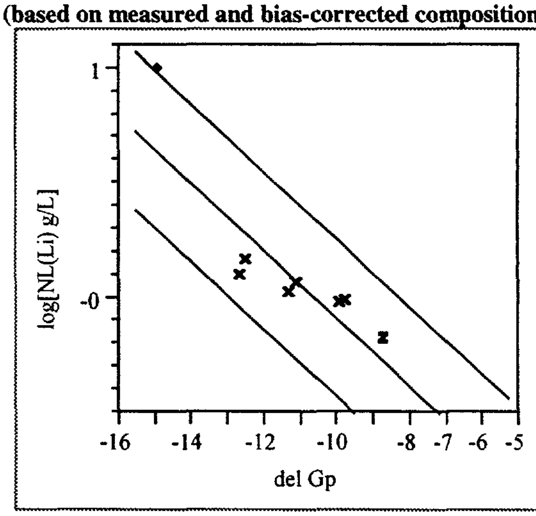

**Exhibit A.8: Viscosity Measurements, Fulcher Fits, and Predictions at 1150 °C**

# pha07

| Parameter | Estimate | ApproxStdErr |
|---|---|---|
| A | -4.44557977 | 0.27581109 |
| B | 8725.688255 | 535.07267 |
| C | 112.1582176 | 29.5925881 |

## Graph

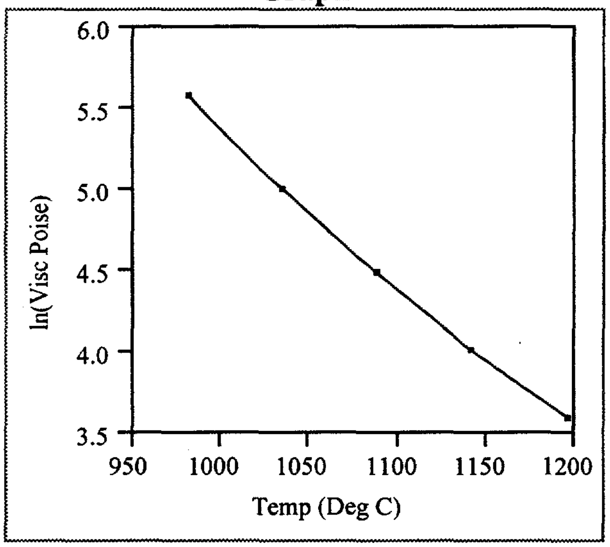


| Temp (Deg C) | Visc (Poise) | ln Visc (Fulcher) | ln(Visc Poise) | Visc Pred (poise) |
|---|---|---|---|---|
| 1197.5 | 36.41812 | 3.593997 | 3.595066 | 36.38 |
| 1142 | 55.93637 | 4.027264 | 4.024215 | 56.11 |
| 1089 | 89.10828 | 4.48697 | 4.489852 | 88.85 |
| 1035.5 | 148.9483 | 5.004538 | 5.003599 | 149.09 |
| 982.5 | 265.0833 | 5.580008 | 5.580044 | 265.07 |
| 1150 | ? | 3.961952 | ? | 52.56 |

**Exhibit A.8: Viscosity Measurements, Fulcher Fits, and Predictions at 1150 °C**
(continued)

# pha08

| Parameter | Estimate | ApproxStdErr |
|---|---|---|
| A | -4.49084159 | 0.98191161 |
| B | 8510.326797 | 1911.8085 |
| C | 108.0934978 | 108.800145 |

**Graph**

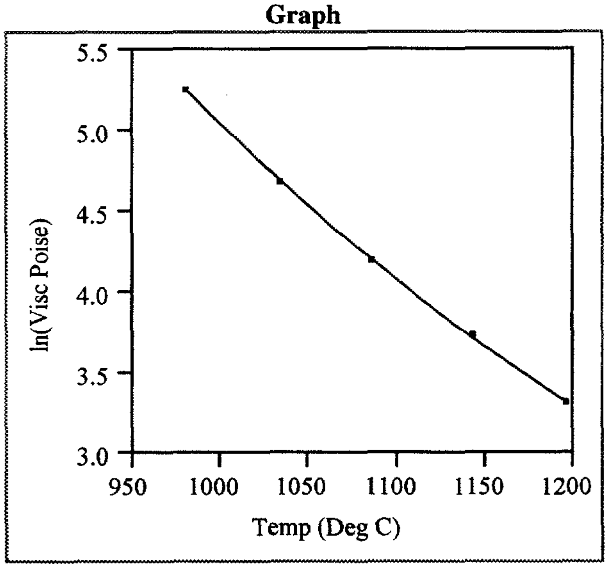


| Temp (Deg C) | Visc (Poise) | ln Visc (Fulcher) | ln(Visc Poise) | Visc Pred (poise) |
|---|---|---|---|---|
| 1196.7 | 27.71782 | 3.326792 | 3.322076 | 27.85 |
| 1143 | 42.27204 | 3.732439 | 3.744126 | 41.78 |
| 1086.5 | 66.56259 | 4.207309 | 4.198143 | 67.18 |
| 1034.5 | 109.635 | 4.695543 | 4.697157 | 109.46 |
| 981.5 | 191.2485 | 5.252991 | 5.253573 | 191.14 |
| 1150 | ? | 3.677192 | ? | 39.54 |

**Exhibit A.8: Viscosity Measurements, Fulcher Fits, and Predictions at 1150 °C**
(continued)

## pha09

| Parameter | Estimate | ApproxStdErr |
|---|---|---|
| A | -3.836806001 | 0.5317635 |
| B | 7294.3847955 | 911.326186 |
| C | 223.85402492 | 53.185137 |

Graph

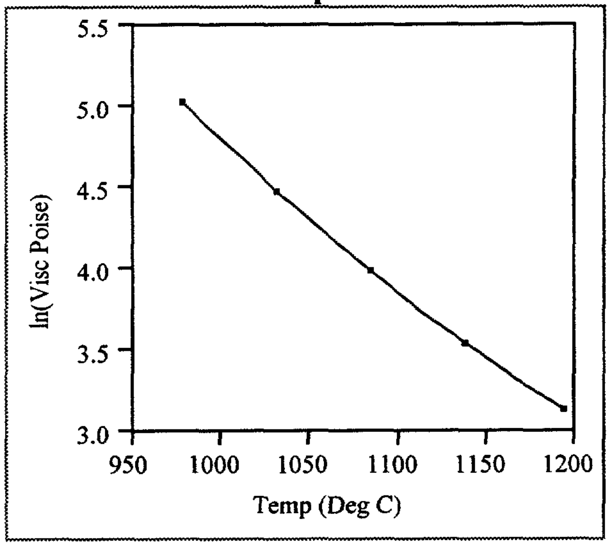


| Temp (Deg C) | Visc (Poise) | ln Visc (Fulcher) | ln(Visc Poise) | Visc Pred (poise) |
|---|---|---|---|---|
| 1194.5 | 22.98829 | 3.134217 | 3.134985 | 22.97 |
| 1139 | 34.57952 | 3.544709 | 3.543261 | 34.63 |
| 1085 | 54.08813 | 3.990508 | 3.990615 | 54.08 |
| 1032 | 88.38879 | 4.480684 | 4.481745 | 88.3 |
| 979 | 153.3134 | 5.032972 | 5.032484 | 153.39 |
| 1150 | ? | 3.459757 | ? | 31.81 |

**Exhibit A.8: Viscosity Measurements, Fulcher Fits, and Predictions at 1150 °C**
(continued)

## pha10

| Parameter | Estimate | ApproxStdErr |
|---|---|---|
| A | -4.211228647 | 0.68336661 |
| B | 8265.118085 | 1293.93434 |
| C | 134.6714148 | 73.7151825 |

**Graph**

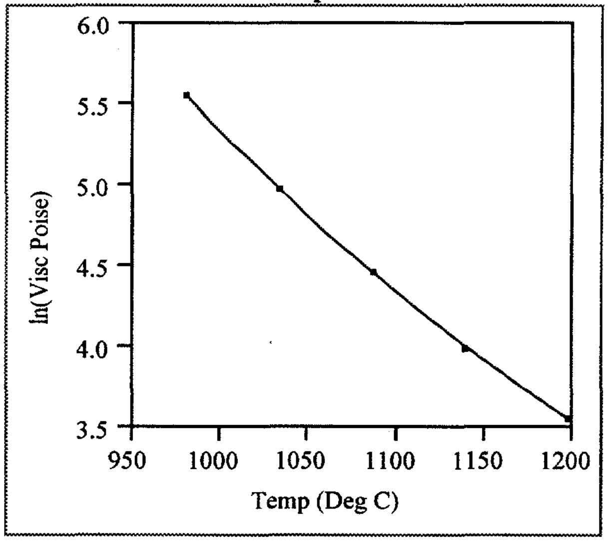


| Temp (Deg C) | Visc (Poise) | ln Visc (Fulcher) | ln(Visc Poise) | Visc Pred (poise) |
|---|---|---|---|---|
| 1198.5 | 35.23691 | 3.557991 | 3.562094 | 35.09 |
| 1140.5 | 54.40326 | 4.005995 | 3.996424 | 54.93 |
| 1088 | 86.78037 | 4.458519 | 4.46338 | 86.36 |
| 1034.5 | 144.9262 | 4.973985 | 4.976225 | 144.6 |
| 981 | 258.0073 | 5.554621 | 5.552988 | 258.43 |
| 1150 | ? | 3.92911 | ? | 50.86 |

**Exhibit A.8: Viscosity Measurements, Fulcher Fits, and Predictions at 1150 °C**
(continued)

# pha11

| Parameter | Estimate | ApproxStdErr |
|---|---|---|
| A | -4.401679211 | 0.68822425 |
| B | 8245.499811 | 1319.7412 |
| C | 123.1634512 | 76.3370491 |

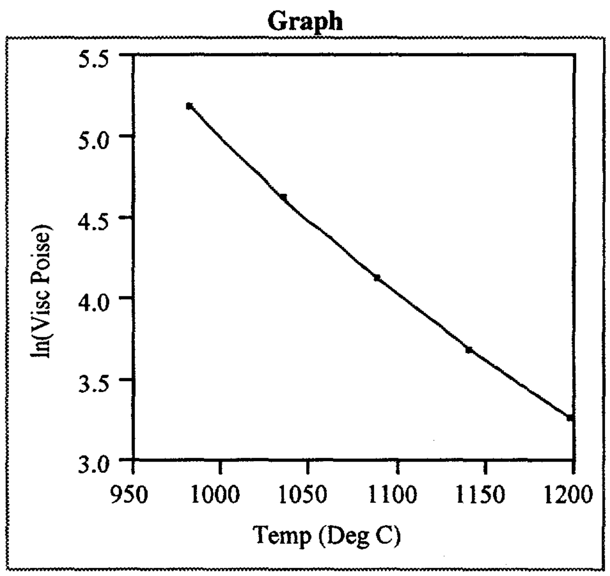


| Temp (Deg C) | Visc (Poise) | ln Visc (Fulcher) | ln(Visc Poise) | Visc Pred (poise) |
|---|---|---|---|---|
| 1198 | 26.41414 | 3.26972 | 3.273899 | 26.3 |
| 1141.5 | 39.88963 | 3.695349 | 3.686116 | 40.26 |
| 1088.5 | 63.04207 | 4.139901 | 4.143802 | 62.8 |
| 1035 | 103.968 | 4.64106 | 4.644083 | 103.65 |
| 982 | 180.7705 | 5.1991 | 5.197228 | 181.11 |
| 1150 | ? | 3.628323 | ? | 37.65 |

**Exhibit A.8: Viscosity Measurements, Fulcher Fits, and Predictions at 1150 °C**
(continued)

## pha12

| Parameter | Estimate | ApproxStdErr |
|---|---|---|
| A | -4.528030191 | 0.34283287 |
| B | 8160.360348 | 661.787426 |
| C | 117.3960937 | 38.9389514 |

**Graph**

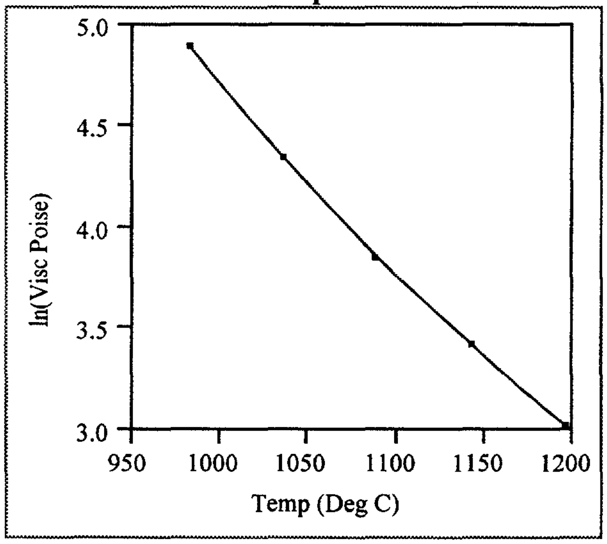


| Temp (Deg C) | Visc (Poise) | ln Visc (Fulcher) | ln(Visc Poise) | Visc Pred (poise) |
|---|---|---|---|---|
| 1197.5 | 20.60633 | 3.027132 | 3.025598 | 20.64 |
| 1144 | 30.71827 | 3.420859 | 3.424858 | 30.6 |
| 1089.5 | 47.6133 | 3.866505 | 3.863112 | 47.78 |
| 1036.5 | 77.58851 | 4.350575 | 4.351419 | 77.52 |
| 983 | 134.2111 | 4.899331 | 4.899414 | 134.2 |
| 1150 | ? | 3.374671 | ? | 29.21 |

**Exhibit A.8: Viscosity Measurements, Fulcher Fits, and Predictions at 1150 °C**
(continued)

## Batch 1
(Measured using Crucible/Spindle Set A after CST glasses)

| Parameter | Estimate | ApproxStdErr |
|---|---|---|
| A | -4.163417666 | 0.26297363 |
| B | 8160.6533445 | 498.124624 |
| C | 136.65295042 | 28.7540657 |

**Graph**

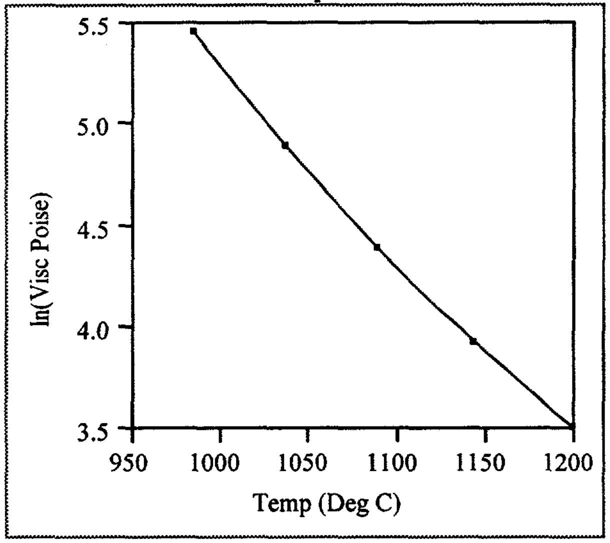


| Temp (Deg C) | Visc (Poise) | ln Visc (Fulcher) | ln(Visc Poise) | Visc Pred (poise) |
|---|---|---|---|---|
| 1199.5 | 33.6289 | 3.514689 | 3.515386 | 33.61 |
| 1143.5 | 51.48968 | 3.941739 | 3.941381 | 51.51 |
| 1089.5 | 81.3304 | 4.401077 | 4.39852 | 81.54 |
| 1037 | 134.8082 | 4.90048 | 4.903853 | 134.35 |
| 984 | 236.5726 | 5.46741 | 5.466255 | 236.85 |
| 1150 | ? | 3.88975 | ? | 48.90 |

**Exhibit A.8: Viscosity Measurements, Fulcher Fits, and Predictions at 1150 °C**
(continued)

# Batch 1

(Measured using Crucible/Spindle Set B after CST glasses)

| Parameter | Estimate | ApproxStdErr |
|---|---|---|
| A | -3.478220023 | 0.37284869 |
| B | 6922.5011794 | 652.766354 |
| C | 206.14511702 | 41.019357 |

**Graph**

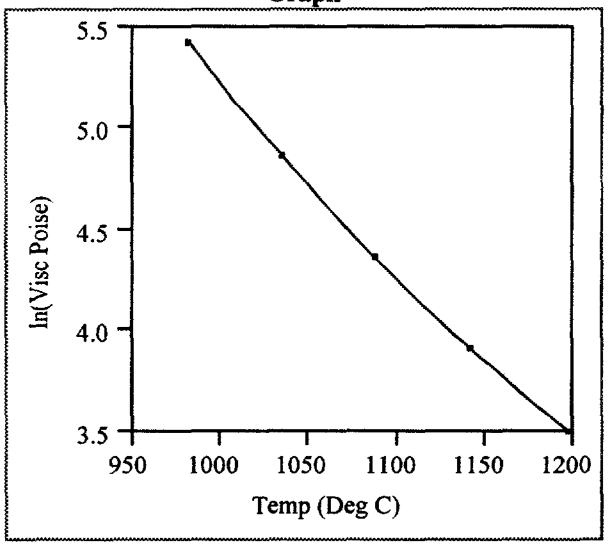


| Temp (Deg C) | Visc (Poise) | ln Visc (Fulcher) | ln(Visc Poise) | Visc Pred (poise) |
|---|---|---|---|---|
| 1198 | 33.24714 | 3.501129 | 3.503969 | 33.15 |
| 1142 | 50.05937 | 3.918761 | 3.91321 | 50.34 |
| 1089 | 78.5489 | 4.362821 | 4.363721 | 78.48 |
| 1035.5 | 130.5924 | 4.86863 | 4.872081 | 130.14 |
| 982.5 | 229.7086 | 5.438451 | 5.436812 | 230.09 |
| 1150 | ? | 3.856065 | ? | 47.28 |

# APPENDIX B.

## Discussion of Results from Re-batched Glasses

As plans were being made to measure the $T_L$'s for these PHA Phase 1 glasses, it was determined that there may not sufficient quantities of these glasses to support all desired property measurements. This led to a second set of 6 glasses (with the same target compositions as the first set) being batched and fabricated. These additional glasses were denoted (using an "r" for re-batch) as pha07r through pha12r and were submitted to the SRTC-ML for composition analyses. The analytical plan provided to the SRTC-ML is given as Attachment V of [4], and the resulting data are provided in Chart B.1 of this appendix. Display B.1 in this appendix provides plots of these data by glass sample id and oxide. Plots of the standards over the analytical blocks by oxide are provided in Display B.2 of this appendix. Table B.1 provides the average measured composition for the two standards included in this analytical plan. The reference values for the standards are also provided in this table.

**Table B.1: Measurements from Glass Standards for Re-Batched Glasses**

| | std (Batch 1) | | | u-std (Uranium-bearing Standard) | | |
|---|---|---|---|---|---|---|
| | Analytical Block | | | Analytical Block | | |
| | 1 | 2 | Reference | 1 | 2 | Reference |
| Oxide | 3 obs | 3 obs | Value | 2 obs | 2 obs | Value |
| $Al_2O_3$ | 4.535 | 4.554 | 4.877 | 3.694 | 3.817 | 4.100 |
| $B_2O_3$ | 8.136 | 7.492 | 7.777 | 9.000 | 9.515 | 9.209 |
| CaO | 1.171 | 1.176 | 1.220 | 1.233 | 1.293 | 1.301 |
| $Cr_2O_3$ | 0.138 | 0.073 | 0.107 | 0.272 | 0.225 | 0.000 |
| CuO | 0.379 | 0.384 | 0.399 | 0.013 | 0.009 | 0.000 |
| $Fe_2O_3$ | 13.048 | 13.573 | 12.839 | 13.046 | 14.075 | 13.196 |
| $K_2O$ | 3.168 | 3.321 | 3.327 | 2.885 | 2.933 | 2.999 |
| $Li_2O$ | 4.887 | 4.378 | 4.429 | 3.100 | 2.842 | 3.057 |
| MgO | 1.378 | 1.447 | 1.419 | 1.169 | 1.202 | 1.210 |
| MnO | 1.709 | 1.752 | 1.726 | 2.737 | 2.828 | 2.892 |
| $Na_2O$ | 9.036 | 9.054 | 9.003 | 11.748 | 11.849 | 11.795 |
| NiO | 0.742 | 0.791 | 0.751 | 1.049 | 1.126 | 1.120 |
| $SiO_2$ | 48.277 | 49.133 | 50.220 | 44.925 | 45.674 | 45.353 |
| $TiO_2$ | 0.643 | 0.688 | 0.677 | 0.951 | 0.973 | 1.049 |
| $U_3O_8$ | 0.295 | 0.295 | 0.000 | 2.305 | 2.317 | 2.406 |
| $ZrO_2$ | 0.091 | 0.088 | 0.098 | 0.007 | 0.012 | 0.000 |
| Sum of Oxides | 97.682 | 98.262 | 98.869 | 98.198 | 100.773 | 99.687 |

The information appearing in Table B.1 was used to bias-correct all measurements generated when the SRTC-ML conducted composition analyses for the re-batched glasses. Display B.3 in this appendix provides plots of these PHA Phase 1 glasses showing the targeted and measured compositions (for both the initial and re-batched glasses). Some observations regarding these plots are warranted. The measured boron values for the re-batched glasses (especially pha09r and pha12r) are much larger than their target values. Similarly, the sodium values for pha09r and pha12r are higher than targeted. A problem was discovered in the PHA batch used for these glasses. The PHA used for re-batching these Phase 1 glasses (PHA and CST) was also used in batching the Phase 2 glasses. It is anticipated that the anomalies for boron and sodium seen in these re-batched glasses may also occur in Phase 2 of these studies.

Finally, the $TiO_2$ values are lower than targeted for both the initial and re-batched glasses. For TiO2, the same behavior was seen in the CST Phase 1 glasses (i.e., measurements less than targeted). As discussed in [4], a larger than expected moisture content in the MST was discovered but not until after the Phase 1 and 2 glasses for both programs, PHA and CST, had been batched. Glasses for Phases 3 and 4 are to be batched in a manner fully accounting for the loss of the additional MST moisture. In addition, Phase 4 is to include selected glasses from the first two phases that are to re-batched using the new formulations. This will provide better coverage of the higher MST loadings for these phases of the PHA study.

Table B.2 also provides a complete look at the compositions from Phase 1, both the initial and the re-batched glasses.

## Table B.2: Target, Measured and Bias-Corrected Compositions (in wt%) for the Phase 1 Glasses

| | Batch 1 | | | | | Uranium Standard (u-std) | | | | |
|---|---|---|---|---|---|---|---|---|---|---|
| | | | Measured | Re-Batched | | | | Meas. | Re-Batched | |
| | Target | Measured | Bias-cor. | Meas. | Bias-cor. | Target | Meas. | Bias-cor. | Meas. | Bias-cor. |
| $Al_2O_3$ | 4.877 | 4.544 | 4.877 | 4.686 | 4.911 | 4.100 | 3.755 | 4.030 | 3.840 | 3.997 |
| $B_2O_3$ | 7.777 | 7.814 | 7.777 | 8.077 | 7.777 | 9.209 | 9.257 | 9.220 | 9.370 | 9.027 |
| CaO | 1.220 | 1.173 | 1.220 | 1.299 | 1.220 | 1.301 | 1.263 | 1.313 | 1.379 | 1.295 |
| $Cr_2O_3$ | 0.107 | 0.105 | 0.107 | 0.100 | 0.109 | 0.000 | 0.248 | 0.271 | 0.232 | 0.248 |
| CuO | 0.399 | 0.381 | 0.399 | 0.382 | 0.404 | 0.000 | 0.011 | 0.012 | 0.010 | 0.011 |
| $Fe_2O_3$ | 12.839 | 13.311 | 12.839 | 12.195 | 12.601 | 13.196 | 13.561 | 13.076 | 12.288 | 12.944 |
| $K_2O$ | 3.327 | 3.244 | 3.327 | 3.341 | 3.327 | 2.999 | 2.909 | 2.984 | 2.966 | 2.954 |
| $Li_2O$ | 4.429 | 4.632 | 4.429 | 4.198 | 4.429 | 3.057 | 2.971 | 2.838 | 2.831 | 2.987 |
| MgO | 1.419 | 1.413 | 1.419 | 1.384 | 1.414 | 1.210 | 1.186 | 1.191 | 1.121 | 1.150 |
| MnO | 1.726 | 1.730 | 1.726 | 1.659 | 1.738 | 2.892 | 2.783 | 2.776 | 2.618 | 2.723 |
| $Na_2O$ | 9.003 | 9.045 | 9.003 | 9.189 | 9.003 | 11.795 | 11.798 | 11.744 | 12.159 | 11.915 |
| NiO | 0.751 | 0.766 | 0.751 | 0.721 | 0.753 | 1.120 | 1.087 | 1.065 | 1.020 | 1.063 |
| $SiO_2$ | 50.220 | 48.705 | 50.220 | 49.453 | 50.220 | 45.353 | 45.300 | 46.711 | 46.369 | 47.048 |
| $TiO_2$ | 0.677 | 0.666 | 0.677 | 0.679 | 0.673 | 1.049 | 0.962 | 0.979 | 0.983 | 0.981 |
| $U_3O_8$ | 0.000 | 0.295 | 0.295 | 0.590 | 0.590 | 2.406 | 2.311 | 2.311 | 2.258 | 2.258 |
| $ZrO_2$ | 0.098 | 0.090 | 0.098 | 0.092 | 0.097 | 0.000 | 0.009 | 0.010 | 0.010 | 0.011 |
| Sum of Oxides | 98.869 | 97.972 | 99.221 | 98.092 | 99.744 | 99.687 | 99.485 | 100.604 | 99.518 | 100.673 |
| | **pha07** | | | | | **pha08** | | | | |
| | | | Measured | Re-Batched | | | | Meas. | Re-Batched | |
| | Target | Measured | Bias-cor. | Meas. | Bias-cor. | Target | Meas. | Bias-cor. | Meas. | Bias-cor. |
| $Al_2O_3$ | 2.901 | 2.650 | 2.758 | 2.693 | 2.890 | 2.883 | 2.711 | 2.822 | 2.768 | 2.971 |
| $B_2O_3$ | 7.660 | 7.688 | 7.403 | 7.832 | 7.801 | 8.488 | 8.766 | 8.435 | 9.434 | 9.393 |
| CaO | 1.092 | 1.119 | 1.051 | 0.983 | 1.021 | 1.088 | 1.129 | 1.060 | 1.049 | 1.091 |
| $Cr_2O_3$ | 0.125 | 0.121 | 0.129 | 0.117 | 0.121 | 0.125 | 0.113 | 0.120 | 0.129 | 0.135 |
| CuO | 0.576 | 0.492 | 0.514 | 0.524 | 0.548 | 0.800 | 0.693 | 0.725 | 0.641 | 0.671 |
| $Fe_2O_3$ | 11.685 | 10.308 | 10.855 | 10.973 | 10.583 | 11.683 | 10.626 | 11.201 | 10.787 | 10.404 |
| $K_2O$ | 3.365 | 3.084 | 3.071 | 3.632 | 3.725 | 4.745 | 4.352 | 4.335 | 4.526 | 4.643 |
| $Li_2O$ | 4.510 | 4.236 | 4.468 | 4.586 | 4.380 | 4.305 | 4.080 | 4.304 | 4.225 | 4.040 |
| MgO | 1.381 | 1.382 | 1.417 | 1.408 | 1.415 | 1.322 | 1.331 | 1.365 | 1.346 | 1.352 |
| MnO | 2.041 | 1.863 | 1.938 | 1.946 | 1.941 | 2.041 | 1.875 | 1.950 | 2.105 | 2.099 |
| $Na_2O$ | 8.116 | 8.071 | 7.910 | 8.068 | 8.030 | 8.264 | 8.391 | 8.222 | 8.711 | 8.671 |
| NiO | 1.099 | 0.866 | 0.902 | 0.927 | 0.908 | 1.099 | 0.861 | 0.897 | 0.980 | 0.959 |
| $SiO_2$ | 50.766 | 50.274 | 51.040 | 50.113 | 51.679 | 48.486 | 50.006 | 50.778 | 48.776 | 50.297 |
| $TiO_2$ | 1.126 | 0.691 | 0.689 | 0.665 | 0.676 | 1.125 | 0.698 | 0.697 | 0.675 | 0.686 |
| $U_3O_8$ | 2.367 | 2.633 | 2.633 | 2.426 | 2.426 | 2.367 | 2.161 | 2.161 | 1.928 | 1.928 |
| $ZrO_2$ | 0.129 | 0.128 | 0.137 | 0.125 | 0.137 | 0.129 | 0.126 | 0.134 | 0.138 | 0.151 |
| Sum of Oxides | 98.939 | 95.647 | 96.958 | 97.069 | 98.333 | 98.950 | 97.963 | 99.250 | 98.270 | 99.542 |
| | **pha09** | | | | | **pha10** | | | | |
| | | | Measured | Re-Batched | | | | Meas. | Re-Batched | |
| | Target | Measured | Bias-cor. | Meas. | Bias-cor. | Target | Meas. | Bias-cor. | Meas. | Bias-cor. |
| $Al_2O_3$ | 2.865 | 2.707 | 2.817 | 2.664 | 2.859 | 2.894 | 2.636 | 2.743 | 2.820 | 3.026 |
| $B_2O_3$ | 9.317 | 9.410 | 9.068 | 11.503 | 11.449 | 7.561 | 7.985 | 7.693 | 7.293 | 7.231 |
| CaO | 1.083 | 1.099 | 1.032 | 0.983 | 1.022 | 1.090 | 1.109 | 1.043 | 1.027 | 1.067 |
| $Cr_2O_3$ | 0.125 | 0.113 | 0.121 | 0.121 | 0.125 | 0.125 | 0.113 | 0.121 | 0.128 | 0.133 |
| CuO | 1.023 | 0.761 | 0.795 | 0.853 | 0.892 | 0.576 | 0.501 | 0.523 | 0.460 | 0.482 |
| $Fe_2O_3$ | 11.681 | 9.951 | 10.475 | 11.287 | 10.888 | 11.684 | 9.701 | 10.205 | 11.477 | 11.068 |
| $K_2O$ | 6.125 | 5.294 | 5.273 | 4.638 | 4.756 | 3.365 | 3.123 | 3.111 | 3.635 | 3.730 |
| $Li_2O$ | 4.099 | 4.037 | 4.259 | 3.789 | 3.624 | 4.425 | 4.295 | 4.533 | 4.516 | 4.308 |
| MgO | 1.262 | 1.272 | 1.304 | 1.221 | 1.227 | 1.356 | 1.337 | 1.370 | 1.375 | 1.381 |
| MnO | 2.041 | 1.905 | 1.981 | 1.717 | 1.713 | 2.041 | 1.853 | 1.928 | 2.066 | 2.061 |
| $Na_2O$ | 8.412 | 8.374 | 8.206 | 9.001 | 8.959 | 8.191 | 8.341 | 8.178 | 8.206 | 8.168 |
| NiO | 1.099 | 0.857 | 0.893 | 0.880 | 0.862 | 1.099 | 0.838 | 0.873 | 0.983 | 0.963 |
| $SiO_2$ | 46.206 | 48.081 | 48.940 | 44.979 | 46.369 | 49.816 | 51.343 | 52.180 | 49.685 | 51.234 |
| $TiO_2$ | 1.124 | 0.707 | 0.705 | 0.663 | 0.674 | 2.224 | 1.369 | 1.365 | 1.301 | 1.322 |
| $U_3O_8$ | 2.367 | 2.565 | 2.565 | 2.314 | 2.314 | 2.367 | 2.409 | 2.409 | 1.698 | 1.698 |
| $ZrO_2$ | 0.129 | 0.132 | 0.140 | 0.147 | 0.160 | 0.129 | 0.126 | 0.134 | 0.132 | 0.144 |
| Sum of Oxides | 98.958 | 97.306 | 98.618 | 96.816 | 97.950 | 98.943 | 97.171 | 98.504 | 96.903 | 98.119 |

**Table B.2: Target, Measured and Bias-Corrected Compositions (in wt%) for the Phase 1 Glasses (continued)**

| | pha11 | | | | | pha12 | | | | |
|---|---|---|---|---|---|---|---|---|---|---|
| | | | Measured | Re-Batched | | | | Meas. | Re-Batched | |
| | Target | Measured | Bias-cor. | Meas. | Bias-cor. | Target | Meas. | Bias-cor. | Meas. | Bias-cor. |
| $Al_2O_3$ | 2.876 | 2.664 | 2.773 | 3.080 | 3.305 | 2.858 | 2.626 | 2.733 | 2.749 | 2.950 |
| $B_2O_3$ | 8.390 | 8.967 | 8.646 | 9.893 | 9.843 | 9.219 | 9.724 | 9.375 | 12.244 | 12.225 |
| CaO | 1.086 | 1.102 | 1.036 | 0.999 | 1.039 | 1.081 | 1.114 | 1.047 | 1.018 | 1.059 |
| $Cr_2O_3$ | 0.125 | 0.117 | 0.124 | 0.117 | 0.120 | 0.125 | 0.111 | 0.119 | 0.121 | 0.126 |
| CuO | 0.800 | 0.676 | 0.707 | 0.643 | 0.673 | 1.023 | 0.818 | 0.855 | 0.905 | 0.947 |
| $Fe_2O_3$ | 11.682 | 9.879 | 10.403 | 11.084 | 10.696 | 11.680 | 10.344 | 10.880 | 10.462 | 10.092 |
| $K_2O$ | 4.745 | 4.255 | 4.239 | 4.135 | 4.239 | 6.125 | 5.514 | 5.491 | 4.752 | 4.876 |
| $Li_2O$ | 4.219 | 4.091 | 4.315 | 4.150 | 3.968 | 4.013 | 3.929 | 4.145 | 3.908 | 3.718 |
| MgO | 1.297 | 1.285 | 1.317 | 1.266 | 1.272 | 1.237 | 1.230 | 1.261 | 1.249 | 1.255 |
| MnO | 2.041 | 1.840 | 1.914 | 1.804 | 1.800 | 2.041 | 1.837 | 1.910 | 1.979 | 1.974 |
| $Na_2O$ | 8.339 | 8.432 | 8.266 | 8.314 | 8.275 | 8.487 | 8.543 | 8.373 | 9.601 | 9.556 |
| NiO | 1.099 | 0.861 | 0.898 | 0.894 | 0.876 | 1.099 | 0.849 | 0.885 | 0.938 | 0.919 |
| $SiO_2$ | 47.536 | 51.236 | 52.113 | 46.476 | 47.929 | 45.256 | 48.669 | 49.502 | 44.551 | 45.937 |
| $TiO_2$ | 2.223 | 1.337 | 1.334 | 1.269 | 1.290 | 2.222 | 1.350 | 1.346 | 1.316 | 1.339 |
| $U_3O_8$ | 2.367 | 2.462 | 2.462 | 2.072 | 2.072 | 2.367 | 2.456 | 2.456 | 2.158 | 2.158 |
| $ZrO_2$ | 0.129 | 0.122 | 0.130 | 0.134 | 0.147 | 0.129 | 0.122 | 0.129 | 0.135 | 0.147 |
| Sum of Oxides | 98.954 | 99.415 | 100.764 | 96.432 | 97.647 | 98.962 | 99.327 | 100.600 | 98.192 | 99.385 |

The liquidus temperature for each re-batched glass was estimated by performing isothermal holds (as discussed in the body of this report) at 900°C, 950°C, 1000°C, and 1050°C. Approximately 5 grams of glass were placed in a small platinum crucible and transferred to a furnace already heated to 1150°C. After a four-hour hold period, the temperature was reduced to 900°C, 950°C, 1000°C, or 1050°C and held at that temperature for 24 hours. The crucible was then removed from the furnace and the glass allowed to cool within the crucible at room temperature. For these experiments, twelve glasses were treated together. The twelve glasses consisted of the six re-batched CST and six re-batched PHA glasses containing 26 wt% Purex simulated sludge. Therefore, the CST and PHA glasses experienced essentially identical heat treatments. The six PHA glasses at 900°C were submitted for XRD analysis. Care was taken to obtain glass that was not part of the top glass surface. The glass pieces, although mainly from the bulk, usually included part of the bottom surface (i.e., that surface in contact with the crucible).

The XRD analysis revealed no crystals in any of the glasses to the detection limit of the technique (~0.7 to 1.0 wt%). Therefore, the approximate liquidus temperatures for the six PHA glasses were:

**Table B.3: Liquidus Temperatures**

| GLASS ID | LIQUIDUS TEMPERATURE |
|---|---|
| pha07 | <900°C |
| pha08 | <900°C |
| pha09 | <900°C |
| pha10 | <900°C |
| pha11 | <900°C |
| pha12 | <900°C |

To the scale of XRD, the liquidus temperatures for these glasses are likely well below the nominal property acceptance region (PAR) value of 1025 °C [10] and readily meet DWPF processing requirements for liquidus temperature. The model predictions for these six glasses are given in Table B.4.

**Table B.4: Liquidus Temperature Predictions**

| | Liquidus Temperature Property Prediction based on | | | | |
|---|---|---|---|---|---|
| Glass ID | Target Composition | Measured Composition | Bias-Corrected Composition | Re-batched Measured Composition | Re-batched Bias-Corrected Composition |
| pha07 | 988.0 | 966.8 | 973.2 | 978.2 | 967.4 |
| pha08 | 997.3 | 973.2 | 980.0 | 980.7 | 969.8 |
| pha09 | 1007.6 | 969.2 | 975.2 | 1005.3 | 993.0 |
| pha10 | 991.8 | 953.7 | 959.3 | 988.6 | 977.2 |
| pha11 | 1001.5 | 957.0 | 962.7 | 997.3 | 985.6 |
| pha12 | 1012.2 | 973.1 | 979.2 | 993.0 | 981.5 |

These data suggest that the predictions may be too conservative for these glasses. A new liquidus temperature model is being developed with a goal of preventing unnecessarily conservative constraints on this property.

## Surface Crystallization

For liquidus measurements, crystal formation is considered only in the interior or bulk glass region. Therefore, samples submitted for XRD analysis were bulk samples. However, crystals can form at the interface of the glass and the crucible and/or the glass and air. For completeness, the detection of these surface crystals on the top of the glass is provided in Table B.5 as a function of temperature.

**Table B.5. Surface Crystals for the Six PHA Glasses as Function of Temperature after the 24 hour heat treatment.**

| | pha07 | pha 08 | pha 09 | pha 10 | pha 11 | pha 12 |
|---|---|---|---|---|---|---|
| 1150°C | None | None | None | None | None | None |
| 1000°C | None | None | None | None | None | None |
| 950°C | None | None | None | None | None | None |
| 900°C | None | None | None | None | None | None |

As shown in Table B.5, no surface crystallization was detected for any of the glasses at these temperatures.

## Summary of Information for Appendix B

The information provided in this appendix regarding the six re-batched glasses is included for completeness. A problem was seen in the PHA batch used for these glasses. The higher boron and sodium levels seen in these glasses pushes components of the PHA beyond the target levels intended. Only liquidus temperature and surface crystallization were investigated for these glasses, and no problems were seen. Additional discussion is anticipated in Phase 2 due to the PHA batch being used in the preparation of the glasses for that phase.

## Chart B.1: Composition Measurements for Re-Batched Glasses
(expressed as cation wt%'s)

| Planning | Glass | Lithium Metaborate Dissolution | | | | | | | | | | | | | | | | Lithium Metaborate Dissolution | | | | | | Peroxide Fusion Dissolution | | | | |
|---|---|---|---|---|---|---|---|---|---|---|---|---|---|---|---|---|---|---|---|---|---|---|---|---|---|---|---|---|
| Sample ID | Sample ID | Block | Seq | Lab ID | Al | Ca | Cr | Cu | Fe | Mg | Mn | Ni | Si | Ti | U | Zr | | Block | Seq | Lab ID | Na | K | | Block | Seq | Lab ID | Li | B |
| std | std | 1 | 1 | stdlm11 | 2.42 | 0.845 | 0.093 | 0.307 | 9.36 | 0.88 | 1.35 | 0.578 | 22.8 | 0.414 | <0.500 | 0.07 | | 1 | 1 | stdlm11 | 6.80 | 2.64 | | 1 | 1 | stdpf11 | 2.42 | 2.64 |
| std | std | 1 | 14 | stdlm12 | 2.47 | 0.844 | 0.093 | 0.296 | 8.86 | 0.816 | 1.31 | 0.593 | 22.0 | 0.367 | <0.500 | 0.067 | | 1 | 15 | stdlm12 | 6.74 | 2.66 | | 1 | 15 | stdpf12 | 2.15 | 2.81 |
| std | std | 1 | 29 | stdlm13 | 2.31 | 0.821 | 0.098 | 0.305 | 9.16 | 0.798 | 1.31 | 0.578 | 22.9 | 0.376 | <0.500 | 0.065 | | 1 | 29 | stdlm13 | 6.57 | 2.59 | | 1 | 29 | stdpf13 | 2.24 | 2.13 |
| std | std | 2 | 1 | stdlm21 | 2.56 | 0.883 | 0.051 | 0.324 | 9.72 | 0.871 | 1.32 | 0.607 | 23.6 | 0.415 | <0.500 | 0.068 | | 2 | 1 | stdlm21 | 6.62 | 2.78 | | 2 | 1 | stdpf21 | 2.08 | 2.36 |
| std | std | 2 | 14 | stdlm22 | 2.37 | 0.848 | 0.049 | 0.3 | 9.22 | 0.852 | 1.38 | 0.618 | 22.5 | 0.412 | <0.500 | 0.064 | | 2 | 15 | stdlm22 | 6.82 | 2.77 | | 2 | 15 | stdpf22 | 1.91 | 2.10 |
| std | std | 2 | 29 | stdlm23 | 2.3 | 0.791 | 0.049 | 0.296 | 9.54 | 0.895 | 1.37 | 0.64 | 22.8 | 0.41 | <0.500 | 0.064 | | 2 | 29 | stdlm23 | 6.71 | 2.72 | | 2 | 29 | stdpf23 | 2.11 | 2.52 |
| u-std | u-std | 1 | 8 | ustdlm11 | 1.89 | 0.893 | 0.182 | 0.011 | 8.83 | 0.719 | 2.13 | 0.824 | 21.1 | 0.583 | 1.92 | <0.010 | | 1 | 8 | ustdlm11 | 8.73 | 2.36 | | 1 | 8 | ustdpf11 | 1.58 | 2.84 |
| u-std | u-std | 2 | 8 | ustdlm21 | 2 | 0.909 | 0.157 | 0.01 | 9.49 | 0.737 | 2.14 | 0.854 | 21.1 | 0.588 | 1.87 | <0.010 | | 1 | 22 | ustdlm12 | 8.84 | 2.43 | | 1 | 22 | ustdpf12 | 1.38 | 3.06 |
| u-std | u-std | 2 | 21 | ustdlm22 | 2.04 | 0.939 | 0.151 | <0.010 | 10.2 | 0.713 | 2.24 | 0.915 | 21.6 | 0.579 | 2.06 | 0.013 | | 2 | 8 | ustdlm21 | 8.74 | 2.44 | | 2 | 8 | ustdpf21 | 1.26 | 2.85 |
| u-std | u-std | 1 | 21 | ustlm12 | 2.02 | 0.87 | 0.19 | 0.01 | 9.42 | 0.691 | 2.11 | 0.824 | 20.9 | 0.557 | 1.99 | <0.010 | | 2 | 22 | ustdlm22 | 8.70 | 2.43 | | 2 | 22 | ustdpf22 | 1.30 | 2.75 |
| pha11r | pha09r | 1 | 10 | w1lm11 | 1.38 | 0.689 | 0.105 | 0.678 | 7.69 | 0.711 | 1.31 | 0.678 | 20.2 | 0.386 | 1.9 | 0.111 | | 1 | 16 | w1lm11 | 6.71 | 3.87 | | 1 | 10 | w1pf11 | 1.98 | 3.68 |
| pha11r | pha09r | 2 | 6 | w1lm12 | 1.45 | 0.717 | 0.062 | 0.702 | 8.01 | 0.745 | 1.36 | 0.718 | 22.1 | 0.415 | 2.02 | 0.111 | | 2 | 4 | w1lm12 | 6.63 | 3.91 | | 2 | 7 | w1pf12 | 1.73 | 3.43 |
| pha11r | pha09r | 1 | 15 | w1lm21 | 1.38 | 0.687 | 0.103 | 0.637 | 7.81 | 0.749 | 1.32 | 0.682 | 20.5 | 0.379 | 1.96 | 0.106 | | 1 | 24 | w1lm21 | 6.57 | 3.68 | | 1 | 24 | w1pf21 | 1.72 | 3.76 |
| pha11r | pha09r | 2 | 12 | w1lm22 | 1.43 | 0.716 | 0.061 | 0.709 | 8.07 | 0.74 | 1.33 | 0.687 | 21.3 | 0.409 | 1.97 | 0.106 | | 2 | 21 | w1lm22 | 6.80 | 3.94 | | 2 | 12 | w1pf22 | 1.61 | 3.42 |
| pha07r | pha07r | 1 | 22 | w3lm11 | 1.38 | 0.682 | 0.099 | 0.41 | 7.58 | 0.842 | 1.48 | 0.708 | 23.5 | 0.372 | 2.03 | 0.095 | | 1 | 7 | w3lm11 | 6.01 | 2.95 | | 1 | 28 | w3pf11 | 2.29 | 2.67 |
| pha07r | pha07r | 2 | 15 | w3lm12 | 1.44 | 0.732 | 0.061 | 0.416 | 7.95 | 0.85 | 1.54 | 0.758 | 23.5 | 0.431 | 2.18 | 0.091 | | 2 | 19 | w3lm12 | 5.93 | 3.06 | | 2 | 21 | w3pf12 | 1.88 | 2.30 |
| pha07r | pha07r | 1 | 17 | w3lm21 | 1.43 | 0.682 | 0.102 | 0.413 | 7.36 | 0.848 | 1.46 | 0.705 | 23.6 | 0.388 | 1.98 | 0.093 | | 1 | 14 | w3lm21 | 6.08 | 2.99 | | 1 | 19 | w3pf21 | 2.29 | 2.32 |
| pha07r | pha07r | 2 | 9 | w3lm22 | 1.45 | 0.713 | 0.059 | 0.434 | 7.81 | 0.856 | 1.55 | 0.742 | 23.1 | 0.403 | 2.04 | 0.091 | | 2 | 5 | w3lm22 | 5.92 | 3.06 | | 2 | 17 | w3pf22 | 2.06 | 2.44 |
| pha08r | pha10r | 1 | 25 | w5lm11 | 1.47 | 0.718 | 0.109 | 0.353 | 7.77 | 0.805 | 1.56 | 0.757 | 23.4 | 0.726 | 1.49 | 0.096 | | 1 | 2 | w5lm11 | 6.18 | 2.98 | | 1 | 6 | w5pf11 | 2.36 | 2.45 |
| pha08r | pha10r | 2 | 25 | w5lm12 | 1.48 | 0.75 | 0.065 | 0.377 | 8.3 | 0.851 | 1.64 | 0.793 | 23.0 | 0.839 | 1.44 | 0.1 | | 2 | 10 | w5lm12 | 5.93 | 2.96 | | 2 | 13 | w5pf12 | 1.85 | 2.02 |
| pha08r | pha10r | 1 | 18 | w5lm21 | 1.46 | 0.717 | 0.108 | 0.359 | 7.82 | 0.803 | 1.57 | 0.761 | 22.9 | 0.737 | 1.43 | 0.097 | | 1 | 10 | w5lm21 | 6.13 | 3.08 | | 1 | 23 | w5pf21 | 2.23 | 2.69 |
| pha08r | pha10r | 2 | 18 | w5lm22 | 1.56 | 0.75 | 0.069 | 0.382 | 8.22 | 0.858 | 1.63 | 0.778 | 23.6 | 0.817 | 1.4 | 0.098 | | 2 | 18 | w5lm22 | 6.11 | 3.05 | | 2 | 10 | w5pf22 | 1.95 | 1.90 |
| pha09r | pha08r | 1 | 26 | w6lm11 | 1.4 | 0.746 | 0.114 | 0.5 | 7.34 | 0.798 | 1.6 | 0.744 | 22.4 | 0.378 | 1.67 | 0.099 | | 1 | 26 | w6lm11 | 6.41 | 3.68 | | 1 | 27 | w6pf11 | 2.16 | 2.98 |
| pha09r | pha08r | 2 | 2 | w6lm12 | 1.52 | 0.787 | 0.071 | 0.538 | 7.76 | 0.817 | 1.65 | 0.805 | 23.0 | 0.447 | 1.63 | 0.104 | | 2 | 6 | w6lm12 | 6.53 | 3.81 | | 2 | 6 | w6pf12 | 1.73 | 2.51 |
| pha09r | pha08r | 1 | 20 | w6lm21 | 1.46 | 0.707 | 0.103 | 0.503 | 7.4 | 0.808 | 1.59 | 0.722 | 23.2 | 0.379 | 1.61 | 0.104 | | 1 | 6 | w6lm21 | 6.42 | 3.75 | | 1 | 4 | w6pf21 | 1.97 | 3.08 |
| pha09r | pha08r | 2 | 23 | w6lm22 | 1.48 | 0.76 | 0.066 | 0.508 | 7.68 | 0.824 | 1.68 | 0.808 | 22.6 | 0.414 | 1.63 | 0.101 | | 2 | 20 | w6lm22 | 6.49 | 3.79 | | 2 | 19 | w6pf22 | 1.99 | 3.15 |
| pha10r | pha11r | 1 | 12 | w7lm11 | 1.53 | 0.706 | 0.106 | 0.511 | 7.86 | 0.746 | 1.38 | 0.674 | 21.4 | 0.749 | 1.66 | 0.101 | | 1 | 27 | w7lm11 | 5.97 | 3.27 | | 1 | 25 | w7pf11 | 2.00 | 3.18 |
| pha10r | pha11r | 2 | 13 | w7lm12 | 1.69 | 0.725 | 0.061 | 0.517 | 7.63 | 0.796 | 1.42 | 0.703 | 21.7 | 0.817 | 1.76 | 0.098 | | 2 | 28 | w7lm12 | 6.06 | 3.53 | | 2 | 2 | w7pf12 | 1.86 | 3.12 |
| pha10r | pha11r | 1 | 24 | w7lm21 | 1.57 | 0.672 | 0.097 | 0.496 | 7.73 | 0.753 | 1.4 | 0.703 | 22.4 | 0.697 | 1.84 | 0.098 | | 1 | 20 | w7lm21 | 6.11 | 3.39 | | 1 | 17 | w7pf21 | 2.06 | 3.27 |
| pha10r | pha11r | 2 | 7 | w7lm22 | 1.73 | 0.753 | 0.056 | 0.531 | 7.79 | 0.76 | 1.39 | 0.729 | 21.4 | 0.78 | 1.77 | 0.101 | | 2 | 14 | w7lm22 | 6.53 | 3.54 | | 2 | 9 | w7pf22 | 1.79 | 2.72 |
| pha12r | pha12r | 1 | 11 | w9lm11 | 1.39 | 0.693 | 0.103 | 0.711 | 7.13 | 0.758 | 1.52 | 0.705 | 20.6 | 0.76 | 1.84 | 0.099 | | 1 | 13 | w9lm11 | 7.24 | 4 | | 1 | 2 | w9pf11 | 2.13 | 3.79 |
| pha12r | pha12r | 2 | 4 | w9lm12 | 1.52 | 0.751 | 0.064 | 0.733 | 7.42 | 0.767 | 1.54 | 0.756 | 20.8 | 0.799 | 1.9 | 0.101 | | 2 | 25 | w9lm12 | 7.24 | 3.88 | | 2 | 27 | w9pf12 | 1.55 | 3.97 |
| pha12r | pha12r | 1 | 6 | w9lm21 | 1.43 | 0.733 | 0.101 | 0.705 | 7.28 | 0.735 | 1.5 | 0.724 | 20.7 | 0.769 | 1.76 | 0.1 | | 1 | 4 | w9lm21 | 6.95 | 3.89 | | 1 | 20 | w9pf21 | 2.02 | 3.54 |
| pha12r | pha12r | 2 | 3 | w9lm22 | 1.48 | 0.734 | 0.062 | 0.744 | 7.44 | 0.752 | 1.57 | 0.762 | 21.2 | 0.828 | 1.82 | 0.099 | | 2 | 27 | w9lm22 | 7.06 | 4.01 | | 2 | 23 | w9pf22 | 1.56 | 3.91 |

**Display B.1: Measurements of Re-Batched Glasses by Oxide**

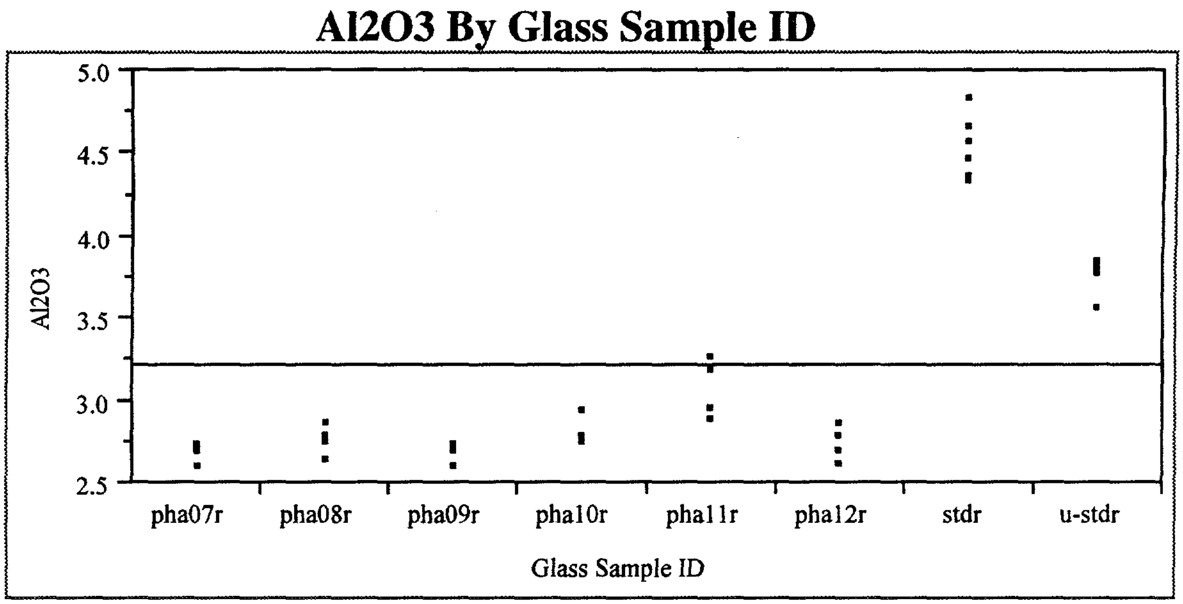


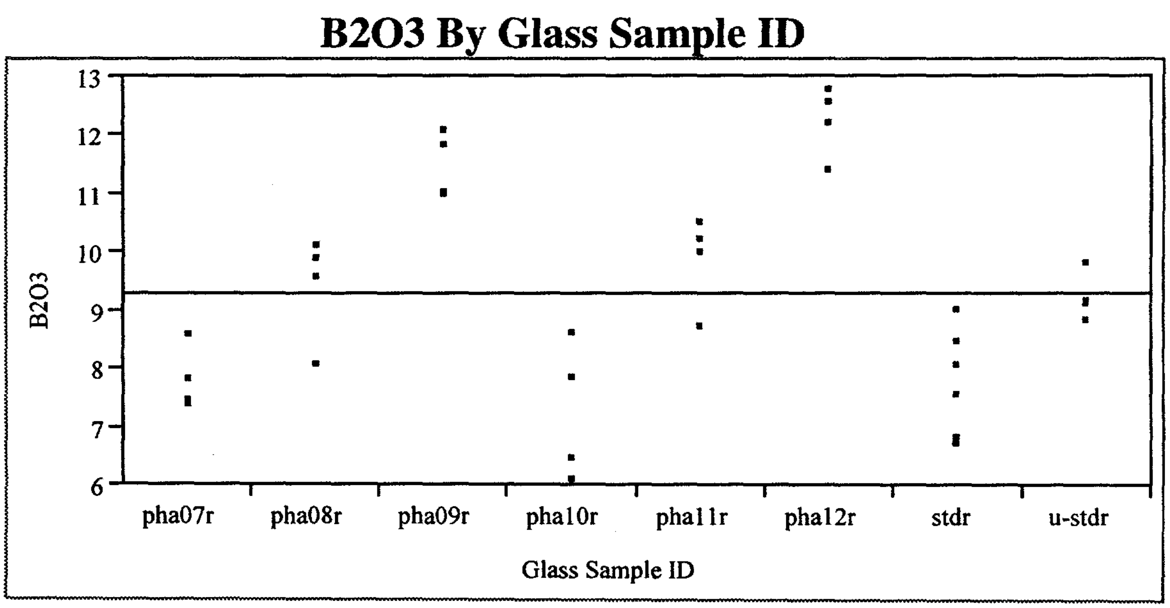

**Display B.1: Measurements of Re-Batched Glasses by Oxide**
(continued)

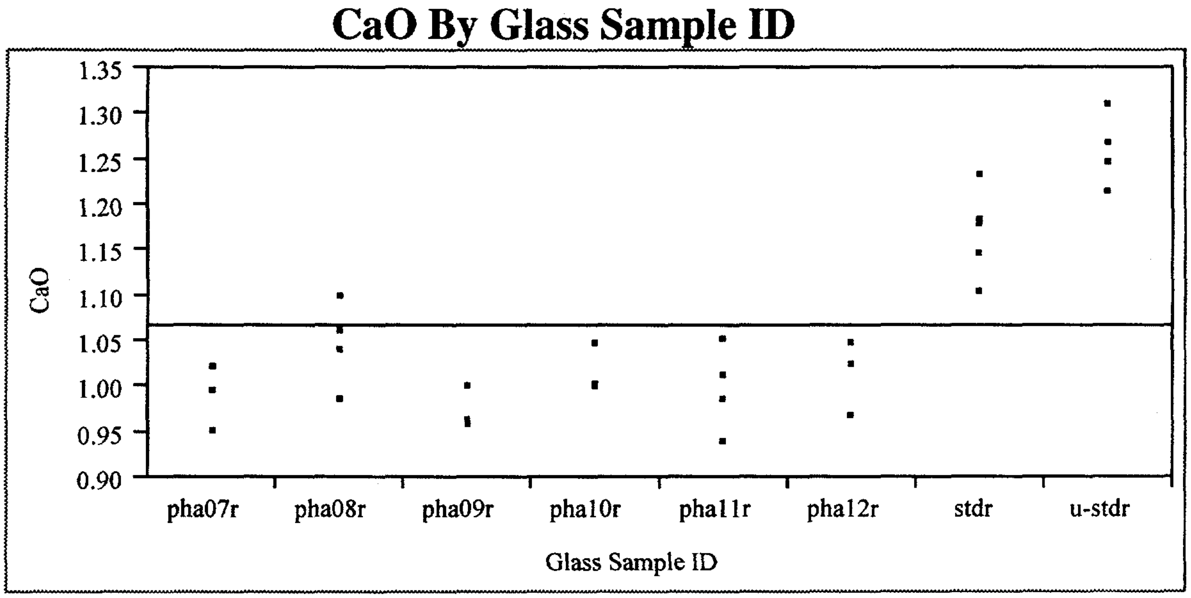


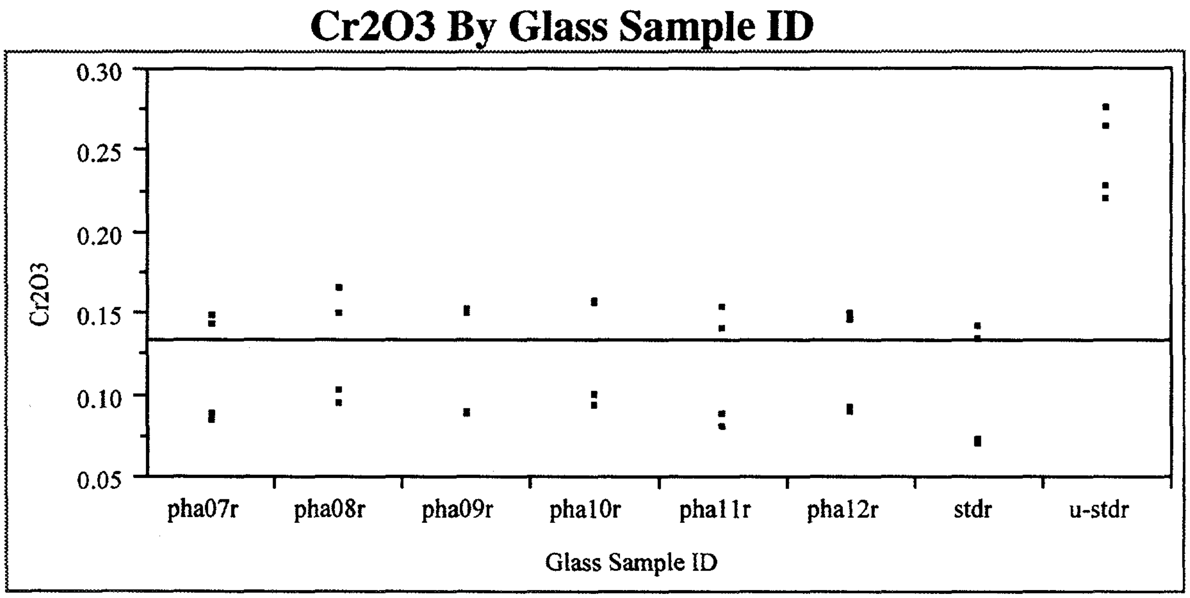

**Display B.1: Measurements of Re-Batched Glasses by Oxide**
(continued)

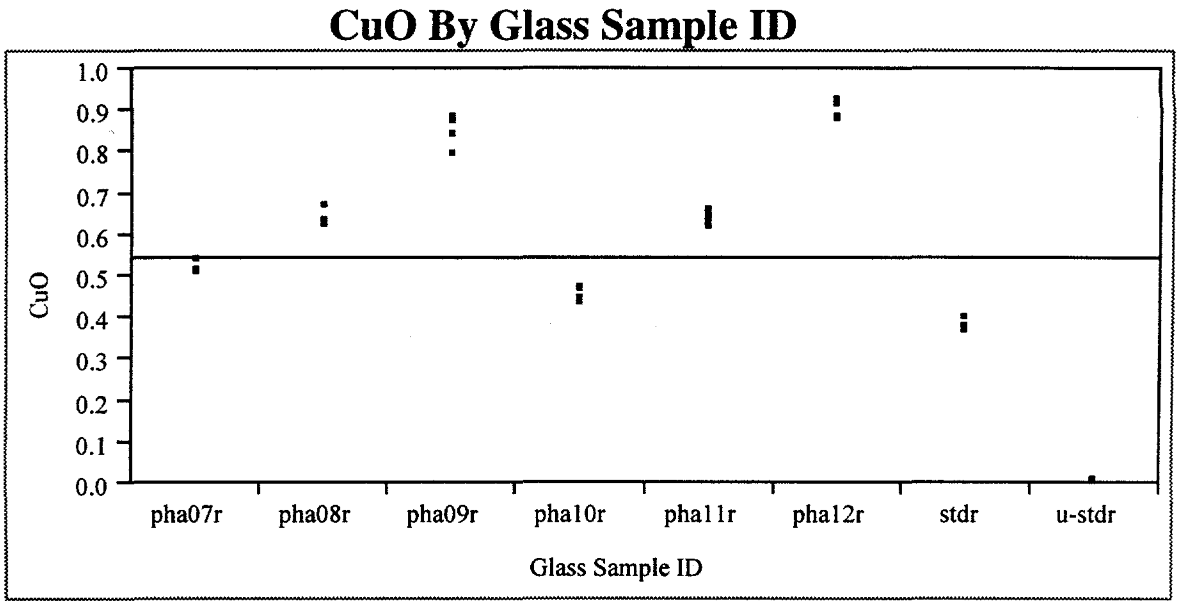


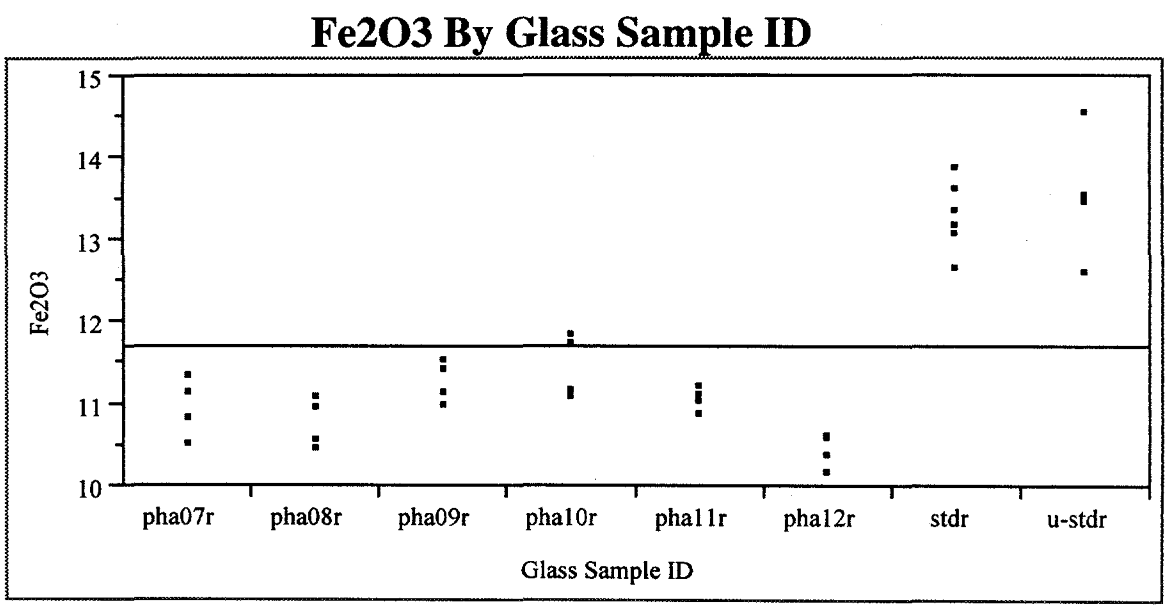

**Display B.1: Measurements of Re-Batched Glasses by Oxide**
**(continued)**

## K2O By Glass Sample ID

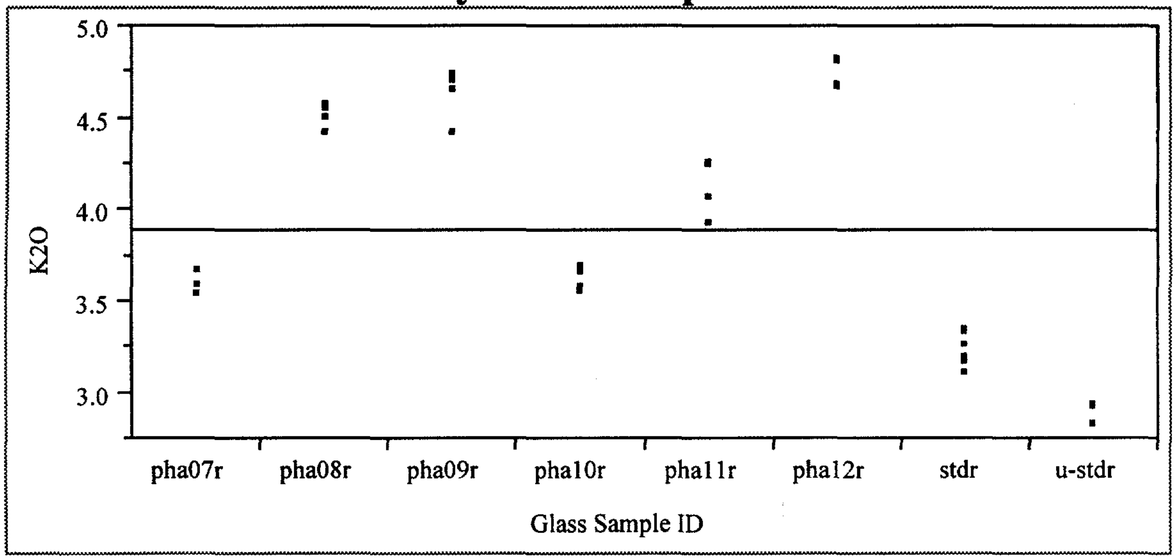


## Li2O By Glass Sample ID

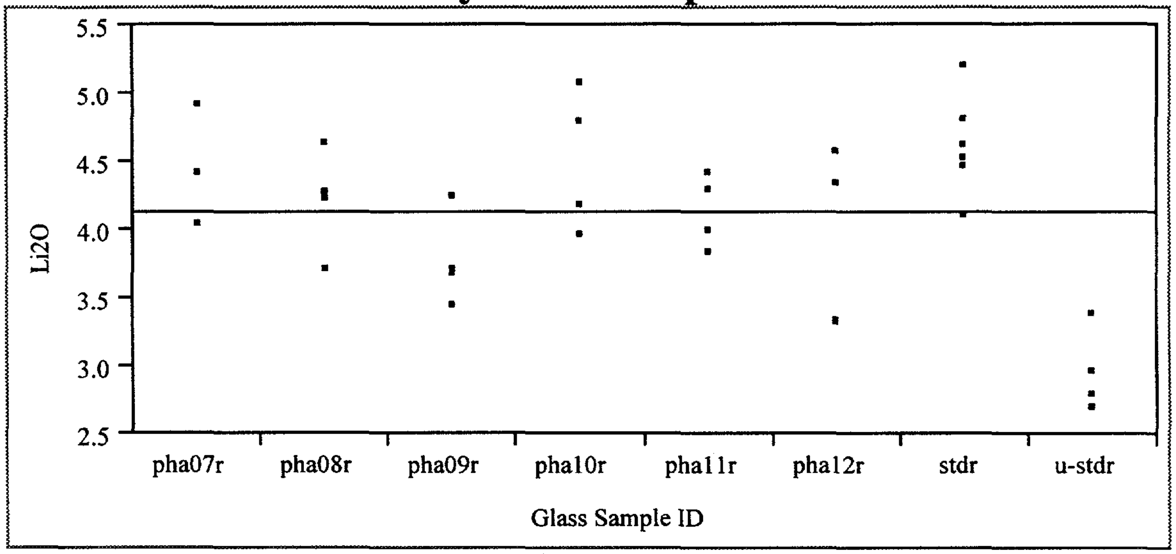

**Display B.1: Measurements of Re-Batched Glasses by Oxide**
**(continued)**

## MgO By Glass Sample ID

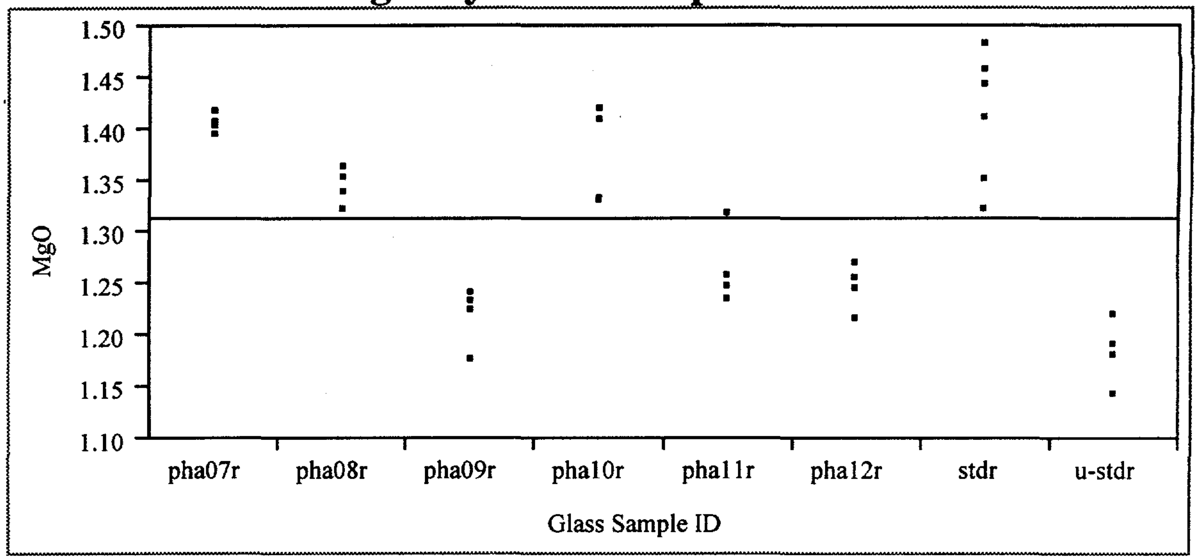


## MnO By Glass Sample ID

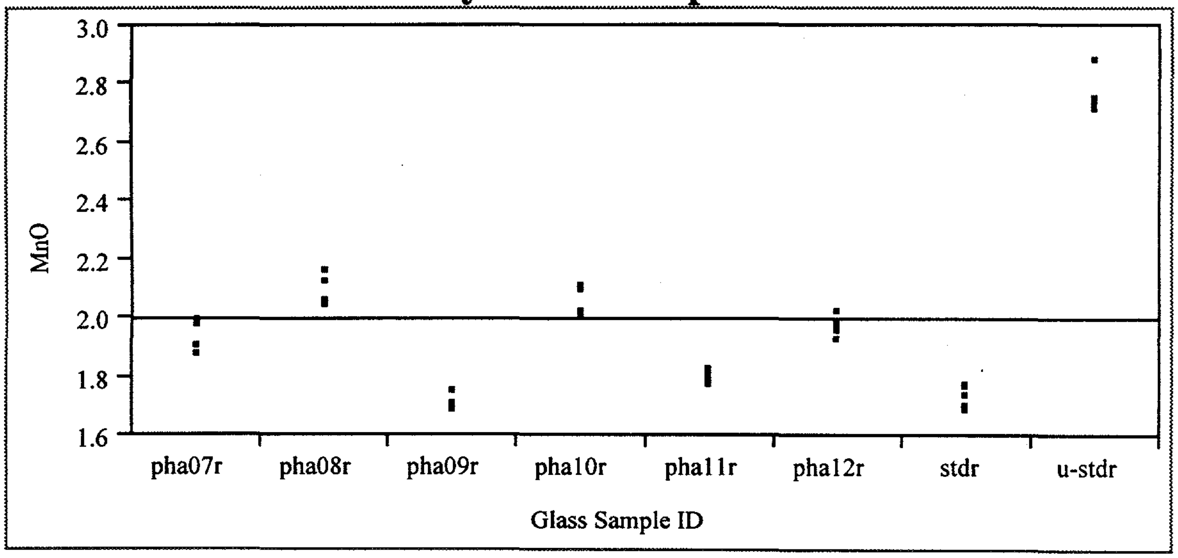

**Display B.1: Measurements of Re-Batched Glasses by Oxide**
(continued)

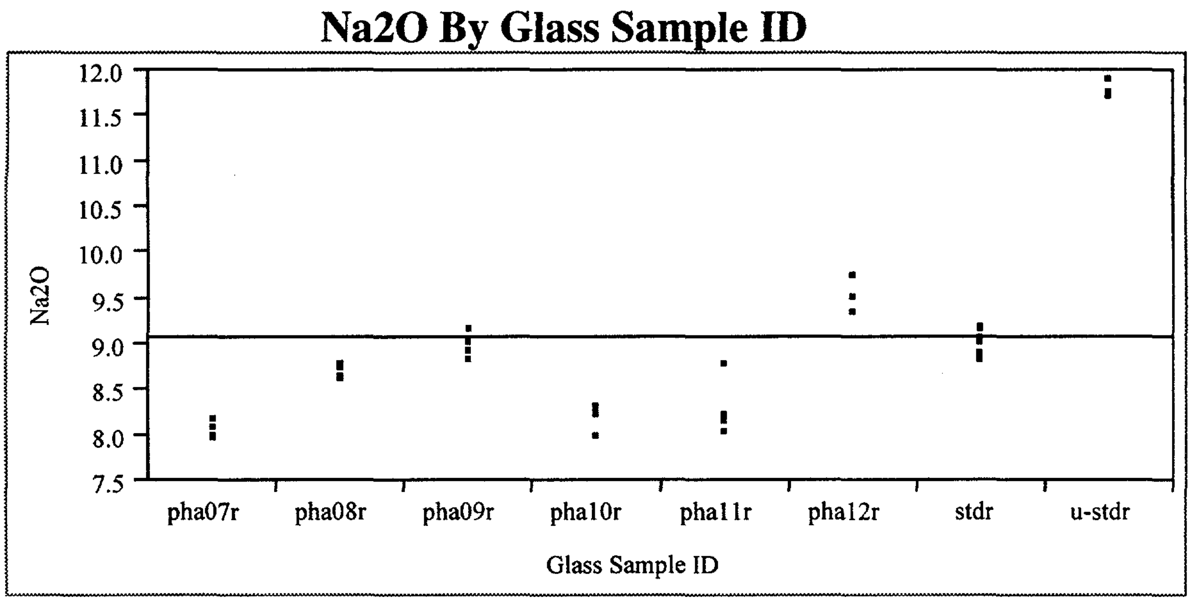


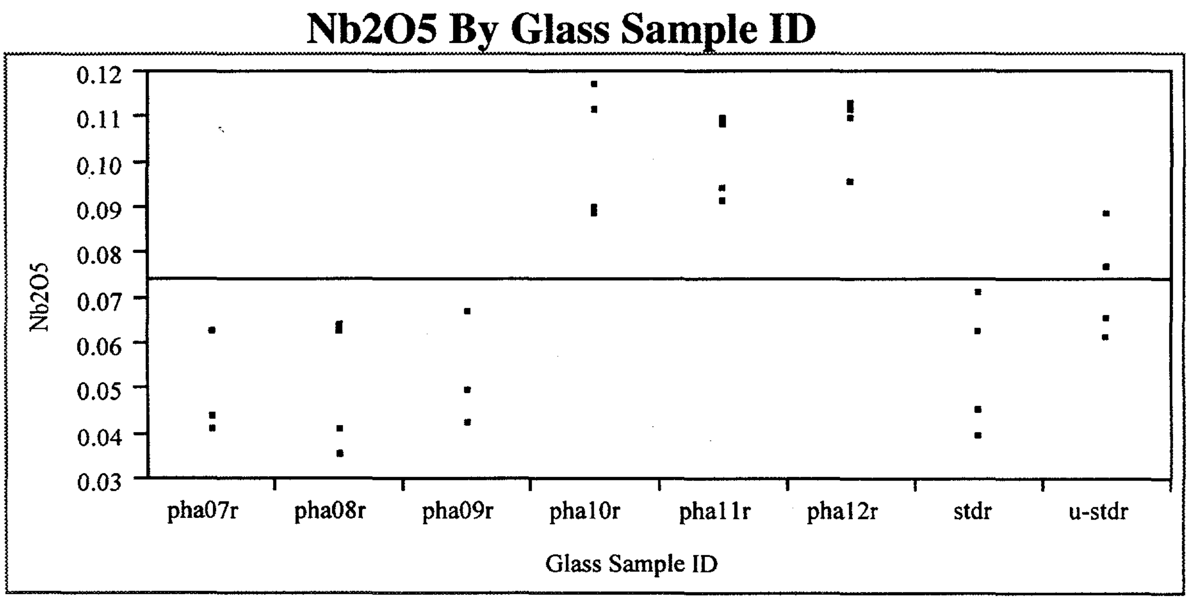

**Display B.1: Measurements of Re-Batched Glasses by Oxide**
**(continued)**

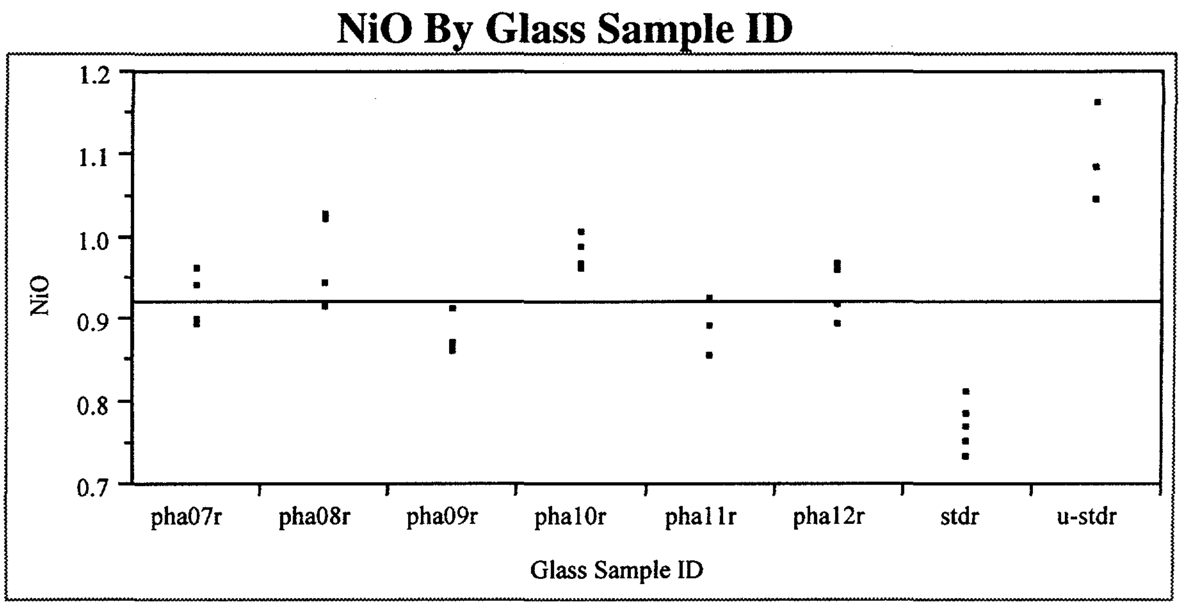


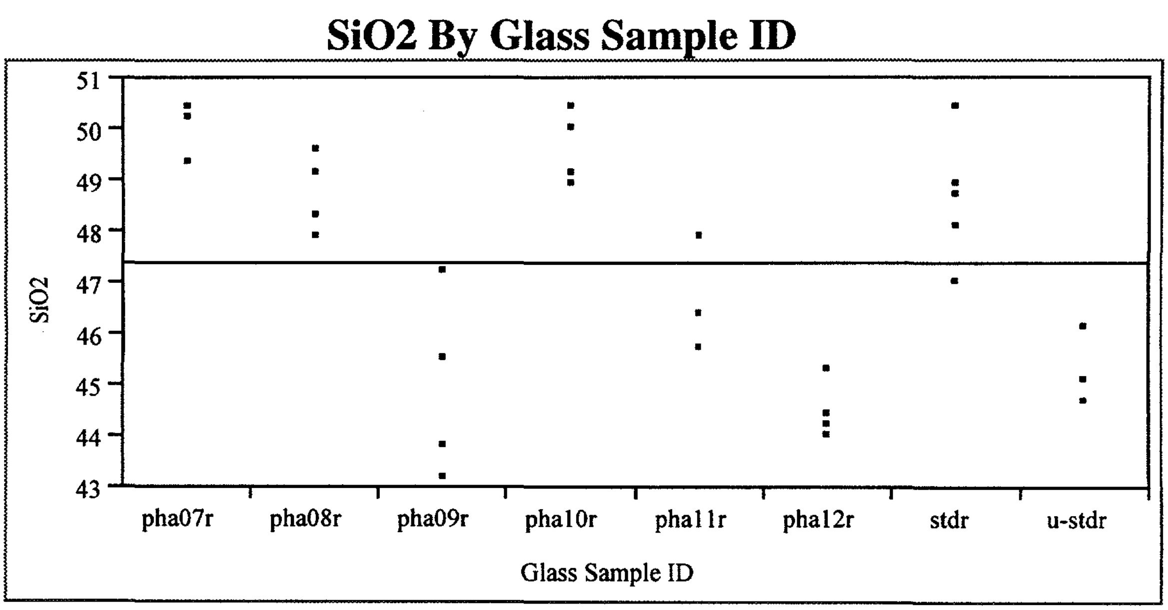

**Display B.1: Measurements of Re-Batched Glasses by Oxide**
(continued)

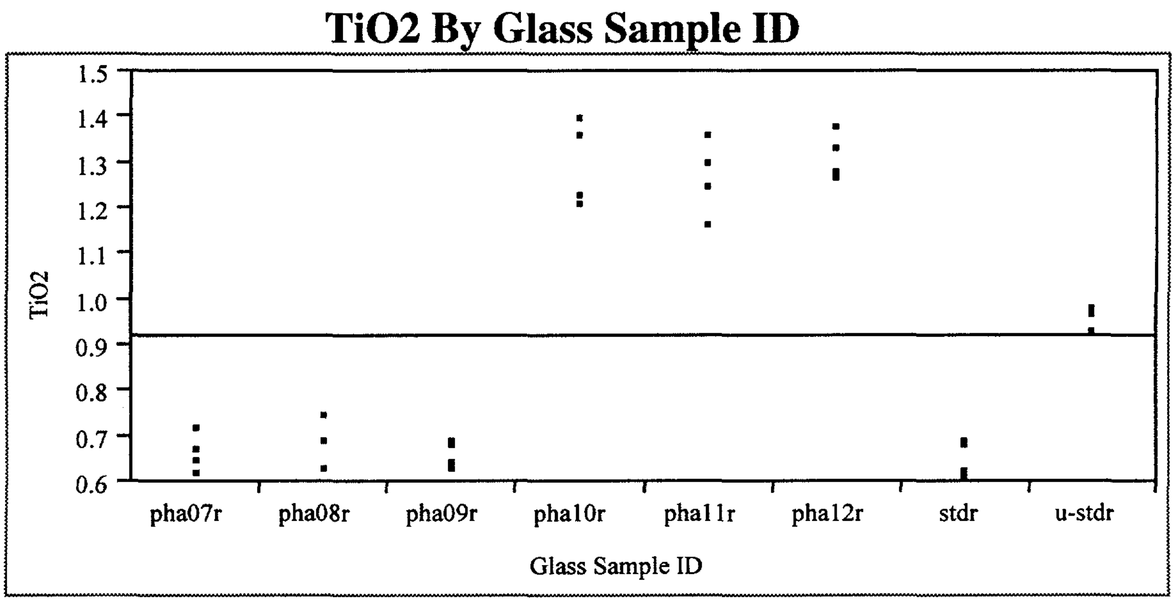


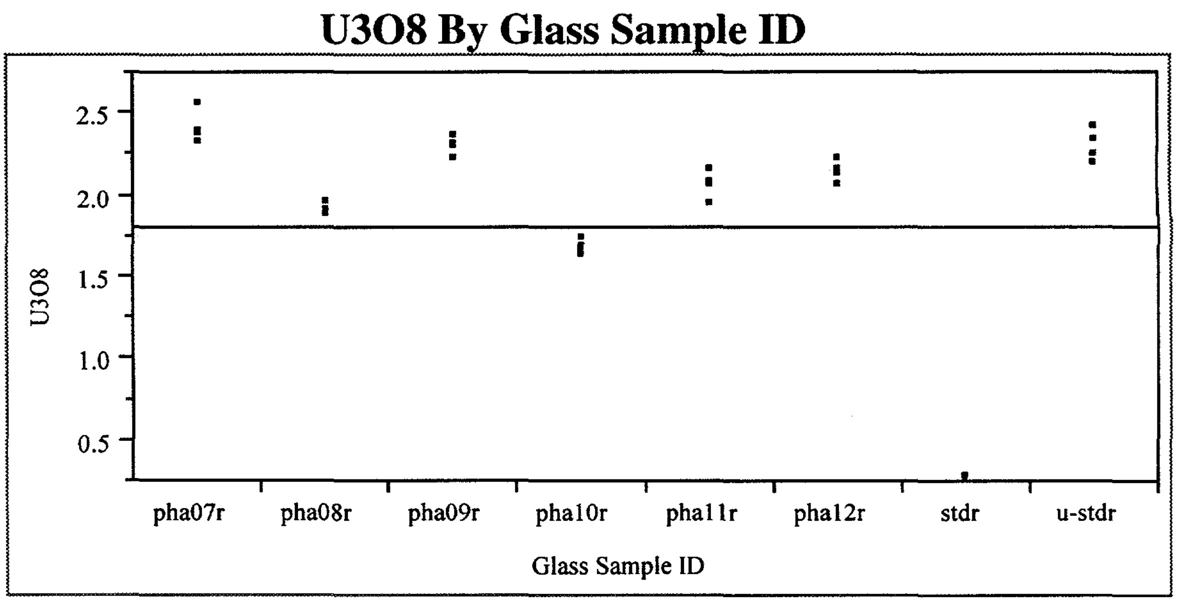

**Display B.1: Measurements of Re-Batched Glasses by Oxide**
(continued)

## ZrO2 By Glass Sample ID

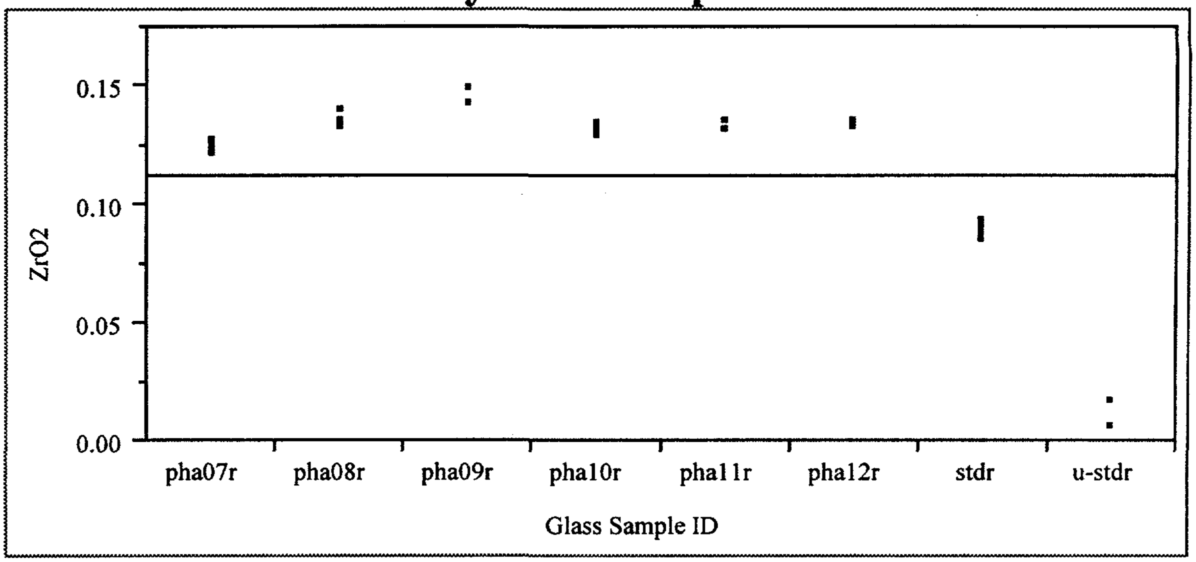


## Sum of Oxides By Glass Sample ID

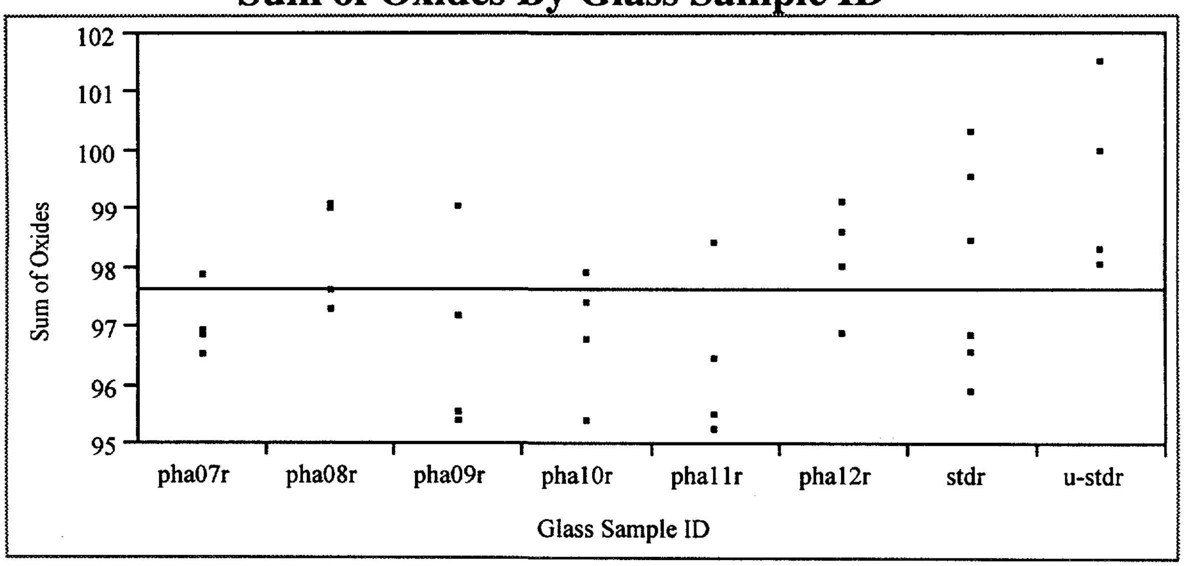

**Display B.2: Measurements of Glass Standards by Oxide**
(+ u-std; small square Batch 1 standard)

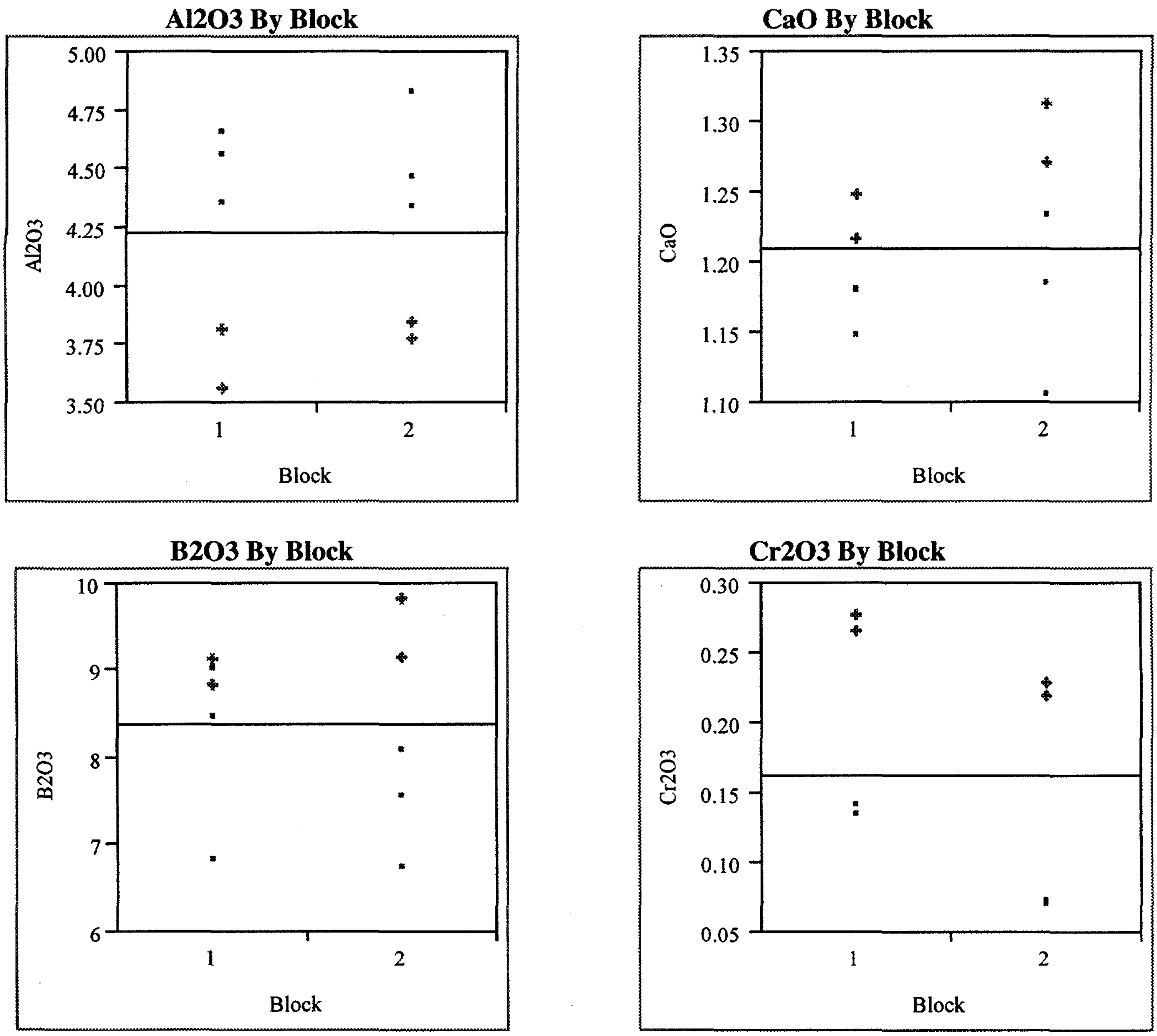

**Display B.2: Measurements of Glass Standards by Oxide**
(+ u-std; small square Batch 1 standard)
(continued)

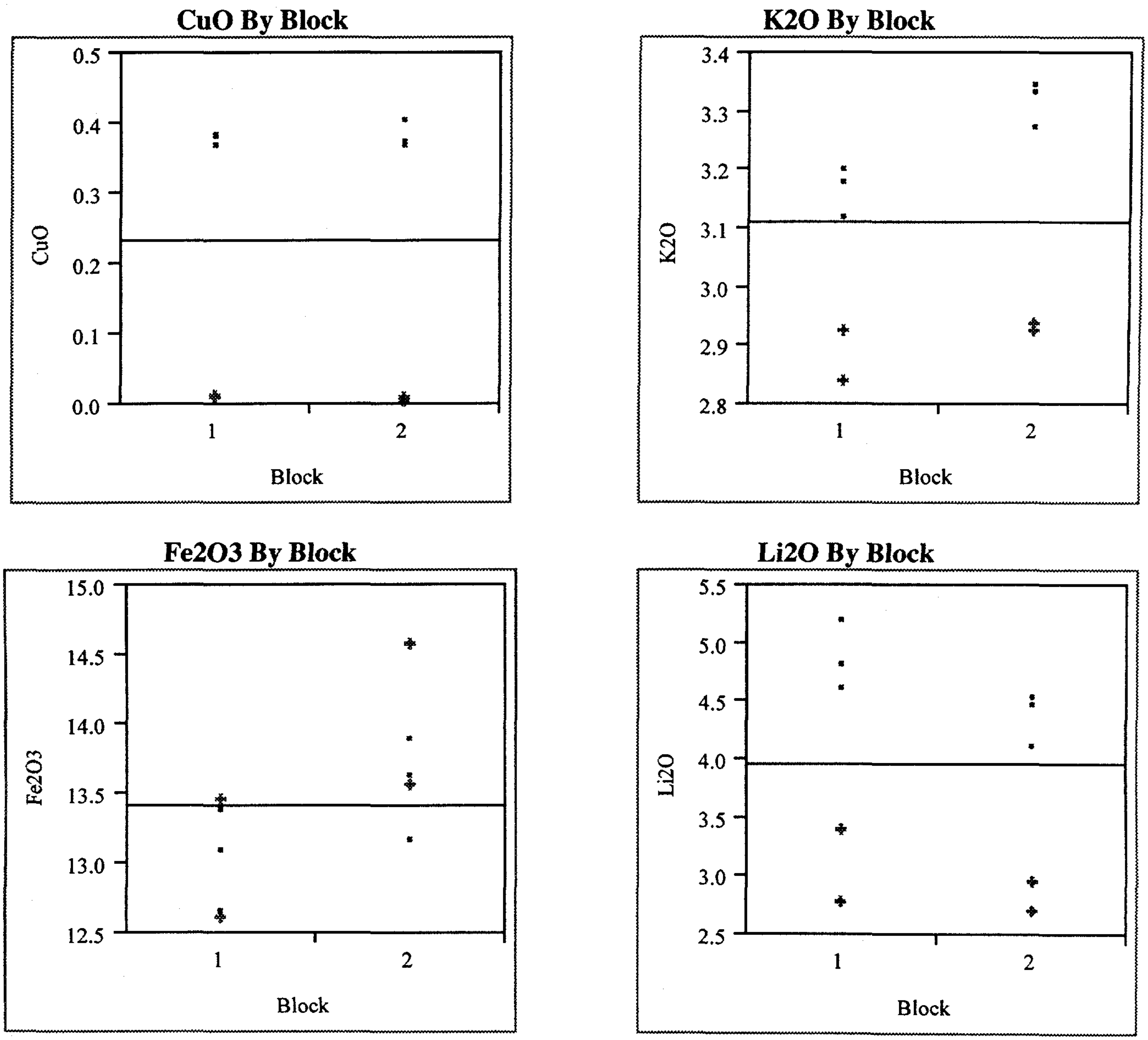

**Display B.2: Measurements of Glass Standards by Oxide**
(+ u-std; small square Batch 1 standard)
(continued)

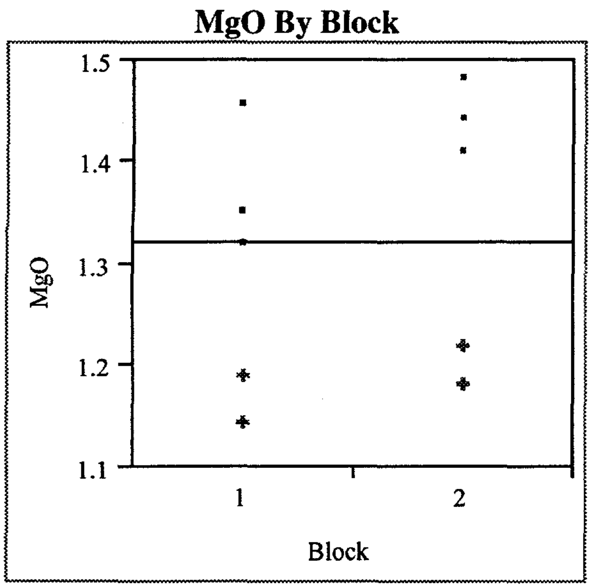


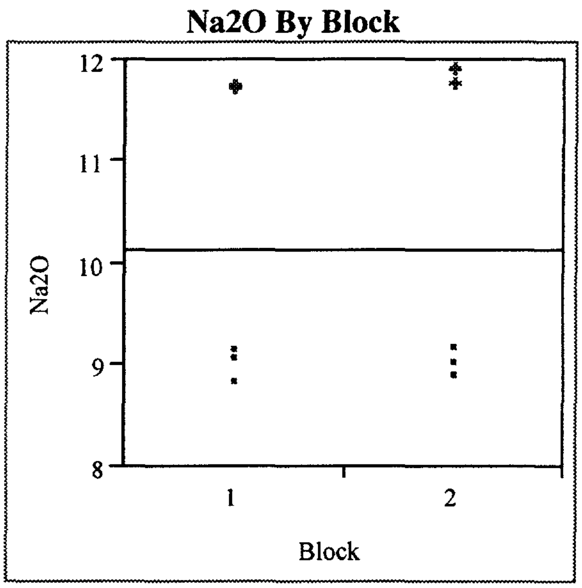


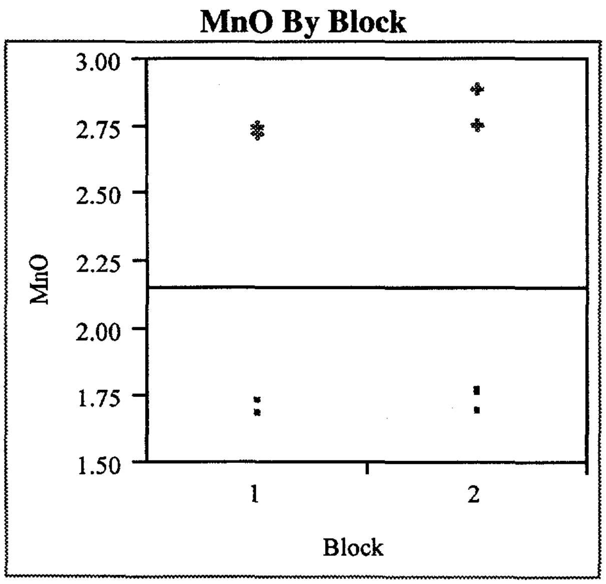


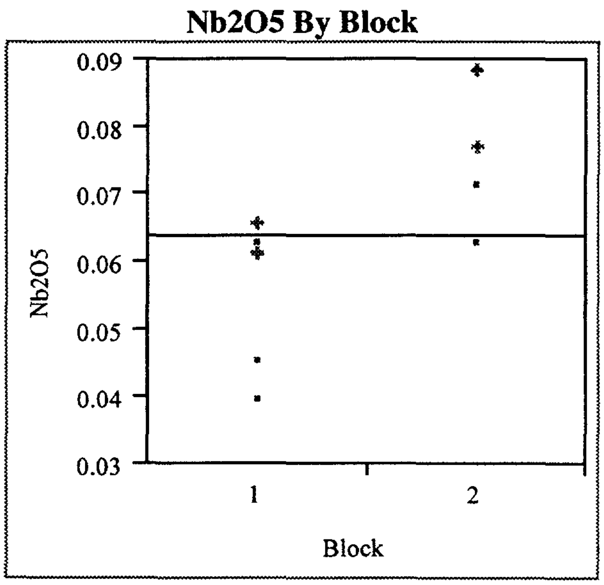

**Display B.2: Measurements of Glass Standards by Oxide**
(+ u-std; small square Batch 1 standard)
(continued)

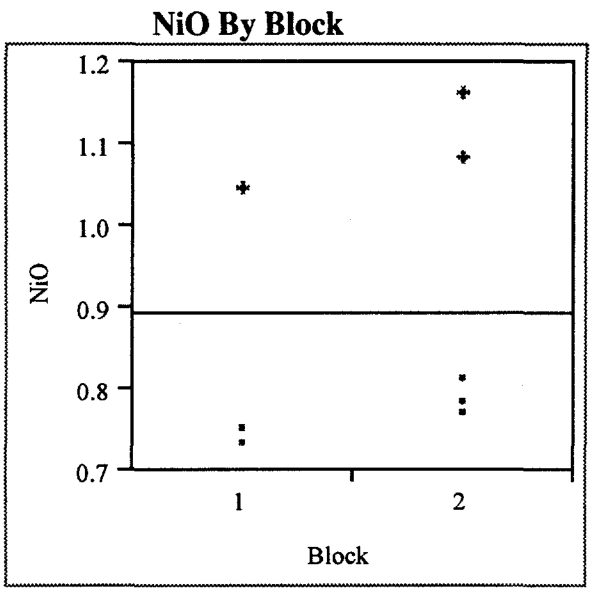


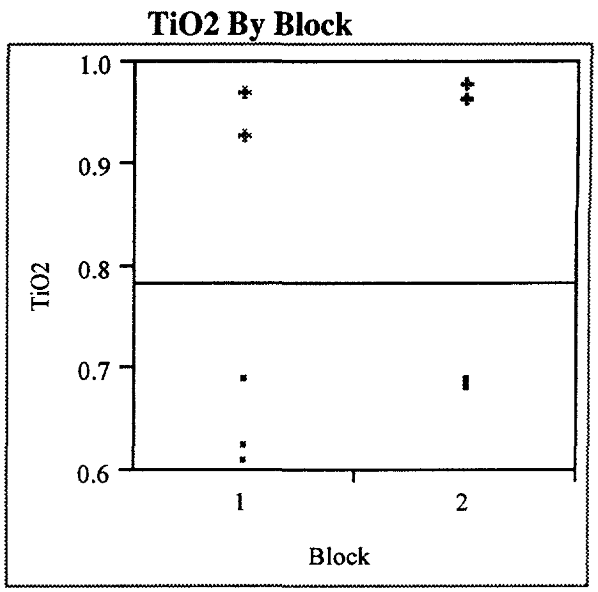


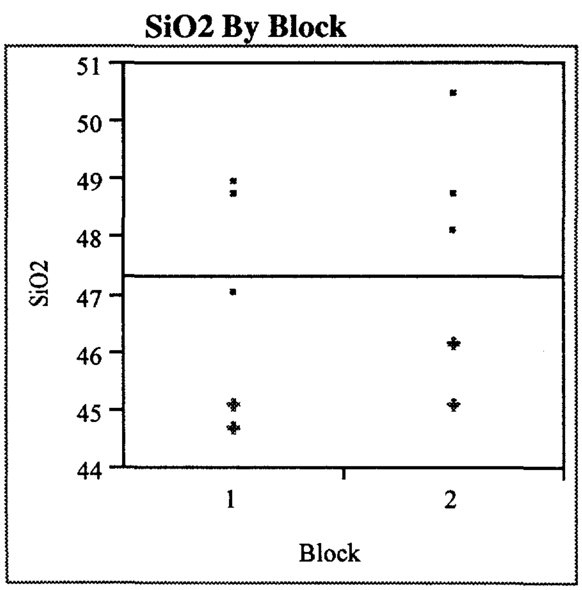


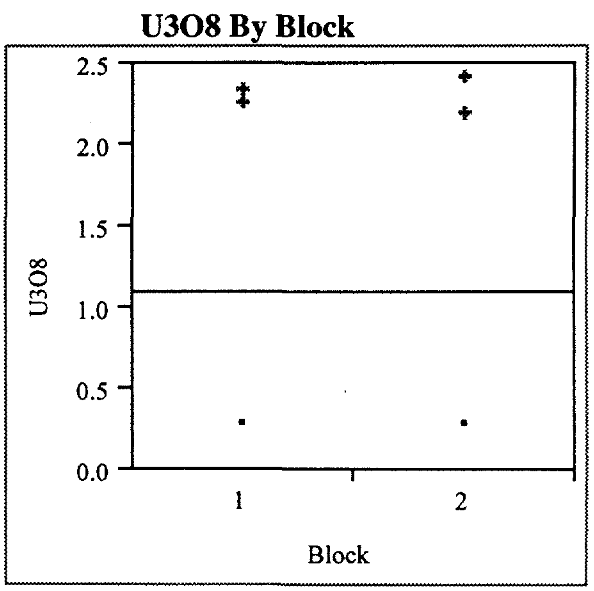

**Display B.2: Measurements of Glass Standards by Oxide**
(+ u-std; small square Batch 1 standard)
(continued)

ZrO2 By Block

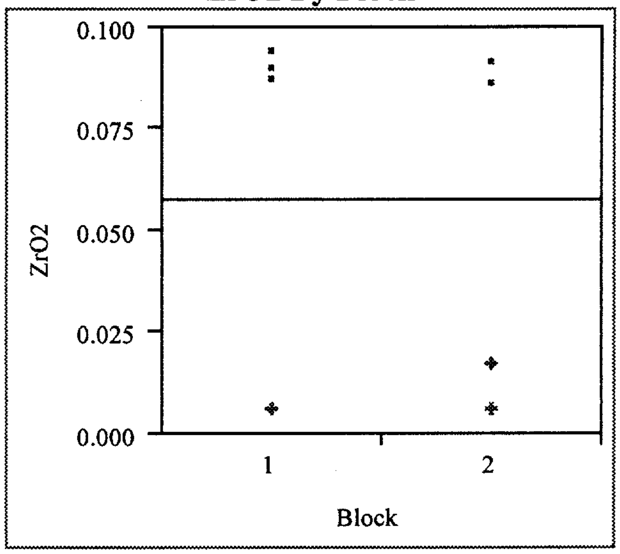

**Display B.3: Comparisons of Measurements versus Target Compositions**
(concentrations in weight percents)
**$Al_2O_3$**

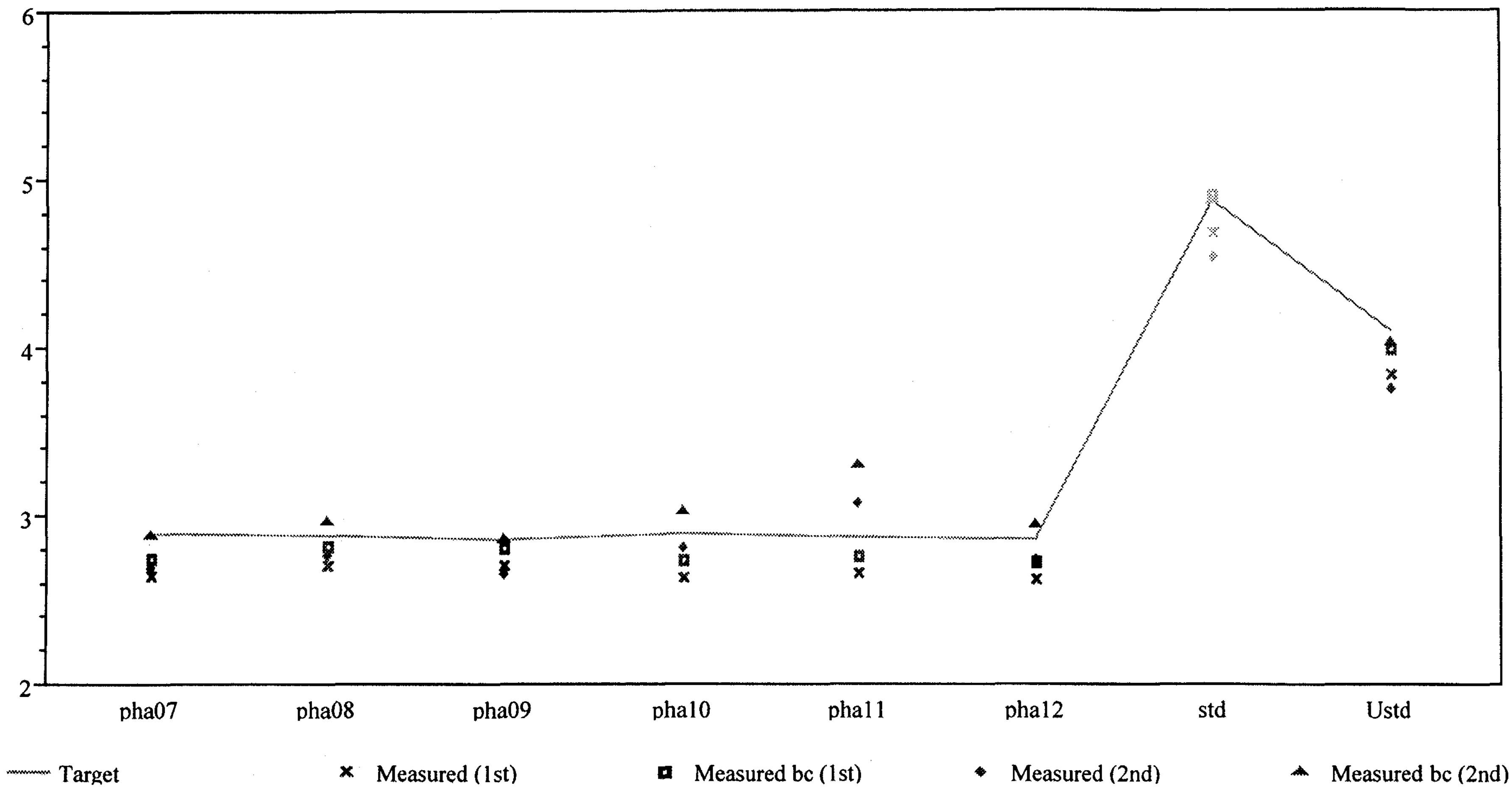

**Display B.3: Comparisons of Measurements versus Target Compositions**
(concentrations in weight percents)

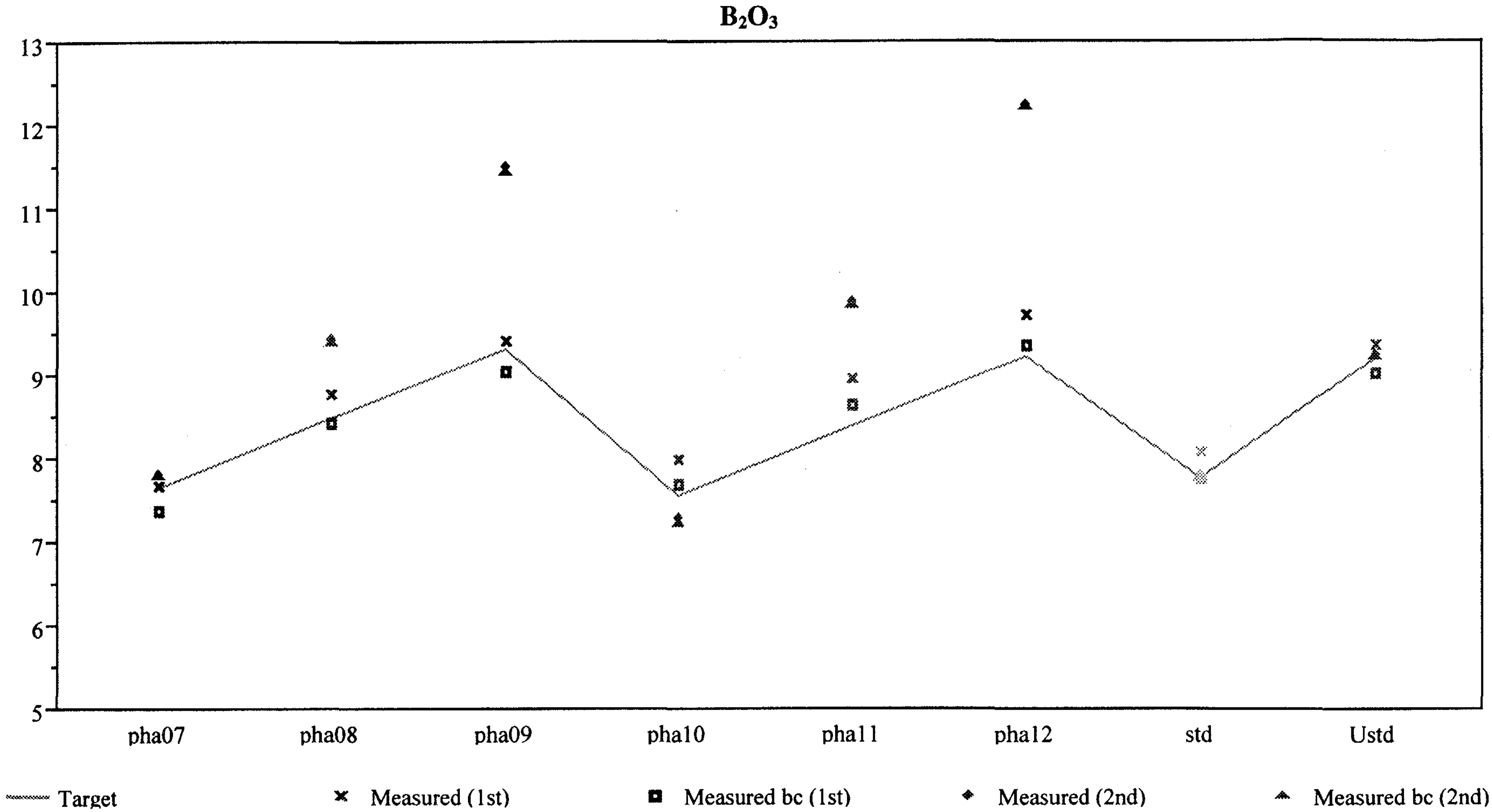

**Display B.3: Comparisons of Measurements versus Target Compositions**
(concentrations in weight percents)

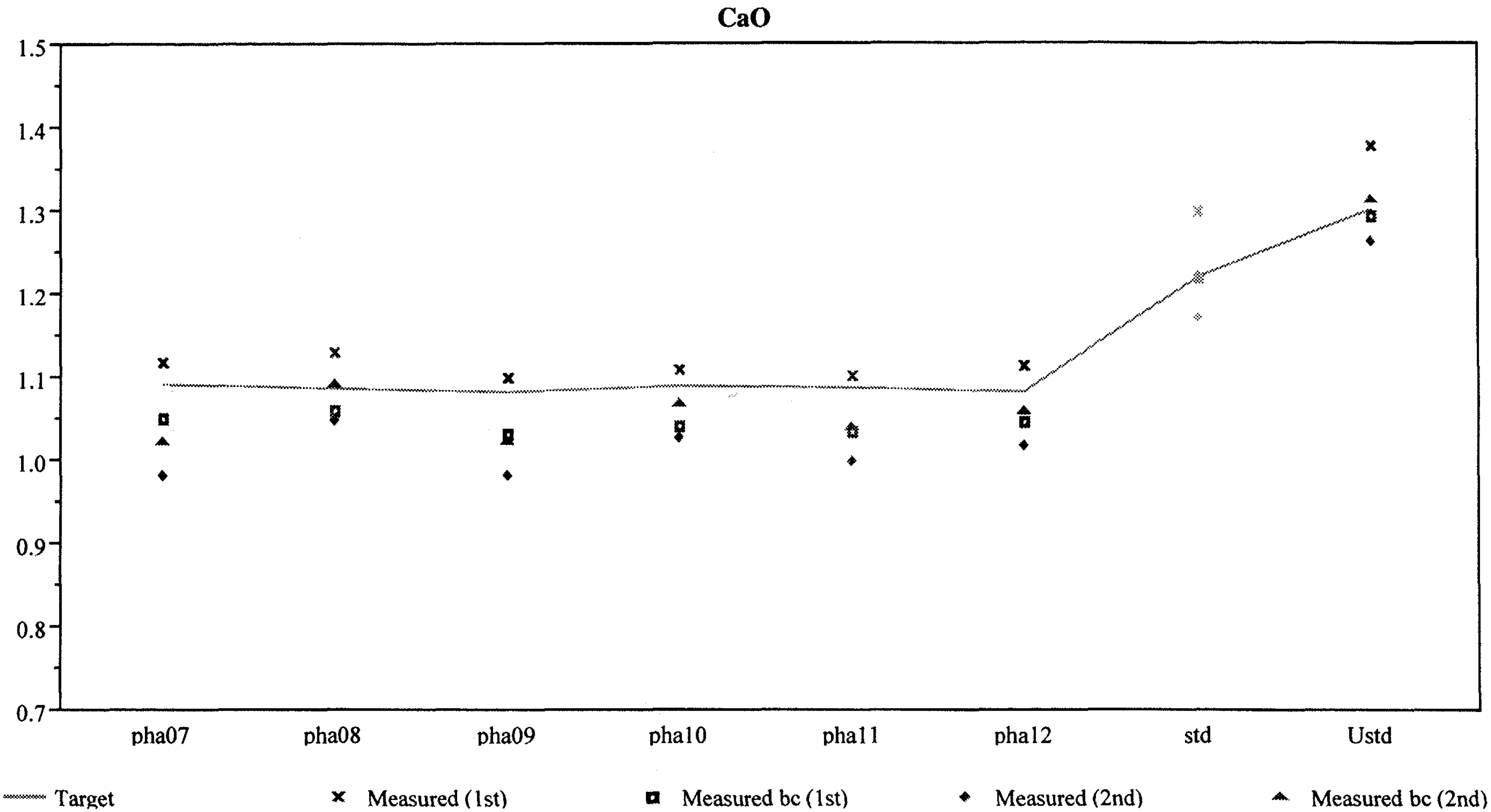

**Display B.3: Comparisons of Measurements versus Target Compositions**
(concentrations in weight percents)

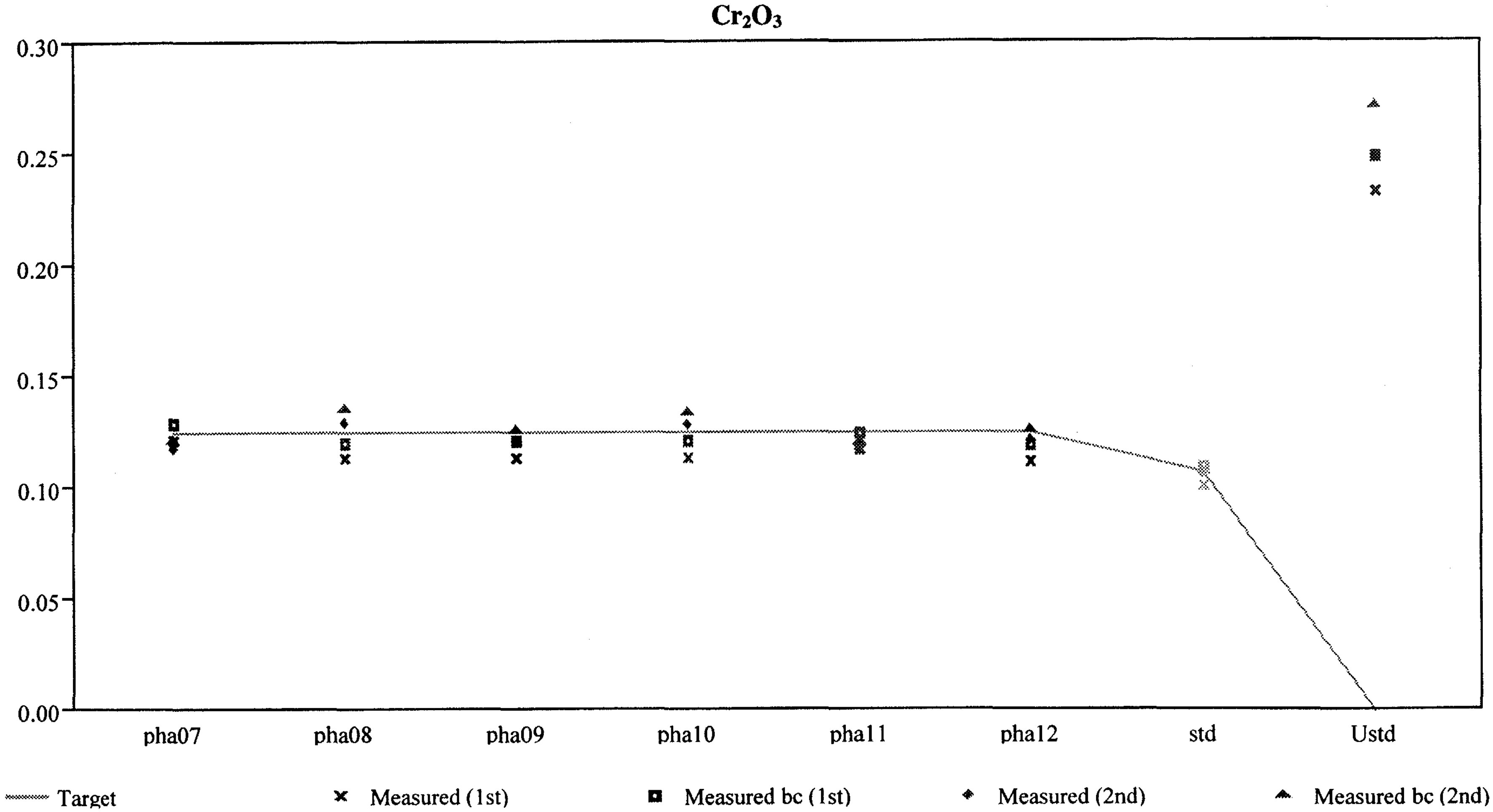

**Display B.3: Comparisons of Measurements versus Target Compositions**
(concentrations in weight percents)

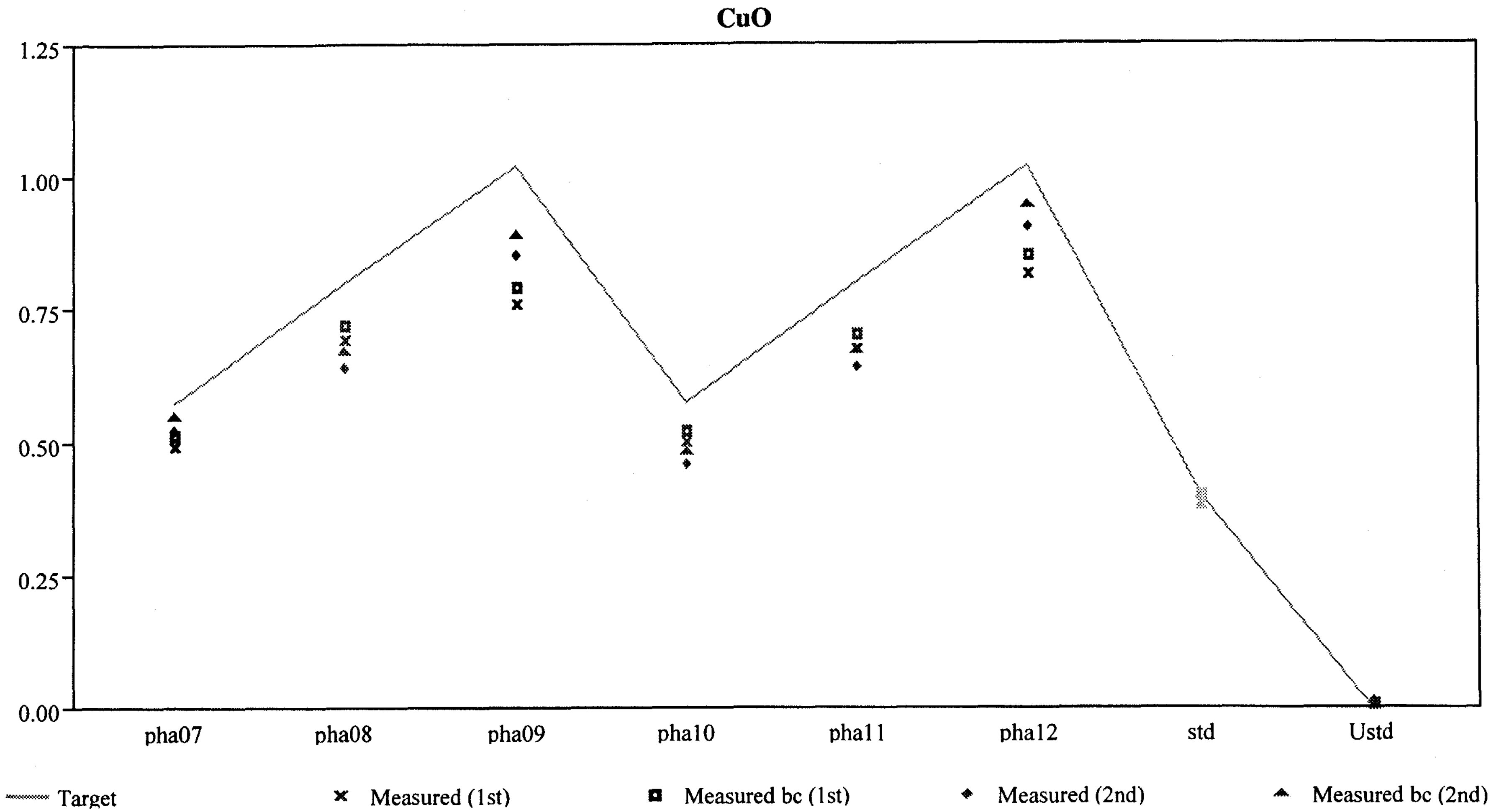

**Display B.3: Comparisons of Measurements versus Target Compositions**
(concentrations in weight percents)

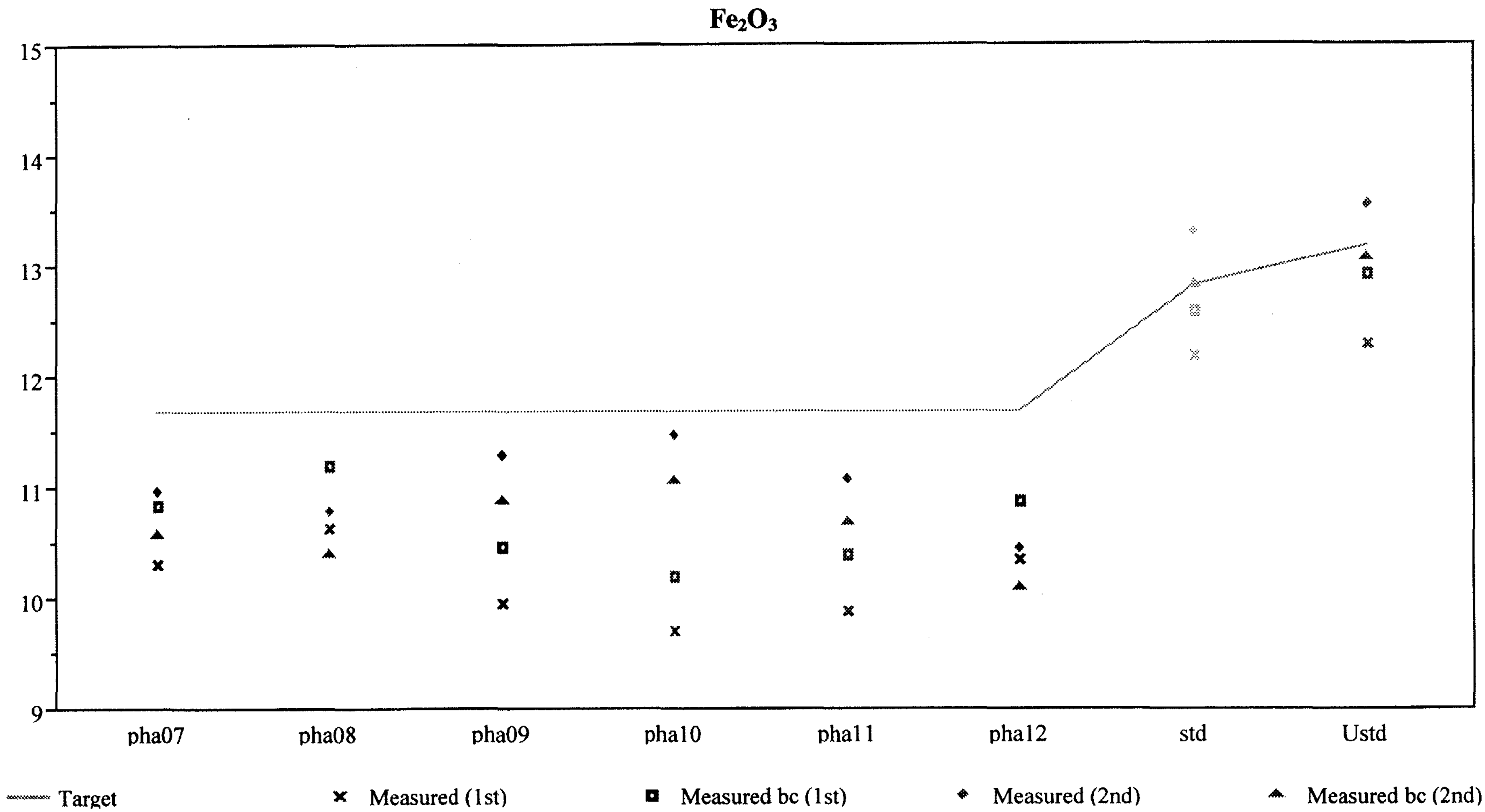

**Display B.3: Comparisons of Measurements versus Target Compositions**
(concentrations in weight percents)

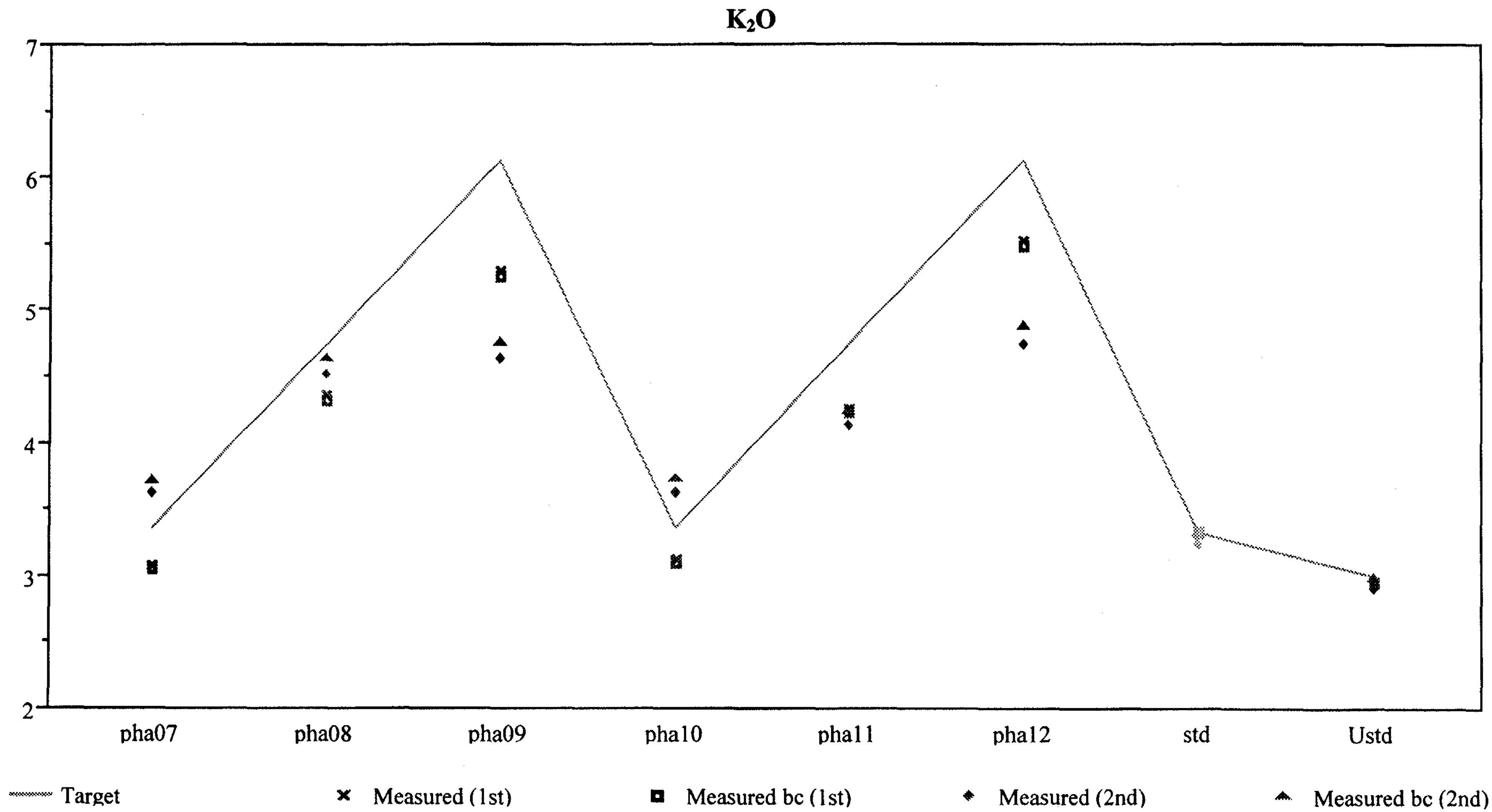

**Display B.3: Comparisons of Measurements versus Target Compositions**
(concentrations in weight percents)

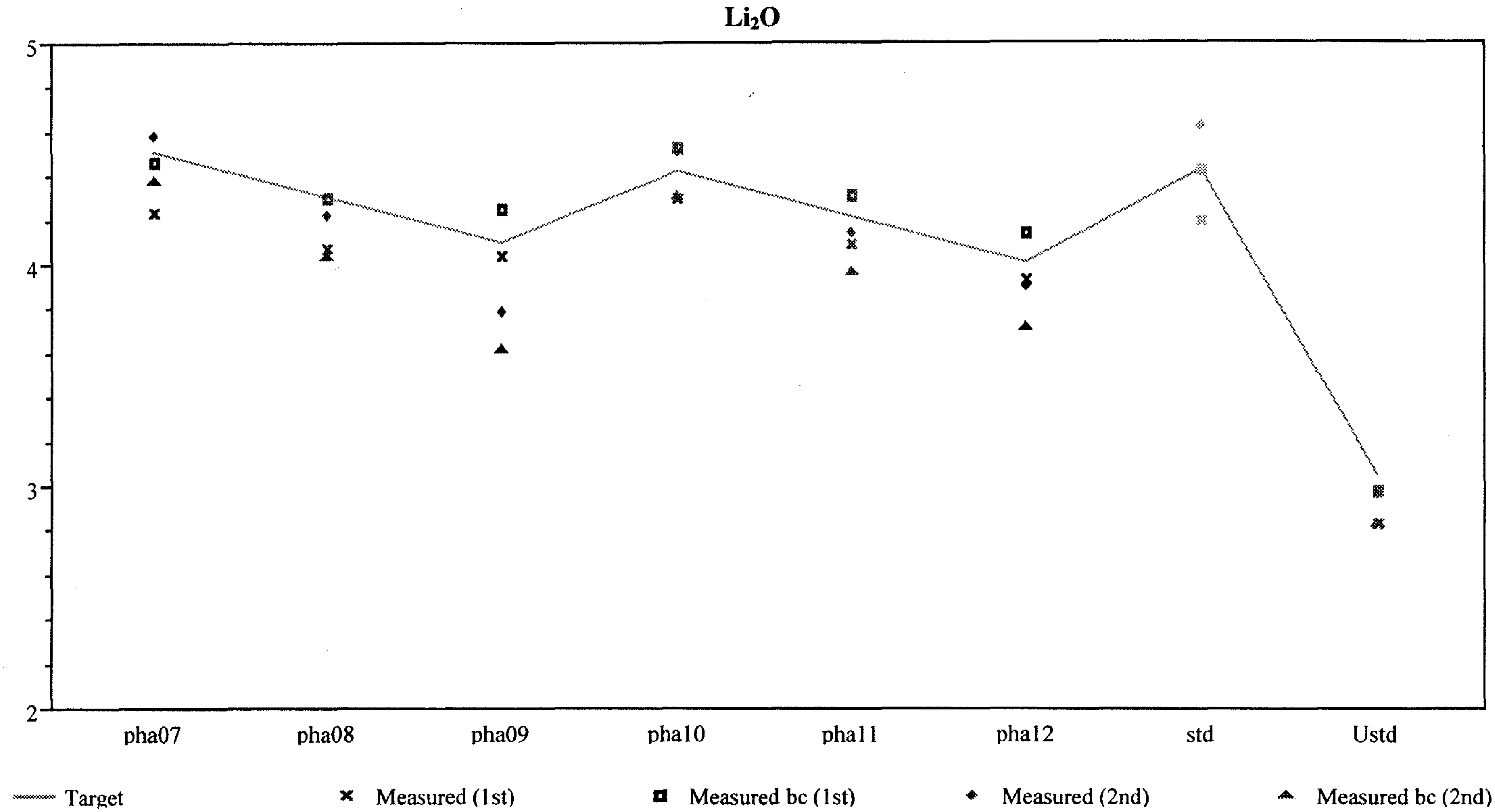

**Display B.3: Comparisons of Measurements versus Target Compositions**
(concentrations in weight percents)

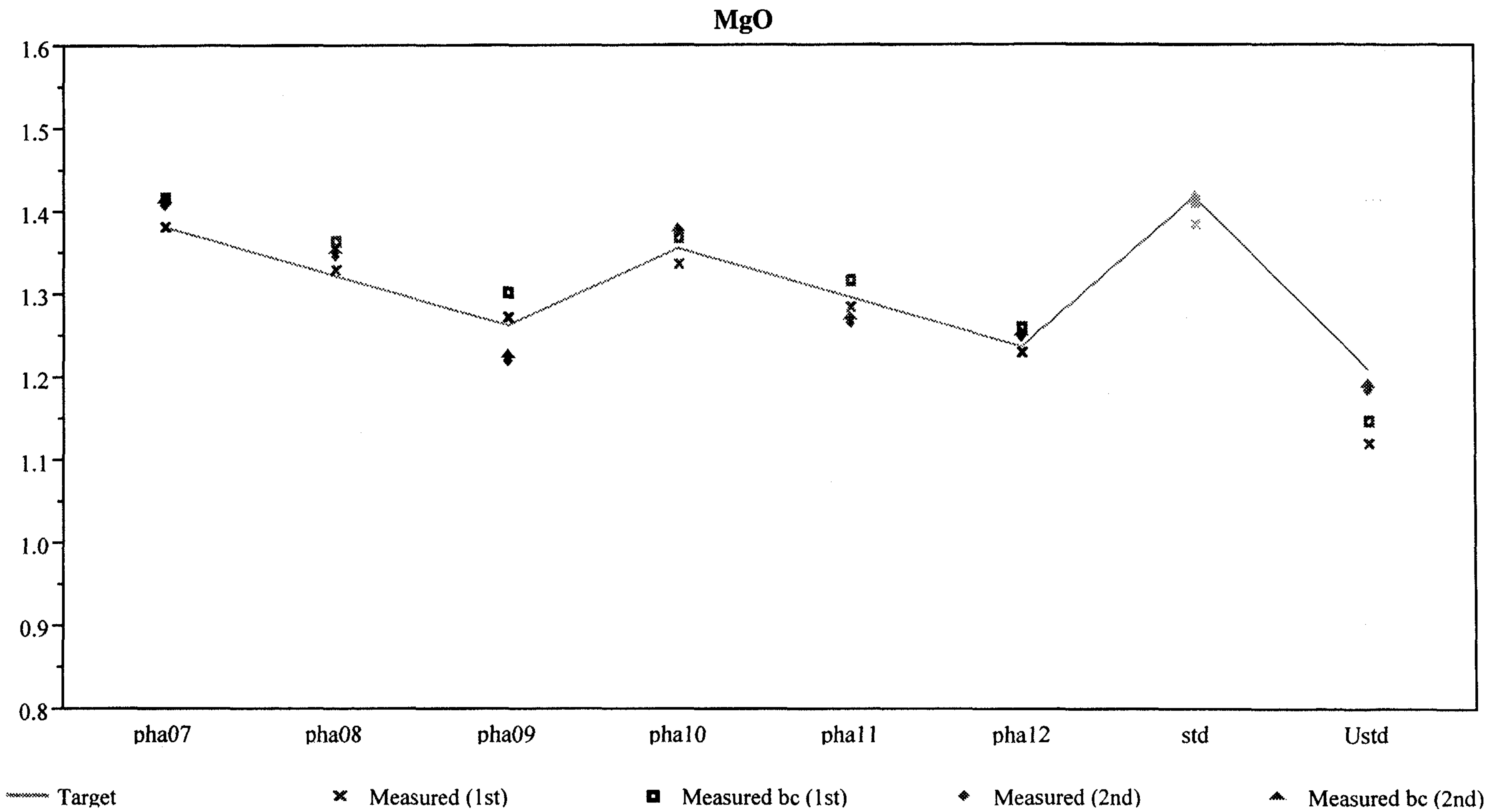

**Display B.3: Comparisons of Measurements versus Target Compositions**
(concentrations in weight percents)

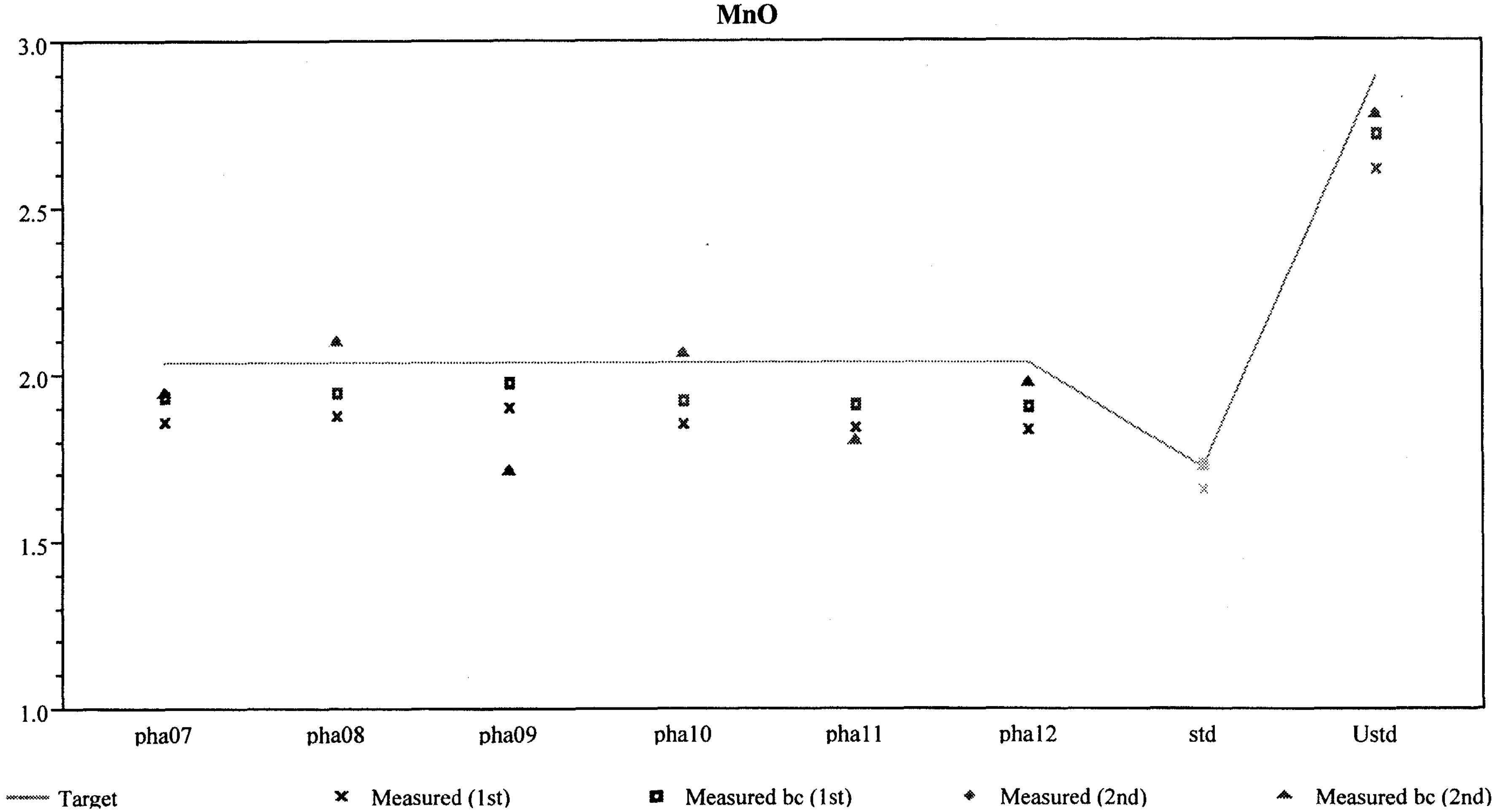

**Display B.3: Comparisons of Measurements versus Target Compositions**
(concentrations in weight percents)

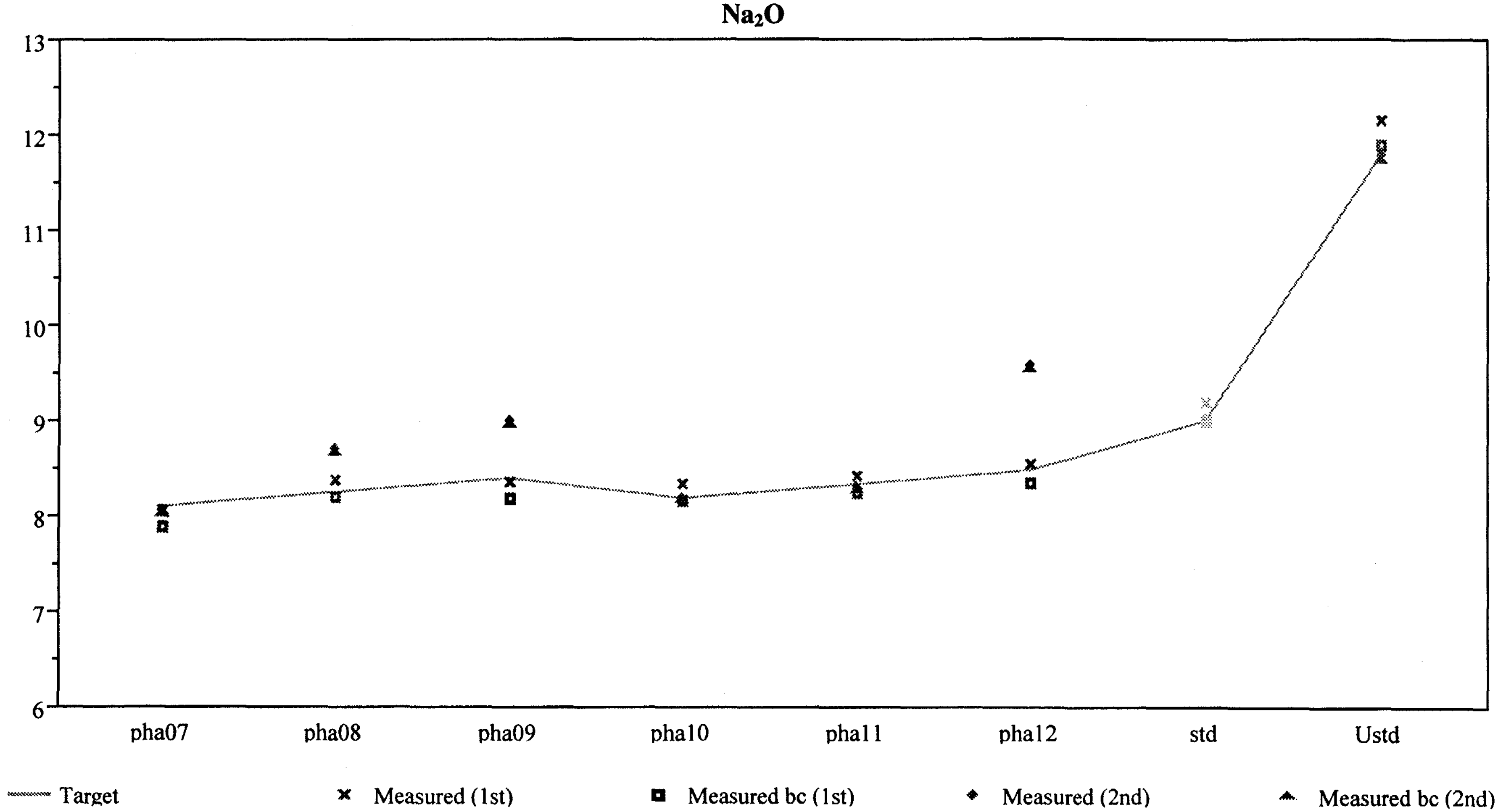

**Display B.3: Comparisons of Measurements versus Target Compositions**
(concentrations in weight percents)

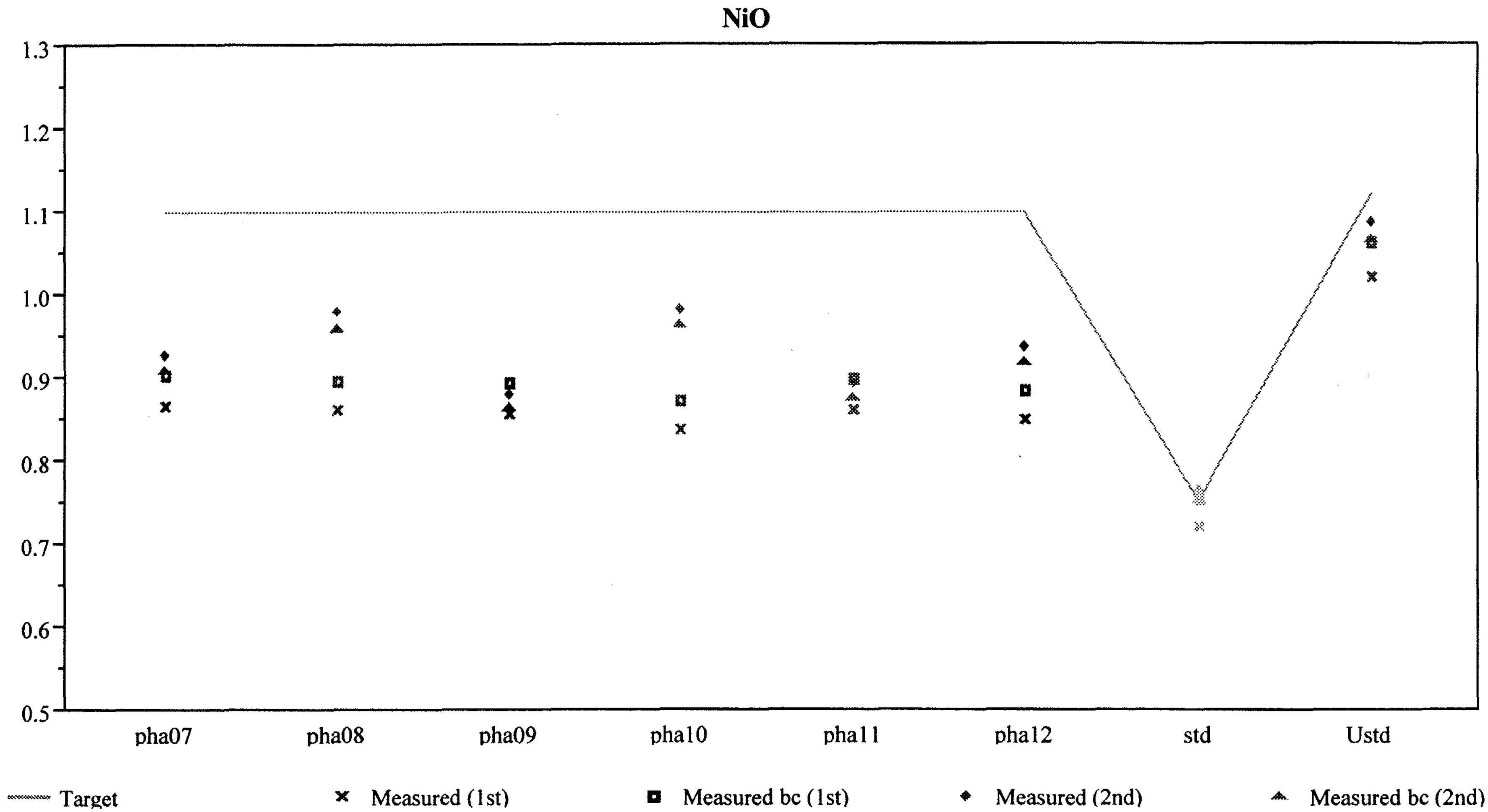

**Display B.3: Comparisons of Measurements versus Target Compositions**
(concentrations in weight percents)

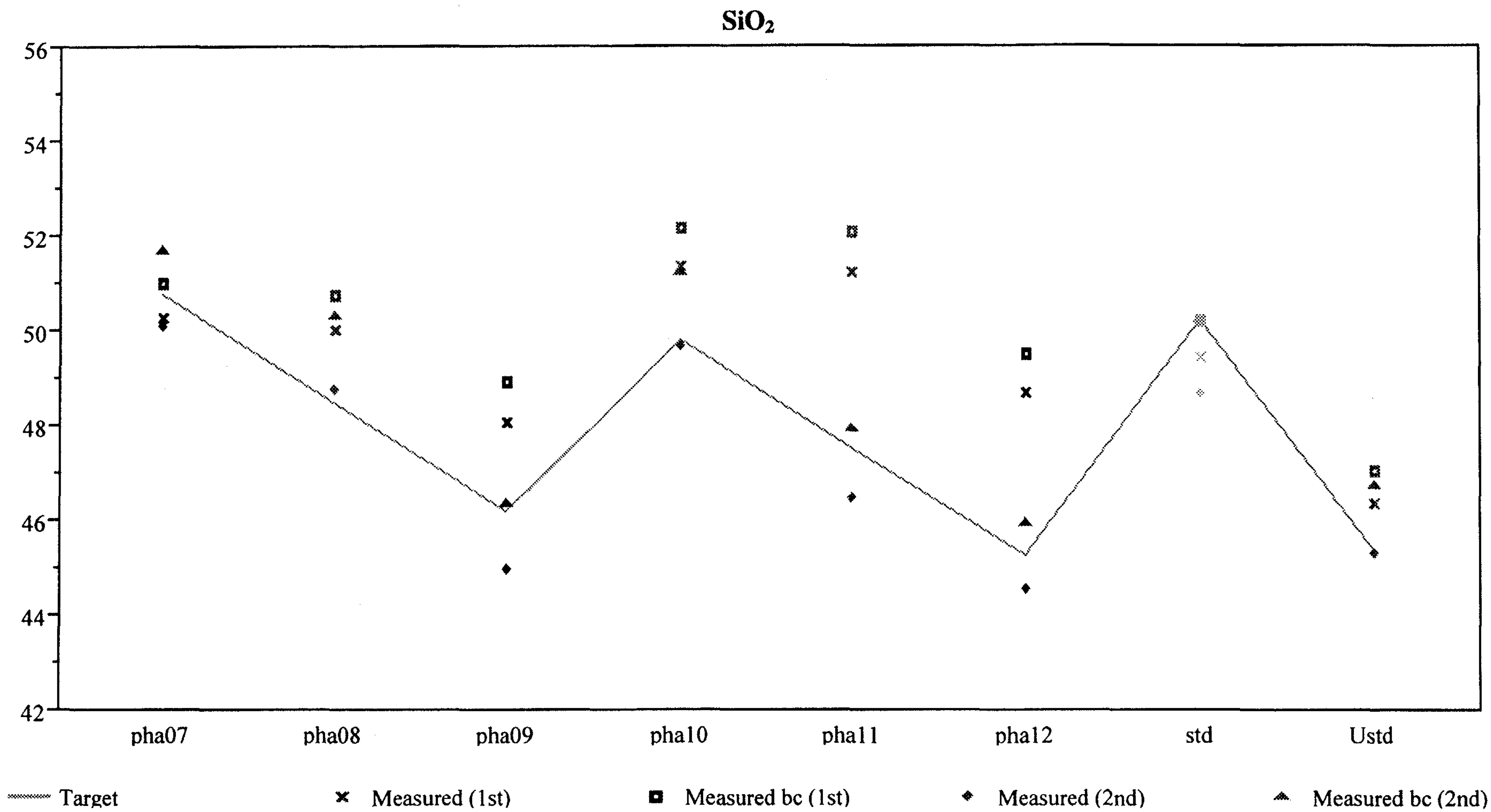

**Display B.3: Comparisons of Measurements versus Target Compositions**
(concentrations in weight percents)

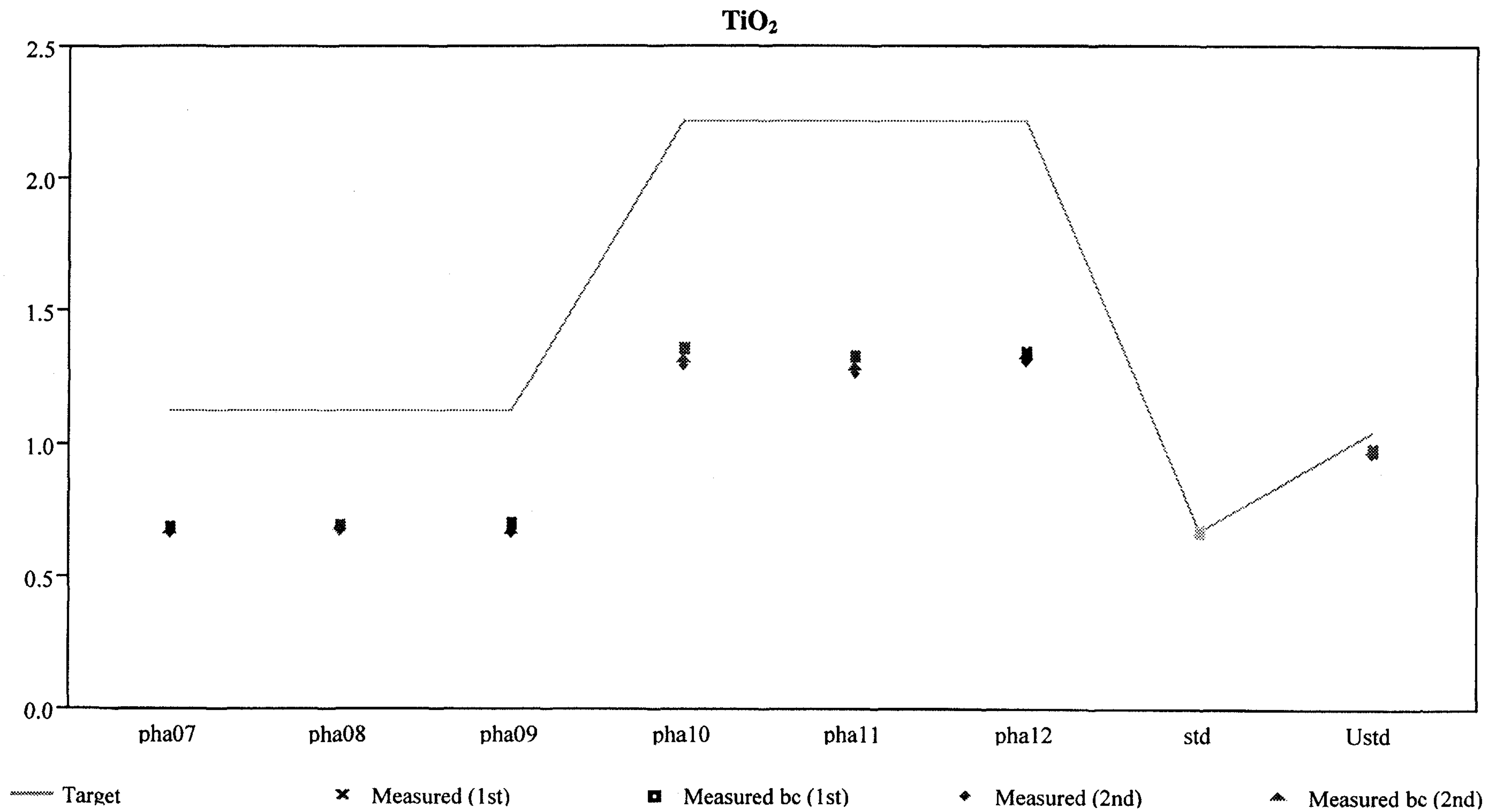

**Display B.3: Comparisons of Measurements versus Target Compositions**
(concentrations in weight percents)

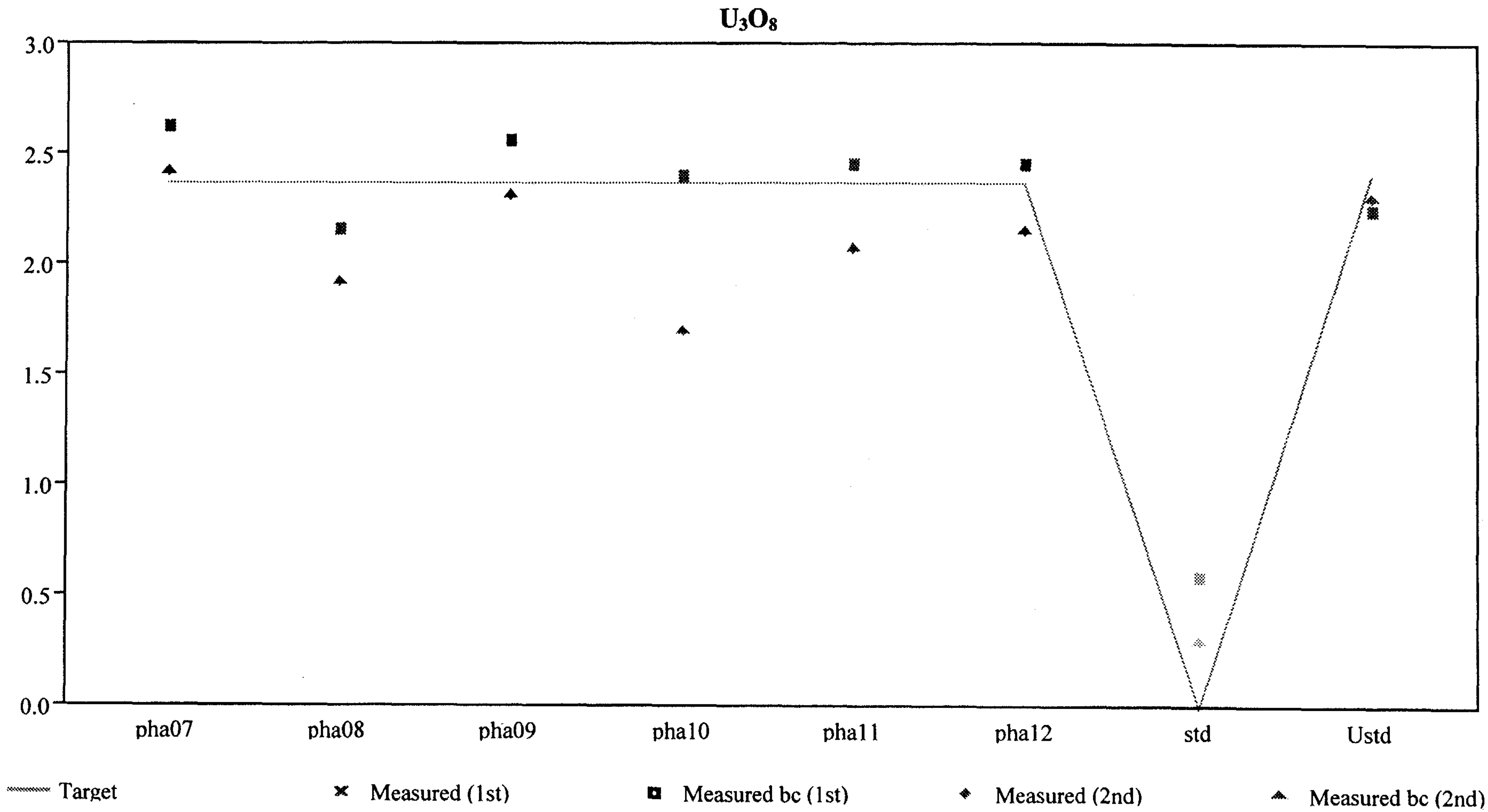

**Display B.3: Comparisons of Measurements versus Target Compositions**
(concentrations in weight percents)

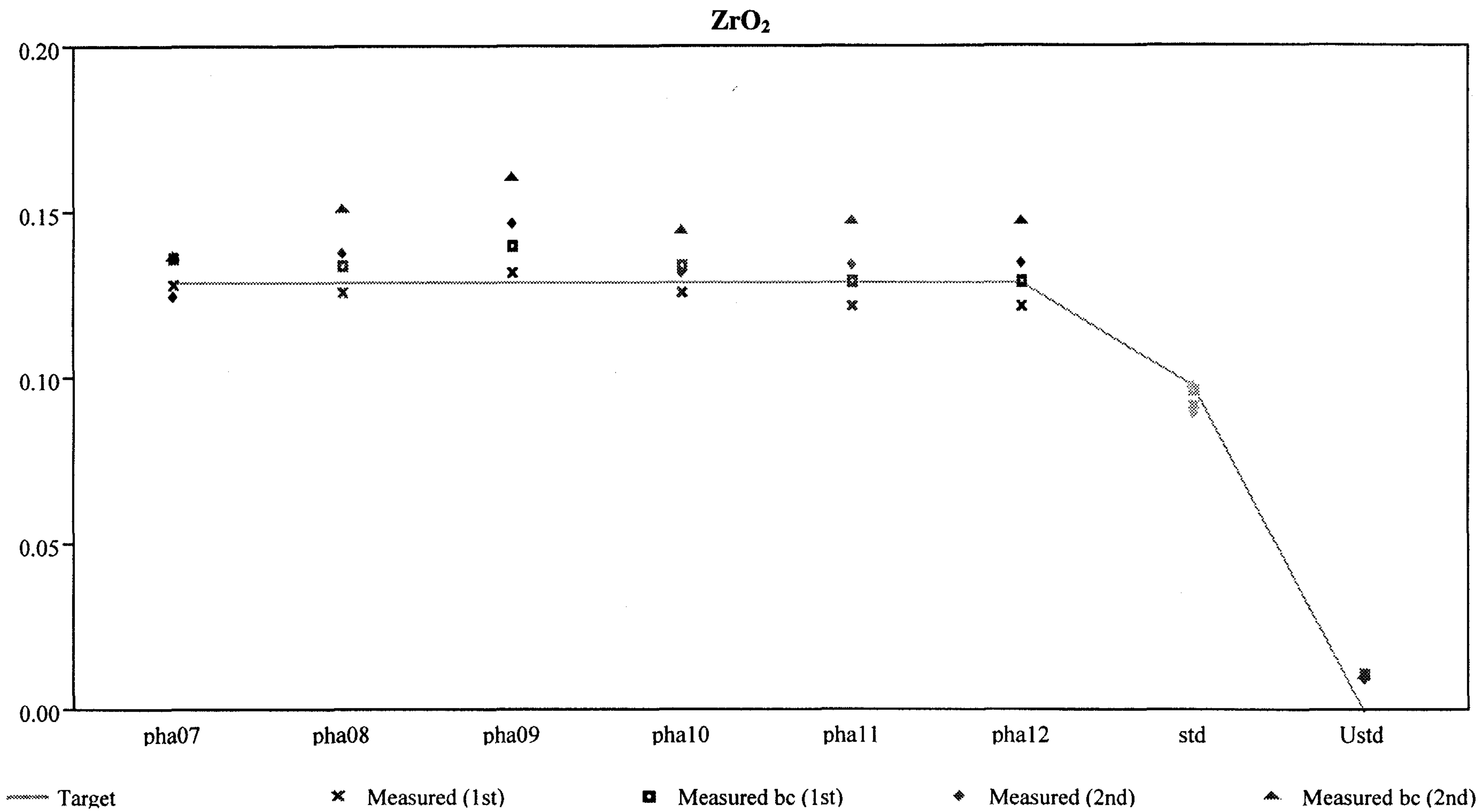

**Display B.3: Comparisons of Measurements versus Target Compositions**
(concentrations in weight percents)

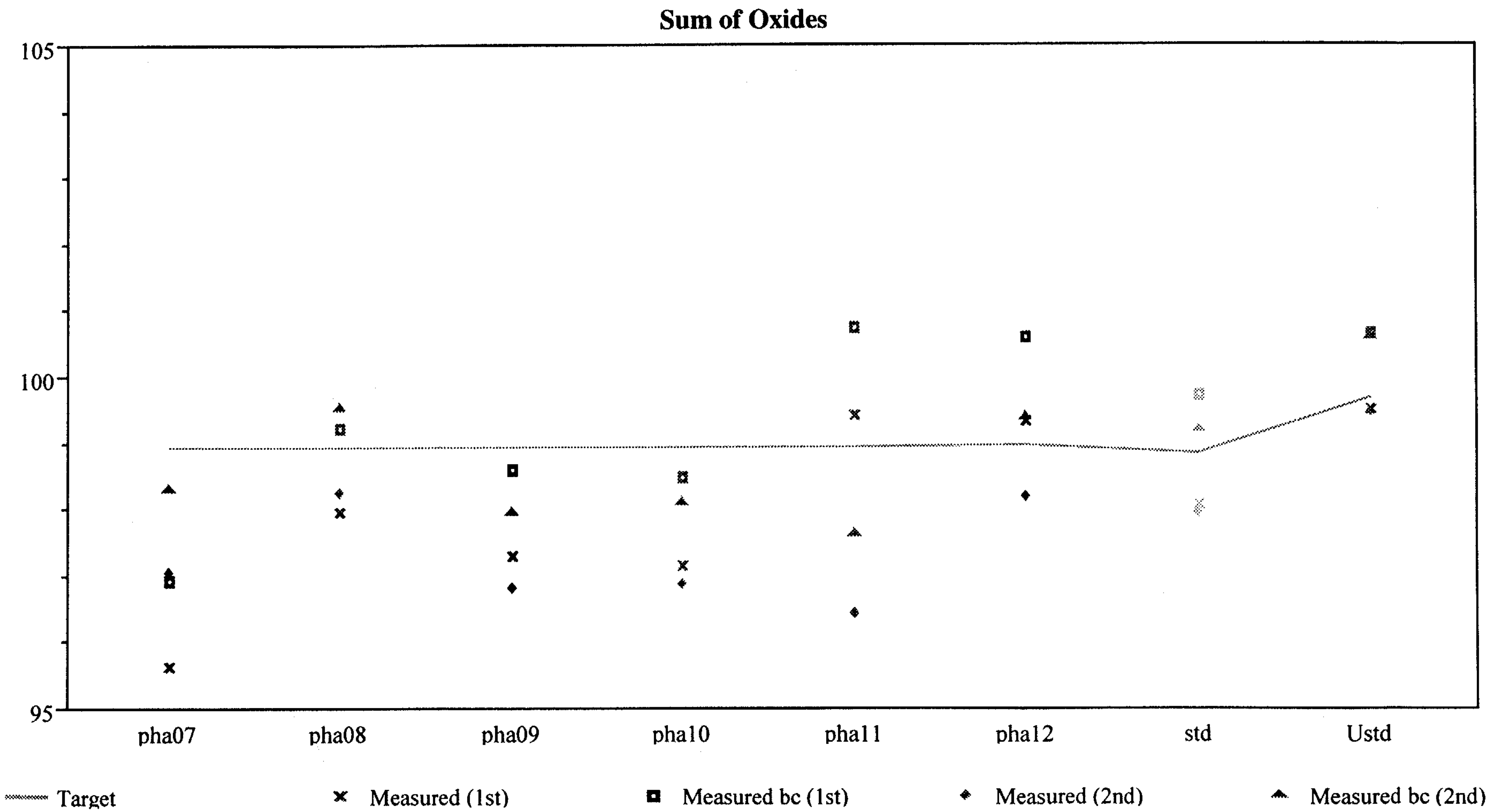

**This page intentionally left blank.**

## Attachment I

"Glass Compositions and Their Property Predictions for the PHA Alternative (U),"
SRT-SCS-99-010

March 18, 1999

13 Pages

**This page intentionally left blank.**

OSR 31-688 (Rev 11-20-97)
Stores: 26-8910.00

**WESTINGHOUSE SAVANNAH RIVER COMPANY**
# INTEROFFICE MEMORANDUM

BNFL

**SRT-SCS-99-010**

March 18, 1999

To: J. R. Harbour, 773-43A

cc: D. R. Best, 773-A
K. G. Brown, 704-1T
J. T. Carter, 704-3N
H. H. Elder, 704-S
C. R. Goetzman, 773-A
S. P. Harris, 773-42A (es)
E. W. Holtzscheiter, 773-A (es)
R. A. Jacobs, 704-3N
C. M. Jantzen, 773-A
D. Moore-Shedrow, 773-A (es)
C. T. Randall, 704-T (es)
R. C. Tuckfield, 773-42A

es - executive summary only

From: T. B. Edwards, 773-42A (5-5148)
Statistical Consulting Section

S. P. Harris, Technical Reviewer — 3/23/99 Date

R. C. Tuckfield, Manager
Statistical Consulting Section — 3/23/99 Date

# GLASS COMPOSITIONS AND THEIR PROPERTY PREDICTIONS FOR THE PHA ALTERNATIVE (U)

# *EXECUTIVE SUMMARY*

A task technical request (HLW SDT-TTR-99-07.0) has been submitted to the Savannah River Technology Center (SRTC) to initiate a study of the feasibility of incorporating anticipated levels of PHA into DWPF glass with and without doubling the nominal MST concentration.

A task technical & QA plan (WSRC-RP-99-00218) has been issued in response to the TTR. This memorandum provides details in support of the TT& QA plan in the form of target compositions for the glasses identified in the plan (including Purex, HM and Blend sludge types). The property models currently utilized by DWPF's Product Composition Control System (PCCS) are used to predict processability and product quality (durability) for these glasses. These predictions (although somewhat questionable due to expanded component ranges, beyond those over which the models were developed, that are required to cover the PHA contributions in the glass) provide insight that may be helpful in planning and sequencing the batching, fabricating, and testing of the glasses for this study.

This information provides the customer and SRTC reviewers/analysts an opportunity to gain a better understanding of some of the issues being considered as decisions on the sequencing and testing of these PHA glasses are made.

# *INTRODUCTION*

The Alternative Salt Disposition Flowsheet requires that the Defense Waste Processing Facility (DWPF) vitrify a coupled feed consisting of high level waste (HLW) and Precipitate Hydrolysis Aqueous (PHA). A technical task request (TTR) was received by the Savannah River Technology Center (SRTC) requesting that a glass variability study be conducted to explore the processability and product quality of the glass composition region for this alternative to the In-Tank Precipitation (ITP) Process [1]. A task technical and quality assurance (TT&QA) plan was issued by SRTC in response to the TTR [2]. The objective of that task is to obtain information on the feasibility of incorporating anticipated levels of PHA into DWPF glass with and without doubling the nominal levels of monosodium titanate (MST).

The objective of this memorandum is to provide the set of target compositions from which the glasses supporting this study are to be selected and to determine their process and product property predictions for the models utilized by DWPF's Product Composition Control System (PCCS).

# *DISCUSSION*

A limited PHA variability study is underway to analyze and test glasses generated from selected variations in the amounts of frit, PHA, MST, and sludge in the glass [2]. The MST concentrations are to be either 1.25% or 2.5% in the glass. The composition of MST is given in Table 1.

**Table 1: Oxide Composition of MST**

| Oxide | Weight Percent (wt%) |
|---|---|
| $Na_2O$ | 12.106 |
| $TiO_2$ | 87.894 |

The PHA formulation is provided in Table 2, and the PHA loadings in the glass are to be 7, 10, or 13 wt% on an oxide basis.

**Table 2: Oxide Composition of PHA**

| Oxide | Weight Percent (wt%) |
|---|---|
| $B_2O_3$ | 35.50 |
| CuO | 7.44 |
| $K_2O$ | 46.05 |
| $Na_2O$ | 11.02 |

The next component of the glass to identify is the sludge. Purex sludge is of primary interest in this study, and most of the glasses (18 of the planned 22) are expected to use this sludge. HM sludge is to be used for the remaining glasses (4 of the 22). The cation and anion compositions (and corresponding oxide compositions) used to represent these two types of sludge are provided in Tables 3 and 4.

**Table 3: Composition of Purex Sludge**

| Cation | Elemental wt% | Oxide | Gravimetric Factor | Oxide wt% in Sludge | Zeolite | Oxide wt% in Glass |
|---|---|---|---|---|---|---|
| Al | 3.780 | $Al_2O_3$ | 1.890 | 7.142 | 0.201 | 9.642 |
| B | 0.000 | $B_2O_3$ | 3.220 | 0.000 | | 0.000 |
| Ba | 0.260 | BaO | 1.117 | 0.290 | | 0.381 |
| Ca | 2.040 | CaO | 1.399 | 2.854 | 0.056 | 3.821 |
| Cr | 0.250 | $Cr_2O_3$ | 1.462 | 0.365 | | 0.480 |
| Cu | 0.130 | CuO | 1.252 | 0.163 | | 0.214 |
| Fe | 23.800 | $Fe_2O_3$ | 1.430 | 34.027 | 0.048 | 44.742 |
| K | 0.250 | $K_2O$ | 1.205 | 0.301 | 0.018 | 0.418 |
| Li | 0.000 | $Li_2O$ | 2.153 | 0.000 | | 0.000 |
| Mg | 0.130 | MgO | 1.658 | 0.216 | 0.016 | 0.304 |
| Mn | 4.630 | MnO | 1.291 | 5.978 | | 7.850 |
| Na | 6.900 | $Na_2O$ | 1.348 | 9.301 | 0.040 | 12.266 |
| Ni | 2.530 | NiO | 1.273 | 3.219 | | 4.227 |
| P | 0.046 | $P_2O_5$ | 2.291 | 0.105 | | 0.137 |
| Pb | 0.310 | PbO | 1.077 | 0.334 | | 0.438 |
| Si | 0.690 | $SiO_2$ | 2.139 | 1.476 | 0.857 | 3.063 |
| Ti | 0.000 | $TiO_2$ | 1.668 | 0.000 | | 0.000 |
| U | 5.880 | $U_3O_8$ | 1.179 | 6.934 | | 9.104 |
| Zn | 0.240 | ZnO | 1.245 | 0.299 | | 0.392 |
| Zr | 0.290 | $ZrO_2$ | 1.306 | 0.379 | | 0.497 |
| Wet Zeolite | 1.470 | Dry Zeolite | 0.841 | 1.236 | 1.236 | 0.000 |
| Anions | | Anions | | | | |
| F- | 0.110 | F- | 1.000 | 0.110 | | 0.144 |
| Cl- | 0.830 | Cl- | 1.000 | 0.830 | | 1.090 |
| $(SO_4)$- | 0.720 | $SO_3$ | 0.833 | 0.600 | | 0.788 |
| | | | Total | 76.160 | | 100.000 |

**Table 4: Composition of HM Sludge**

| Cation | Elemental wt% | Oxide | Gravimetric Factor | Oxide wt% in Sludge | Zeolite | Oxide wt% in Glass |
|---|---|---|---|---|---|---|
| Al | 8.930 | $Al_2O_3$ | 1.890 | 16.873 | 1.318 | 25.661 |
| B | 0.000 | $B_2O_3$ | 3.220 | 0.000 | | 0.000 |
| Ba | 0.130 | BaO | 1.117 | 0.145 | | 0.205 |
| Ca | 0.650 | CaO | 1.399 | 0.909 | 0.366 | 1.799 |
| Cr | 0.160 | $Cr_2O_3$ | 1.462 | 0.234 | | 0.330 |
| Cu | 0.044 | CuO | 1.252 | 0.055 | | 0.078 |
| Fe | 14.000 | $Fe_2O_3$ | 1.430 | 20.016 | 0.317 | 28.682 |
| K | 0.130 | $K_2O$ | 1.205 | 0.157 | 0.115 | 0.383 |
| Li | 0.000 | $Li_2O$ | 2.153 | 0.000 | | 0.000 |
| Mg | 0.210 | MgO | 1.658 | 0.348 | 0.106 | 0.641 |
| Mn | 4.880 | MnO | 1.291 | 6.301 | | 8.889 |
| Na | 5.680 | $Na_2O$ | 1.348 | 7.657 | 0.263 | 11.172 |
| Ni | 0.850 | NiO | 1.273 | 1.082 | | 1.526 |
| P | 0.046 | $P_2O_5$ | 2.291 | 0.105 | | 0.148 |
| Pb | 0.160 | PbO | 1.077 | 0.172 | | 0.243 |
| Si | 2.430 | $SiO_2$ | 2.139 | 5.198 | 5.614 | 15.253 |
| Ti | 0.000 | $TiO_2$ | 1.668 | 0.000 | | 0.000 |
| U | 1.850 | $U_3O_8$ | 1.179 | 2.182 | | 3.077 |
| Zn | 0.036 | ZnO | 1.245 | 0.045 | | 0.063 |
| Zr | 0.285 | $ZrO_2$ | 1.351 | 0.385 | | 0.543 |
| Wet Zeolite | 9.630 | Dry Zeolite | 0.841 | 8.098 | 8.099 | 0.000 |
| Anions | | Anions | | | | |
| F- | 0.120 | F- | 1.000 | 0.120 | | 0.169 |
| Cl- | 0.400 | Cl- | 1.000 | 0.400 | | 0.564 |
| $(SO_4)$- | 0.490 | $SO_3$ | 0.833 | 0.408 | | 0.576 |
| | | | Total | 70.890 | | 100.001 |

Note that zeolite is represented in these two tables. The amount of wet zeolite is provided in the cation column and the gravimetric factor for this component of the sludge represents its dry weight fraction. The normalized composition of zeolite is provided in Table 5.

**Table 5: Oxide Composition of Zeolite**

| Oxide | Weight Percent (wt%) |
|---|---|
| $Al_2O_3$ | 16.27 |
| CaO | 4.52 |
| $Fe_2O_3$ | 3.91 |
| $K_2O$ | 1.42 |
| MgO | 1.31 |
| $Na_2O$ | 3.25 |
| $SiO_2$ | 69.33 |

As discussed in the TT&QA plan, glasses made using Blend sludge are to be considered as candidate compositions as this study progresses depending on the process and product performance of the glasses tested. Table 6 provides the composition used to represent Blend sludge.

**Table 6: Composition of Blend Sludge**

| Cation | Elemental wt% | Oxide | Gravimetric Factor | Oxide wt% in Sludge | Oxide wt% in Zeolite | Oxide wt% in Glass |
|---|---|---|---|---|---|---|
| Al | 5.810 | $Al_2O_3$ | 1.890 | 10.978 | 0.646 | 15.138 |
| B | 0.000 | $B_2O_3$ | 3.220 | 0.000 | | 0.000 |
| Ba | 0.240 | BaO | 1.117 | 0.268 | | 0.349 |
| Ca | 1.690 | CaO | 1.399 | 2.365 | 0.179 | 3.313 |
| Cr | 0.240 | $Cr_2O_3$ | 1.462 | 0.351 | | 0.457 |
| Cu | 0.120 | CuO | 1.252 | 0.150 | | 0.196 |
| Fe | 22.300 | $Fe_2O_3$ | 1.430 | 31.882 | 0.155 | 41.723 |
| K | 0.320 | $K_2O$ | 1.205 | 0.385 | 0.056 | 0.575 |
| Li | 0.000 | $Li_2O$ | 2.153 | 0.000 | | 0.000 |
| Mg | 0.200 | MgO | 1.658 | 0.332 | 0.052 | 0.499 |
| Mn | 5.360 | MnO | 1.291 | 6.921 | | 9.013 |
| Na | 3.560 | $Na_2O$ | 1.348 | 4.799 | 0.129 | 6.418 |
| Ni | 2.140 | NiO | 1.273 | 2.723 | | 3.546 |
| P | 0.046 | $P_2O_5$ | 2.291 | 0.105 | | 0.136 |
| Pb | 0.280 | PbO | 1.077 | 0.302 | | 0.393 |
| Si | 2.160 | $SiO_2$ | 2.139 | 4.621 | 2.752 | 9.602 |
| Ti | 0.000 | $TiO_2$ | 1.668 | 0.000 | | 0.000 |
| U | 3.910 | $U_3O_8$ | 1.179 | 4.611 | | 6.005 |
| Zn | 0.190 | ZnO | 1.245 | 0.237 | | 0.308 |
| Zr | 0.285 | $ZrO_2$ | 1.351 | 0.385 | | 0.501 |
| Wet Zeolite | 4.720 | Dry Zeolite | 0.841 | 3.969 | 3.969 | 0.000 |
| Anions | | Anions | | | | |
| F- | 0.120 | F- | 1.000 | 0.120 | | 0.156 |
| Cl- | 0.700 | Cl- | 1.000 | 0.700 | | 0.912 |
| $(SO_4)$- | 0.700 | $SO_3$ | 0.834 | 0.584 | | 0.760 |
| | | | Total | 76.786 | | 100.000 |

The sludge oxide loadings to be considered in this study, regardless of sludge type, are 22, 26, and 30 wt% in the glass.

Finally, the formulation of the frit to be used in this study, Frit 202, will be based on measurements of the actual lot to be used for batching these glasses, Frit 202 Lot 14 [4]. These measurements are provided in Table 7.

**Table 7: Composition of Frit 202 Lot 14**

| Oxide | Weight Percent (wt%) |
|---|---|
| $Al_2O_3$ | 0.600 |
| $B_2O_3$ | 7.870 |
| CaO | 0.150 |
| $Fe_2O_3$ | 0.080 |
| $K_2O$ | 0.050 |
| $Li_2O$ | 6.860 |
| MgO | 1.980 |
| $Na_2O$ | 6.090 |
| $SiO_2$ | 76.000 |
| $TiO_2$ | 0.042 |

## *DEFINING THE GLASS COMPOSITIONS OF INTEREST*

The information appearing in the previous section is all that is necessary to develop the compositions from which glasses for this study are to be selected. Tables 8, 9, and 10 provide the compositions for glasses developed using Purex, HM, and Blend sludge, respectively.

## Table 8: Glasses of Interest for Purex Sludge

| Sludge | MST | PHA | Frit | Glass ID | $Al_2O_3$ | $B_2O_3$ | BaO | CaO | $Cr_2O_3$ | CuO | $Fe_2O_3$ | $K_2O$ | $Li_2O$ | MgO | MnO | Na2O | NiO | $P_2O_5$ | PbO | $SiO_2$ | $TiO_2$ | $U_3O_8$ | ZnO | $ZrO_2$ | F- | Cl- | $SO_3$ |
|---|---|---|---|---|---|---|---|---|---|---|---|---|---|---|---|---|---|---|---|---|---|---|---|---|---|---|---|
| 22 | 1.250 | 7 | 69.750 | pha01 | 2.540 | 7.974 | 0.084 | 0.945 | 0.106 | 0.568 | 9.899 | 3.350 | 4.785 | 1.448 | 1.727 | 7.869 | 0.930 | 0.030 | 0.096 | 53.684 | 1.128 | 2.003 | 0.086 | 0.109 | 0.032 | 0.240 | 0.173 |
| 22 | 1.250 | 10 | 66.750 | pha02 | 2.522 | 8.803 | 0.084 | 0.941 | 0.106 | 0.791 | 9.897 | 4.730 | 4.579 | 1.389 | 1.727 | 8.017 | 0.930 | 0.030 | 0.096 | 51.404 | 1.127 | 2.003 | 0.086 | 0.109 | 0.032 | 0.240 | 0.173 |
| 22 | 1.250 | 13 | 63.750 | pha03 | 2.504 | 9.632 | 0.084 | 0.936 | 0.106 | 1.014 | 9.894 | 6.110 | 4.373 | 1.329 | 1.727 | 8.165 | 0.930 | 0.030 | 0.096 | 49.124 | 1.125 | 2.003 | 0.086 | 0.109 | 0.032 | 0.240 | 0.173 |
| 22 | 2.500 | 7 | 68.500 | pha04 | 2.532 | 7.876 | 0.084 | 0.943 | 0.106 | 0.568 | 9.898 | 3.350 | 4.699 | 1.423 | 1.727 | 7.944 | 0.930 | 0.030 | 0.096 | 52.734 | 2.226 | 2.003 | 0.086 | 0.109 | 0.032 | 0.240 | 0.173 |
| 22 | 2.500 | 10 | 65.500 | pha05 | 2.514 | 8.705 | 0.084 | 0.939 | 0.106 | 0.791 | 9.896 | 4.730 | 4.493 | 1.364 | 1.727 | 8.092 | 0.930 | 0.030 | 0.096 | 50.454 | 2.225 | 2.003 | 0.086 | 0.109 | 0.032 | 0.240 | 0.173 |
| 22 | 2.500 | 13 | 62.500 | pha06 | 2.496 | 9.534 | 0.084 | 0.934 | 0.106 | 1.014 | 9.893 | 6.110 | 4.288 | 1.304 | 1.727 | 8.240 | 0.930 | 0.030 | 0.096 | 48.174 | 2.224 | 2.003 | 0.086 | 0.109 | 0.032 | 0.240 | 0.173 |
| 26 | 1.250 | 7 | 65.750 | pha07 | 2.901 | 7.660 | 0.099 | 1.092 | 0.125 | 0.576 | 11.685 | 3.365 | 4.510 | 1.381 | 2.041 | 8.116 | 1.099 | 0.036 | 0.114 | 50.766 | 1.126 | 2.367 | 0.102 | 0.129 | 0.038 | 0.283 | 0.205 |
| 26 | 1.250 | 10 | 62.750 | pha08 | 2.883 | 8.488 | 0.099 | 1.088 | 0.125 | 0.800 | 11.683 | 4.745 | 4.305 | 1.322 | 2.041 | 8.264 | 1.099 | 0.036 | 0.114 | 48.486 | 1.125 | 2.367 | 0.102 | 0.129 | 0.038 | 0.283 | 0.205 |
| 26 | 1.250 | 13 | 59.750 | pha09 | 2.865 | 9.317 | 0.099 | 1.083 | 0.125 | 1.023 | 11.681 | 6.125 | 4.099 | 1.262 | 2.041 | 8.412 | 1.099 | 0.036 | 0.114 | 46.206 | 1.124 | 2.367 | 0.102 | 0.129 | 0.038 | 0.283 | 0.205 |
| 26 | 2.500 | 7 | 64.500 | pha10 | 2.894 | 7.561 | 0.099 | 1.090 | 0.125 | 0.576 | 11.684 | 3.365 | 4.425 | 1.356 | 2.041 | 8.191 | 1.099 | 0.036 | 0.114 | 49.816 | 2.224 | 2.367 | 0.102 | 0.129 | 0.038 | 0.283 | 0.205 |
| 26 | 2.500 | 10 | 61.500 | pha11 | 2.876 | 8.390 | 0.099 | 1.086 | 0.125 | 0.800 | 11.682 | 4.745 | 4.219 | 1.297 | 2.041 | 8.339 | 1.099 | 0.036 | 0.114 | 47.536 | 2.223 | 2.367 | 0.102 | 0.129 | 0.038 | 0.283 | 0.205 |
| 26 | 2.500 | 13 | 58.500 | pha12 | 2.858 | 9.219 | 0.099 | 1.081 | 0.125 | 1.023 | 11.680 | 6.125 | 4.013 | 1.237 | 2.041 | 8.487 | 1.099 | 0.036 | 0.114 | 45.256 | 2.222 | 2.367 | 0.102 | 0.129 | 0.038 | 0.283 | 0.205 |
| 30 | 1.250 | 7 | 61.750 | pha13 | 3.263 | 7.345 | 0.114 | 1.239 | 0.144 | 0.585 | 13.472 | 3.380 | 4.236 | 1.314 | 2.355 | 8.363 | 1.268 | 0.041 | 0.132 | 47.849 | 1.125 | 2.731 | 0.118 | 0.149 | 0.043 | 0.327 | 0.236 |
| 30 | 1.250 | 10 | 58.750 | pha14 | 3.245 | 8.174 | 0.114 | 1.234 | 0.144 | 0.808 | 13.470 | 4.760 | 4.030 | 1.255 | 2.355 | 8.511 | 1.268 | 0.041 | 0.132 | 45.569 | 1.123 | 2.731 | 0.118 | 0.149 | 0.043 | 0.327 | 0.236 |
| 30 | 1.250 | 13 | 55.750 | pha15 | 3.227 | 9.003 | 0.114 | 1.230 | 0.144 | 1.031 | 13.467 | 6.140 | 3.824 | 1.195 | 2.355 | 8.659 | 1.268 | 0.041 | 0.132 | 43.289 | 1.122 | 2.731 | 0.118 | 0.149 | 0.043 | 0.327 | 0.236 |
| 30 | 2.500 | 7 | 60.500 | pha16 | 3.256 | 7.246 | 0.114 | 1.237 | 0.144 | 0.585 | 13.471 | 3.379 | 4.150 | 1.289 | 2.355 | 8.438 | 1.268 | 0.041 | 0.132 | 46.899 | 2.223 | 2.731 | 0.118 | 0.149 | 0.043 | 0.327 | 0.236 |
| 30 | 2.500 | 10 | 57.500 | pha17 | 3.238 | 8.075 | 0.114 | 1.233 | 0.144 | 0.808 | 13.469 | 4.759 | 3.945 | 1.230 | 2.355 | 8.586 | 1.268 | 0.041 | 0.132 | 44.619 | 2.221 | 2.731 | 0.118 | 0.149 | 0.043 | 0.327 | 0.236 |
| 30 | 2.500 | 13 | 54.500 | pha18 | 3.220 | 8.904 | 0.114 | 1.228 | 0.144 | 1.031 | 13.466 | 6.139 | 3.739 | 1.170 | 2.355 | 8.734 | 1.268 | 0.041 | 0.132 | 42.339 | 2.220 | 2.731 | 0.118 | 0.149 | 0.043 | 0.327 | 0.236 |

## Table 9: Glasses of Interest for HM Sludge

| Sludge | MST | PHA | Frit | Glass ID | $Al_2O_3$ | $B_2O_3$ | BaO | CaO | $Cr_2O_3$ | CuO | $Fe_2O_3$ | $K_2O$ | $Li_2O$ | MgO | MnO | Na2O | NiO | $P_2O_5$ | PbO | $SiO_2$ | $TiO_2$ | $U_3O_8$ | ZnO | $ZrO_2$ | F- | Cl- | $SO_3$ |
|---|---|---|---|---|---|---|---|---|---|---|---|---|---|---|---|---|---|---|---|---|---|---|---|---|---|---|---|
| 22 | 1.250 | 7 | 69.750 | pha19 | 6.064 | 7.974 | 0.045 | 0.500 | 0.073 | 0.538 | 6.366 | 3.343 | 4.785 | 1.522 | 1.955 | 7.628 | 0.336 | 0.032 | 0.053 | 56.366 | 1.128 | 0.677 | 0.014 | 0.119 | 0.037 | 0.124 | 0.127 |
| 22 | 1.250 | 10 | 66.750 | pha20 | 6.046 | 8.803 | 0.045 | 0.496 | 0.073 | 0.761 | 6.363 | 4.723 | 4.579 | 1.463 | 1.955 | 7.776 | 0.336 | 0.032 | 0.053 | 54.086 | 1.127 | 0.677 | 0.014 | 0.119 | 0.037 | 0.124 | 0.127 |
| 22 | 1.250 | 13 | 63.750 | pha21 | 6.028 | 9.632 | 0.045 | 0.491 | 0.073 | 0.984 | 6.361 | 6.103 | 4.373 | 1.403 | 1.955 | 7.924 | 0.336 | 0.032 | 0.053 | 51.806 | 1.125 | 0.677 | 0.014 | 0.119 | 0.037 | 0.124 | 0.127 |
| 22 | 2.500 | 7 | 68.500 | pha22 | 6.056 | 7.876 | 0.045 | 0.499 | 0.073 | 0.538 | 6.365 | 3.342 | 4.699 | 1.497 | 1.955 | 7.704 | 0.336 | 0.032 | 0.053 | 55.416 | 2.226 | 0.677 | 0.014 | 0.119 | 0.037 | 0.124 | 0.127 |
| 22 | 2.500 | 10 | 65.500 | pha23 | 6.038 | 8.705 | 0.045 | 0.494 | 0.073 | 0.761 | 6.362 | 4.722 | 4.493 | 1.438 | 1.955 | 7.851 | 0.336 | 0.032 | 0.053 | 53.136 | 2.225 | 0.677 | 0.014 | 0.119 | 0.037 | 0.124 | 0.127 |
| 22 | 2.500 | 13 | 62.500 | pha24 | 6.020 | 9.534 | 0.045 | 0.490 | 0.073 | 0.984 | 6.360 | 6.102 | 4.288 | 1.378 | 1.955 | 7.999 | 0.336 | 0.032 | 0.053 | 50.856 | 2.224 | 0.677 | 0.014 | 0.119 | 0.037 | 0.124 | 0.127 |
| 26 | 1.250 | 7 | 65.750 | pha25 | 7.066 | 7.660 | 0.053 | 0.566 | 0.086 | 0.541 | 7.510 | 3.356 | 4.510 | 1.468 | 2.311 | 7.832 | 0.397 | 0.038 | 0.063 | 53.936 | 1.126 | 0.800 | 0.016 | 0.141 | 0.044 | 0.147 | 0.150 |
| 26 | 1.250 | 10 | 62.750 | pha26 | 7.048 | 8.488 | 0.053 | 0.562 | 0.086 | 0.764 | 7.507 | 4.736 | 4.305 | 1.409 | 2.311 | 7.980 | 0.397 | 0.038 | 0.063 | 51.656 | 1.125 | 0.800 | 0.016 | 0.141 | 0.044 | 0.147 | 0.150 |
| 26 | 1.250 | 13 | 59.750 | pha27 | 7.030 | 9.317 | 0.053 | 0.557 | 0.086 | 0.987 | 7.505 | 6.116 | 4.099 | 1.350 | 2.311 | 8.127 | 0.397 | 0.038 | 0.063 | 49.376 | 1.124 | 0.800 | 0.016 | 0.141 | 0.044 | 0.147 | 0.150 |
| 26 | 2.500 | 7 | 64.500 | pha28 | 7.059 | 7.561 | 0.053 | 0.565 | 0.086 | 0.541 | 7.509 | 3.355 | 4.425 | 1.444 | 2.311 | 7.907 | 0.397 | 0.038 | 0.063 | 52.986 | 2.224 | 0.800 | 0.016 | 0.141 | 0.044 | 0.147 | 0.150 |
| 26 | 2.500 | 10 | 61.500 | pha29 | 7.041 | 8.390 | 0.053 | 0.560 | 0.086 | 0.764 | 7.506 | 4.735 | 4.219 | 1.384 | 2.311 | 8.055 | 0.397 | 0.038 | 0.063 | 50.706 | 2.223 | 0.800 | 0.016 | 0.141 | 0.044 | 0.147 | 0.150 |
| 26 | 2.500 | 13 | 58.500 | pha30 | 7.023 | 9.219 | 0.053 | 0.556 | 0.086 | 0.987 | 7.504 | 6.115 | 4.013 | 1.325 | 2.311 | 8.203 | 0.397 | 0.038 | 0.063 | 48.426 | 2.222 | 0.800 | 0.016 | 0.141 | 0.044 | 0.147 | 0.150 |
| 30 | 1.250 | 7 | 61.750 | pha31 | 8.069 | 7.345 | 0.061 | 0.632 | 0.099 | 0.544 | 8.654 | 3.369 | 4.236 | 1.415 | 2.667 | 8.035 | 0.458 | 0.044 | 0.073 | 51.506 | 1.125 | 0.923 | 0.019 | 0.163 | 0.051 | 0.169 | 0.173 |
| 30 | 1.250 | 10 | 58.750 | pha32 | 8.051 | 8.174 | 0.061 | 0.628 | 0.099 | 0.767 | 8.652 | 4.749 | 4.030 | 1.355 | 2.667 | 8.183 | 0.458 | 0.044 | 0.073 | 49.226 | 1.123 | 0.923 | 0.019 | 0.163 | 0.051 | 0.169 | 0.173 |
| 30 | 1.250 | 13 | 55.750 | pha33 | 8.033 | 9.003 | 0.061 | 0.623 | 0.099 | 0.991 | 8.649 | 6.129 | 3.824 | 1.296 | 2.667 | 8.331 | 0.458 | 0.044 | 0.073 | 46.946 | 1.122 | 0.923 | 0.019 | 0.163 | 0.051 | 0.169 | 0.173 |
| 30 | 2.500 | 7 | 60.500 | pha34 | 8.061 | 7.246 | 0.061 | 0.631 | 0.099 | 0.544 | 8.653 | 3.369 | 4.150 | 1.390 | 2.667 | 8.110 | 0.458 | 0.044 | 0.073 | 50.556 | 2.223 | 0.923 | 0.019 | 0.163 | 0.051 | 0.169 | 0.173 |
| 30 | 2.500 | 10 | 57.500 | pha35 | 8.043 | 8.075 | 0.061 | 0.626 | 0.099 | 0.767 | 8.651 | 4.749 | 3.945 | 1.331 | 2.667 | 8.258 | 0.458 | 0.044 | 0.073 | 48.276 | 2.221 | 0.923 | 0.019 | 0.163 | 0.051 | 0.169 | 0.173 |
| 30 | 2.500 | 13 | 54.500 | pha36 | 8.025 | 8.904 | 0.061 | 0.622 | 0.099 | 0.991 | 8.648 | 6.129 | 3.739 | 1.271 | 2.667 | 8.406 | 0.458 | 0.044 | 0.073 | 45.996 | 2.220 | 0.923 | 0.019 | 0.163 | 0.051 | 0.169 | 0.173 |

**Table 10: Glasses of Interest for Blend Sludge**

| Sludge | MST | PHA | Frit | Glass ID | $Al_2O_3$ | $B_2O_3$ | BaO | CaO | $Cr_2O_3$ | CuO | $Fe_2O_3$ | $K_2O$ | $Li_2O$ | MgO | MnO | Na2O | NiO | $P_2O_5$ | PbO | $SiO_2$ | $TiO_2$ | $U_3O_8$ | ZnO | $ZrO_2$ | F- | Cl- | $SO_3$ |
|---|---|---|---|---|---|---|---|---|---|---|---|---|---|---|---|---|---|---|---|---|---|---|---|---|---|---|---|
| 22 | 1.250 | 7 | 69.750 | pha37 | 3.749 | 7.974 | 0.077 | 0.834 | 0.101 | 0.564 | 9.235 | 3.385 | 4.785 | 1.491 | 1.983 | 6.582 | 0.780 | 0.030 | 0.086 | 55.122 | 1.128 | 1.321 | 0.068 | 0.110 | 0.034 | 0.201 | 0.167 |
| 22 | 1.250 | 10 | 66.750 | pha38 | 3.731 | 8.803 | 0.077 | 0.829 | 0.101 | 0.787 | 9.232 | 4.765 | 4.579 | 1.432 | 1.983 | 6.730 | 0.780 | 0.030 | 0.086 | 52.842 | 1.127 | 1.321 | 0.068 | 0.110 | 0.034 | 0.201 | 0.167 |
| 22 | 1.250 | 13 | 63.750 | pha39 | 3.713 | 9.632 | 0.077 | 0.825 | 0.101 | 1.010 | 9.230 | 6.145 | 4.373 | 1.372 | 1.983 | 6.878 | 0.780 | 0.030 | 0.086 | 50.562 | 1.125 | 1.321 | 0.068 | 0.110 | 0.034 | 0.201 | 0.167 |
| 22 | 2.500 | 7 | 68.500 | pha40 | 3.741 | 7.876 | 0.077 | 0.832 | 0.101 | 0.564 | 9.234 | 3.384 | 4.699 | 1.466 | 1.983 | 6.658 | 0.780 | 0.030 | 0.086 | 54.172 | 2.226 | 1.321 | 0.068 | 0.110 | 0.034 | 0.201 | 0.167 |
| 22 | 2.500 | 10 | 65.500 | pha41 | 3.723 | 8.705 | 0.077 | 0.827 | 0.101 | 0.787 | 9.231 | 4.764 | 4.493 | 1.407 | 1.983 | 6.805 | 0.780 | 0.030 | 0.086 | 51.892 | 2.225 | 1.321 | 0.068 | 0.110 | 0.034 | 0.201 | 0.167 |
| 22 | 2.500 | 13 | 62.500 | pha42 | 3.705 | 9.534 | 0.077 | 0.823 | 0.101 | 1.010 | 9.229 | 6.144 | 4.288 | 1.347 | 1.983 | 6.953 | 0.780 | 0.030 | 0.086 | 49.612 | 2.224 | 1.321 | 0.068 | 0.110 | 0.034 | 0.201 | 0.167 |
| 26 | 1.250 | 7 | 65.750 | pha43 | 4.330 | 7.660 | 0.091 | 0.960 | 0.119 | 0.572 | 10.901 | 3.406 | 4.510 | 1.432 | 2.343 | 6.595 | 0.922 | 0.035 | 0.102 | 52.466 | 1.126 | 1.561 | 0.080 | 0.130 | 0.041 | 0.237 | 0.198 |
| 26 | 1.250 | 10 | 62.750 | pha44 | 4.312 | 8.488 | 0.091 | 0.956 | 0.119 | 0.795 | 10.898 | 4.786 | 4.305 | 1.372 | 2.343 | 6.743 | 0.922 | 0.035 | 0.102 | 50.186 | 1.125 | 1.561 | 0.080 | 0.130 | 0.041 | 0.237 | 0.198 |
| 26 | 1.250 | 13 | 59.750 | pha45 | 4.294 | 9.317 | 0.091 | 0.951 | 0.119 | 1.018 | 10.896 | 6.166 | 4.099 | 1.313 | 2.343 | 6.891 | 0.922 | 0.035 | 0.102 | 47.906 | 1.124 | 1.561 | 0.080 | 0.130 | 0.041 | 0.237 | 0.198 |
| 26 | 2.500 | 7 | 64.500 | pha46 | 4.323 | 7.561 | 0.091 | 0.958 | 0.119 | 0.572 | 10.900 | 3.405 | 4.425 | 1.407 | 2.343 | 6.671 | 0.922 | 0.035 | 0.102 | 51.516 | 2.224 | 1.561 | 0.080 | 0.130 | 0.041 | 0.237 | 0.198 |
| 26 | 2.500 | 10 | 61.500 | pha47 | 4.305 | 8.390 | 0.091 | 0.954 | 0.119 | 0.795 | 10.897 | 4.785 | 4.219 | 1.348 | 2.343 | 6.819 | 0.922 | 0.035 | 0.102 | 49.236 | 2.223 | 1.561 | 0.080 | 0.130 | 0.041 | 0.237 | 0.198 |
| 26 | 2.500 | 13 | 58.500 | pha48 | 4.287 | 9.219 | 0.091 | 0.949 | 0.119 | 1.018 | 10.895 | 6.165 | 4.013 | 1.288 | 2.343 | 6.966 | 0.922 | 0.035 | 0.102 | 46.956 | 2.222 | 1.561 | 0.080 | 0.130 | 0.041 | 0.237 | 0.198 |
| 30 | 1.250 | 7 | 61.750 | pha49 | 4.912 | 7.345 | 0.105 | 1.087 | 0.137 | 0.579 | 12.566 | 3.427 | 4.236 | 1.372 | 2.704 | 6.609 | 1.064 | 0.041 | 0.118 | 49.810 | 1.125 | 1.801 | 0.092 | 0.150 | 0.047 | 0.273 | 0.228 |
| 30 | 1.250 | 10 | 58.750 | pha50 | 4.894 | 8.174 | 0.105 | 1.082 | 0.137 | 0.803 | 12.564 | 4.807 | 4.030 | 1.313 | 2.704 | 6.757 | 1.064 | 0.041 | 0.118 | 47.530 | 1.123 | 1.801 | 0.092 | 0.150 | 0.047 | 0.273 | 0.228 |
| 30 | 1.250 | 13 | 55.750 | pha51 | 4.876 | 9.003 | 0.105 | 1.078 | 0.137 | 1.026 | 12.562 | 6.187 | 3.824 | 1.254 | 2.704 | 6.904 | 1.064 | 0.041 | 0.118 | 45.250 | 1.122 | 1.801 | 0.092 | 0.150 | 0.047 | 0.273 | 0.228 |
| 30 | 2.500 | 7 | 60.500 | pha52 | 4.904 | 7.246 | 0.105 | 1.085 | 0.137 | 0.579 | 12.565 | 3.426 | 4.150 | 1.348 | 2.704 | 6.684 | 1.064 | 0.041 | 0.118 | 48.860 | 2.223 | 1.801 | 0.092 | 0.150 | 0.047 | 0.273 | 0.228 |
| 30 | 2.500 | 10 | 57.500 | pha53 | 4.886 | 8.075 | 0.105 | 1.080 | 0.137 | 0.803 | 12.563 | 4.806 | 3.945 | 1.288 | 2.704 | 6.832 | 1.064 | 0.041 | 0.118 | 46.580 | 2.221 | 1.801 | 0.092 | 0.150 | 0.047 | 0.273 | 0.228 |
| 30 | 2.500 | 13 | 54.500 | pha54 | 4.868 | 8.904 | 0.105 | 1.076 | 0.137 | 1.026 | 12.561 | 6.186 | 3.739 | 1.229 | 2.704 | 6.980 | 1.064 | 0.041 | 0.118 | 44.300 | 2.220 | 1.801 | 0.092 | 0.150 | 0.047 | 0.273 | 0.228 |

The glasses that are to be batched, fabricated, and tested as part of this study are to be taken from this set of 54 compositions. Although Purex glasses are of primary interest (followed by glasses prepared using the HM sludge), process and product property predictions are to be determined and used to direct the sequencing of the testing of these glasses.

### *PROCESS AND PRODUCT PROPERTY PREDICTIONS*

DWPF uses the Product Composition Control System (PCCS) to determine the acceptability of each Slurry Mix Evaporator (SME) batch. There are constraints for boron, lithium, and sodium leaching, liquidus temperature, high and low viscosity, homogeneity, alumina, low and high conservation (sum of oxides), low and high frit loading, titanium, chloride, fluoride, chromium, sulfate, copper, and phosphorus. The development of the coefficients relating each of these property constraints to glass composition is explained in the SME acceptability document [3]. Each of the constraints involving property predictions based on a statistical model of glass composition has two sources of uncertainty that must be addressed: model uncertainty and measurement uncertainty. (Constraints directly related to glass composition have, at most, measurement uncertainty that must be addressed.) Each model's uncertainty leads to the definition of the property acceptance region (PAR) for that property model. Historical correlation matrices and coefficients of variation for measurements are used by the PCCS algorithms to estimate the measurement uncertainty associated with model predictions based on the average composition of the SME material. These considerations lead to the development of the measurement acceptance region (MAR) for each property model.

The coefficients relating each of the other property constraints to glass composition (in molar oxides) are given in Table 11.[1] The determination of the PAR and MAR regions for these constraints is discussed in [3]. For the target compositions being considered in this study, some of the constraints listed above are not involved and/or are easily satisfied, and they are not included in the discussion that follows.[2] In addition, the current PCCS limit for $TiO_2$ of 1 wt% (in the glass) is violated for each of the candidate compositions. Process and product property behavior for glasses containing this much titanium is of interest for this study.

---

1 The molar oxide concentration, c, corresponding to a cation concentration, expressed as weight percent, x, is determined equation $c = x*g/m$ where g is the gravimetric factor for the corresponding oxide and m is the molecular weight for this oxide.

2 The amounts of chromium, sulfate, chloride, and fluoride targeted in the batching of these glasses were well below the waste solubility limits represented by the corresponding constraints in Table 11.

### Table 11: Constraint Coefficients Relating Molar Oxide Concentrations to the Property Models

| Oxide | B Leaching | Li Leaching | Na Leaching | Liquidus Temp | High Viscosity | Low Viscosity | Homogeneity | $Al_2O_3$ | Low Conserv | High Conserv | Low Frit | High Frit | TiO2 | Cr2O3 | Cu | P2O5 |
|---|---|---|---|---|---|---|---|---|---|---|---|---|---|---|---|---|
| $Al_2O_3$ | 37.680 | 37.680 | 37.680 | -34.9431 | -2 | 2 | 575.85645 | 101.961 | 101.9612 | -101.9612 | 0 | 0 | 0 | 0 | 0 | 0 |
| $B_2O_3$ | -10.430 | -10.430 | -10.430 | 0 | 1 | -1 | 111.635994 | 0 | 69.6202 | -69.6202 | 69.6202 | -69.6202 | 0 | 0 | 0 | 0 |
| CaO | -13.790 | -13.790 | -13.790 | 0 | 0 | 0 | 316.72525 | 0 | 56.0794 | -56.0794 | 0 | 0 | 0 | 0 | 0 | 0 |
| $Cr_2O_3$ | 11.950 | 11.950 | 11.950 | 0 | 0 | 0 | 0 | 0 | 151.9902 | -151.9902 | 0 | 0 | 0 | -151.9902 | 0 | 0 |
| CuO | -4.955 | -4.955 | -4.955 | 0 | 0 | 0 | 0 | 0 | 75.5439 | -75.5439 | 0 | 0 | 0 | 0 | -63.5383 | 0 |
| $Fe_2O_3$ | 14.560 | 14.560 | 14.560 | -134 | 2 | -2 | 901.9096 | 0 | 159.6922 | -159.6922 | 0 | 0 | 0 | 0 | 0 | 0 |
| $K_2O$ | -76.410 | -76.410 | -76.410 | 0 | 2 | -2 | 151.05515 | 0 | 94.2034 | -94.2034 | 94.2034 | -94.2034 | 0 | 0 | 0 | 0 |
| $Li_2O$ | -24.040 | -24.040 | -24.040 | 0 | 2 | -2 | 47.90841 | 0 | 29.8774 | -29.8774 | 29.8774 | -29.8774 | 0 | 0 | 0 | 0 |
| MgO | -6.570 | -6.570 | -6.570 | 0 | 0 | 0 | 0 | 0 | 40.3114 | -40.3114 | 0 | 0 | 0 | 0 | 0 | 0 |
| MnO | -24.440 | -24.440 | -24.440 | 0 | 0 | 0 | 0 | 0 | 70.9374 | -70.9374 | 0 | 0 | 0 | 0 | 0 | 0 |
| $Na_2O$ | -53.090 | -53.090 | -53.090 | 0 | 2 | -2 | 99.38332 | 0 | 61.9790 | -61.9790 | 61.9790 | -61.9790 | 0 | 0 | 0 | 0 |
| NiO | 0.370 | 0.370 | 0.370 | 0 | 0 | 0 | 0 | 0 | 74.7094 | -74.7094 | 0 | 0 | 0 | 0 | 0 | 0 |
| $P_2O_5$ | -26..550 | -26..550 | -26..550 | 0 | 0 | 0 | 0 | 0 | 141.945 | -141.945 | 0 | 0 | 0 | 0 | 0 | -141.945 |
| $SiO_2$ | 4.050 | 4.050 | 4.050 | 15.1082 | -0.8471 | 1.2682 | 96.34598 | 0 | 60.0848 | -60.0848 | 60.0848 | -60.0848 | 0 | 0 | 0 | 0 |
| $TiO_2$ | 16.270 | 16.270 | 16.270 | 0 | 0 | 0 | 0 | 0 | 79.8988 | -79.8988 | 0 | 0 | -79.8988 | 0 | 0 | 0 |
| $U_3O_8$ | -23.770 | -23.770 | -23.770 | 0 | 0 | 0 | 0 | 0 | 842.085 | -842.085 | 0 | 0 | 0 | 0 | 0 | 0 |
| PAR | -12.8215 | -12.7178 | -13.0167 | 0 | 0 | 0 | 210.9203 | 3 | 95 | -105 | 70 | -85 | -1 | -0.3 | -0.5 | -2.25 |

*Note: PAR represents the boundary of the property acceptance region for the given constraint. Each of the constraints is expressed as a greater-than inequality implying that the constraint evaluated for the average molar oxides concentrations should be greater than the corresponding PAR value. The PAR values for the liquidus temperature constraint may be re-expressed as 1024.9 degrees Celsius, and the viscosity PAR interval as 21.5 to 95.3 poise[3].*

Also, the presence of PHA and MST in the glass at the levels considered in this study leads to an expanded composition region beyond that over which the current PCCS models were developed. Thus, there is some question as to the appropriateness of one or more of these property models. They are the best available tools, however, for providing insight into the likely behavior of the glasses of interest, before the glasses are batched and tested. Process and product properties of interest have been evaluated for the 54 glasses identified in Tables 8-10 using their target oxide compositions and the predictive models as represented by Table 11 and as discussed in [3], and the results appear in Table 12.

**Table 12: Property Predictions by Glass ID**

| Sludge Type | Sludge | Loadings MST | PHA | Frit | Glass ID | del $G_p$ | NL[B (g/L)] | NL[Li (g/L)] | NL[Na (g/L)] | Frit wt% | Homo. Wt% | Visc. poise | $T_L$ Deg. C |
|---|---|---|---|---|---|---|---|---|---|---|---|---|---|
| Purex | 22 | 1.25 | 7 | 69.75 | pha01 | -9.948 | 0.797 | 0.821 | 0.794 | 77.66 | 200.12 | 70.20 | 949.30 |
| Purex | 22 | 1.25 | 10 | 66.75 | pha02 | -11.317 | 1.410 | 1.304 | 1.361 | 77.53 | 199.78 | 53.10 | 956.10 |
| Purex | 22 | 1.25 | 13 | 63.75 | pha03 | -12.685 | 2.495 | 2.071 | 2.333 | 77.40 | 199.43 | 39.10 | 963.60 |
| Purex | 22 | 2.5 | 7 | 68.5 | pha04 | -9.767 | 0.739 | 0.773 | 0.740 | 76.60 | 198.36 | 67.40 | 952.00 |
| Purex | 22 | 2.5 | 10 | 65.5 | pha05 | -11.136 | 1.307 | 1.227 | 1.268 | 76.47 | 198.02 | 50.60 | 959.10 |
| Purex | 22 | 2.5 | 13 | 62.5 | pha06 | -12.505 | 2.315 | 1.94'9 | 2.173 | 76.35 | 197.67 | 36.90 | 966.90 |
| Purex | 26 | 1.25 | 7 | 65.75 | pha07 | -9.945 | 0.795 | 0.820 | 0.793 | 74.42 | 207.87 | 58.00 | 988.00 |
| Purex | 26 | 1.25 | 10 | 62.75 | pha08 | -11.314 | 1.408 | 1.303 | 1.360 | 74.29 | 207.53 | 42.70 | 997.30 |
| Purex | 26 | 1.25 | 13 | 59.75 | pha09 | -12.682 | 2.493 | 2.070 | 2.331 | 74.16 | 207.18 | 30.50 | 1007.60 |
| Purex | 26 | 2.5 | 7 | 64.5 | pha10 | -9.765 | 0.738 | 0.772 | 0.739 | 73.36 | 206.12 | 55.30 | 991.80 |
| Purex | 26 | 2.5 | 10 | 61.5 | pha11 | -11.133 | 1.306 | 1.226 | 1.266 | 73.23 | 205.78 | 40.40 | 1001.50 |
| Purex | 26 | 2.5 | 13 | 58.5 | pha12 | -12.501 | 2.311 | 1.947 | 2.170 | 73.10 | 205.43 | 28.50 | 1012.20 |
| Purex | 30 | 1.25 | 7 | 61.75 | pha13 | -9.942 | 0.794 | 0.819 | 0.792 | 71.17 | 215.64 | 46.70 | 1032.90 |
| Purex | 30 | 1.25 | 10 | 58.75 | pha14 | -11.310 | 1.406 | 1.301 | 1.358 | 71.04 | 215.29 | 33.30 | 1045.40 |
| Purex | 30 | 1.25 | 13 | 55.75 | pha15 | -12.679 | 2.489 | 2.067 | 2.327 | 70.92 | 214.94 | 23.00 | 1059.30 |
| Purex | 30 | 2.5 | 7 | 60.5 | pha16 | -9.760 | 0.736 | 0.771 | 0.737 | 70.11 | 213.88 | 44.30 | 1037.90 |
| Purex | 30 | 2.5 | 10 | 57.5 | pha17 | -11.129 | 1.304 | 1.224 | 1.264 | 69.98 | 213.54 | 31.30 | 1051.00 |
| Purex | 30 | 2.5 | 13 | 54.5 | pha18 | -12.497 | 2.307 | 1.944 | 2.167 | 69.86 | 213.19 | 21.30 | 1065.70 |
| HM | 22 | 1.25 | 7 | 69.75 | pha19 | -8.520 | 0.439 | 0.507 | 0.453 | 80.10 | 201.46 | 129.80 | 901.50 |
| HM | 22 | 1.25 | 10 | 66.75 | pha20 | -9.889 | 0.777 | 0.805 | 0.776 | 79.97 | 201.11 | 102.00 | 906.30 |
| HM | 22 | 1.25 | 13 | 63.75 | pha21 | -11.257 | 1.375 | 1.278 | 1.330 | 79.84 | 200.76 | 78.50 | 911.50 |
| HM | 22 | 2.5 | 7 | 68.5 | pha22 | -8.340 | 0.407 | 0.477 | 0.422 | 79.04 | 199.71 | 126.10 | 903.40 |
| HM | 22 | 2.5 | 10 | 65.5 | pha23 | -9.708 | 0.720 | 0.757 | 0.722 | 78.91 | 199.35 | 98.60 | 908.40 |
| HM | 22 | 2.5 | 13 | 62.5 | pha24 | -11.077 | 1.276 | 1.203 | 1.239 | 78.78 | 199.01 | 75.40 | 913.90 |
| HM | 26 | 1.25 | 7 | 65.75 | pha25 | -8.258 | 0.393 | 0.464 | 0.408 | 77.29 | 209.46 | 125.10 | 928.90 |
| HM | 26 | 1.25 | 10 | 62.75 | pha26 | -9.627 | 0.697 | 0.737 | 0.700 | 77.16 | 209.11 | 97.00 | 935.60 |
| HM | 26 | 1.25 | 13 | 59.75 | pha27 | -10.994 | 1.232 | 1.170 | 1.199 | 77.04 | 208.76 | 73.60 | 943.00 |
| HM | 26 | 2.5 | 7 | 64.5 | pha28 | -8.077 | 0.365 | 0.436 | 0.380 | 76.23 | 207.71 | 121.30 | 931.60 |
| HM | 26 | 2.5 | 10 | 61.5 | pha29 | -9.445 | 0.646 | 0.693 | 0.651 | 76.11 | 207.36 | 93.60 | 938.60 |
| HM | 26 | 2.5 | 13 | 58.5 | pha30 | -10.814 | 1.143 | 1.100 | 1.117 | 75.98 | 207.01 | 70.40 | 946.40 |
| HM | 30 | 1.25 | 7 | 61.75 | pha31 | -7.994 | 0.352 | 0.424 | 0.368 | 74.49 | 217.46 | 120.20 | 961.50 |
| HM | 30 | 1.25 | 10 | 58.75 | pha32 | -9.363 | 0.624 | 0.674 | 0.631 | 74.36 | 217.12 | 91.90 | 970.70 |
| HM | 30 | 1.25 | 13 | 55.75 | pha33 | -10.731 | 1.104 | 1.070 | 1.081 | 74.23 | 216.77 | 68.50 | 981.10 |
| HM | 30 | 2.5 | 7 | 60.5 | pha34 | -7.814 | 0.327 | 0.399 | 0.343 | 73.43 | 215.71 | 116.30 | 965.20 |
| HM | 30 | 2.5 | 10 | 57.5 | pha35 | -9.183 | 0.579 | 0.634 | 0.588 | 73.30 | 215.36 | 88.30 | 974.90 |
| HM | 30 | 2.5 | 13 | 54.5 | pha36 | -10.552 | 1.025 | 1.007 | 1.007 | 73.17 | 215.01 | 65.30 | 985.90 |
| Blend | 22 | 1.25 | 7 | 73.75 | pha37 | -8.440 | 0.425 | 0.493 | 0.439 | 77.85 | 202.87 | 101.30 | 940.10 |
| Blend | 22 | 1.25 | 10 | 70.75 | pha38 | -9.809 | 0.752 | 0.783 | 0.752 | 77.72 | 202.52 | 78.40 | 946.50 |
| Blend | 22 | 1.25 | 13 | 67.75 | pha39 | -11.177 | 1.330 | 1.244 | 1.289 | 77.59 | 202.17 | 59.20 | 953.50 |
| Blend | 22 | 2.5 | 7 | 72.5 | pha40 | -8.260 | 0.394 | 0.464 | 0.409 | 76.79 | 201.11 | 98.00 | 942.70 |
| Blend | 22 | 2.5 | 10 | 69.5 | pha41 | -9.627 | 0.697 | 0.737 | 0.700 | 76.66 | 200.76 | 75.30 | 949.30 |
| Blend | 22 | 2.5 | 13 | 66.5 | pha42 | -10.997 | 1.234 | 1.171 | 1.200 | 76.53 | 200.41 | 56.50 | 956.70 |
| Blend | 26 | 1.25 | 7 | 69.75 | pha43 | -8.162 | 0.378 | 0.449 | 0.393 | 74.64 | 211.12 | 91.90 | 976.60 |
| Blend | 26 | 1.25 | 10 | 66.75 | pha44 | -9.531 | 0.669 | 0.713 | 0.674 | 74.51 | 210.78 | 69.80 | 985.30 |
| Blend | 26 | 1.25 | 13 | 63.75 | pha45 | -10.900 | 1.185 | 1.133 | 1.155 | 74.38 | 210.43 | 51.60 | 995.00 |
| Blend | 26 | 2.5 | 7 | 68.5 | pha46 | -7.982 | 0.351 | 0.423 | 0.366 | 73.58 | 209.37 | 88.60 | 980.10 |
| Blend | 26 | 2.5 | 10 | 65.5 | pha47 | -9.351 | 0.621 | 0.671 | 0.628 | 73.45 | 209.02 | 66.80 | 989.20 |
| Blend | 26 | 2.5 | 13 | 62.5 | pha48 | -10.718 | 1.098 | 1.065 | 1.075 | 73.32 | 208.67 | 49.00 | 999.40 |
| Blend | 30 | 1.25 | 7 | 65.75 | pha49 | -7.886 | 0.337 | 0.409 | 0.353 | 71.43 | 219.38 | 82.50 | 1018.90 |
| Blend | 30 | 1.25 | 10 | 62.75 | pha50 | -9.254 | 0.596 | 0.650 | 0.604 | 71.30 | 219.04 | 61.40 | 1030.70 |
| Blend | 30 | 1.25 | 13 | 59.75 | pha51 | -10.622 | 1.055 | 1.031 | 1.035 | 71.17 | 218.69 | 44.30 | 1043.90 |
| Blend | 30 | 2.5 | 7 | 64.5 | pha52 | -7.704 | 0.312 | 0.385 | 0.328 | 70.37 | 217.62 | 79.20 | 1023.70 |
| Blend | 30 | 2.5 | 10 | 61.5 | pha53 | -9.073 | 0.553 | 0.611 | 0.563 | 70.24 | 217.27 | 58.40 | 1036.00 |
| Blend | 30 | 2.5 | 13 | 58.5 | pha54 | -10.442 | 0.979 | 0.970 | 0.965 | 70.11 | 216.93 | 41.80 | 1049.90 |

The first, and most significant observation from Table 12 is that all of these glasses are predicted to have acceptable durabilities based upon the PAR for these constraints, with the caveat that many of these glasses do fall outside of the PAR for one or more of the constraints supporting the durability models such as frit, alumina, or homogeneity. Table 13 summarizes this information for each sludge type and loading. (Note that measurement uncertainties are not being considered.)

**Table 13: Predicted Behavior versus PAR for Each Set of 6 Glasses**

| Sludge Type | Sludge Loading | Durability Met in | Alumina Met in | Frit Met in | Homogeneity Met in | Viscosity Met in | Liquidus Temperature Met in |
|---|---|---|---|---|---|---|---|
| Purex | 22 | 6 of 6 | 0 of 6 | 6 of 6 | 0 of 6 | 6 of 6 | 6 of 6 |
| | 26 | 6 of 6 | 0 of 6 | 6 of 6 | 0 of 6 | 6 of 6 | 6 of 6 |
| | 30 | 6 of 6 | 6 of 6 | 4 of 6 | 6 of 6 | 5 of 6 | 0 of 6 |
| HM | 22 | 6 of 6 | 6 of 6 | 6 of 6 | 0 of 6 | 2 of 6 | 6 of 6 |
| | 26 | 6 of 6 | 6 of 6 | 6 of 6 | 0 of 6 | 3 of 6 | 6 of 6 |
| | 30 | 6 of 6 | 6 of 6 | 6 of 6 | 6 of 6 | 4 of 6 | 6 of 6 |
| Blend | 22 | 6 of 6 | 6 of 6 | 6 of 6 | 0 of 6 | 4 of 6 | 6 of 6 |
| | 26 | 6 of 6 | 6 of 6 | 6 of 6 | 3 of 6 | 6 of 6 | 6 of 6 |
| | 30 | 6 of 6 | 6 of 6 | 6of 6 | 6 of 6 | 6 of 6 | 2 of 6 |

Meeting the frit constraint appears to be a concern only for the Purex glasses at the highest (30 wt%) sludge loading. Most of the glasses (regardless of sludge type) fall outside of the PAR for the homogeneity constraint implying possible phase separation and less reliable durability predictions. Acceptable viscosities appear less likely for HM glasses, and Purex glasses with high waste loadings may fall outside the PAR for liquidus temperature. The low alumina for the Purex glasses (at 22 and 26 wt% waste loadings) is a concern as well.

### *STRATEGY FOR SEQUENCING GLASS BATCHING AND TESTING*

How is the information presented in Table 13 to be used for determining which glasses should be batched and/or tested for which properties? The specific answer depends on how the test results progress. For example, the current plan is to batch the set of six Purex glasses at 26 wt% waste loading. Poor durability results (obvious phase separation, unpredictability for the current models, or high leach rates) for this set of glasses may indicate a high probability of similar problems for the set of Purex glasses at the 22 wt% waste loading. In such a case, a set of Blend glasses (at e.g., 26 wt%) might be considered for testing in lieu of the set of Purex glasses. Once again, as these tests progress and their results are evaluated, the information in Table 13 provides some, albeit limited, insight into possible property outcomes for these candidate glass compositions. This information is being provided in this memorandum to provide the customer and SRTC reviewers/analysts an opportunity to gain a better understanding of some of these issues as decisions on the sequencing and testing of these PHA glasses are made.

# CONCLUDING COMMENTS

This memorandum provides a set of target compositions from which the glasses supporting this study of the PHA alternative are to be selected. These target compositions are used to determine process and product property predictions for the models utilized by DWPF's PCCS. These predictions (although somewhat questionable due to the introduction by PHA of unique component(s) and/or component ranges over which the models are being used) provide insight that may be helpful in planning and sequencing the batching, fabricating, and testing of the glasses for this study. This information is being provided to provide the customer and SRTC reviewers/analysts an opportunity to gain a better understanding of some of the issues being considered as decisions on the sequencing and testing of these PHA glasses are made.

# REFERENCES

[1] H. H. Elder, "Technical Task Request: DWPF Coupled Operation Chemistry – PHA Glass Testing," HLW-SDT-TTR-99-07.0, February 2, 1999.

[2] Harbour, J. R. and T. B. Edwards, "Task Technical & QA Plan: DWPF Coupled Operation Chemistry – PHA Glass Testing," WSRC-RP-99-00218, March 8, 1999.

[3] Brown, K. G. and R. L. Postles, "SME Acceptability Determination for DWPF Process Control (U)," WSRC-TR-95-0364, Revision 3, February 21, 1996.

[4] Sproull, Jim, "Frit 202 Data," E-mail to Tommy Edwards and John Harbour, March 5, 1999.

This page intentionally left blank.

## Distribution

J. L. Barnes, 704-3N
N. E. Bibler, 773-A
D. F. Bickford, 773-43A
K. G. Brown, 704-1T
J. T. Carter, 704-3N
J. J. Connelly, 773-41A
A. D. Cozzi, 77-43A
D. A. Crowley, 773-43A
T. B. Edwards, 773-42A
H. H. Elder, 704-S
S. D. Fink, 773-A
J. R. Harbour, 773-43A
E. W. Holtzscheiter, 773-A
R. A. Jacobs, 704-3N
C. M. Jantzen, 773-A
R. T. Jones, 704-3N
D. P. Lambert, 704-1T
L. F. Landon, 704-1T
S. L. Marra, 704-25S
D. B. Moore-Shedrow, 773-A
L. M. Papouchado, 773-A
D. K. Peeler, 773-43A
J. A. Pike, 704-3N
K. J. Rueter, 704-3N
R. F. Schumacher, 773-43A
M. E. Smith, 773-43A
T. K. Snyder, 704-1T
P. C. Suggs, 704-196N
W. L. Tamosaitis, 773-A
R. C. Tuckfield, 773-43A
R. J. Workman, 773-A
TIM (4 copies), 703-43A